CALCINATION AND SYNERGISTIC RATIO OPTIMISATION IN THE PRODUCTION OF HYBRID AGRICULTURAL POZZOLANS FROM AGRICULTURAL WASTES FOR THE CONSTRUCTION INDUSTRY

BY

Happiness Davies MAC-ETELI
B.Eng. Civil Engineering (NDU), M.Sc. Civil Engineering (Leeds).
Matric No: 202463

A Thesis in the Department of Agricultural and Environmental Engineering
Submitted to the Faculty of Technology
In partial fulfilment of the requirements for the Degree of

DOCTOR OF PHILOSOPHY

of the

UNIVERSITY OF IBADAN

June, 2023.

CERTIFICATION

This is to certify that this work was carried out under our joint supervision by Happiness D. Mac-Eteli in the Department of Agricultural and Environmental Engineering, Faculty of Technology, University of Ibadan, Ibadan, Nigeria.

……..…….

Supervisor
J.C. Igbeka
B.Sc., M.Sc. (Technion, Israel), Ph.D. (Ohio State),
FNIAE, FNSE, Regd. Engr. (COREN)
Emeritus Professor, Department of Agricultural and Environmental Engineering,
Faculty of Technology
University of Ibadan, Ibadan, Nigeria

……..…….

Co-Supervisor
B.I.O. Dahunsi
B.Sc. (Ife), M.Sc. (Ibadan), Ph.D. (Ibadan),
MNSE, MNIAE, MIEE, Regd. Engr. (COREN)
Professor, Department of Civil Engineering,
Faculty of Technology
University of Ibadan, Ibadan, Nigeria

DEDICATION

This thesis is dedicated to Almighty God for His grace and love, as well as to the blessed memories of my lovely mum and grand mum; Mrs Gloria O. Mac-Eteli (Late) and Madam Lucy Edua (Late).

ACKNOWLEDGEMENTS

I acknowledge the meticulous and outstanding supervision and guidance from my lead supervisor, Engr. Emeritus Prof. J.C. Igbeka, an astute academic mentor and father, whose zeal for perfection was at the core of this research progress, having successfully instilled in me the consciousness that there is always a room for improvement. In same vein, my heartfelt gratitude goes to Engr. Prof. B.I.O. Dahunsi, the co-supervisor, who zealously and selflessly assisted in offering a comprehensive guidance towards the successful completion of this research. Special thanks go to Engr. Dr. M. Omobowale (HOD), an epitomic academic, a father and a dearest friend, who successfully adopted me as an academic son and groomed out success through me. Many thanks also goes to Prof. Y. Mijinyawa, Prof. A. K. Aremu, Prof. T. A. Ewemoje, Prof. A. O. Raji, Prof. K. Ogedengbe, Prof. E. A. Ajav, Prof. A. I. Bamgboye, Prof. A. Y. Sangodoyin, Dr Mrs O. E. Ewemoje, Dr B. O. Oyefeso and other non-academic staff at the Department of Agricultural and Environmental Engineering, University of Ibadan, who collectively played significant roles in making this journey worthwhile.

My appreciation goes to the stakeholders of Nigerian Agip Exploration (NAE) Scheme, for partly funding this research work. Similarly, I deeply appreciate the part funding facilitated by the management of Niger Delta University, and the Federal Government of Nigeria through the Federal Government Needs Assessment Scheme. I equally acknowledge Engr. Prof. Solomon Orumu and members of Staff of the Department of Civil Engineering, Niger Delta University, for their collective support.

Special appreciation goes to my father, Mr Morris Mac-Eteli, for his selfless sacrifice and investments on his children; my grand-mum, Madam Lucy Edua (Late), who always believed we're made for more. Boundless appreciation to my beautiful wife, Dayagha D. Mac-Eteli, members of my dearest blessed family, HajefMoria Conglomerate, Great Martha's Descendants, and my choco-milo boys, Arimor A. Mac-Eteli and Arionin R. Mac-Eteli, for collectively being the reason behind the extra effort.

Special recognition goes to Dr. Goodluck E. Jonathan, Rtd. Rear Admiral Gborigbiogha J. Jonah, Prof. Humphrey Ogoni, Prof. Allen Agih, Prof. Charles Owaba, Prof. M. Adigio, Prof. and Prof Mrs Oshinowo, Prof. Z. Yelebe, Dr. Mrs Alice Atuwo, Dr. Richard Okojaja, Engr. Boyibim Edoghotu, Mr Ayebaikieri Jonah, CSP. Ebi Okoyen, Mr. Selepre Mathew, Engr. Luke Dima, Engr. Dr. Kuti Abayomi, Engr. Lucky Edeh, Engr. Sopakirite Somina, Engr. Keme Nelson, Engr Habib, Engr. Omale, Engr. Audu John, Engr. Kadiri, Engr. Tari Kilakime, Engr Yabefa, Engr. Jonathan, Chidoski, Evans, Bright, Metong, Ebiarede, Godson, Osiakeme, Emmanual, Adila, Dangana, Esther, Peretiemo, Ogari, Abilo, Jumbo, Courage, Osain, Oworodo, Moses, Lucas, Inspector, Shenkomaya, and a host of friends, colleagues, undergraduate project

students, students, and well-wishers too numerous to mention, for their respective, peculiar and immense contributions leading to the realization of this research exercise. Thank you all.

ABSTRACT

Cement is an important material in the construction industry. However, the environmental problems associated with the mining and calcination of limestone for cement production necessitates the search for supplementary cementitious materials with minimal threat to the environment.

Periwinkle and clam shells, processed into ash are potential substitutes for cement in concrete. This study was designed to investigate the suitability of Periwinkle Shell Ash (PSA) and Clam Shell Ash (CSA) and a hybrid of both as partial replacements for cement in concrete. Shells were sourced from Amassoma, Bayelsa State, Nigeria, washed, sun dried and calcined at varying temperatures (200, 400, 600 and 800 ^{o}C). These were pulverised to pass through 75 µm sieve to produce PSA, CSA, and hybrids of both, mixed at 70:30, 60:40, 50:50, 40:60 and 30:70. Grade M20 concrete specimens were produced at varying Portland limestone cement (PLC) replacement levels (0, 20, 30, 40 and 50%) with 0% as control, and cured for 28 days prior to testing. Specific gravity, flexural strength, compressive strength, Water Absorption Index (WAI), Chloride Induced Strength Loss Index (CISLI), and Sulphate Induced Strength Loss Index (SISLI), were conducted in accordance with British Standards. Combined mixture methodology was used to develop regression models from laboratory data, analysed and optimised at 95% confidence interval to ascertain Optimum Pozzolanic Reactivity (OPR) based on Strength Activity Index (SAI). Emissions of CO_2 associated with calcination of samples were analysed and compared to that of PLC using data from energy demand and carbon footprint.

Specific gravities were 3.12±0.24, 2.96±0.01, 3.00±0.10, 3.14±0.03, while flexural and compressive strengths were 5.29±0.14, 2.83±0.10, 2.83±0.08, 3.36±0.21 and 27.74±1.41, 18.27±1.10, 19.21±0.25, 21.67±2.29 N/mm2 for PLC, PSA, CSA and 60% PSA:40% CSA, respectively, at 40% cement replacement level, produced at 600 ^{o}C. Compressive strengths of 60% PSA:40% CSA, were 78.1% of PLC, 118.6% of PSA and 112.8% of CSA; implying that the hybrid was stronger than PSA or CSA. Also, WAI, CISLI, and SISLI, were 1.98±0.19, 2.84±0.08, 3.25±0.17, 2.75±0.13; 24.56±2.15, 19.34±0.37, 0.44±0.08, 6.10±0.84; and 16.47±1.43, -10.97±1.32, -16.88±0.68, 4.09±0.62 for PLC, PSA, CSA and 60% PSA:40% CSA. The PLC had the least WAI but diminished more in strength due to chemical attacks and absence of pozzolans compared to PSA and CSA. The OPR based on SAI was 55.5% PSA:44.5% CSA, and cement replacement levels were 19.7, 23.2, and 44.0%, for PSA, CSA and 55.5% PSA:44.5% CSA, respectively, produced at 425, 527, and 607 ^{o}C. A uniform compressive strength of 20.8 N/mm2 was obtained for PSA, CSA and 55.5% PSA:44.5% CSA, produced at 425, 527, and 607 ^{o}C, respectively, satisfying the SAI criteria. Optimised WAI, CISLI, and SISLI of PSA, CSA and 55.5% PSA:44.5% CSA were 2.46, 2.52, 2.51; 2.10, 3.06, 12.72; and -33.16, -31.48, -0.08%, when produced at 425, 527, and 607 ^{o}C. A kilogram of pozzolan emitted 350g of CO_2 at calcination, while that of PLC was 490g; providing a 28.60% savings in CO_2 emissions.

Periwinkle and clam shells enhanced cement replaceability and satisfied the strength activity index pozzolanic criteria, when synergised and ashed optimally. Consequently, environmental pollution associated with excessive limestone harvest and processing was mitigated.

Keywords: Cement replacement, Pozzolans, Calcination, Strength activity index

Word count: 497

TABLE OF CONTENTS

LIST OF TABLES

LIST OF FIGURES

LIST OF PLATES

APPENDICES

LIST OF ABBREVIATIONS

ABBREVIATION	FULL MEANING
AP:	Agricultural Pozzolans
HAP:	Hybrid Agricultural Pozzolans
MCA:	Maize Cob Ash
MHA:	Maize Husk Ash
RHA:	Rice Husk Ash
SCM:	Supplementary Cementitious Materials
PSA:	Periwinkle Shell Ash
CSA:	Clam Shell Ash
SAI:	Strength Activity Index
SISLI:	Sulphate Induced Strength Loss Index
CISLI:	Chloride Induced Strength Loss Index
SIMLI:	Sulphate Induced Mass Loss Index
PBA:	Palm Bunch Ash
PKA:	Palm Kernel Ash
CHA:	Coconut Husk Ash
CPA:	Cassava Peel Ash
SSA:	Snail Shell Ash
OSA:	Oyster Shell Ash
BWA:	Bagasse Waste Ash
GGBS:	Ground Granulated Blast-Furnace Slag
RLR:	Recommended Level of Replacement
CRL:	Cement Replacement Level

CHAPTER ONE

INTRODUCTION

1.1. Background to the Study

Sustainability is the goal behind any and every advanced profession, as it demands for a preserved tomorrow irrespective of the activities of today. Currently and globally, there is constant pressure on all sectors of society to limit greenhouse gas emissions into space, as well as the unsustainable exploitation of natural resources, (IPCC, 2022).

Locally, there is a demand for population growth rate to be balanced with available resources through boosting human capital development, reducing waste, creating job possibilities and increasing the quality and standard of living, (Anyanwu et al., 2015). On the other hand, those who work in civil engineering, as well as other engineering, environmental, and science-related fields, have a responsibility to deliver engineering facilities in the most cost-effective, environmentally sound, and socially responsible manner possible without sacrificing the facilities' quality, (Qureshi, and Nawab, 2013).

Nigeria does have a vast population exceeding 213 million and growing at a rate of 2.4% annually (Data Commons 2023). Nigeria's Real Gross Domestic Product (GDP) is currently at $2,066, which equates to an average ₦2,600 per day (Data Commons, 2023). This implies that average Nigerians are expected to cater for their education, clothing, health, food, shelter and general maintenance from daily income of ₦2,600. Worse still, Nigeria’s average GDP growth rate decreases at -3.1% annually (Premium Times, 2023).

The over reliance of Nigeria on the oil sector is has greatly impacted on her productivity as a Nation, (Anyanwu et al., 2015). Because of these unpleasant realities, experts in economics, academia, accounting, and other business-related professions have underlined the necessity for economic diversification in the country, but it is clear from the track record so far that little has been done to that end. As a result, the population that should be her greatest asset is now having a negative impact on her ability to live on her rich and fertile land.

With its many chains of production, including fertilizer manufacturing, real farming, processing, preserving, packaging, marketing, and management, agriculture is one industry that has the ability to employ more than 50% of the country's healthy population, (Jobberman, 2023). It will be unrealistic to expect the current administration to cover the initial costs necessary to establish and equip such agricultural institutions as well as the ongoing costs associated with providing for this proportion of the country's population. So, a good strategy would be to increase the allure of farming beyond what it already has by maybe adding value to both farm waste and by products (Jobberman, 2023).

A good example would be the establishment of businesses that would purchase farm items from adjacent communities and then sell the finished, attractively packaged goods to these communities at reasonable prices, making fantastic use of the parts that were first deemed waste. Some of these are; the husk from processed rice, the chaff and cob from maize, the bunch of palm fruit, the shells of coconut, palm kernel, snail, oyster, clam, eggs, periwinkle and crab etc. Such an industry would have created a means for locally empowering locals and provided more motivation to farmers thereby ensuring a better livelihood. Moreover, the environment would be better protected from careless garbage disposal, (Kalkanis *et al*., 2022)

There are far too many advantages and benefits of effective waste management for a country. For instance, "ground granulated blast furnace slag" (GGBS), a by-product from the steel industry, could replace as much as 70% of cement in concrete or sand-crete structures, (Walker and Pavia, 2011). The cement industry over the years has developed greater attention towards integrating by-products from the agricultural as well as industrial sectors into the manufacture of cement, hence the existence of CEM II, CEM III, CEM IV and CEM V, which are either pozzolanic cements with low or high concentrations of pozzolans or slag cements. This is all in a bid to answer the global call towards sustainability (Isaksson and Steimle, 2009).

Cement types in engineering are basically five in number; CEM I, (Ordinary Portland cement), CEM II (Portland composite cement), CEM III (Blast furnace slag cement), CEM IV (Pozzolanic cement) and CEM V (composite cement). Of these, it is evident that excluding CEM I, the other types of cement are seen integrating two major forms

of by-products as additives in cement production process. These are of the hydraulic forms and pozzolanic forms. The hydraulic additives are known to exhibit close resemblance with cement in terms of its formation of calcium silicate hydrate gel when it reacts with water, and as such, literature reports that such materials (e.g. Slag), when used as a replacement material, replaces up to 70% of cement in cement structures (Walker and Pavia, 2011). However, the second form of additive is of a pozzolanic nature, and these must react with calcium hydroxide and water to develop secondary calcium silicate hydrate gels; These have been seen to replace between 10 – 25% of cement in cement structures (Walker and Pavia, 2011).

Agriculturally produced pozzolanic cementitious materials are predominantly manufactured. The majority of them are produced by pulverisation and controlled or uncontrolled combustion. Providing an ideal and optimised temperature for the dihydroxylation of Agricultural Pozzolans (AP), via calcination, and for use as partial substitutes for cement in the construction industry, is of global interest (Danner and Justnes, 2018).

1.2. Problem Statement

The structural maturity of Portland cement in terms of its setting time, rate of hydration or strength gaining is faster compared to lime binder. Regardless, neither Portland cement nor lime can be regarded as the ideal binder as these are unsustainable in areas of energy demand, carbon footprint, and cost associated with their production. Cement production for instance requiring calcination temperatures ranging between 1450 to 1600 ^{o}C for the formation of clinker, results in the consumption of about 4.5 GJ of energy and emission of about 850 gCO_2 per ton of clinker produced ((Habert, 2013), of which about 50-63% is attributed to the calcination phase and about 37-50% attributed to the combustion of fossil fuels (BREF, 2010). Similarly, lime, which is superior to cement in areas of durability, workability and long term strength, requires calcination temperatures ranging between 800 ^{o}C and 1200 ^{o}C hence consuming an average of 4.25 GJ of energy and emitting about 1.092 tons per tonne of quicklime produced, of which about 68% is attributed to the calcination process, 30% attributed to fuel combustion and 2% attributed to electricity (Stork *et al*., 2014).

While in desperate search for a material that possesses the beneficial properties of both lime and cement binders, the greater challenge for the engineering and research community remains developing sustainable means of reducing energy demand, carbon footprint as well as cost. As such, current trends are in energy efficiency (optimising materials and processes associated with the production phase such as the switching from horizontal kilns to vertical kilns (Schorcht *et al*., 2013)); lower carbon energy sources (switching from fossil fuels to gas or biomass (Stork et al., 2014)); end of pipe solution (Carbon Capture and Storage/Utilization, (TNO, 2012; Stork *et al*., 2014; CEFIC, 2013)); carbonation (lime structures exhibit greater tendencies towards carbonation when compared to cement). Campo *et al*., (2021), reports that between 80 – 92% of emitted carbon is reabsorbed over a period of 100 years in lime mortar structures); and use of Supplementary Cementitious Materials (SCM's).

In Nigeria, approximately 54 Mta of cement is produced annually, of these, Dangote dominates the industry with a 32.25Mta capacity and roughly a 60% market share; BUA Group comes in second with 11 Mta and a market share of roughly 20.4%; followed by Lafarge Africa with 10.5 Mta and a market share of roughly 19.5%, (AsokoInsights, 2023, Cemnet 2023**).** Dangote's flagship plant at Obagaja in Kogi State Nigeria, commissioned in 2008 is the largest plant in Nigeria and responsible for about 30% of Nigerian annual cement production. However, Dangote has reported that in 45 years, its 647 million tons of limestone reserves would be completely used up in course of cement production, (AsokoInsights, 2023), see figure 1.1. This is a significant threat to Nigeria and Nigerians as the country might be forced into limestone/cement importation at very unsustainable costs. It is therefore a timely necessity to search for alternative and sustainable sources of $CaCO_3$, for complete or partial replacement of cement.

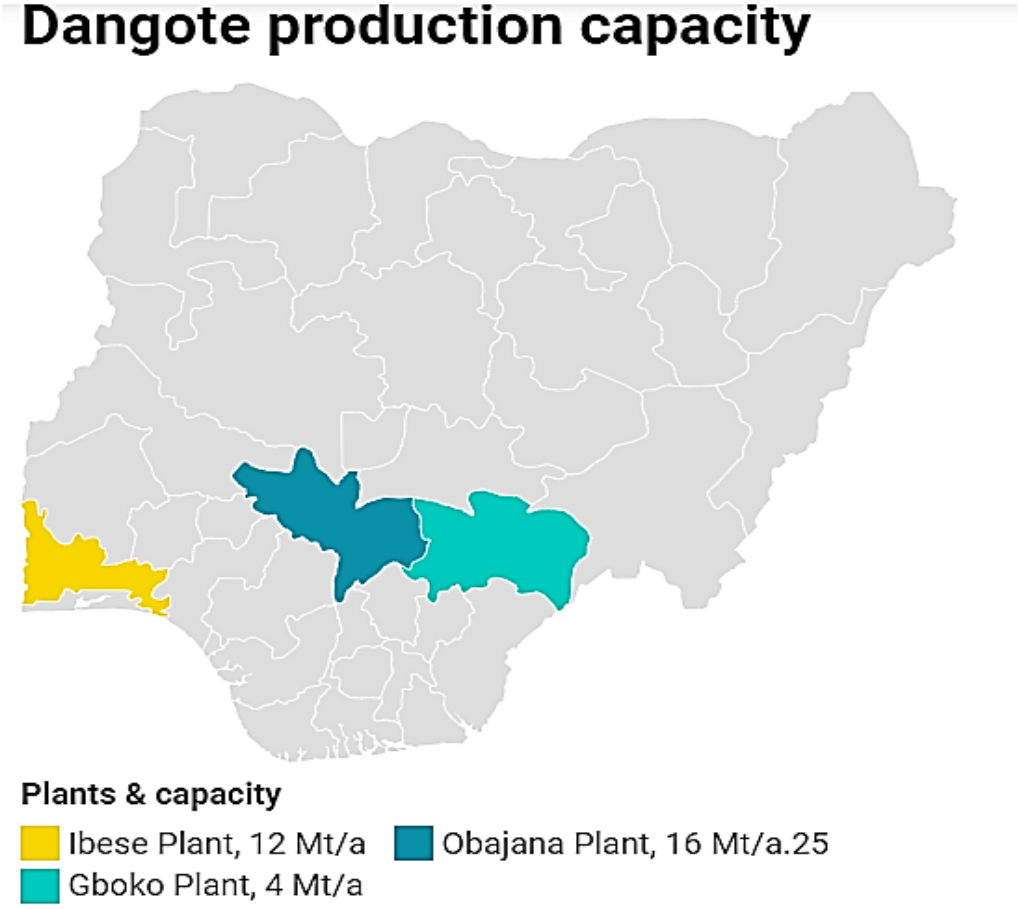

Figure 1.1: Dangote's Cement Plants in Nigeria

Source: AsokoInsights, 2023

Research into the use of agro-based SCM's can be traced as far back as the late 70s (Cook *et al*., 1977). A great number of publications exist in the area of optimising partial replacement levels of cement or lime binder using agro based SCM's such as rice husk (Cook *et al*., 1977; Zhang and Malhotra, 1996; Abalaka, 2012; Ettu *et al*., 2013; Kumar *et al*., 2016). Further agro based SCM's researched on are Periwinkle shell (Umoh and Ujene, 2015; Eziefula *et al*., 2020; Antia *et al*., 2020), Palm kernel shell (Olowe and Adebayo, 2015; Oti *et al*., 2015; Fadele and Ata, 2016), clam/oyster shell (Lertwattanaruk *et al*., 2012; Olutoge *et al*., 2016; Ephraim *et al*., 2019), coconut shell (Kumar and Kumar, 2014; Bheel *et al*., 2021) cassava peels (Salau *et al*., 2012; Ofuyatan *et al*., 2018; Ogbonna *et al*., 2020), maize husk (Kevern and Wang, 2010; Ndububa and Nurudeen, 2015; Kamau *et al*., 2016), and snail shell (Etuk *et al*., 2012; Syed and Vaishali, 2014), etc. In a bid to obtain more practicable results, researchers have equally opened a window into hybrid agro based SCM in which agro based SCM's synergised to form single partial cement replacement materials (Ajay *et al*., 2007, Kannan and Ganesan, 2012; Umoh *et al*., 2013; Inti *et al*., 2016; Ban and Nobert 2016; Dankwah and Nkrumah, 2016).

While these researchers have obtained excellent results thus far, optimum cement replaceability can only be achieved when the best materials are produced under the best conditions. For instance, the chemistry of Portland cement clinker, built at very high calcination temperature contains four distinct elements which are CaO, SiO_2, Al_2O_3 and Fe_2O_3. These elements are in definite proportions which give the cement its binding and strength giving qualities. As such, cement substitutes are expected to have a chemical resemblance of a sort to cement in order to maximise their potential to sustainably and partially replace cement. While previous research delved more on single agro based SCM's, and more recent researchers into agro hybrid SCM, only Dankwah and Nkrumah, (2016) was cited to have published findings on the synergy of agro based SCM's rich in both CaO and SiO_2, no marvel his sample could effectively replace up to 30% of cement which is one of the best results cited in this research. In their work, the synergy of rice husk ash (RHA) and Snail Shell Ash (SSA) was not varied but fixed at a ratio of 20:80. Also, knowledge on the effect of variations in calcination temperature was absent.

Having established the independent roles played by calcination temperature and synergistic ratio in building cement-like sample's chemical signature, it will be of great value to establish the combined effect of variations in these production parameters in order to open a doorway into greater cement replacement possibilities. This is the focal point and knowledge gap aimed to be filled after the successful completion of this research work. A simplified breakdown of the problem statement is as shown in Table 1.1.

1.3. Aim and Objectives

This study is aimed at optimising the production parameters for periwinkle shell ash, clam shell ash, and a hybrid of both for enhanced cement replaceability in concrete, that yields comparatively practical mechanical and durability properties.

The objectives are:

1. determination of the physical and mechanical properties of Clam Shell Ash, Periwinkle Shell Ash and Clam/Periwinkle ash synergised samples produced under varying calcination temperatures and synergistic ratios as well as durability contribution to Concrete specimens, when used as partial cement substitutes;
2. analysis experimental data and develop models for the optimisation of calcination temperature, synergistic ratio and cement replacement level, in the production of PSA/CSA hybrid pozzolan as partial cement replacement material in concrete; and
3. evaluate the sustainability features of using optimized agricultural by-products/wastes as partial replacements to Portland cement in Engineering structures.

Table 1.1: Basic Research Questions

S/N	RESEARCH QUESTIONS	ANSWER	AVAILABLE LITERATURE?	OBJ.
1	Is the partial / complete replacement of Portland cement a timely necessity	Sustainability *(Economic, Social and Environmentally related costs)*	Yes	NO
2	Are the materials readily available for the effective replacement of Portland cement?	Yes and No *(availability and material quality)*	Yes (GGBS, MetaStar, PFA, Agro-based Pozzolans)	NO
3	Are there solutions for the improvement of Pozzolan properties for effective cement replaceability?	Limited	Knowledge Gap	YES
4	What is the optimum temperature for the calcining of Clam shell ash for improved pozzolanicity?	N.A.	Knowledge Gap	YES
5	What is the optimum temperature for the calcining of Periwinkle shell ash for improved pozzolanicity?	N.A.	Knowledge Gap	YES
6	Are there descriptive analysis on the Calcination temperature and hybrid ratio variations of clam and periwinkle shell ash on the Physico-mechanical and durability properties cement blended concrete	N.A.	Knowledge Gap	YES
7	Are there analyzed and optimized models on the Calcination temperature and hybrid ratio variations of agro-based pozzolans with complementing SiO2 and CaO content on the mechanical and durability properties cement blended concrete	N.A.	Knowledge Gap	YES

1.4. Justification of Research

The environmental indices of limestone harvest and processing in Nigeria are not friendly. Lung diseases, CO_2 emissions and the destruction of the habitat of man, plants and animals, are some fundamental concerns in the cement industry. Economically, the cost of harvesting limestone, processing and transportation of cement is not sustainable due to the decentralized locations of limestone in the country. Socially, employment opportunities in the country relative to cement manufacturing cannot be said to be equal, and this is also as a result of the decentralized locations of the primary raw material for cement manufacturing (limestone).

This research is geared towards mitigating the challenges associated with cement binder by looking into the use of agro based Supplementary Cementitious Materials as these do not necessarily share the expensive and high technological know-how demands associated with the other abatement measures as expressly outlined by a technical report published by the European lime Association in 2014 (Stork et al., 2014). More so, the use of well-produced agriculturally based Supplementary Cementitious Materials holds promise in increasing strength and durability of cement structures while promoting the quality of the agricultural sector by attaching value to agricultural by-products/waste (Walker and Pavia, 2011).

1.5. Scope and Limitations

The fundamental areas covered in this research are strength, durability and sustainability. The strength of concrete samples was measured in terms of compressive and flexural strength at ages 28 days, 56 days and 90 days. However, analytical models developed for strength features at ages 28 days alone. Durability indices were recorded in terms of water absorption, chloride attack and sulphate attack at ages 28 days, 56 days and 90 days. However, analytical models will be developed for durability features at ages 28 days, noting that while PLC concrete reaches maximum strength at 28days, pozzolan-cement blended concrete exceeds 28 days in its rate of hydration and at such, 28 day findings for pozzolan-cement blended concrete is the minimum benchmark for industrial applications. Fineness, specific gravity and water demand were also covered in course of this study.

Sustainability analysis was measured in terms of cost, energy demand and CO_2 emissions. Due to very high financial implications, physical findings such as amorphousness and surface area will not be covered. Sample preparation required a high capacity milling machine as well as a high temperature capacity furnace, which were locally fabricated.

CHAPTER TWO

LITERATURE REVIEW

2.1 Waste as a Binder Replacement

Using waste to partially replace binders is not a novel idea. Actually, pozzolans are a subset of additional cementitious materials, a more general concept (SCMs). These compounds have the ability to make binders more reactive, either on their own or in response to hydration by-products of cement or lime. They have been known to aid in long term strength gain, as well as resistance of concrete against chemical attacks and hazardous exposure conditions, (Adam, 2004). Adam (2014) further divided supplementary cementitious materials into hydraulic and pozzolanic, adding that an increase in calcium oxide content promotes Hydraulic effects but reduces pozzolanicity as shown in Figure 2.1.

Ground granulated blast-furnace slag (GGBS), an example of an SCM, forms cementitious compounds simply by reacting with water, whereas pozzolanic SCMs, which contain siliceous or aluminous amorphous oxide, only form secondary binding properties when reacting with CaO or $Ca(OH)_2$ in puverised state. The amorphous content plays a significant role in the pozzolanic index of SCMs' as sheown in Figure 2.2.

About 50% of tobermorite (C-S-H gel) is a hydration product of cement and water, while 25 – 50% is portlandite (CaOH) and the remaining proportion of the hydration product is ettringite (Adam, 2004). In essence, the hydration products of cement and water are tobermorite, portlandite and ettringite. Portlandite is a filler with minimal strength value but however, reacts with Sulphate ions to form expansive ettringite which is a threat to the matrix of the cement structure, as enormous expansive reactions can lead to the development of cracks. Calcium silicate hydrate gel (C-S-H gel) is responsible for the strength within the cement matric. Curiously, portlandite is the needed material by pozzolans to develop secondary C-S-H gel and hence giving the cement structure more strength.

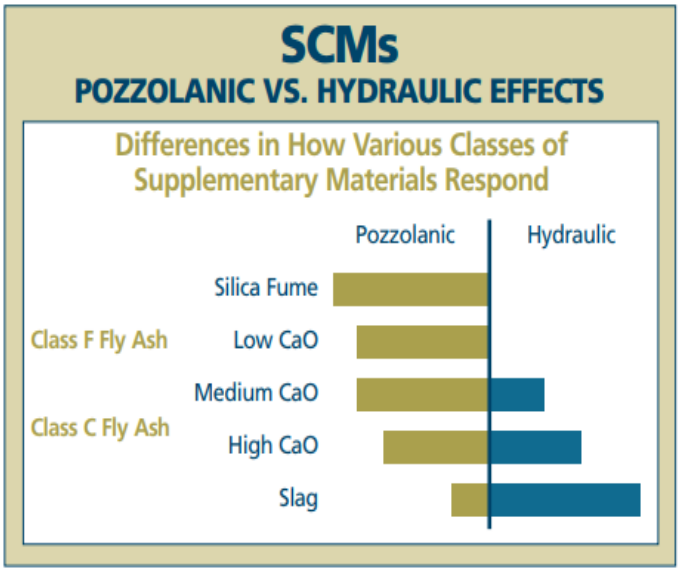

Figure 2.1: Pozzolanic and Hydraulic Supplementary Cementitious materials

Source: Adam, (2014)

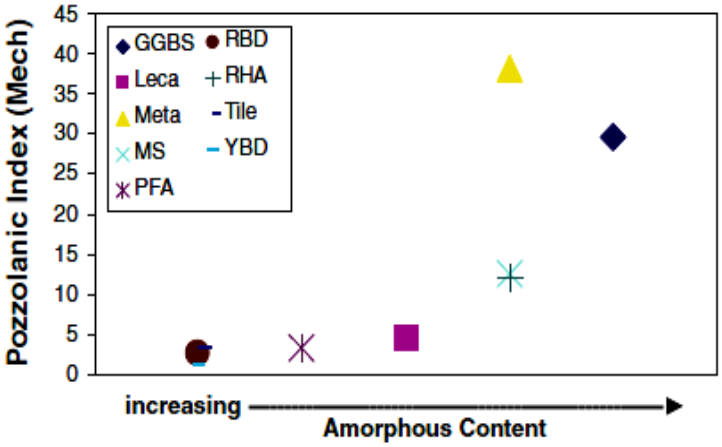

Figure 2.2: Effect of Amorphous content on the pozzolanic reactivity of Pozzolan cement

Source: Walker and Pavia (2011)

Along with being a by-product of cement's hydration, calcium oxide ($Ca(OH)_2$) is also a component of lime binder, which is created by the calcination of limestone and slaking of quicklime.

As such, both binders (cement and lime) generate portlandite as a by-product of hydration and require the presence of pozzolans to activate the portlandite, mitigate the formation of delayed ettringite as well as enhance the development of strength at ages beyond 28 days.

2.2 Agricultural Wastes and Pozzolans

A Roman architect named Marcus Vitruvius Pollio, who was also an engineer and lived in the first century BCE (15–25 BC), is known to have discovered the use of pozzolans and how they were used to improve the performance of lime binders even in the presence of water. The volcanic ash was found in Pozzuoli, a village close to Mount Vesuvius, and was thus given the name Pozzolan. Marcus Vitruvius Pollio wrote 'Ten Books of Architecture' and asserted that there is a certain powder that exhibits astounding outcomes from natural sources. This material, when mixed with lime and rubble, not only reinforces other construction types but also hardens underwater when used to construct seashore piers (Marcus, 1960).

In order to meet the global need of reducing greenhouse gas emissions as well as reduce the rate at which naturally resources are being harvested; improving on human capacity development for meeting local empowerment needs; and ensure a safe working environment, researchers have therefore put a lot of effort into determining the feasibility of incorporating natural, industrial, and agricultural pozzolans into the building industry. Knowledge Exchange for Young Scientists (KEYS) presented its findings in the following areas at its first international conference:

i. Developing nations are expected to contribute 80% of the global increase in cement demand.
ii. The total amount of CO_2 released by the cement industry accounts for between 5-8% of all carbon dioxide emissions worldwide.
iii. The availability of these materials (SCMs) in nature has a major impact on the viability of clinker substitution methods.

iv. Fly ash and slag are excellent examples of materials that can replace approximately 70% of cement; however, their global availability is less than 5%.

Major physical traits influencing pozzolans' pozzolanic reactivity include fineness, specific gravity, amorphousness, and specific surface area. Walker and Pavia (2011) found that amorphousness, rather than other pozzolan physical characteristics, significantly influences the reactivity of the material.

The classes of pozzolans are summarized in Table 2.1 below in accordance with ASTM C-618.

Table 2.1: Pozzolan classification according to ASTM C-618 (2012)

POZZOLANIC PROPERTIES	NATURAL	ARTIFICIAL	
	Class N	Class F	Class C
Fineness (max. Ret. When wet sieved on 45μ sieve), (%)	34	34	34
28 day Strength Activity Index (SAI), (%)	75	75	75
Min. "$SiO_2 + Al_2O_3 + Fe_2O_3$" (%)	70	70	70
Loss on ignition (LOI) (%)	10	6-12	6
Sulphur trioxide (SO_3) max. (%)	4	5	5
Water requirement max.% of control	115	105	105
Autoclave soundness %	0.8	0.8	0.8

The European Standard EN 197-1 (2000) which is a standard for the classification of cement further added that a pozzolan consists essentially of Silicon dioxide (SiO_2) and aluminium oxide (Al_2O_3). It further adds that the reactive SiO_2 content shall not be less than 25% by mass. However, presence of CaO is negligible in pozzolan classification.

If all key sectors are actively involved, agriculture has the ability to meet local demands for developing human capital and producing plenty of job opportunities, both of which can make living safer and cheaper. Due to this, scholars in various fields of science and engineering have focused on optimising the value chain in the agricultural industry by devising methods to efficiently transform by-products from agricultural sector to beneficial resources in the building and construction industry where they are termed supplementary cementitious materials (SCM's) some of which include;

i. Rice Husk Ash (ASH) gotten from rice husk
ii. Maize Husk Ash (MHA) gotten from maize husk
iii. Maize Cob Ash (MCA) produced from maize cob
iv. Palm Bunch Ash (PBA) produced from the frond (bunch) of palm trees
v. Palm Kernel Ash (PKA) produced from the kernel of Palm oil fruits
vi. Coconut Husk Ash (CHA) produced from the husk of coconut fruit
vii. Coconut Shell Ash (COSA) produced from the shell of coconut fruit
viii. Cassava Peel Ash (CPA) produced from cassava peels
ix. Periwinkle Shell Ash (PSA) produced from periwinkle shells
x. Snail Shell Ash (SSA) produced from snail shells
xi. Clam Shell Ash (CSA) produced from waste clam shells
xii. Oyster Shell Ash (OSA) produced from waste oyster shells
xiii. Moon-snail Shell Ash (MSA) produced from waste moon-snail shells
xiv. Bagasse Waste Ash (BWA) produced from sugarcane back waste

2.2.1. Rice Husk Ash (RHA)

About 20% of the weight of rice is made up of the agricultural waste product known as rice husk, which is produced from the milling of rice and 483.1 million tons of rice were produced worldwide in 2016 (FAO, 2023). To satisfy its yearly need of 7.9 million tons, Nigeria increased its production of milled rice from 2.8 million tons in 2010 to 5.4 million tons in 2022, (Statista, 2023). As a result, with Nigeria's present pace of rice production, no less than 1.16 million tons of husk are generated as waste each year, (Science Nigeria, 2023).

The usage of rice husk ash, blended with lime cement mixtures for use in the productions of sandcrete blocks was studied (Cook *et al.,* 1977), which was one of the earliest revelations of RHA as a potential partial substitute for binders. According to their research, the calcination process used to produce RHA should be managed and kept between 450 and 500 °C.

The cost of producing husk is around 32% of the cost of producing ASTM Type 1 cement, they stated, and 25% of the husk is transformed to ash during calcination (Cook *et al.*, 1977). Their findings revealed exceptionally high level of SiO_2—roughly 93%—along with extremely small amounts of other oxides. A certain amount of sodium aluminate was added to the blended lime mix to improve its tensile strength. Results further demonstrated that a reduction in the initial and final setting times of both lime and cement mixes is caused by a rise in rice husk ash and $NaAlO_2$ concentration, (Cook *et al.,* 1977).

At 40%RHA concentration, there was also no discernible difference between the mortar specimens' compressive strength and the control's at 90 days of age. In contrast to the control, ash-containing lime specimens demonstrated a greater rate of strength increase after 90 days - the existence of a pozzolan with significant activity index was cited as the cause of this. The RHA replacement level recommendations ranged from 10 to 20%.

Zhang and Malhotra (1996) burnt rice husk at temperatures below 800 ^{o}C for a short period of time (unspecified) in order to observe the impact of RHA on the characteristics of fresh and cured concrete. According to a chemical investigation, the

RHA contains 0.5% CaO and 82.7% SiO_2. Results for compressive strength demonstrated that at 15% RHA, the RHA-blend concrete's compressive strength was higher than the control at 1, 7, and 28 days. Additionally, it was demonstrated that as the water/RHA blended cement ratio was lowered, the strength of the concrete rose. The RHA cement blended concrete was found to set up more quickly than the control. Regarding resistance to penetration of chloride ions and freeze-thaw cycling, the concrete made with RHA cement combined with other materials fared better relative to PLC concrete (Zhang and Malhotra, 1996).

Many studies on the viability of replacing cement and lime in the construction sector with RHA were published in the 20th and 21st centuries (Zaid *et al*., 2021). They produced their ash at a calcination temperature of 700 ^{o}C, and at 10% cement replacement levels, optimum the 28-day result relative to compressive strength and durability was reached. Also, between 5–10% RHA content, growth in strength of concrete was demonstrated relative to the PLC control, particularly at ages longer than 28 days. Furthermore, superior durability findings were noted. Abalaka (2012)'s production of RHA at 758 ^{o}C and with various replacement amounts was shown to have lower compressive strength than the control excluding the concrete produced with 10% RHA as partial cement substitute and measured at 90 days, which was somewhat stronger relative to PLC control concrete. Therefore, he advised that if early strength is a priority, RHA percentages in concrete should not exceed 25%. (Abalaka, 2012).

Rice husk ash was the focus of research by Ettu *et al*., (2013) and Deepa *et al*., (2013), whose studies were on evaluating the optimal and structurally feasible cement replacement level using RHA. The rice husk was calcined by Ettu *et al*., (2013) at temperatures below 650 ^{o}C and ground till it could pass a 600 μm sieve. He achieved outcomes at all ages that were comparable to controls at a replacement level of 15%. The amorphous phase content, the degree of dehydroxylation, the specific surface area, the amount of $Ca(OH)_2$ in the cement paste, the admixture content, and the water to binder ratio in the material appear to be the most significant factors that affect pozzolanic activity, (Kulkani *et al*., 2014). A review of the responsiveness of RHA employed in the construction industry was published by Das and Patel (2018). The SiO_2 content was determined to be the primary determinant of pozzolanic reactivity.

Other elements such as the amorphous phase content, the degree of dehydroxylation, the specific surface area, the amount of $Ca(OH)_2$ in the cement paste, the admixture content, and the water to binder ratio, as highlighted by Kulkani *et al*., (2014), where also recalled by Das and Patel (2018). Studies on the strength of concrete have indicated that rice husk ash in concrete fails to enhance early strength because of the time needed for SiO_2 to form a bond with $Ca(OH)_2$. It was discovered that 20% replacement represented the ideal RHA concentration in terms of strength. However, after 90 days, the 40% RHA embedded concrete outperformed the control in terms of strength. With more RHA concrete, durability improvements include decreased chloride attack, increased corrosion resistance, decreased acid attack mass loss, increased sulphate resistance, and improved carbonation performance. (Das and Patel, 2018).

Future studied by the authors were recommended in the areas of; costs of concrete containing or not containing RHA; long-term durability and strength measured beyond 180 days and one year; capacity for increased RHA replenishment of cement; and effect of chemical activators on the reactivity of RHA as a pozzolan

Similar to Das and Patel, (2018) this study recommends using the Strength activity Index (SAI), to assess the reactivity of RHA in concrete after reviewing papers on its use as a partial cement replacement. They came to the conclusion that RHA is a promising material in the construction sector if manufactured under regulated conditions after recognizing the interaction taking place between the silicon dioxide in pozzolans with free Portlandite in cement. Shen *et al*., (2011) looked into how calcination affected the silica content, specific gravity, and setting times of fresh mortar in 2016. Results showed that as temperature rises, SiO_2 content gradually rises. On the other hand, specific gravity drops as temperature rises. Results generally showed that there was room for energy savings as well as reduction in carbon dioxide emission by optimising the burning temperature in the manufacture of rice husk ash (Shen *et al*., 2011). In lieu of early strength (14 – 28 days), Kumar *et al*., (2016) supports the provisions of earlier studies by recommending maximum RHA content in concrete to fall below 20%. Table 2.2 provides an overview of the key discoveries found in the studied literatures.

Table 2.2: Summarised literature on rice husk ash as a pozzolanic material

S/N	Source	Dehydroxyl.		Pas.	Oxides (%)					RLR
		Calc. (^oC)	Dur. (min)	(μm)	SiO_2	FAS	CaO	MgO	SO_3	(%)
1	Cook et al., (1977)	450– 500	-	-	93.0	93.7	0.43	0.42	-	10 – 20
2	Zhang and Malhotra (1996)	800	-	45	87.2	87.5	0.5	0.35	0.24	15
3	Zaid *et al*., (2021)	700	-	-	62.3	78.9	12.6	3.5	0.6	5
4	Abalaka A.E (2012)	758	240		95.4	96.2	-	1.24	0.07	25
5	Ettu *et al*. (2013)	650	-	600	-	-	-	-	-	15
6	Kumar *et al*. (2016)	400 – 600[x]	4320	75	-	-	-	-	-	20

FAS = $SiO2 + Al_2O_3 + Fe_2O_3$

x = Open air burning

2.2.2. Maize Husk/Corn Cob Ash

The most significant grain crop in sub-Saharan Africa is maize or corn and more than a billion tons of corn is produced worldwide (Olafusi and Olutoge, 2013). According to Mr. Phillip Ojo, Nigeria's National Seed Council's Director General (NSCN), Nigeria is the region's top seed provider, providing 70% of the seeds for maize used in West Africa, (Beef2Live, 2017). Nigeria, which produces 6.9 million tons of corn annually, is the 15th-largest producer of the grain in the world, (Beef2Live, 2017).

According to Sokhansanj *et al*., (2002), 15%, 22% and 50% by mass constitutes the cobs, leaves and stalks respectively, for every kilogram of dry corn grains grown. Inferring that the husk makes up at least 20% of the maize produced, Nigeria generates no fewer than 1.38 million metric tons of husk and a million tons or more of cob each year.

Studies on RHA as a pozzolanic material and alternative or partial cement replacement material greatly exceeds that of maize husk and corn cobs as potential binder additives in the co nstruction sector. However, Murthi *et al*., (2020) conducted an extensive review on maize husk and how it might be effectively incorporated into concrete. They covered different calcination methods and ultimately observed that heating the husk to between 500 and 600 °C in an open reactor was a more feasible approach, transferring it into a furnace, maintaining the temperature for 12 hours, and then cooling it for 24 hours. Before being ground, the specimen goes through two cycles of calcination at 600°C. At this mode of production, when compared to control, 28 day compressive strength lost roughly 24.5% of its strength at 10% replacement level. Thus, the recommendations provided restricted the usage of MHA to less than 10% in concrete (Murthi *et al*., 2020). Regardless of the outcomes, using so much energy during the production phase to only replace around 10% of the cement is not a sustainable strategy.

Suwanmaneechot *et al*. (2015) studied the chemical composition, physical characteristics, and engineering properties of maize cob ash. According to the findings, corn cob ash that had a 4-hour heat treatment at 600 °C, was composed of FAS of 72% (SiO_2 + Al_2O_3 + Fe_2O_3) and hence can be categorised as Class N calcined natural pozzolan in accordance with ASTM C618.

When compared to reference samples, the motar cubes, which replaced cement with 20% treated corn cob ash, had a 28-day compressive strength of 103%. Olafusi and Olutoge (2013) conducted more research on the usage of CCA in concrete and suggested that if early strength is a requirement, cement replacement levels should not exceed 10%.

The effects of CCA in concrete as a partial replacement of concrete was studied (Isado *et al*., 2014). In each of the three cases, the corn cobs were burned with oxygen present in the open, creating the ash. All three publications recommended a maximum CCA of 10% when initial strength and durability characteristics have to be retained. In agreement, 10% MHA was recommended as the appropriate replacement amount when used as a cement replacement by Ndububa and Nurudeen (2015). Comparatively, Kamau *et al*. (2016) generated CCA in the presence of oxygen for more than 8 hours at temperatures between 650°C and 800°C. Results for compressive strength indicate that 7.5%, which was slightly less than the control, was the ideal replacement level. The mechanism of combustion of the CCA was cited by the authors as the cause of the results being unfeasible (Kamau *et al*., 2016). Table 2.3 is a summary of the key discoveries found in the reviewed literatures;

Table 2.3: Summarised literature on maize husk ash as a pozzolanic material

S/N	Source	Dehydroxyl.		Pas.	Oxides (%)					RLR
		Calc. (^oC)	Dur. (min)	(µm)	SiO_2	FAS	CaO	MgO	SO_3	(%)
1	Kevein and Wang, (2010)	500–600	2160	-	38.3	39.0	7.83	5.0	1.7	10
2	Ndububa and Nurudeen, (2015)	600	-	75	78.2	80.3	3.3	3.8	0.5	10
3	Kamau *et al*., (2016)	650 – 800[x]	-	-	38.8	54.1	1.8	2.1	0.6	7.5

FAS = $SiO2 + Al_2O_3 + Fe_2O_3$

2.2.3. Palm Bunch Ash (PBA)

Global oil Production (2017) asserted that the production of palm oil reached 58.8 million tons globally in 2016, but it was anticipated to rise to 62.88 million tons by 2017-2018, an increase of 6.94%. At a yearly production rate of 970,000 tons, Nigeria was positioned as the 5th largest oil producers globally (World Oil Production, 2017), with Indonesia and Malaysia occupying the top two spots. However, Otunye and Azuma (2016) stated the significance of Nigeria in oil production, been the first producers of the palm seedlings for Indonesia and Malaysia (2016).

As a result of the fueling of the palm oil production system with palm bunches (Fronde) and palm kernels, palm oil production facilities naturally produce palm oil fuel ash. However, this research chose to concentrate only on palm bunches and palm kernels in order to facilitate control as well as management of the majority of palm bunches and kernels that are now available as waste.

Amaziah and Zumah (2016) looked into the impact of PBA on concrete when it was used in place of some of the cement. Palm bunch was created by open burning the palm to ashes and sieving through a 600 µm sieve. For regular concrete and light weight concrete, the ideal replacement level was proposed at 5% and 20%, respectively.

2.2.4. Palm Kernel Ash (PKA)

Both the husk and the shells of the palm fruit are used as fuel in the boiler of palm oil mills after the palm oil has been recovered from the fruits (Olowe and Adebayo, 2015). According to the United States Environmental Protection Agency (EPA, 2023), 5-25% PKA by weight of solid waste is created following burning.

One of the many researchers that have studied the impact of palm kernel ash in concrete when used as a partial substitute for cement in concrete is Olowe and Adebayo, (2015). The ash prior to integration in a cement mix, was sieved to pass a 45 µm sieve, albeit their report did not specify how it was prepared. The findings of the compression test showed that strength decreased with higher percentage replacement levels and increased with age, which is consistent with the majority of earlier papers on pozzolans that are particularly rich in silicon oxide and poor in calcium oxide. 10% PKA was the ideal and suggested replacement level (Olowe and Adebayo, 2015).

Oti *et al*., (2015) suggested replacing up to 50% of the cement in concrete. The mode or temperature at which the ash was formed is unknown, but it was sieved to pass a 36 micron meter sieve. A super-plasticiser was also used in the research to regulate workability and compaction factor. The 25% PKA content replacement level was ideal, but using the strength activity index as a guide, a 50% replacement level produced outcomes in terms of strength that could be used.

Oti *et al*., (2015) adjusted the rate of burning at which PKA was to be manufactured between 350 ^{o}C and 750 ^{o}C in order to conserve energy and safeguard the environment. They claim that 750 ^{o}C increases PKA's potentials for cement replacement in concrete.

Recent studies on PKA's effects on concrete's compressive strength were reported by Fadele and Ata, (2016). A 212 mm BS sieve was used to filter the ash after it was produced by open burning for an unknown period of time or at an unknown temperature. They recommended replacing cement up to 30% by weight at 5% intervals, with 5% levels of replacement for grade M25 concrete and 15% levels of replacement for grade M20 concrete. An overview of the major discoveries made in the research reviewed may be found in Table 2.4;

Table 2.4: Summarised literature on palm kernel ash as a pozzolanic material

S/N	Source	Dehydroxyl.		Pas.	Oxides (%)					RLR
		Calc. (^oC)	Dur. (min)	(µm)	SiO_2	FAS	CaO	MgO	SO_3	(%)
1	Olowe and Adebayo (2015)	-	-	45	-	-	-	-	-	10
2	Oti *et al.*, (2015)	350-750	-	45	-	-	-	-	-	25-50
3	Fadele and Ata (2016)	-	-	71	-	-	-	-	-	5-15

FAS = $SiO2 + Al_2O_3 + Fe_2O_3$

2.2.5. Coconut Husk Ash (CHA)

The outer layer of the coconut fruit before the shells is known as the husk. Nigeria is listed as the 18 th country with the biggest capacity for coconut production by World. Nigeria's annual manufacturing capacity was estimated to be 265,000 tons. The coconut's flesh makes up between 40 and 70 percent of the entire fruit. This indicates that the husk and shell make up more than 30% of the 265,000 tons of coconuts produced in Nigeria. Around 61 million tons of coconuts were produced worldwide in 2014 (Atlas, 2017).

Arum *et al*. (2013), produced the samples by allowing the husk to air dry for three (3) months before calcining it for six (6) hours at 700 ^{o}C and allowing it to cool for 72 hours before filtering through a 45 µm sieve, provided more exact results. Their specimens had longer setting periods than the control, like with all pozzolanic effects. It's interesting to note that the compressive strength increased with increasing CHA content up to 15%, before declining as the CHA content exceeds 15%. Thus, a partial cement substitution level of 15% using CHA was advised (Arum *et al*., 2013). Kurniawan *et al*. (2016) also looked into the results gotten by combining fly ash and CHA in concrete. At 650 ^{o}C, the synergised sample was calcinated in an oven to create the ash specimen. Strength effects were seen at ages 3 days and 7 days, and replacement levels up to 30% were made. At a synergistic combination of 5% fly-ash: 25% CHA, the best compressive strength result was attained. Early observations on strength (7 days curing) showed a strength increment of 8.4% larger than the control specimen, and seen to be likely influenced by the fly-ash, which was found to contain roughly 7.31% CaO. Nevertheless, 10% replacement level provided the best and most acceptable outcomes for cement replacement utilizing solely CHA.

Anifowoshe and Nwaiwu (2016), thoroughly dried coconut fiber, calcined for 1 hour and 40 minutes at a burning rate of 600 - 700 °C, and then allowed to cool before filtering through a 150 micron screen. Replacement levels ranged from 0 - 100%, and 40% replacement level was recommended for light concrete structures. However, for all curing ages reported as well as levels of substitution, it was observed that the control retained superior compressive strength indices. Table 2.5 is a summary of the key discoveries found in the reviewed literatures;

Table 2.5: Summarised literature on coconut husk ash as a pozzolanic material

S/N	Source	Dehydroxyl.		Pas.	Oxides (%)					RLR (%)
		Calc. (^oC)	Dur. (min)	(µm)	SiO_2	FAS	CaO	MgO	SO_3	
1	Arum *et al*. (2013)	700	360	45	48.0	74.5	6.6	-	-	15
2	Kurniawan *et al*. (2016)	600	360	-	63.3	64.0	0.77	0.29	0.53	10

FAS = $SiO2 + Al_2O_3 + Fe_2O_3$

2.2.6. Coconut Shell Ash (COSA)

Bheel *et al*. (2021), examined multiple papers on the impact of COSA, which serves as a partial substitute for cement, on the compressive strength, density, and setting times of concrete. The shells were dried in the air for 48 hours and then allowed to burn wildly in oxygen-rich environment before being sieved to pass a 75 µm sieve. Based on the findings of the 28-day compressive strength test, a replacement percentage range of 10–15 percent was recommended as ideal. With rising COSA content, density was seen to decline. Setting times and compressive strength findings followed the trend of earlier pozzolan studies in that an increase in COSA content decreases both strength characteristics and setting times.

In order to study the impact of COSA's partial cement replacement on concrete, Oyedepo *et al*., (2015) restricted their replacement amount to no more than 5% COSA. Ash production was place throughout the course of two phases. Calcination of the charred ashes to a temperature of 800 ^{o}C for 8 hours was required in phase two before sifting to pass through a 75 micron screen. Phase one entailed uncontrolled burning of the air dried shells for 3 hours. It is surprising that the oxide composition results matched perfectly those of Bheel *et al*., (2021), which is unlikely given the different fabrication methods for the specimens. The technique and objective sections of the article are in conflict with the published compressive strength results, which were for levels of 30% replacement. The paper did not include the results for the 5% replacement level.

Findings on the impact of COSA on several concrete properties were also published by Kumar and Kumar, (2014). The ash was created by uncontrolled burning for three hours when there was oxygen present. The ashes were employed in startling amounts to replace up to 30% of cement; the sieve size was not stated. Based on results for compressive strength, the ideal and suggested replacement level was set at 10% COSA content. Similarly, Olusunle *et al*., (2015) published findings on the effect of COSA in cement structures and recommended 10% COSA as ideal level of cement substitution relative to optimum strength and durability indices.

Between ages 3 -7 days, Ahmed *et al*. (2016) observed the pace at which cement concrete gained strength in comparison to 10%COSA-cement blended concrete. It was

found that the compressive strength of the control specimen increased by 59% between ages 3 and 7 days, whereas the specimen made up of 10% COSA-cement increased by 67%. When compared to the 10% COSA-cement blended specimen, the control specimen had 4% more compressive strength at age 3 (3 days), but by age 7, this difference had decreased to 2.5%. (7 days). The authors came to the conclusion that there would be no negative impact on the compressive strength of the final concrete specimen at 10% replacement levels based on the results of the compressive strength tests after 7 days.

The impact of COSA on the engineering characteristics of COSA-cement blended concrete was the subject of research results published by Bheel *et al*., (2021). The shells were calcined at 700 °C for 5 hours, and cooled at room temperature for an additional hour prior to filtering through a 90 µm sieve. According to results on compressive and tensile strength of the COSA-cement blended concrete at ages 28 days, as measured between 0 – 20% COSA content, a recommendation of 10% COSA cement substitution level was made. Table 2.6 provides a summary of the key discoveries in the literatures analysed;

Table 2.6: Summarised literature on coconut shell ash as a pozzolanic material

S/N	Source	Dehydroxyl.		Pas.	Oxides (%)					RLR
		Calc. (^{O}C)	Dur. (min)	(µm)	SiO_2	FAS	CaO	MgO	SO_3	(%)
1	Utsev and Taku (2012)	X	-	75	37.9	77.6	4.98	1.89	0.71	10-15
2	Kumar and Kumar (2014)	X	180	-	-	-	-	-	-	10
3	Bheel *et al*., (2021)	700	300	90	-	-	-	-	-	10

FAS = $SiO_2 + Al_2O_3 + Fe_2O_3$

x = Open air burning

2.2.7. Cassava Peel Ash (CPA)

Food and Agricultural Organization of the United Nations published that Nigeria was the lead cassava producer as at 2017 (Ikuemonisan et al., 2020), which accounted for 20% of the cassava produced globally with a production capacity of 54.8 million tons, or around 20.4% of the total capacity for the production of cassava in the globe.

In concrete, cassava peel ash was also used to substitute cement to amounts as high as 25% at intervals of 5% (Salau *et al*., 2012). A 150 µm sieve was used to further separate the ash after it had been produced at 700^{o}C for 90 minutes. When the percentage of CPA grew, it was noticed that the workability and compacting factor decreased. According to suggestions provided in light of 28-day compressive strength data, replacement levels shouldn't exceed 15% of CPA content. Raheem *et al*. (2020), on the other hand, denied the viability of CPA use in concrete based on the unfeasible 28-day compressive strength result. The ash was produced by controlled burning at 500 degrees Celsius with an unidentified filter size for an unknown period of time or rate. Using the peels from processed cassava as a partial substitute for cement in concrete, they however observed that at ages 28 day, the compressive strength values at 5% CPA content had a strength activity index (SAI) of 55% which is below the 75% SAI requirement and hence recommended CPA levels to be below 5% if compressive strength is of priority (Raheem *et al*., 2020).

Additional research on the impacts of CPA in cement structures when used as a partial cement substitution utilizing various manufacturing techniques was reported by Ogbonna *et al*. (2020) and Ofuyatan *et al*. (2018). According to Ogbonna *et al*. (2020), 5-10% is the maximum and appropriate level of replacement for cement based on 28-day compressive strength using CPA. Strength activity index at this level was above 75%, and hence satisfies the mechanical criteria for pozzolanicity.

Table 2.7 is a summary of some literatures on cassava peel ash as a supplementary cementitious material.

Table 2.7: Summarised literature on cassava peel ash as a pozzolanic material

S/N	Source	Dehydroxyl.		Pas.	Oxides (%)					RLR (%)
		Calc. (^{O}C)	Dur. (min)	(µm)	SiO_2	FAS	CaO	MgO	SO_3	
1	Salau *et al*. (2012)	700	90	150	58.0	72.2	8.53	5.02	2.18	15
2	Ogbonna *et al*. (2020)	-	-	75	-	-	-	-	-	5-10
3	Ofuyatan *et al*. 2018	700	70	600	59.7	72.3	8.4	5.2	2.1	10

FAS = $SiO_2 + Al_2O_3 + Fe_2O_3$

x = Open air burning

2.2.8. Periwinkle Shell Ash (PSA)

The Littorinidae family of sea snails includes the periwinkle kind of sea snail which is widely distributed throughout Nigeria's coastal regions and the rest of the world. The shell is an unneeded by-product that is generally haphazardly disposed of or used in unconventional ways as a substitute for coarse aggregate in the building sector after the edible section has been removed. These snails are found in the Niger Delta lagoons between the Nigerian cities of Calabar in the east and Badagry in the west. (Antia *et al*., 2020). One of the seashells with a high CaO content that can improve the pozzolanicity of waste materials with a high SiO_2 content for use in the engineering and building industries is the periwinkle shell.

The results of using PSA in place of up to 40% of the cement in concrete were published by Eziefula *et al*. (2020). A furnace was calcined at a temperature of 800^{o}C to make PSA. To allow it to pass through a 45 µm sieve, the ash was ground up. Strength and workability/slump were shown to decrease with increasing PSA content. Nonetheless, as stated by earlier studies, compressive strength was shown to increase with age. According to results from 28 days of compressive strength tests, a replacement level of 10% PSA was advised; however, results from replacement levels of 10% to 30% were seen to exceed 80% of the mean compressive strength, and as such, 30% of the cement could be substituted with PSA without negatively impacting on the compressive strength of the cement structure.

Antia *et al*. (2020) produced PSA to blend with cement in the production of laterite blocks. Cement was replaced up to 30% and results obtained on water absorption as well as shrinkage observed to be feasible even at 30% cement replacement level. Eziefula *et al*. (2020), produced PSA at 800 ^{o}C calcination temperature and Passinga 45 µm sieve. According to the results of the compressive strength tests, the ideal replacement level should be between 10% and 20% of the cement content. By adding sodium nitrate ($NaNO_3$) as an admixture, the replacement level could be increased to 30% without adversely affecting strength and durability (Eziefula *et al*., 2020).

Umoh and Ujene (2015) employed a distinctive manufacturing technique that involved calcining the shells at 600 ^{o}C for 20 to 30 minutes, allowed to cool for 24 hours, and then crushed to pass through a 75 µm sieve. It was demonstrated that the 28-day compressive strength was 0.96% greater at 30% PSA + 2% $NaNO_3$ than the

control specimen when its level of substitution was set at 30% while the $NaNO_3$ proportions were altered. Therefore, if larger PSA concentrations were to be used, the scientists suggested adding 2% $NaNO_3$ to the cement mixture. (Umoh and Ujene, 2015).

According to Amarachi *et al*. (2021), PSA manufactured at 1000^{o}C and sieved to pass a 75 micron meter BS sieve possess potentials to substitute no less than 10% of PLC in cement structures without degrading the compressive strength of the material by more than 0.4% at age 28 compared to the control specimen. He went on to assert that durability is enhanced at such high PSA concentrations due to increased resistance to acid and sulphate attacks.

Table 2.8 presents an overview of the key discoveries found in the studied literatures.

Table 2.8: Summarised literature on periwinkle shell ash as a pozzolanic material

S/N	Source	Dehydroxyl.		Pas.	Oxides (%)					RLR (%)
		Calc. (^oC)	Time (min)	(µm)	SiO_2	FAS	CaO	MgO	SO_3	
1	Eziefula *et al*. (2020)	800	-	45	33.8	50.0	40.8	0.48	0.26	10-30
2	Antia *et al*., (2020)		-	75	3.56	7.6	44.3	9.0	-	5-30
4	Umoh and Ujene (2015)	600	20-30	75	27.2	38.3	52.1	0.82	0.26	30

FAS = $SiO2 + Al_2O_3 + Fe_2O_3$

x = Open air burning

2.2.9 Snail Shell Ash (SSA)

In the Eastern and Western areas of Nigeria, snails are extensively gathered, with the edible half being eaten while the shell is dumped in landfills. It has enormous promise in the building business, particularly as a cementitious alternative, just like most if not all molluscs because it possesses a high concentration of calcium oxides (Tayeh *et al*., 2019).

In order to use the ash as a partial substitute for cement in concrete, Etuk *et al*. (2012) sun-dried the shells for three days prior to calcination for a period of four hours at 800 ^{o}C and grinding them till they passed through a 63 µm screen. He found that raising the SSA percentage always lengthens setting periods and decreases strength. A 15% replacement level was suggested as the ideal threshold. In addition, Zaid and Ghorpade (2014) noted that snail shell ash when sieved using a 90micron meter BS sieve can efficiently substitute 15–20% of cement in concrete and cement structures, without significantly reducing strength.

Inyang and Etuk (2016) changed the SSA calcination range to 900 -1600 ^{o}C to observe how temperature affected the chemical characteristics of the ash. The chemical oxides in the ash were not significantly affected by temperatures above 900 ^{o}C, according to the results. It follows logically that calcining shouldn't be done over 1000 ^{o}C to conserve energy.

Regarding the impact of using SSA as a partial replacement for cement in concrete, Syed and Vaishali (2014) discovered some quite unique and intriguing results. The ash was made by first washing to remove organic waste, calcining at a temperature between 600 °C and 800 °C, and then further grinding into fine powder. Compressive strength for the 7 and 28 day tests was best at 20% SSA content, which was 5% and 8% more than control, respectively. 40% replacement level, however, was also higher than the control at ages 7 and 28 days. About 50% SSA was recommended to replace cement in an effective manner without sacrificing strength (Syed and Vaishali, 2014).

Raheem *et al*. (2016) observed the impact of dehydroxylation on the pozzolanic indices of SSA, just like Inyang and Etuk (2016) did. They experimented with temperatures between 650 and 1000 °C at various time intervals and found that

calcining at 650 °C for 90 minutes is the best method, which they utilized to produce the ash. The authors suggested a 20% optimal replacement amount based on the Strength Activity Index (SAI). Table 2.9 is a summary of the key discoveries found in the reviewed literatures.

2.2.10. Clam/Oyster Shell Ash (CSA)

Clams and oysters are both aquatic organisms that are abundant in Nigeria's coastal regions and are known to be calcium-rich. Oyster shell, Short-necked clam shell, cockle shell, and green mussel shell, were the four marine shells that Lertwattanaruk *et al*. (2012) studied (OS). They were cleaned, ground to pass sieve No. 4, wet milled to pass sieve No. 200, and then dried in an oven at 110 + 5 °C for 24 hours to turn them into ashes. The resultant ashes were added to mortar at amounts up to 20% by mass of the total cement as a partial cement substitute. Although the water required demand of the fresh mixes did not quite follow literature, which claimed that water demand decreased as the replacement level increased, setting times were shown to increase with increasing percentages of the ashes. Also, it was found that as the percentage of ashes utilized increased, thermal conductivity decreased.

Although researchers did not specify the particular method for preparation of the ash, Ephraim *et al*. (2019), found that between 5 and 20% the ashes from the shells could be utilized to substitute PL in cement structures successfully. Olutoge *et al*. (2016) also cleaned and sun-dried clam shells for five days before they spontaneously caught fire and sieved through a 4.75 µm sieve. The resultant ash was utilized in concrete to partially replace cement. Maximum cement replacement amount was determined to be 5%, which had a SAI of 82.23% and was 17.8% lower than the control specimen. Table 2.10 is a summary of the key discoveries found in the reviewed literatures;

Table 2.9: Summarised literature on snail shell ash as a pozzolanic material replacement

S/N	Source	Dehydroxyl.		Pas.	Oxides (%)					RLR
		Calc. (^oC)	Time (min)	(µm)	SiO_2	FAS	CaO	MgO	SO_3	(%)
1	Etuk *et al*. (2012)	800	240	63	26.3	40.2	55.5	0.4	0.18	15
2	Syed and Vaishali (2014)	600-800	-	75	0.6	1.7	56.1	0.69	0.19	10-40
3	Raheem *et al*.(2016)	650	90	-	0.78	2.23	50.1	0.59	0.24	20

FAS = $SiO_2 + Al_2O_3 + Fe_2O_3$

x = Open air burning

Table 2.10: Summarised literature on clam shell ash as a pozzolanic material

S/N	Source	Dehydroxyl.		Pas.	Oxides (%)					RLR
		Calc. (^oC)	Time (min)	(μm)	SiO_2	FAS	CaO	MgO	SO_3	(%)
1	Lertwattanaruk *et al*. (2012)	110	1440	75	0.84	1.04	54.0	0.08	0.16	20
2	Ephraim *et al*., (2019)	-	-	-	4.04	4.46	90.0	0.65	0.72	5-20
3	Olutoge *et al*. (2016)	X	-	4.75	40.7	47.0	51.1	0.18	-	5-10

FAS = $SiO2 + Al_2O_3 + Fe_2O_3$

x = Open air burning

2.2.11. Hybrid Agricultural Pozzolans (HAP)

The term "hybrid agricultural pozzolans" (HAP) refers to pozzolans that have been created by combining two or more pozzolans, either during production or during usage. The majority of the publications listed examined how these pozzolans worked together while being combined at the point of application, in essence, the individual pozzolans were made independently. Wheat straw ash (WSA) and RHA have a synergistic impact, according to studies by Ajay *et al* (2007). The ashes were first calcined at a regulated rate of 2 °C per minute up to 600 °C, followed by 2 hours of grinding. In concrete manufacturing, 15% of cement was replaced with ashes, which ranged between 10% RHA:5% WSA, 5% RHA:10% WSA, and 7.5% RHA:7.5% WHA. In terms of strength and durability, it was claimed that equal amounts of WSA and RHA (7.5% RHA + 7.5% WHA) produced outcomes that were better than control at all ages (Ajay *et al*., 2007). When RHA and Metakaolin are produced at temperatures between 650 and 800 degrees Celsius and 700 and 850 degrees Celsius, respectively.

Kannan and Ganesan (2012) found that an optimal level of cement replacement at 30 percent is feasible with no noticeable drop in neither compressive strength nor durability of the cement concrete. It is seen from the above illustrations that the oxides of Metakaolin, RHA, and WSA, are all poor in CaO and very rich in SiO_2, with little variance. Hence, utilizing only one pozzolan in higher proportions would have the same effect as using the synergy of these pozzolans.

Many studies detailing the synergistic impact of different pozzolans on cement constructions were published by Ettu *et al*. (2013). The individual effects of the pozzolans were found to be either somewhat greater or roughly equivalent to the combined effects in all of these. So, unless it becomes necessary to manage the available resources fairly, there is no longer a necessity to combine pozzolans with similar chemical properties. In general, the synergy of these pozzolans did not produce any additional strength or durability effects.

Umoh *et al*. (2013) blended periwinkle shell ash (PSA), which is high in calcium oxide (CaO), with bamboo leaf ash after taking into account the positive benefits of both silicon oxide (SiO2) and calcium oxide (CaO) (BLA – rich in SiO2). The BLA

proportion was fixed at 10%, and the PSA proportions were adjusted at 5% intervals between 10% and 30%. As such, the 28-day compressive strength results, showed the best mix was a synergy of 15% PSA:10%BLA.

The synergistic effects of RHA and GGBS used in partial cement substituting in geo-polymer concrete were published by Inti *et al*. (2016). With RHA fixed to GGBS at a 30:70% ratio, up to 30% of the cement was changed. Although 30% replacement was only one unit worse than the control level, the optimal replacement level was 20%. Therefore, it's likely that changing the synergistic ratio of the pozzolans could lead to more interesting results. Ban and Nobert (2016) researched on the indices obtainable when synergising RHA and slag in sandcrete, which was similar to Inti *et al*. (2016). Replacement levels were raised to 100% and effects were observed after fixing RHA to GGBS at a ratio of 15:85%. Intriguingly, 70% replacement level was at its highest at age 7, with 16% of the control's compressive strength overtaking it at age 16days and 8.2% at age 28days. These are the first workable results at such young ages as 7 days and 28 days with as high as 70% cement replacement levels in concrete. This is explained by the fact that GGBS has high CaO levels for early strength development and high SiO_2 levels for late strength growth.

RHA and cement kiln dust have a synergistic impact, according to Sulaiman and Aliyu (2020). While it was noted that the RHA was rich in SiO_2, a oxide composition of cement kiln dust (CKD) revealed that it has excess 40% calcium oxides (CaO), making the combination logical. In concrete, the pozzolans were utilized to replace up to 50% of the cement in an equal ratio. The best mix design for this synergy was suggested based on compression strength data between ages 14 and 28 days, which revealed that 15%RHA + 15% CKD demonstrated the greatest strength gain rate. However, the authors also suggested that, should the necessity to raise the replacement level above 30% arise, the pozzolans' proportioning be changed so as to investigate the potentials for more applicable results. The synergy RHA and SSA in masonry manufacturing, as partial substitutes for cement in sandcrete at levels up to 50% was published by Dankwah and Nkrumah (2016). The pozzolans were set at a 20% RHA: 80% SSA ratio.

Without sacrificing the blocks' strength and longevity, a replacement level of 30% was found to be ideal. However, a combination of both has increased replacement levels by

up to 30%, and maybe even more if the proportioning ratio is altered. The majority of RHA and SSA publications were unable to support replacement amounts of more than 20% in the cement mix.

2.3 Measuring Pozzolanic Properties

As previously highlighted, the pozzolanic effect or reactivity of SCM's/Pozzolans is dependent on some characteristics which can be physically, chemically and or mechanically based. Physical characteristics such as fineness, amorphousness, specific surface area have been shown to directly influence the reactivity of pozzolans in concrete and mortar (Walker and Pavia, 2011). The chemical property which is primarily the oxide compositions of the pozzolanic compound, is also a major factor influencing pozzolanic activity as could be seen in the definition of pozzolans (compounds with little or no binding property but develops such when in finely divided form reacts with CaO or CaOH in the presence of water at room temperature). Pozzolans are expected to have sufficient amount of silicon oxide as this is needed to form the silicic acid ($Si(OH)_4$) needed in the acid based reaction with Portlandite ($Ca(OH)_2$), (hydration product of cement or lime) to form secondary Calcium Silicate Hydrate (CSH) gel. This reaction is as shown below;

$Ca(OH)_2 + (Si(OH)_4) = Ca_2 + H_2SiO2^{-}_4 + 2H_2O = CaH_2SiO_4.2H_2O$

Mechanical characteristics of SCM/Pozzolans are detected after they have been integrated in cement or mortar specimens and cured under specific ages ranging from 3 to 90 days. However, 28 day compressive strength of the concrete or mortar specimens are usually used to determine strength activity of the SCM/Pozzolans.

2.3.1 Physical Properties

The basic physical properties guiding the reactivity of SCMs/Pozzolans are Fineness and Shape (Amorphousness) of the materials.

2.3.1.1 Fineness/Surface Area

Fineness is a measure of the quantity of material passing through a specific sieve number/size, in this context, fineness of the material is a relative measure of the area of the material available for hydration also known as Surface Area. In order words, the greater the fineness, the greater the area available for hydration and according to

literature; increases in fineness increases strength (particularly at ages below 28 days), reduces setting times and water absorption rate but increases slump and workability, (Ahmad, 2002; Walker and Pavia, 2011; Sajedi and Razak, 2011; Huajian *et al*., 2015; and Yu *et al*., 2021).

Figures 2.3 and 2.4, represents the effect of pozzolan fineness on compressive strength of concrete. Yu et al., (2021), further added that in regards to the fineness of a SCM/Pozzolan, the uniformity factor (n) which is a measure of the material's homogeneity is a strong variable greatly impacting on the pozzolanicity of the material. It is mathematically expressed as the ratio of the diameter allowing the passage of 60% of the material (D60) to the diameter allowing the passage of 10% of the material (D10)

Whereas fineness is usually detected using either 45 or 90 µm sieve, surface area requires the air permeability apparatus while uniformity factor requires BS sieve set in accordance to BS 410 – part 1 (2000) and standard conforming to BS EN: 933-1 (1997). Standard fineness determination for cement and pozzolans conforms to IS 4031 part 1 (1996), IS 4031 part 15 (1991), BS EN 196-5 (1996), and BS 3892 – 1 (1997).

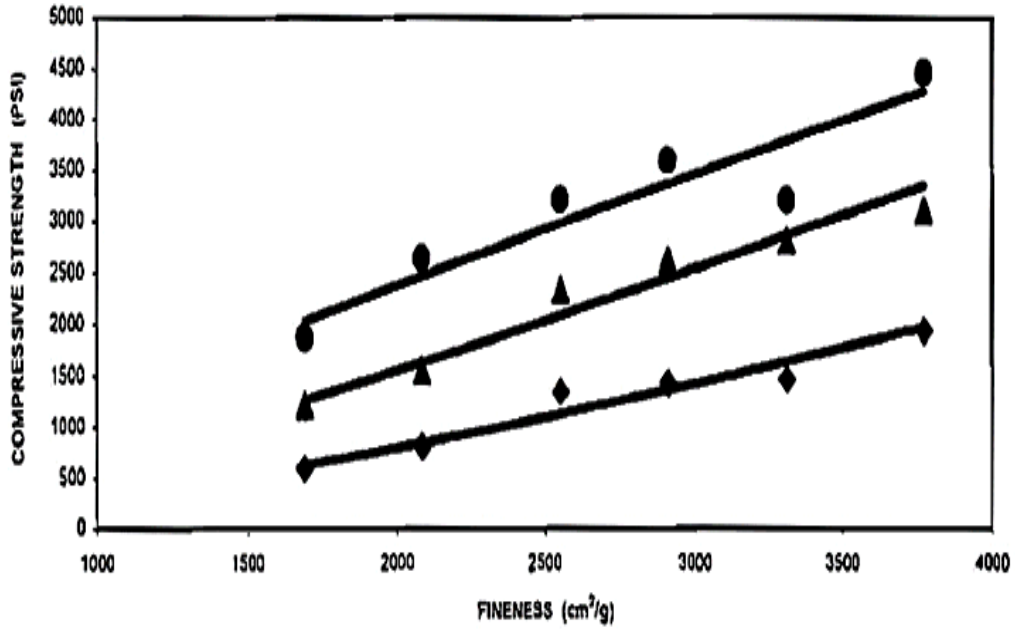

Figure 2.3: Relationship between SCM/pozzolan fineness and concrete compressive strength

Source: Ahmad (2002)

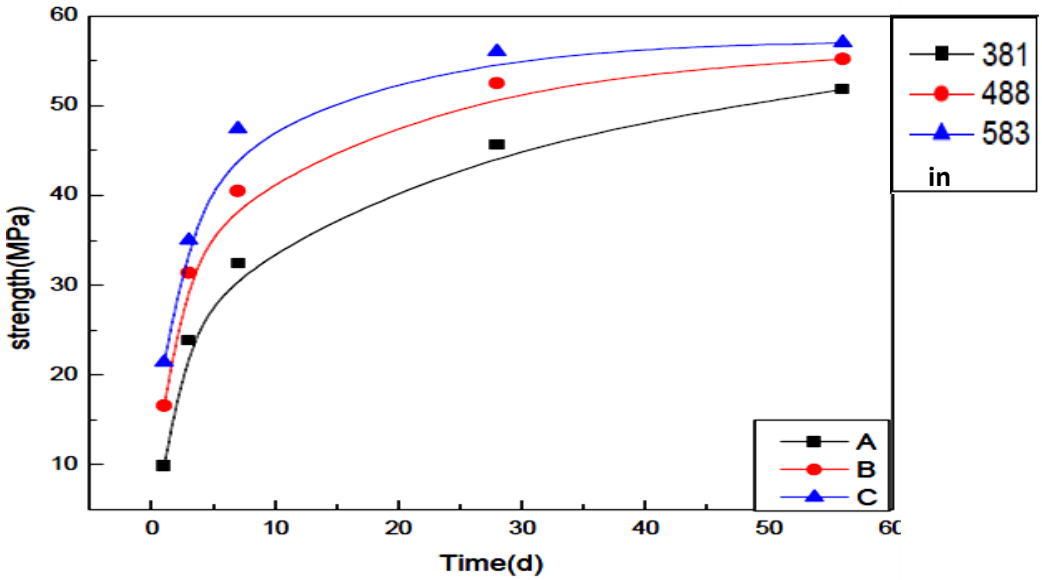

Figure 2.4: Relationship between SCM/pozzolan surface area and compressive strength

Source: Huajian *et al*. (2015)

These international methods generally adopt either wet sieving approach requiring the use of a 45 µm sieve or a dry sieving approach requiring the use of 90 µm sieve. In either case, the percentage of material retained on the specific sieve after sieving is read as the fineness of the material as shown in the equation 2.1 below;

$$F = \frac{WR}{WT} \qquad \text{.....} \quad (2.1)$$

Where;

F = percentage fineness of the material

W_R = Weight retained on the specific sieve in grams (g)

W_T = Total weight of sample before sieving in grams (g)

Figure 2.5 represents a directly relationship between SCM/pozzolan uniformity coefficient and the compressive strength concrete.

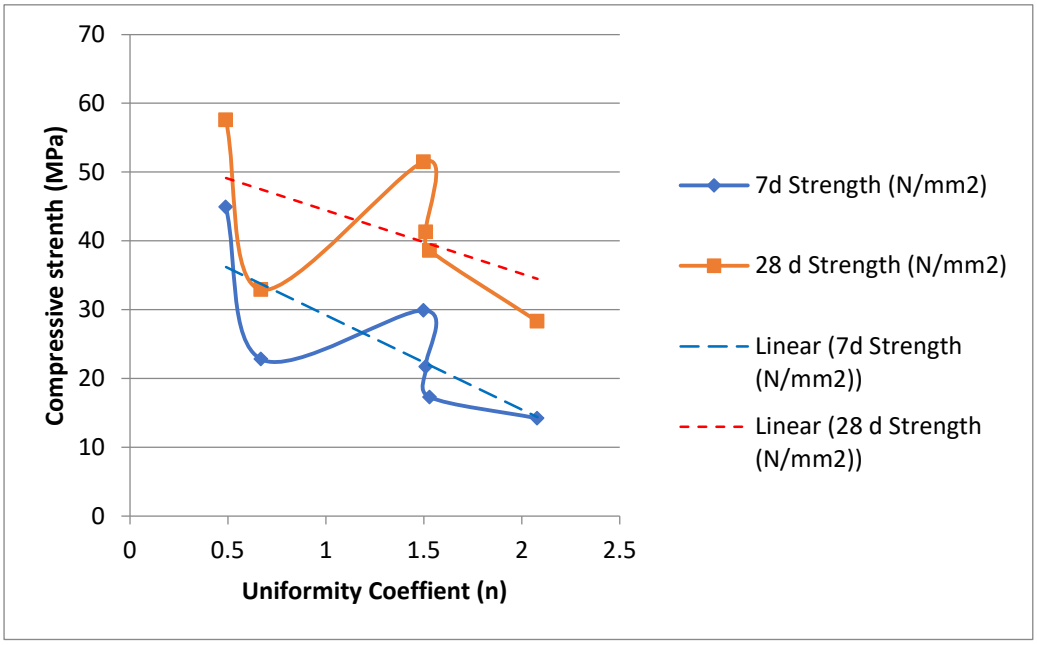

Figure 2.5: Relationship between SCM/Pozzolan uniformity factor and concrete compressive strength

Source: Yu et al. (2021)

2.3.1.2 Amorphousness

Amorphousness is a shape factor. It tends to illustrate how far cementitious or supplementary cementitious particles are from crystalline. Walker and Pavia (2011) illustrated that amorphousness is the major factor determining the reactivity of pozzolans. This is however a rather early conclusion as fineness as well as oxide compositions plays an equally great role.

Table 2.11 Illustrates that Microsilica (MS) has the highest finest, Table 2.12 shows that GGBS is highest in amorphous content, but Figure 2.2 illustrates that Metastar has the highest mechanical reactivity before GGBS and Microsilica. Although, Metastar is shown to be mostly amorphous, with the second best in fineness after GGBS, theory of Walker and Pavia (2011) on amorphousness being the greatest factor determining pozzolanic reactivity did not follow absolutely.

Table 2.11: Rating of pozzolans as a function of fineness (Source: Walker and Pavia 2011)

Pozzolan	Surface area (m2/g)	Fineness rating
MS	23.09	MS
Metastar	18.33	Metastar
RHA	13.70	RHA
RBD	4.29	GGBS
Tile	4.16	PFA
PFA	4.09	Leca
GGBS	2.65	Tile
Leca	1.28	RBD
YBD	0.31	YBD

Table 2.12: Mineralogical Compositions and rate of amorphousness of pozzolans

(Source: Walker and Pavia, 2011)

Pozzolan	Rate of amorphousness	Mineralogical composition
GGBS	(5) Totally amorphous	No crystalline fraction
Leca	(3) Intermediate	Quartz, wadsleyite, mullite and illite
Metastar	(4) Mostly amorphous	Quartz, tohdite, aluminium oxide, wollastonite and paragonite
MS	(4) Mostly amorphous	Quartz and cristobalite
PFA	(3-2) Intermediate to slightly	Quartz and mullite peaks
RBD	(2) Slightly amorphous	Quartz, hematite, anhydrite, gypsum, and anorthite
RHA	(4) Mostly amorphous	Quartz and cristobalite
Tile	(2) Slightly amorphous	Quartz, hematite, gismondine and gypsum
YBD	(2) Slightly amorphous	Mullite and cordierite

2.3.1.3 Water Demand

An increase in water content generally increases water to binder ratio, increases slump/workability, but reduces strength and durability (Eren, 2015). As such, pozzolans with high water demand and higher water/binder ratio will theoretically have lower strength and durability features. On a general note, mixes containing pozzolans as partial cement replacements require more water to attain sufficient workability hence increased water/binder ratio which could alter the strength credentials of the resulting mortar or concrete particularly at early ages.

The effect of water demand of Portland cement on the structural performance of concrete is as shown in Figures 2.6 and 2.7 respectively.

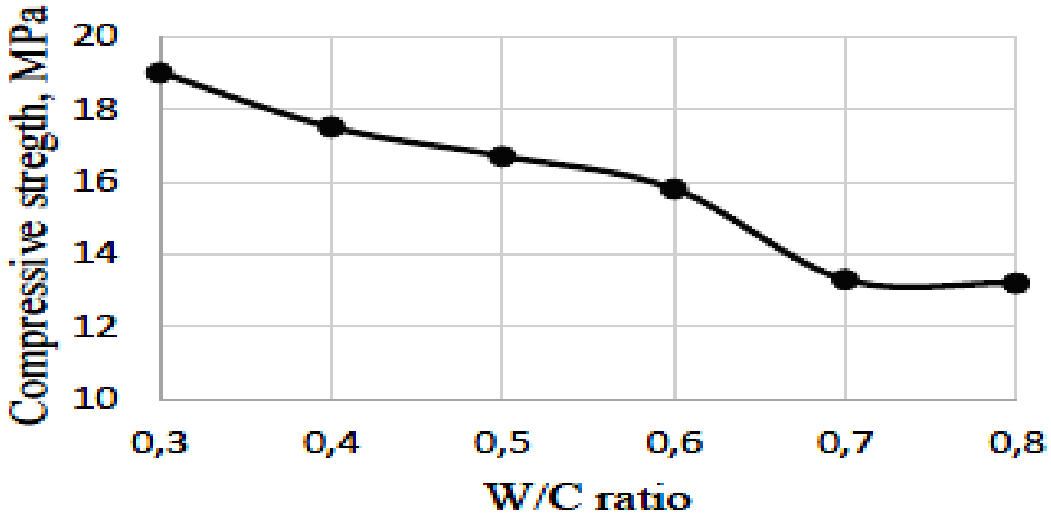

Figure 2.6: Water to binder ratio Vs Compressive Strength

Source: Eren (2015)

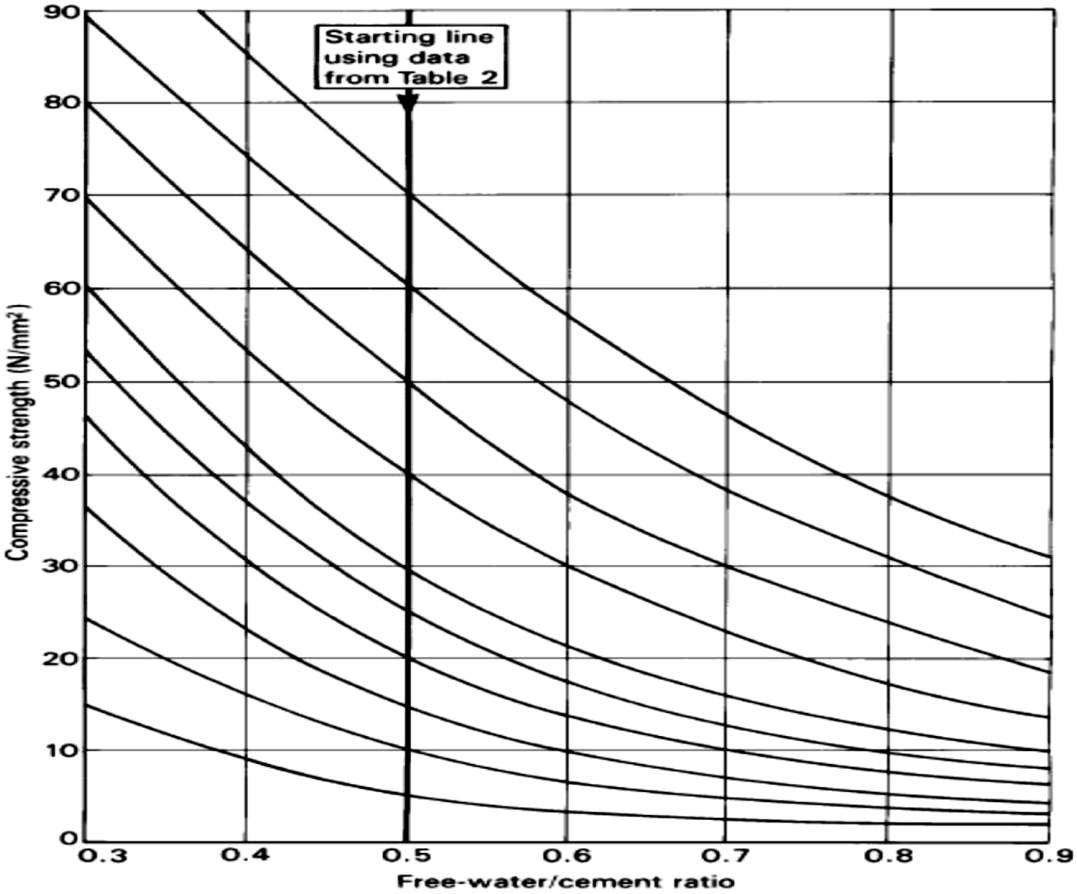

Figure 2.7 Effect of free water – cement ratio on the compressive strength of concrete

Source: Malaiskiene *et al.* (2017)

2.3.2. Chemical/Oxide Composition

Researchers have indicated that chemical oxide composition of binders plays a major role in determining the strengthening as well as durability properties of the resulting concrete or mortar. Cement as a binder is known to be primarily composed of Calcium oxide as well as silicon oxide. Table 2.13 indicates that between 60-66% of Portland cement is made up of calcium oxide (CaO), 19-25% is made up of Silicon Oxide, 3 – 8% of aluminum oxide and 1-5% of Iron Oxide (Eren, 2015).

Table 2.13 clearly shows that C3S constitutes beyond 50% of the cement compound. However, this compound is also responsible for the early rate of hydration as well as early strength gain rate of the cement.

Cement is further known to hydrate beyond 80% at age 28 and above; a property basically attributed to the fineness as well as the major chemical compounds of the cement. This is as shown in the Table 2.14.

It therefore follows that below 28 days, an abundance of calcium oxide is responsible for major strengthening of the resulting mortar or concrete, however, a balancing strength effect beyond 28 days is attributed to the presence of Dicalcium Silicate (C2S) which contains abundance of silicon oxide. Additionally, Tricalcium (C3A) aluminate which is primarily composed of oxides of aluminium constitutes only about 8% of cement clinker and is responsible for the earliest form of hydration (1-6 days) in cement (Eren, 2015) as can be deduced from Tables 2.13- 2.14.

Table 2.13: Major Chemical compounds of Portland cement (Source: Ozgur Eren, 2015)

Name of Compound	Chemical Composition	Abbreviation	Percentage (%)
Tricalcium Silicate	$3CaO.SiO_2$	C3S	51
Dicalcium Silicate	$2CaO.SiO_2$	C2S	23
Tricalcium aluminate	$3CaO.Al_2O_3$	C3A	8
Tetracalcium aluminoferrite	$4CaO.Al_2O_3Fe_2O_3$	C4AF	9

Table 2.14: The rate of Hydration /Strength gain (Source: Eren, 2015)

Chemical Compounds	Time to achieve 80% hydration (days)
C3S	10
C2S	100
C3A	6
C4AF	50

Table 2.15 Oxide Composition of Specific Pozzolans (Source: Walker and Pavia, 2011)

Pozzolan	SiO_2	Al_2O_3	SiO_2+ $Al2O_3$	CaO	Fe_2O_3	SO_3	TiO_2	MnO	K_2O	MgO	P_2O_5
GGBS	34.14	13.85	47.99	39.27	0.41	2.43	0.54	0.25	0.26	8.63	-
Leca	52.78	24.39	77.17	3.59	11.42	0.39	0.88	0.37	2.82	2.70	-
Metastar	51.37	45.26	96.63	-	0.52	-	-	-	2.13	0.5	-
MS	92.10	2.13	94.23	1.10	1.62	0.28	-	-	1.32	1.05	0.23
PFA	65.32	24.72	90.04	0.94	4.84	0.37	0.91	-	1.37	0.68	0.37
RBD	48.24	22.15	70.39	10.31	6.67	6.94	0.91	-	2.97	1.17	0.26
RHA	93.84	1.93	95.77	0.68	0.29	-	-	0.12	1.38	0.45	1.11
Tile	46.61	21.47	68.08	11.34	7.19	7.62	0.96	-	3.05	1.12	0.20
YBD	43.90	44.94	88.84	0.36	2.11	-	0.4	-	1.27	6.28	0.26

Based on the above, it can be confidently stated that the replace-ability of cement using supplementary cementitious materials is greatly dependent on the chemical properties of the SCM and how they complement that of cement. A good combination of calcium, aluminium and silicon oxide is therefore a necessary requirement of SCMs in order to maintain early as well as late strength development of the resulting concrete mix.

Ground granulated Blast Furnace Slag (GGBS) a by-product of the steel industry can replace up to 70% of cement due to its physical as well as chemical credentials. GGBS is composed chiefly of calcium, magnesium and alumina-silicates. The rapid quenching of the molten steel material yields glassy GGBS granules which are air dried and further pulverized to fine powder (BS 6699, 1992). Ground granulated blast furnace slag (GGBS) has been used as a partial replacement for cement in mortar and concrete at replacement levels between 25 and 50%.

A typical compressive strength and percentage GGBS content as a cement replacement is as shown in the Figure 2.8 (Bharnuke and Chore, 2014).

From the illustration in Figure 2.8, for both sand types, increase in GGBS content leads to increasing compressive strength up to 40% replacement. However, results for compressive strengths beyond 45% reduced with increasing GGBS content. Results at 60% replacement level are approximately the same as that of the control implying that 60% replacement level using GGBS as partial replacement is acceptable using compressive strength as a yardstick.

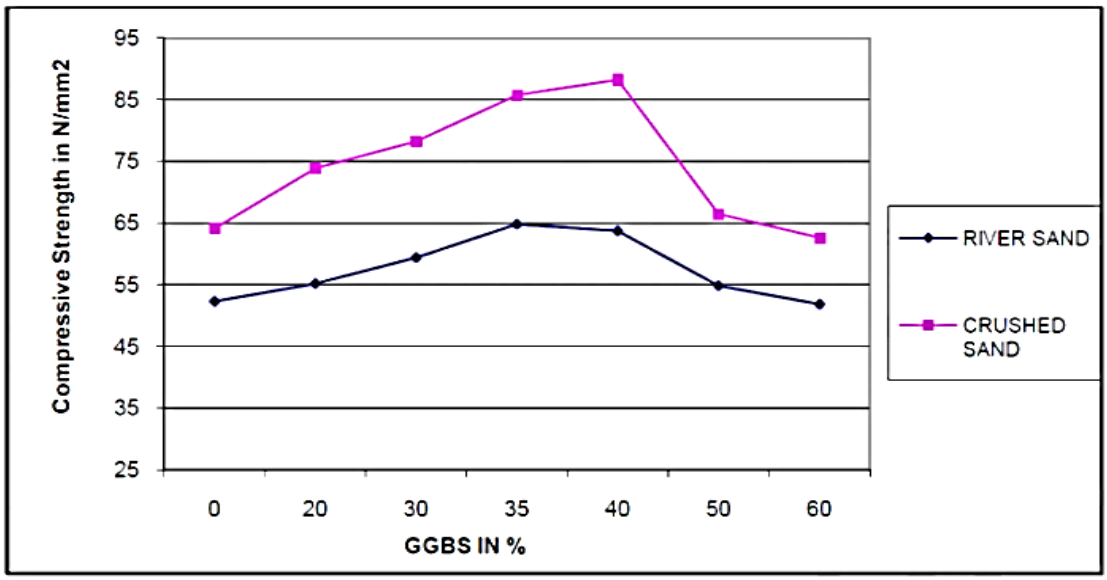

Figure 2.8: 28 Days Compressive Strength (N/mm^2) of the Cylinders for M-30

Source: Bharnuke and Chore (2014)

2.3.3 Cementation and Hydraulicity Indices

Cementation and Hydraulic indexes are parameters mainly dependent on the oxide compositions of Silicon, Aluminium, Iron, magnesium and calcium. Figueredo *et al*., (2016), noted that silicon and aluminium oxides are the primary oxides responsibly for the hydraulic behaviour of a material. In the discussion of their findings, they asserted that at higher calcination temperatures, greater amounts of Alite (C3S) is been produced.

$$Cl = \frac{2.8SiO_2 + 1.1Al_2O_3 + 0.7Fe_2O_3}{CaO + 1.4MgO} \tag{2.2}$$

$$Hl = \frac{SiO_2 + Al_2O_{33}}{CaO} \tag{2.3}$$

Findings of Herbert *et al*., (2019), as shown in Table 2.16, informs that Hydraulicity Index is directly proportional to Cementation Index as well as compressive strength, on the condition that all samples are prepared to have approximate uniform fineness. This could explain the variation observed in the findings of Figueiredo *et al*., (2016), as shown in Table 2.17 in which NHL2-B had a better cementation and Hydraulic Indices when compared to NHL2-A, but was found to be lower in compressive strength as the fineness of both samples was not defined.

Table 2.16: Compressive strength and hydraulic index of calcined pozzolan-cement mortars (Source: Herbert *et al*., 2019)

Pozzolan ID		Calcination Temperature						
Based on 28 day curing age @30 Cem. replacement level		500 °C	600 °C		700 °C	750 °C	800 °C	Ref OPC
Ar – A	Comp. Strength (Mpa)	41.1	45.7		45.7	47.4	47.8	58.4
	Hydraulic Index	-4.22	23.49		23.49	33.73	36.14	
Ar – B	Comp. Strength (Mpa)	42.0	43.1		49.8	48.1	48.2	58.4
	Hydraulic Index	1.45	8.01		48.19	37.83	38.25	
		600 °C	700°C	750°C	800°C	850°C	900°C	Ref OPC
Ar – C	Comp. Strength (Mpa)	40.07	41.0	43.6	43.9	41.3	43.0	59.9
	Hydraulic Index	-6.08	-4.42	9.94	11.82	-2.87	6.57	
Ar – C	Comp. Strength (Mpa)	40.3	41.4	46.5	56.8	48.8	43.3	59.9
	Hydraulic Index	-8.29	-2.21	25.97	82.87	38.67	8.29	

Table 2.17: Oxide composition. Cementation and hydraulicity index (Source: Figueiredo *et al*., 2016)

Oxide	NHL – 2A	NHL – 2B	NHL – 2C
CaO	66.38	66.03	66.41
SiO2	7.80	9.35	4.85
Al_2O_3	1.63	0.38	0.12
MgO	2.37	0.44	1.19
Fe_2O_3	2.10	0.38	0.5
SO_3	0.37	0.46	1.19
K_2O	0.89	0.33	0.46
Na_2O	0.31	0.49	0.49
TiO_2	0.16	0.09	0.09
MnO	0.05	0.01	0.01
LOI	17.95	22.03	24.64
CI	0.36	0.40	0.21
HI	0.14	0.15	0.07

2.3.4. Mechanical Properties

The mechanical activity of pozzolans is measured by compressive, tensile and or flexural tests. A common approach is the strength activity index (SAI) approach which specifies that a cement mix containing pozzolans as partial cement replacement, cured for 28 days should be able to possess compressive strength results that are equal to or greater than 75% of the control specimen containing 100% of cement as binder (Walker and Pavia, 2011). The compressive strength development curve for Natural lime as well Portland cement-based concrete is as shown in Figures 2.19 and 2.10 respectively.

The mechanical activity or strength development rate of cement mixes containing pozzolans is primarily dependent on the physical and chemical factors reviewed above. The rate of strength development in concrete is of great interest to the construction industry. As such, concrete is expected to have achieved certain strength at respective curing ages dependent on the concrete grade. This is a factor that could be used as a guide in monitoring the mechanical pozzolanic reactivity of pozzolans in concrete at defined curing ages

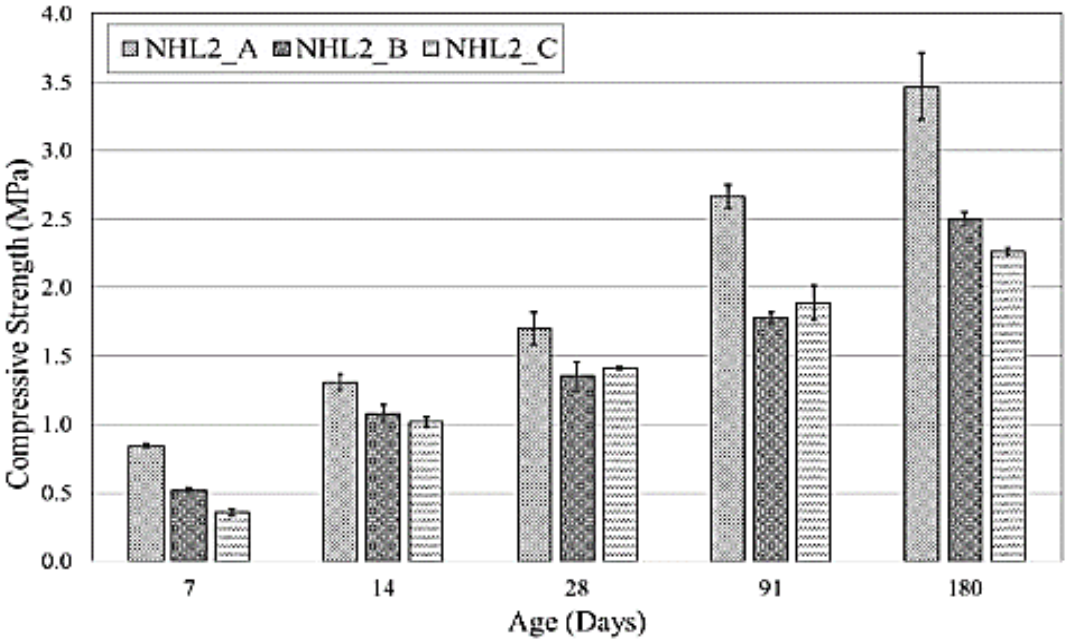

Figure 2.9: Compressive strength of the mortars at 7, 14, 28, 91 and 180 days

Source: Figueiredo et.al. (2016)

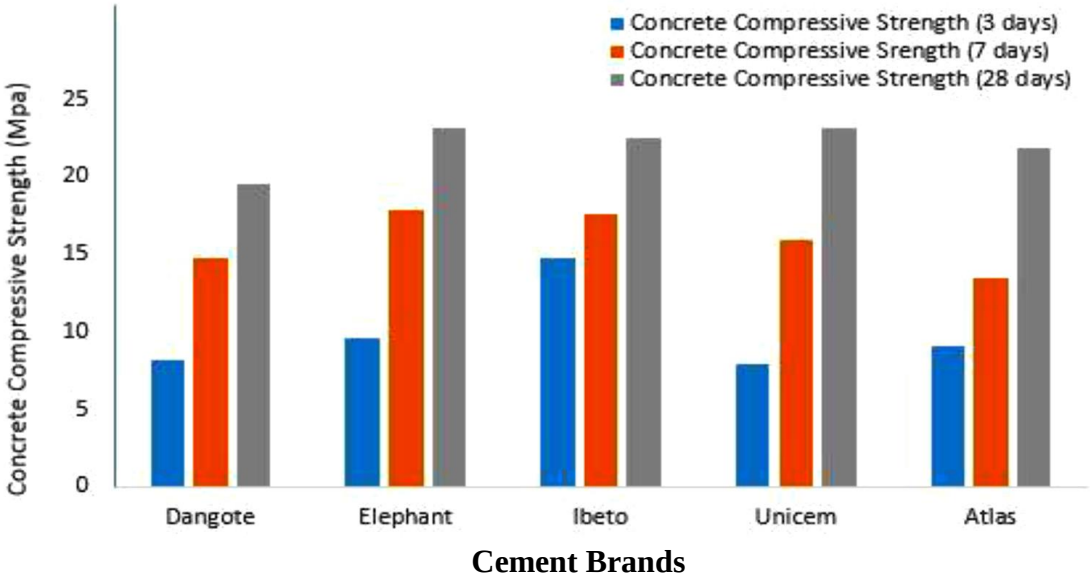

Figure 2.10: Grade M20 Nigerian cements and their concrete compressive strength at different curing ages

Source: Nduka *et al*. (2014).

From Table 2.18, it can be concluded that M20 graded concrete with a mix ratio 1:1.5:3 is expected to have compressive strengths not lower than 41%, 76% and 106% at 3, 7 and 28 days respectively.

Similarly, Figure 2.11 represents a typical strength trend and rate for cement based concrete structures as reported by CIVL 101(2021).

Table 2.18: Average compressive strength achieved by Grade M20 concrete at different curing ages (Source: Nduka *et al* 2014)

Comp. Strength (N/Mm2)	Nigerian Cement Brand						∑ (% G M20).	Avg. % G. M20
	Dangote	Elephant	Unicem	Atlas	Other[x]	Ibeto[xx]		
3DAYS	7.80	9.00	7.50	8.70		15.00		
% of G. M20	39.00	45.00	37.50	43.50	40.00	75.00	205.00	41.00
7DAYS	14.80	17.50	15.00	13.20		17.00		
% of G. M20	74.00	87.00	75.00	67.50	65.00	85.00	453.50	76.00
28 days	19.00	22.50	22.50	22.00		21.80		
% of G. M20	95.00	112.50	112.50	110.00	99.00	109.00	638.00	106.00

xx – Ibeto was not used in arriving at the average results

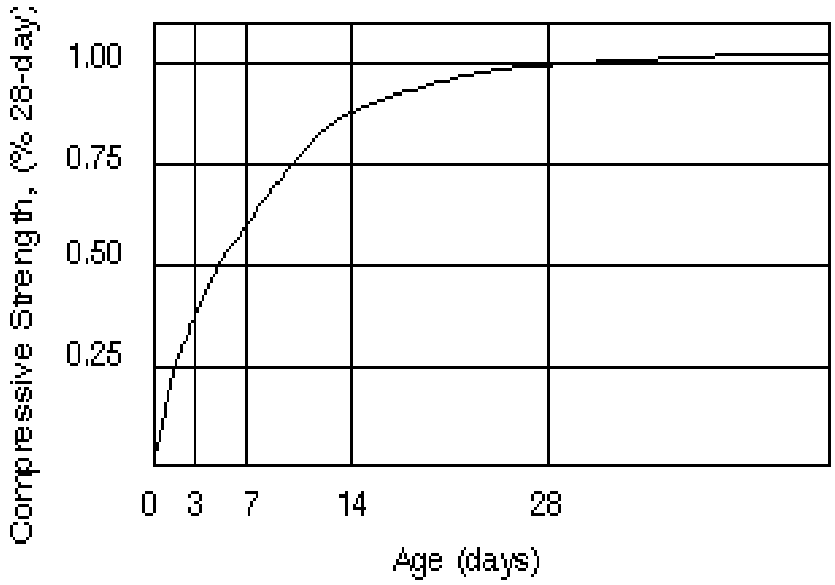

Figure 2.11: Typical Strength gain curve of Portland Cement Based Concrete

Source: CIVL 1101 (2021)

2.4. Summary of Literature Review

The following briefly summarises the literature as reviewed.

1. The majority of articles used X-ray Florescence (XRF) and X-ray Diffraction (XRD) investigations to identify the elemental (oxide) content and amorphousness of the pozzolans.

2. With the use of equations for hydraulicity and cementation index, oxide compositions are essentially required to forecast the hydraulic nature of samples.

3. Under different calcination temperatures, it was discovered that the cementation index and hydraulic index of pozzolans form a quadratic curve, and this was observed to cause a similar trend in the compressive strength of Pozzolan concretes.

4. The Strength Activity Index technique was primarily used to quantify the mechanical pozzolanic activity of the pozzolans (SAI)

5. Calcination temperatures for the pozzolans' manufactured were found to range from 400 to 1000 °C.

6. It was found that the mechanical and durability properties of the resulting cement structure were directly correlated with the pozzolanic material's fineness.

7. Compressive strength is inversely correlated with the water-to-binder ratio. As a result, methods for lowering concrete water use while preserving a satisfactory slump must be proposed.

8. The precise time for calcination or combustion was hardly mentioned in any publications, and there was no energy comparison between pozzolanic cements and structures made entirely of Portland cement with regard to the environmental and economic values and energy consumed in the production of the pozzolans.

9. The bulk of articles hardly ever mentioned or indicated the cost savings.

10. The appropriate calcination temperature must be determined by reference to other scientific literature since no specific and optimum burning temperature has been determined for the pozzolans according to their particular chemistries.

11. For both SiO_2 and CaO rich pozzolans, cement replacement by single pozzolans was often limited to below 20%. However, a synergy of the hybrid of both exhibited acceptable results when employed over 30% replacement level.

12. The research that is currently available on hybrid pozzolans either combines pozzolans with oxide compositions that are comparable to one another or fixes the proportioning ratio of pozzolans with complementary oxides, leading to limiting conclusion.

13. Previous research on hybrid pozzolans demonstrated that each individual pozzolan was produced separately and independently before being combined to create the hybrids. Given that energy demand and CO_2 emissions will be doubled, this method of producing hybrid pozzolans will unquestionably have a detrimental impact on sustainability.

CHAPTER THREE

MATERIALS AND METHODS

3.1. Research Materials

Grade 42.5 Dangote Portland limestone Cement, river sand, 12.5mm to 19mm granite and borehole water (used at water to binder ratio of 0.55), were the primary materials for concrete production.

Supplementary cementitious materials used in this study are categorized as Primary and Hybrid materials, with Agricultural pozzolans (AP) and Hybrid Agricultural Pozzolans (HAP) being the two types.

Concrete specimens containing these materials as partial replacements for cement were developed, tested in accordance with the research's objectives and the impacts were measured. In light of this, the additional agricultural waste materials under the heading of primary and hybrid materials are explained below, in addition to Portland limestone cement, water, and aggregates (fine and coarse) which are the standard components for concrete.

The study area is Niger Delta University environs of Amassoma community, Bayelsa State, Nigeria, located at 4° 58' 13" N and 6° 6' 32" E, (Mindat.org, 2023). The measured mean atmospheric temperature of the samples in this location was 25 ^{o}C.

3.1.1. Primary Research Materials

The primary research materials for this investigation were grouped under AP. They included PSA and CSA. The primary materials were produced at five (5) respective temperature conditions; atmospheric temperature, 200, 400, 600 and 800 ^{o}C. As such, Ten (10) primary samples were developed as design specimens for the study.

3.1.2. Hybrid Research Materials

The complementary oxides of silicon and calcium made up the five (5) sets of hybrid materials that made up the synergistic synthesis of the hybrid research materials. The hybrids were produced using mass proportioning in the following ratios: 70:30, 60:40, 50:50, 40:60, and 30:70. They were subjected to the same five levels of heat treatment as is the case of the primary materials, to yield 25 hybrid research samples in total, produced for the study. However, including the mix ratios of 100 : 0, and 0 : 100 (i.e. PSA : CSA mix ratios), would bring the complete hybrid sample size to seven (7) which if multiplied by the five (5) temperatures, brings the total number of samples to thirty five (excluding the control.

3.1.3. Laboratory Tools and Equipment

The tools and equipment used were peculiar to the tests being conducted. All tools and equipment were of standard quality and used in careful observation of the guidelines of the relevant standards. On a broad scale, the following laboratory tools and equipment were used in achieving the objectives of this research;

1. Compression testing machine
2. Slump apparatus
3. Reactant frame
4. Dial gauges
5. Cube moulds
6. Rectangular moulds
7. Curing tanks
8. Pulverising machines
9. High capacity furnace
10. Digital infrared thermometer
11. Electric blower
12. Weighing scales
13. Sieve set and shaker
14. 90micron Sieve
15. Electric air blower
16. Concrete mixer
17. Wheel barrows

18. Head pans
19. Camera
20. Pycnometer
21. Shovel
22. Head pans
23. Buckets
24. Trowels

3.2. Research Design

Table 3.1 is a summary of the research variables related and covered by this work. Tables 3.2 and 3.3 are the temperatures and synergistic ratios adopted to achieve the objectives of the study.

Table 3.1: Research Variables

Independent Variables	**Physical Dependent Variables**	**Mechanical Dependent Variables**	**Durability Dependent Variables**
Calcination Temperature	Colour	Compressive Strength	Water Absorption (WAI)
Synergistic Ratio	Fineness	Flexural Strength	Sulphate Attack (SISLI) and (SIMLI)
Cement Replacement Level	Specific Gravity (Density)		Chloride Attack (CISLI)
	Water Demand		

Table 3.2: Calcination Temperatures

Calcination Temperatures (^{o}C)				
25	200	400	600	800

Table 3.3: Synergistic Ratios

Synergistic Ratio by Mass of Total Pozzolan content							
PLC	100% PSA	70% PSA: 30% CSA	60% PSA: 40% CSA	50% PSA: 50% CSA	40% PSA: 60% CSA	30% PSA: 70% CSA	100% CSA

3.3. Independent Variables

The independent Variables of this research exercise are Calcination temperature, Synergistic Ratio and Cement Replacement Level.

3.3.1. Calcination Temperature (The Grinding Process)

Clam and Periwinkle shells were sourced from the environs of Amassoma Community, in Bayelsa State. The samples were washed and sun dried for at least 48hours to a moisture content of less than 3.0%, before subjected to a pre-pulverisation process. A 50 kg bag of periwinkle shell required about 15 minutes to be broken down and prepared for calcination. A 50 kg of calm shell required a minimum of 45 minutes to be broken down and prepared for calcination (requiring a hammer mill and followed by an artesian mill). However, a synergy of both was ground for at-least 60 minutes prior to Calcination.

Calcination on the clam shells, periwinkle shells and their synergies was done with the aim of producing ash from the samples, releasing impurities such as CO_2, and opening up the trapped elements for oxidization. This was done at temperatures ranging between 200 and 800 ^{o}C at 200 ^{o}C intervals. For the sake of a more detailed study, non-calcined samples at atmospheric temperature were included in the study. Calcination temperatures are as shown in Table 3.2.

3.3.2 Synergistic Ratio

Clam Shell Ash and Periwinkle Shell Ash were synergised to observe for possible improvement in the Physico-mechanical behaviour of materials to be used in concrete. For clarity of pattern, both materials were observed independently as well as when synergised. Synergistic ratios are as shown in Table 3.3. The total number of samples therefore incorporates the total number of temperatures as well as the synergies. The sample configuration arising from the synergistic ratio and calcination temperature necessitated the production of a total of 36 sample types for this research exercise as shown in Table 3.4. Tables 3.5 and 3.6 represent the mix configurations for AP and HAP concrete specimens.

Table 3.4: Sample number and configuration for descriptive statistical analysis (Objective 1)

SAMPLE ID	CODE	CALCINATION TEMPERATURE (^{o}C)				
PLC	1	25	200	400	600	800
PSA	PSA	2	3	4	5	6
70PSA:30CSA	70P	7	8	9	10	11
60PSA:40CSA	60P	12	13	14	15	16
50PSA:50CSA	50P	17	18	19	20	21
40PSA:60CSA	40P	22	23	24	25	26
30PSA:70CSA	30P	27	28	29	30	31
CSA	CSA	32	33	34	35	36

Note: PLC is the control and its code name remains PLC, however, it is noted as sample No. 1, hence, total sample size is 36

Table 3.5: Mix Configuration for AP concrete specimens

.	Mass of Cement (PC) Replaced							
	20%		30%		40%		50%	
Sample Code	PC	PSA	PC	PSA	PC	PSA	PC	PSA
Control	100	0	100	0	100	0	100	0
PSA	80	20	70	30	60	40	50	50
Sample Code	PC	CSA	PC	CSA	PC	CSA	PC	CSA
Control	100	0	100	0	100	0	100	0
CSA	80	20	70	30	60	40	50	50

Table 3.6: Mix Configuration for HAP concrete specimens

.	Mass proportion of cement (PC)replaced											
	20%			30%			40%			50%		
Sample Code	PC	PSA	CSA	PC	PSA	CSA	PC	PSA	CSA	PC	PSA	CSA
Control	100	0	0	100	0	0	100	0	0	100	0	0
PSA	80	20	0	70	30	0	60	40	0	50	50	0
70P	80	14	6	70	21	9	60	28	12	50	35	15
60P	80	12	8	70	18	12	60	24	16	50	30	20
50P	80	10	10	70	15	15	60	20	20	50	25	25
40P	80	8	12	70	12	18	60	16	24	50	20	30
30P	80	6	14	70	9	21	60	12	28	50	15	35
CSA	80	0	20	70	0	30	60	0	40	50	0	50

3.3.3. Cement Replacement Level

Cement was partially replaced by mass in the production of cube and beam concrete specimens. The replacement levels are 20%, 30%, 40% and 50% respectively.

Based on variations in the cement replacement level, and Pozzolan type, the mix configuration used in this study is as shown in Table 3.5 and 3.6 for AP specimens and HAP specimens respectively

3.3.4. Physical Dependent Variable

Physical dependent variables include colour, fineness, specific gravity and water demand.

3.3.5. Particle Size Distribution

Particle size distribution was conducted in accordance to BS 812 -103 (1985), for the fine and coarse aggregate used in this experimental study in order to establish the suitability of the materials in the production of concrete specimens.

3.3.6. Colour

The colour of the different samples was observed before and after calcination using the British Standard colour chart (British Standard Colour. com, 2023).

3.3.7. Fineness

An indirect approach in accordance to the specifications of BS: 12 (1978) and IS 4031 part 1 (1996) was used to experimentally derive an index for the surface area of the samples.

$$F = \frac{WR}{WT} \tag{3.1}$$

Where;

F = percentage fineness of the material

W_R = Weight retained on the specific sieve (g)

W_T = Total weight of sample before sieving (g)

3.3.8. Specific Gravity

All of the specimens underwent specific gravity testing in line with BS 4450-3 (1978), and a potential correlation with mechanical properties was identified.

3.3.9. Slump and water demand

To determine and subsequently indicate the water demand for each mix, slump tests were carried out on fresh concrete mixtures containing both primary and hybrid samples as cement replacements in accordance with BS EN 12350-2; (2009). They were compared to the outcomes of samples that contained only cement as a binder.

At a constant water/binder ratio, the higher the slump, the lower the water/binder ratio required, the higher the hydraulicity of the material and hence the lower the water demand. As such, water demand was seen as a vital component of this research work to give a preliminary insight into the strength potentials of the samples in concrete.

3.3.10. Mechanical Dependent Variables

Mechanical dependent variables covered in this work are Compressive strength and Flexural Strength.

3.3.11. Compressive Strength Test

Summing up the primary samples (10), hybrid samples (25), and the control (1), a total of 36 samples were used as the research samples of this work. Compressive strength tests were carried out at three (3) ages (28 day, 56day and 90day) using three (3) cube specimens per mix. In essence, each sample had nine (9) cube specimens, hence a total of 315 cube specimens per replacement level and 1260 cube specimens for 4 replacement levels (20%, 30%, 40% and 50%). The control specimens were 9 cubes, which brings the total specimen size to 1269.

The cube specimens' compressive strength was tested in accordance to BS EN 12390-3 (2009). The curing method was full immersion for all concrete specimens produced in course of the investigation. Using the strength activity index (SAI) technique, this served as the main yardstick for assessing the reactivity of the pozzolans, and

contrasting the findings with those found for samples that contained 100% cement as the binder.

The cube specimens were of 150 mm * 150 mm * 150 mm volumetric dimensions and were subjected to submerged fresh water curing after 24 hr of production until the day of testing. The compressive strength was calculated as the ratio of the crushing load at failure (N) to the area of the cube being loaded.

$$Compressive\ strength\ \left(\frac{N}{mm2}\right) = \frac{failure\ load\ (N)}{Area\ under\ loading\ (mm2)} \quad (3.2)$$

Strength Activity Index (SAI) according to ASTM C-618 and BS EN 12390-(3) is a numerical index that measures the percentage relativity between the compressive strengths of cement control concrete specimens and concrete specimens containing pozzolanic/hydraulic materials as partial replacements for cement. According to the cited standards, the compressive strength of cement blended concrete (concrete containing pozzolans as a component of the binder) must not be than 75% of the control concrete specimen (concrete containing cement as 100% binder component).

3.3.12. Flexural Strength test

In order to measure the samples effect in enhancing concretes ability to resist bending due to loading, four point loading flexural strength test was conducted in accordance to BS EN 12390- 5 (2009). The standards measure flexural strength using the following equation.

$$fcf = \frac{pl}{bd^2} \quad (3.3)$$

Where

f_{cf} = the flexural strength (in N/mm²)

P= the breaking load (in N);

B and *d*= the lateral dimensions of the cross-section (in mm) and

I is the distance between the supporting rollers (in mm).

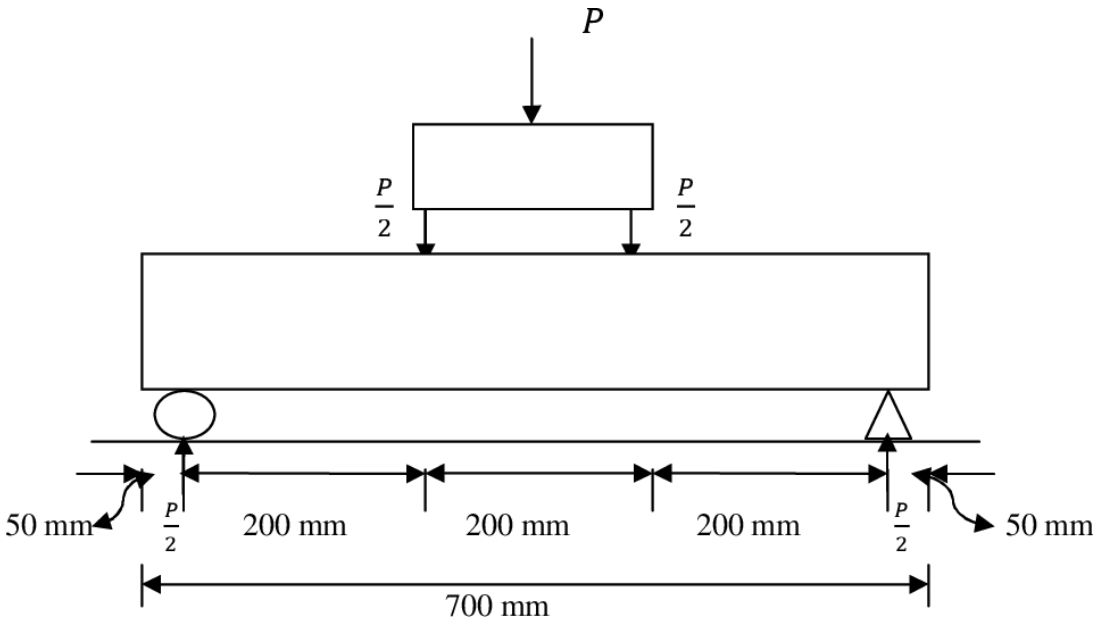

Figure 3.1: Loading mechanism for flexural strength testing
Source: BS EN 12390-5 (2009)

Plate 3.1: Flexural strength testing of cement blended concrete beams

3.3.13. Durability Dependent Variables

Durability dependent variables covered in this research work are water absorption, Chloride attack and sulphate attack.

3.3.14. Water Absorption Index

Water absorption tests required the production of cube specimens of standard dimension of 15 cm. Three (3) cube specimens per day per cement replacement level per temperature amounted to a total of 1269 cube specimens.

Water Absorption Test; in accordance to BS 1881-122 (2011) was conducted on the specimens to ascertain the water retaining capacity of the concrete specimens. Based on recommendations from the BS 1881-122 (2011) and Coull (2014), water absorption results were analysed for at ages 28, 56 and 90 days. Three (3) cubes per mix was produced for this exercise, which after immersion curing, were oven dried at 105 ± 5 ^{o}C for 72 hours and resulting weight recorded as W1, furthermore, the specimens were immersed in water for 24 hours and resulting weights recorded as W2. The ratio of the difference in weights prior to immersion (oven drying weight, W1), and after immersion (W2) to the oven dried weight (W1) expressed as a percentage constitutes the water absorption capacity of the concrete specimen recorded as an index.

$$\mathrm{WAI} = \frac{\mathbf{(W2 - W1)x\ 100}}{\mathbf{W1}} \tag{3.4}$$

3.3.15. Chloride Induced Strength Loss Index

The marine environment is basically responsible for chloride attack. This is particularly so because sea water typically contains about 3.5% of salt, of which Chloride ions (CL^-) make up about 2%, Sodium ions (Na^+) about 1.1%, Magnesium ions (Mg^{2+}) about 0.14%, and Sulphate ions (SO_4^{2-}) of about 0.27% (Shetty, 2005). Hence, with the concentration of chloride ions above 50% of the salt composition in sea water, chloride attack is thus the predominant attack in marine environment. Additionally, as salts, Sodium Chloride makes up 78% while magnesium sulphate makes up 15% of total salt content (3.5%) in sea water (Shetty, 2005).

A 10% sodium chloride solution was developed for the research exercise to create a rapid reaction between the salt and the hydrating concrete structures. Using a modified

approach to the Corrosion Resistance Coefficient (CRC) Method as Per Liu and Huang (2012), Chloride Induced Strength Loss Index (CISLI) was used to relate the strength lost due to chloride attack between a fresh water cured concrete specimens and the chloride solution cured concrete specimens. Two sample sets were produced. One was cured in fresh water and the other cured in chloride solution. Compressive strength of the cured specimens was obtained at ages 28 days, 56 days, and 90 days.

The Weight Loss (%) and chloride induce strength loss index between the concretes cured in fresh water and concrete cured in chloride solution was calculated as follows;

$$CISLI\ (\%) = \frac{Conc.in\ fresh\ water - Strength\ of\ Conc.in\ chloride\ solution}{Strength\ of\ concrete\ in\ fresh\ water} \quad (3.5)$$

3.3.16. Sulphate Induced Strength Loss Index

A 5% Sodium sulphate solution was produced and used for this test method. Analysis was carried out in accordance to Ranganath and Kumari (2018), In conformation with IS 516. Cube specimens of size 150 mm*150 mm*150 mm were produced for the 36 sample types which were cured for 28 days before submerging into the 5% sodium sulphate solution for 28 days, 56 days and 90 days respectively. The specimens were weighed prior to soaking as well as after soaking. The loss in strength was calculated as follows;

$$SISLI\ (\%) = \frac{Conc.in\ fresh\ water - Strength\ of\ Conc.in\ sulphate\ solution}{Strength\ of\ concrete\ in\ fresh\ water} \quad (3.6)$$

Where;

SISLI = Sulphate induced strength loss index (%)

3.3.17. Sulphate Induced Mass Loss Index

Using same method as highlighted under section 3.3.16, the sulphate induced strength loss index was calculated as follows;

$$SIMLI\ (\%) = \frac{Wt.of\ Conc.in\ fresh\ water - Wt\ of\ Conc.in\ sulphate\ solution}{Wt.of\ concrete\ in\ fresh\ water} \quad (3.7)$$

3.3.18. Sustainability Footprint

Analysis of sustainability was done in the areas of CO_2 footprint, energy usage, and cost. They were meticulously measured, and succinct comparisons were made between the findings for the control samples, which had 100% cement as the binder, and samples that contained AP and HAP as partial cement substitutes. The examination of CO_2 footprint was constrained to findings based on fuel consumption for energy generation, publications, and rational/logical assumptions due to the lack of carbon capture equipment.

CO_2 footprint generally results from the fuel burning for energy generation as well as the calcination of the calcined material.

Energy and cost requirement were analysed by measuring the amount of energy used in the production of the pozzolans as well as the cost implications and comparing same to standard publications on the energy and cost requirement for Portland cement.

3.3.19. Experimental Production Summary

The experimental production summary, incorporating all the methods used in this study are as shown in Table 3.7.

3.3.20. Design and Fabrication of Local Coal Powered Furnace

Calcination of the PSA, CSA and PSA/CSA hybrids required a high capacity furnace that could contain no less than 50kg of cementitious materials at a given time, and its internal temperature raised to at least 1000^{o}C. As such, the furnace was designed to have a surface area of 1.20m x 2.85m and a depth of 1.0m. This was partitioned into 4 chambers of 1.2m x 0.6m each, having internal areas as 0.70m * 0.324m at an internal depth of 0.7m. The furnace was constructed with a grade M30 concrete and well reinforced 16mm high tensile steel (Fe 415). The base of the furnace was constructed with a mixture of sand and Plaster of Paris (POP) at a mix ratio of 1:1. Concrete does not have the elastic modulus required to sustain its load bearing capacity when heated to temperatures exceeding 400^{o}C (Alhamad *et al*., 2022), as such, 50mm thick ceramic fibre wool with a minimum insulation capacity of 2000^{o}C was used to line the internal

wall sections of the furnace. The furnace plan design and as fabricated are shown in Appendix A1 and Plate 3.2 respectively.

Table 3.7: Experimental Sample/Specimen Production Summary

S/N	Test Type	Test STD	Synergy	Repl. Level	Temp. levels	Test Age	Spec. per age	Control spec.	Total Spec.
			A	B	C	D	E	F	(A*B*C*D*E) +F
1	Particle Size Distribution for Fine Aggregate	BS 812 -103 (1985)	-	-	-	-	-	-	-
2	Particle Size Distribution for Coarse Aggregate	BS 812 -103 (1985)	-	-	-	-	-	-	-
3	Fineness Test	BS: 12 (1978) and IS 4031 (1996)	7	-	5	-	-	1	36
4	Specific Gravity	BS 4450-3; (1978)	7	-	5	-	-	1	36
5	Water demand/Slump/ Workability	BS EN 12350-2	7	4	5	3	3	9	0
6	Compressive Strength	BSEN 12390- 3	7	4	5	3	3	9	1,269
7	Water Absorption	BSEN 12390- 8 and BS 1881-122	7	4	5	3	3	9	1,269
8	Chloride Attack	BSEN 12390-11	7	4	5	3	3	9	1,269
9	Sulphate Attack	IS 516, Ranganath and Kumari, (2018)	7	4	5	3	3	9	1,269
10	Flexural Strength	BSEN 12390- 5	7	2	5	1	3	3	213

Plate 3.2: The designed and Fabricated Furnace in Use

3.5. Data Analysis

The Results analysis methods were discussed under the headings of the three objectives of this research.

The Excel tool ((Version 14.07268.5000 32-bit) on the Microsoft office application platform was used to study the laboratory findings and develop descriptive statistical relations on the response of varying temperatures and hybrid ratios on the physical properties of CSA and PSA as well as the mixture of both. Furthermore, their mechanical as well as durability contribution to concrete specimens, when used as partial cement substitutes was developed and presented through the Excel tool.

In the development and analysis of models for the optimisation of calcination temperature, synergistic ratio and cement replacement level, for the production of CSA, PSA and CSA/PSA hybrid pozzolan as partial cement substitute, a combined design was developed using Design Expert application (an optimisation application tool, Version 13.0.5.0 64-bit) and the Combined Mixture and Response Surface I optimal design was used. This done to integrate the 'moisture' process as a complimentary factor to the 'calcination temperature' process factor. I optimal design was used to best predict the interaction between variables in the equation (model) as developed.

The design used mixture and process variables templates to generate the runs and configuration required as shown in Table 3.6 to 3.8, to obtain the objective. The design was fed with the independent variables (mixture and processes) as inputs/factors and laboratory results obtained for dependent variables as responses or outputs. On completion of the laboratory works, experimental results obtained at 28 days of curing was used as responses to the application which were used to develop analytic models. The models were analysed using the Analysis of Variance (ANOVA) tools to measure for the significance of the models based on a 95% confidence level. The quality of the regression models was accessed using the R^2 indicator on the regression analysis template to give an overview of the depth to which the variables interact (R^2), the depth to which the model predicts interaction between variables within the boundaries of the experimental framework (R^2 – Adjusted) and the depth to which the model

predicts interaction between variables outside the boundaries of the experimental framework (R^2 – predicted).

Tables, graphs and models were developed using the application that represent the true state or relationship between the inputs (independent variables) and the responses (dependent variables). Table 3.8, 3.9, and 3.10 are the experimental frameworks used in the development and analysis of models for predicting the levels of interactions between variables within and outside the boundaries of the research framework.

To evaluate the sustainability features of using optimized agricultural by-products/wastes as partial replacements to Portland cement binder in Civil Engineering structures, numerical analysis on cost of production was done using tools within Microsoft Excel. Also, Energy demand per sample production and the CO_2 emission associated with fuel combustion was quantified numerically and compared to standard cement values.

Tables 3.8 – 3.10, are the experimental design templates generated with the help of Design Expert application, to develop logical variations in the independent variables prior to commencement of the mechanical and durability experimental works.

Table 3.8: Experimental design template for model development, ANOVA and Optimisation of Periwinkle Shell Ash Pozzolan

Run	Comp.1 A: PC %	Comp.2 B: PSA %	Factor 3 C: TEMP. ^{o}C	Res.1 STRENGTH N/mm^2	Res2 WAI %	Res.3 CISLI %	Res. 4 SISLI %	Res. 5 SIMLI %
1	100	0	800					
2	80	20	600					
3	70	30	25					
4	70	30	400					
5	50	50	400					
6	80	20	400					
7	60	40	200					
8	70	30	600					
9	60	40	25					
10	70	30	800					
11	100	0	25					
12	80	20	200					
13	50	50	800					
14	50	50	25					
15	50	50	400					
16	80	20	800					
17	60	40	600					
18	60	40	800					
19	80	20	25					

Table 3.9: Experimental design template for model development, ANOVA and Optimisation of Clam Shell Ash Pozzolan

Run	Comp.1 A: PC %	Comp.2 B: PSA %	Factor 3 C: TEMP. ^{o}C	Res.1 STRENGTH N/mm^2	Res2 WAI %	Res.3 CISLI %	Res. 4 SISLI %	Res. 5 SIMLI %
1	100	0	800					
2	80	20	600					
3	70	30	25					
4	70	30	400					
5	50	50	400					
6	80	20	400					
7	60	40	200					
8	70	30	600					
9	60	40	25					
10	70	30	800					
11	100	0	25					
12	80	20	200					
13	50	50	800					
14	50	50	25					
15	50	50	400					
16	80	20	800					
17	60	40	600					
18	60	40	800					
19	80	20	25					

Table 3.10: Experimental design template for model development, ANOVA and Optimisation of PSA/CSA hybrid Pozzolan

Run	Comp. 1 A: PC %	Comp. 2 B: PSA %	Comp. 3 C: CSA %	Factor 4 D: Calc. Temp ^{o}C	Resp. 1 Comp. Strength N/mm^2	Resp. 2 WAI %	Resp. 3 CISLI %	Resp. 4 SISLI %	Resp. 5 SIMLI %
1	50	25	25	400					
2	70	0	30	25					
3	50	0	50	25					
4	50	0	50	800					
5	60	24	16	200					
6	70	0	30	400					
7	80	0	20	400					
8	50	25	25	800					
9	70	30	0	400					
10	50	0	50	400					
11	100	0	0	800					
12	60	24	16	600					
13	80	20	0	400					
14	80	20	0	25					
15	80	0	20	25					
16	50	25	25	600					
17	100	0	0	25					
18	60	40	0	800					
19	70	30	0	600					
20	50	50	0	400					
21	60	24	16	400					
22	50	50	0	25					
23	50	50	0	800					
24	60	0	40	800					
25	50	25	25	25					
26	60	16	24	600					
27	60	16	24	200					
28	80	10	10	400					

CHAPTER FOUR
RESULTS AND DISCUSSION

4.1. Physical Properties of Agro-based Pozzolans

Results of the fine and coarse aggregate's particle size distribution, fineness, colour, specific gravity, slump test and water demand as influenced affected by calcination temperature, synergistic ratio and mixture configuration, for Portland limestone cement (PLC), PSA, CSA and HAP hybrids were presented and discussed.

4.1.1 Gradation of aggregates

Figures 4.1 and 4.2 showed the gradations for fine and coarse aggregates indicating a Zone 3 river sand coarse aggregate as per 1S 383 (1970), which is ideal for concrete production. The particle size distribution of the coarse aggregate used for this experimental work ranges between 4.75 mm to 19.10 mm, having a smooth 'S' curve shape which expresses an even distribution of grain sizes across the different coarse aggregate sieves and as such is considered well graded and suitable for concrete production.

.

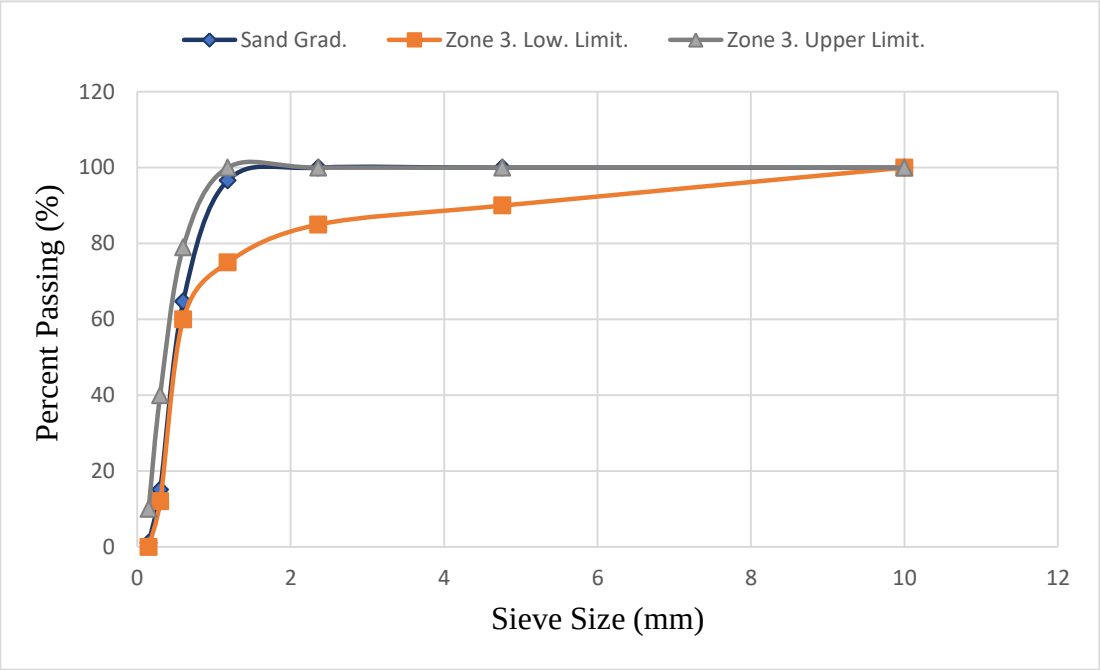

Figure 4.1: Gradation of fine aggregate

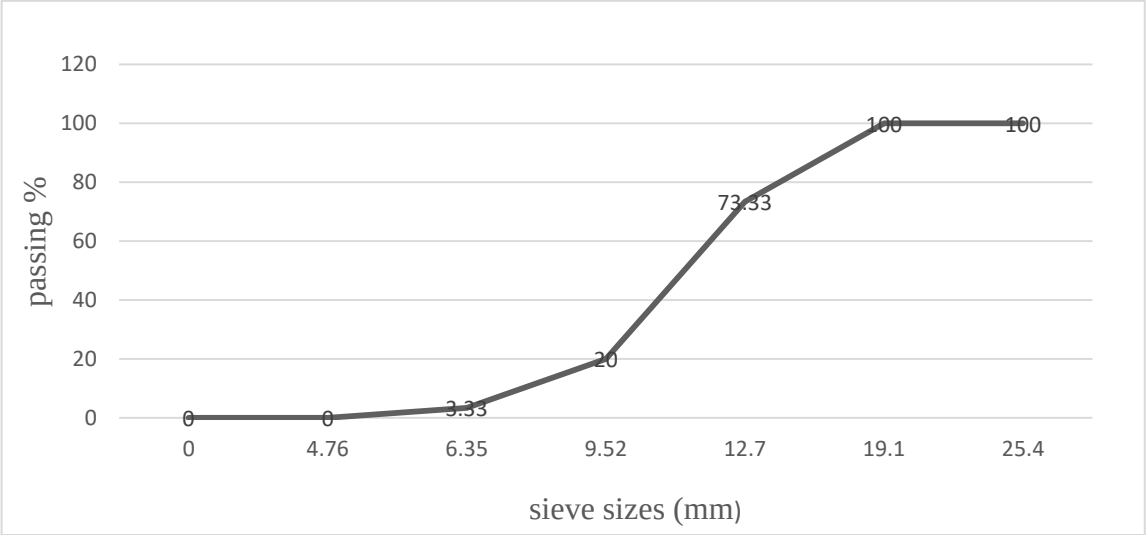

Figure 4.2: Gradation of coarse aggregate

4.1.2. Effect of Calcination on the Colour of Agro-Pozzolans

Periwinkle shell when pulverised atmospheric temperature, has a Manilla/Pale Ivory-BS2660-3040 colour as can be seen in Plate. 4.1. It however changes in colour at increasing calcination temperatures ranging from Cobweb/BS2660-3036 at 200^{o}C to Dark Castle Grey/BS2660-7089 at 800 ^{o}C. Clam shell ash did not change in colour upon calcination as much as periwinkle shell ash as seen in Plate 4.1. Between ATM and 800 ^{o}C, a range of milk coloured shades was observed; from Silver/BS2660-9093 at ATM to Flake Grey/BS2660-9094 colouration at 800 ^{o}C was observed. This is a preliminary indication that higher temperatures are required for clam shell when compared to that of periwinkle shell. Having established that PSA ashes earlier that CSA, the synergistic effect combined with temperature at calcination on the colouration of all 35 samples are as shown in Plate. 4.3.

An increase in CSA content generally increases the brightness of the material and suggests a need for higher calcination temperature.Alternatively, the higher the PSA content the darker the colouration of the hybrid material which suggest a lower calcination temperature requirement

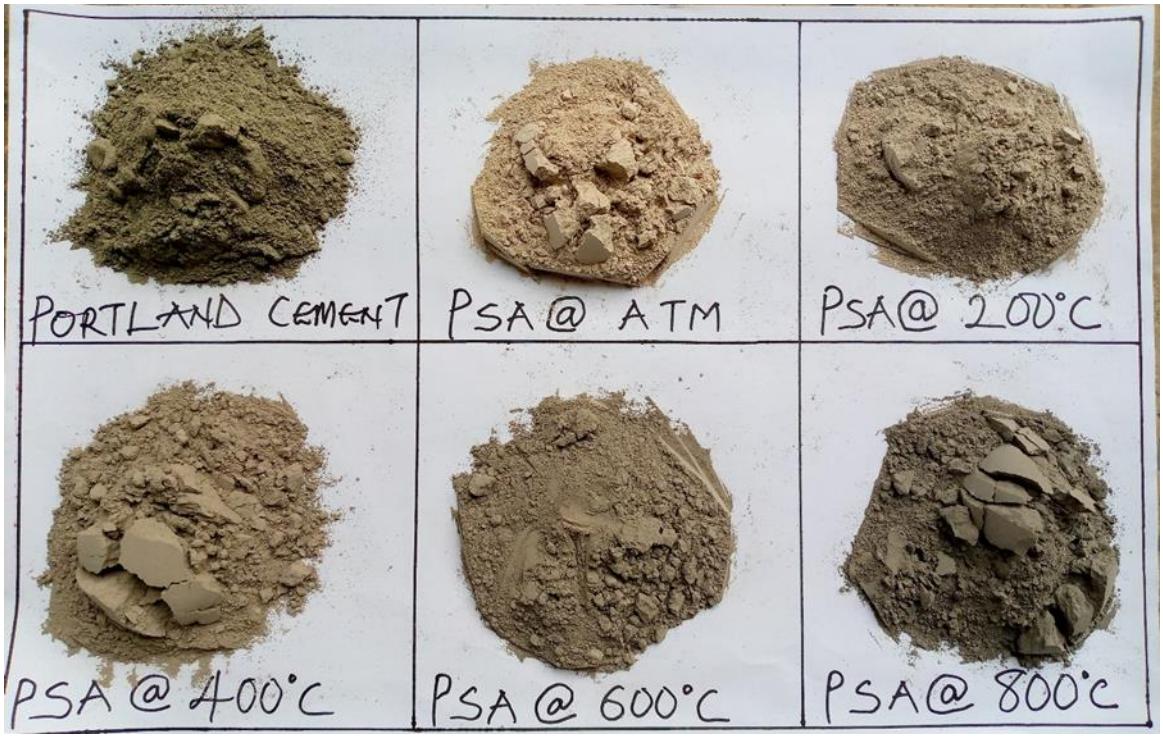

Plate 4.1: Calcination temperature variation on the colour of PSA

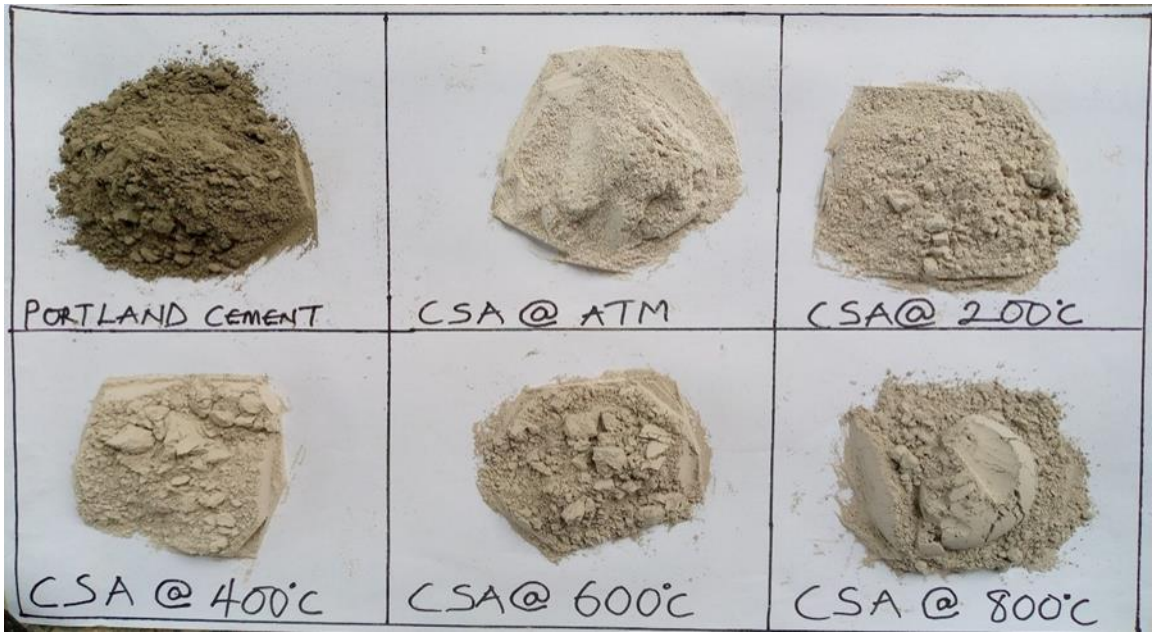

Plate 4.2: Calcination temperature variation on the colour of CSA

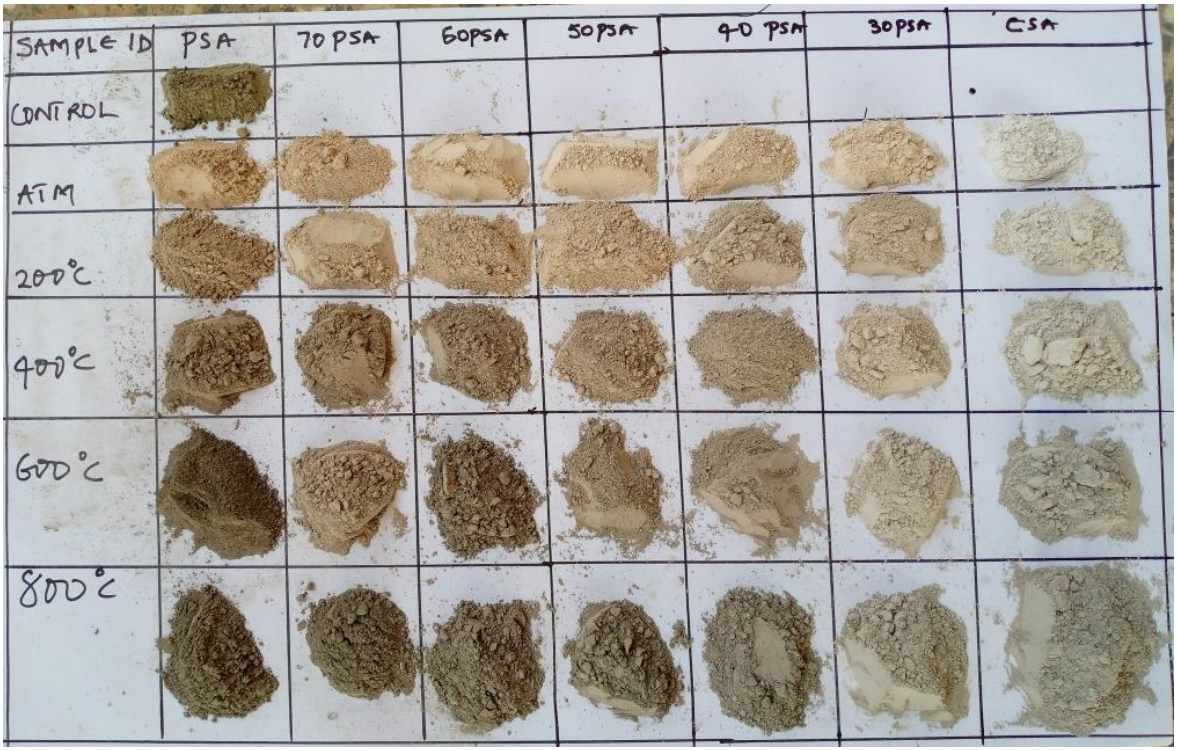

Plate 4.3: Calcination temperature and hybrid ratio variations on the colour of HAP

4.1.3. Effect of Calcination on the Fineness of Agro Pozzolans

Results on Figures 4.3, 4.4 and 4.5 reveals clearly that increasing calcination temperature enhances the fineness of the sample. This is scientifically logical seeing that higher temperatures leads to the expansion and breaking of bonds that make materials monolithic. It can however be seen that optimum temperatures for all synergies but for 50% PSA, are at 800 ^{o}C. In terms of Synergy, linear trend between CSA concentration and the fineness was observed, although not perfectly linear, it was seen that higher CSA content could yield better fineness. 100% CSA at 800 ^{o}C was the best result in terms of fineness having a fineness of 38.43% retained on the 90 µm sieve, which was 98.5% of PLC with a fineness of 37.5% retained the 90 µm sieve.

The cement industry should however note that whilst calcination temperature enhances fineness, increasing calcination temperature has a direct relationship with energy demand, cost and CO_2 emissions. whilst it is elementary to understudy the roe of calcination temperature on fineness, more attention will be made on the mechanical, durability and sustainability indices of the pozzolans before drawing a conclusion on the optimal calcination temperature relative to pozzolan type.

,

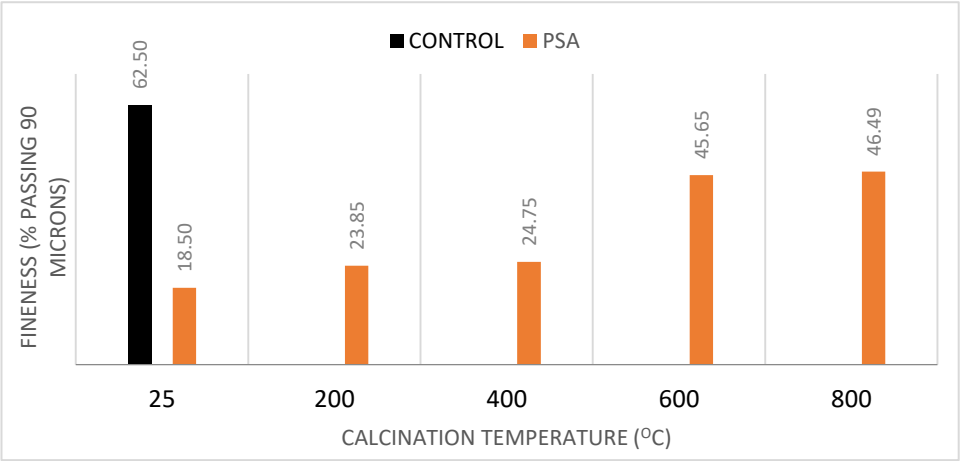

Figure 4.3: **Calcination temperature variation on the fineness of PSA**

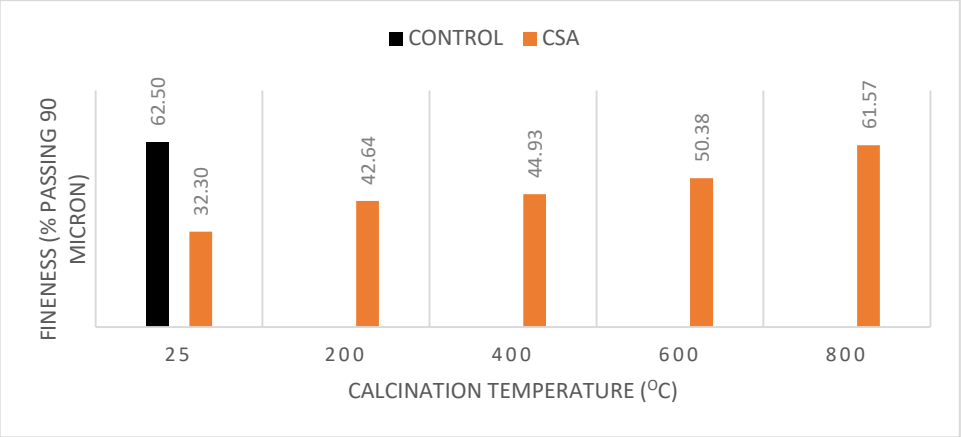

Figure 4.4: **Calcination temperature variations on the fineness of CSA**

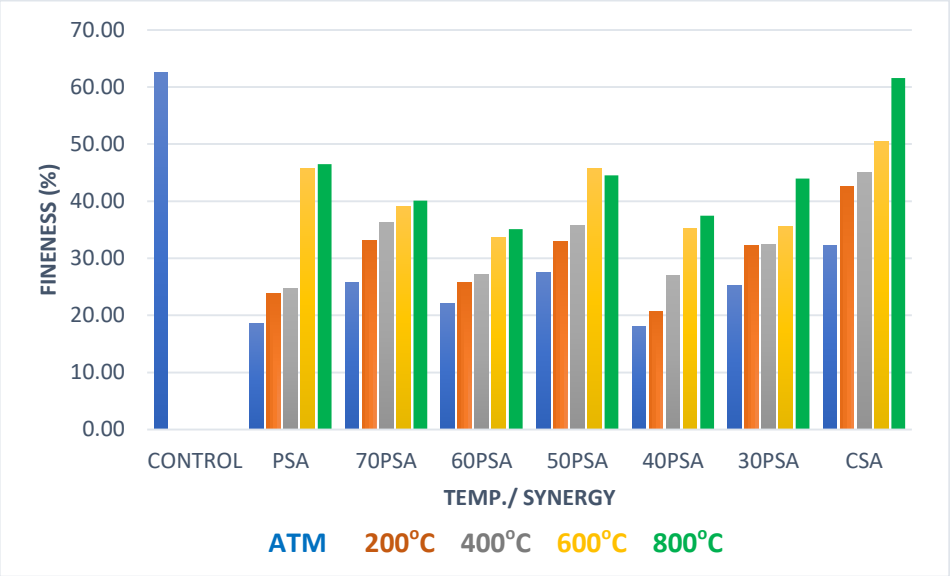

Figure 4.5: Calcination temperature and synergistic ratio variation on the fineness of HAP

4.1.4. Effect of Calcination on the Specific Gravity of HAP

Although the outcome of the calcination of CSA and PSA on specific gravity was largely the same as that of fineness, a drop in specific gravity was seen at 800 ^{o}C. According to Figures 4.6, 4.7, and 4.8, this drop was seen for all synergies. For the five synergies under investigation, calcination temperatures of 400 °C and 600 °C yielded the best specific gravities. The greatest specific gravity ever observed for 60P at 400 °C, however, was 3.14, which was 0.32% higher than the control value, and this was within the sample size (3.13). Hence, all synergies between 400 °C and 800 °C exhibited significant hydraulic parameters and would require sufficient water to binder ratio.

Specific gravity relates to how many times a material is heavier than water. However, in simple terms, materials with higher volume possess lower specific gravity at constant mass. Such materials will require a higher water/binder ratio to achieve hydraulicity and this is a negative implication for the strength property of concretes. It is therefore noteworthy that although 800 ^{o}C gave the best fineness, at that temperature, a significant drop in specific gravity was observed.

The role of specific gravity of cementitious materials hasn't been given much attention, however, noting the specific gravity of the material at desirable conditions is important as this will guide against alterations and errors in the production process. A simple illustration is; if the optimum specific gravity of the pozzolans where to be obtained as 3.14 (yielding the most desirable mechanical and durability indices of the concrete), the fineness of the samples and humidity of the environment where the sample is stored, must be kept constant in all other production scenarios in order to maintain the obtained specific gravity.

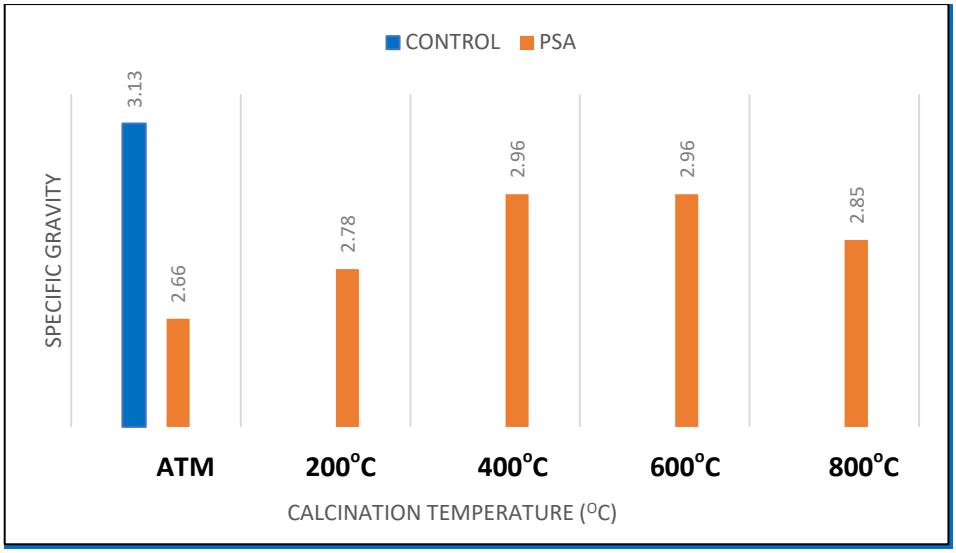

Figure 4.6: Calcination temperature variation on the specific gravity of PSA

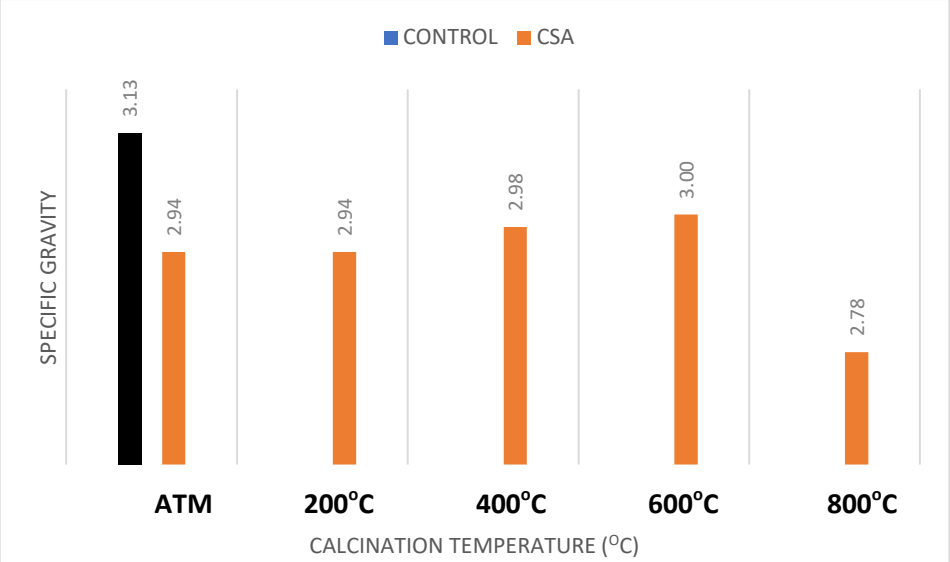

Figure 4.7: Calcination temperature variation on the specific gravity of CSA

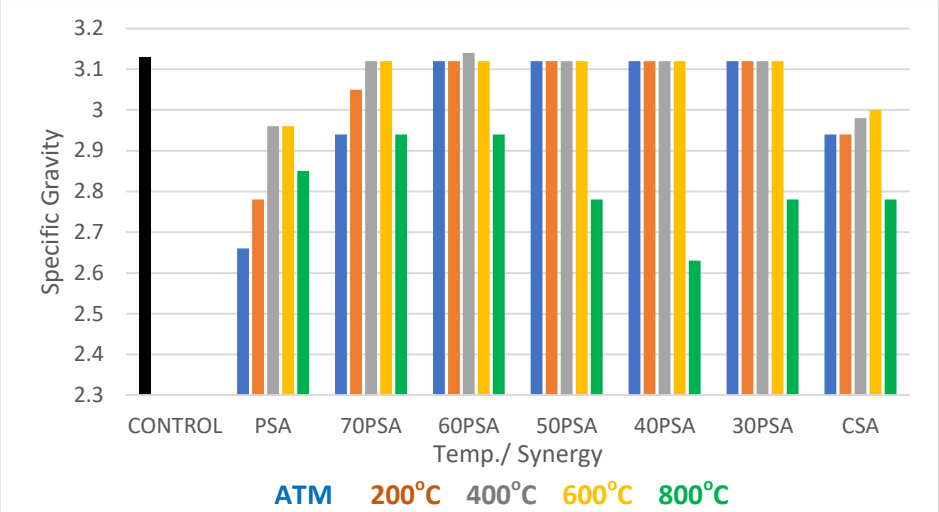

Figure 4.8: Calcination temperature and synergistic ratio variation on the specific gravity of HAP

4.1.5. Calcination and synergistic ratio variation on the Slump/Water Demand of HAP

Figures 4.9 and 4.10 are slump results for all specimens at 40% and 50% cement replacement levels. The primary pattern in calcination temperature is that slump gets high as temperature rises. However, at 50% replacement level, the trend was quite similar to that of specific gravity, revealing a sharp drop in slump at 800^{o}C.

Figures 4.9 and 4.10 show that a sine wave-like trend cresting at 60PSA and troughing between 40P and 30P is generated in terms of synergistic ratio. Water demand of concrete reduces with decreasing PSA up until 60P, increases between 60P and 40P, and then drops once again between 40P and 100CSA; representing the earliest indication of the affinity of PSA and CSA to water demand in concrete.

From Figure 4.10, the slump at 60P/600 ^{o}C was observed to be 165 mm which is approximately 22.22% greater than the control at 135 mm.

The ratio of water to total binder increases with increase in slump and reduces proportional to water demand. At constant water to binder ratio (w/b = 0.55), slump reduces as with increase water demand and increases with strength of concrete, however, excessive slump would imply excess water, which would lead to cement bleeding and subsequent loss in strength.

The effect of calcination temperature on water demand of PSA as represented by the slump, indicates that increasing calcination temperature reduces water demand up to 600 ^{o}C before falling at 800 ^{o}C. This implies that ultimately strength indices of PSA cement blended concrete will be positively affected by calcination up to a temperature of 600^{o}C. The trend obtained for CSA and the hybrid was similar to that of PSA. Hence both primary agro-based pozzolans and the hybrid require calcination treatment at about 600^{o}C for optimum water demand.

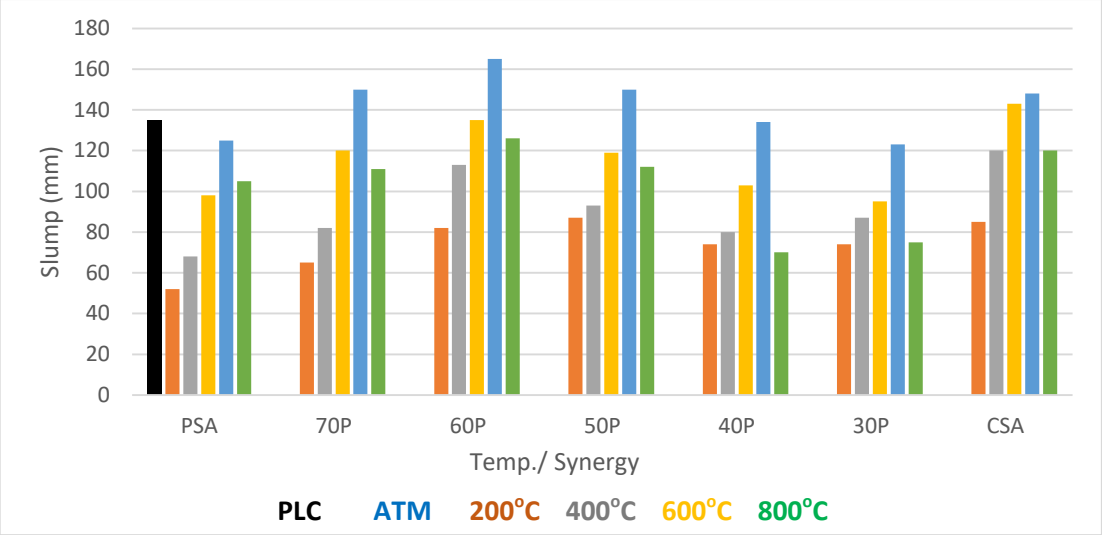

Figure 4.9: Calcination and synergistic ratio variation of HAP on the workability of HAP cement blended concrete at 50% CRL

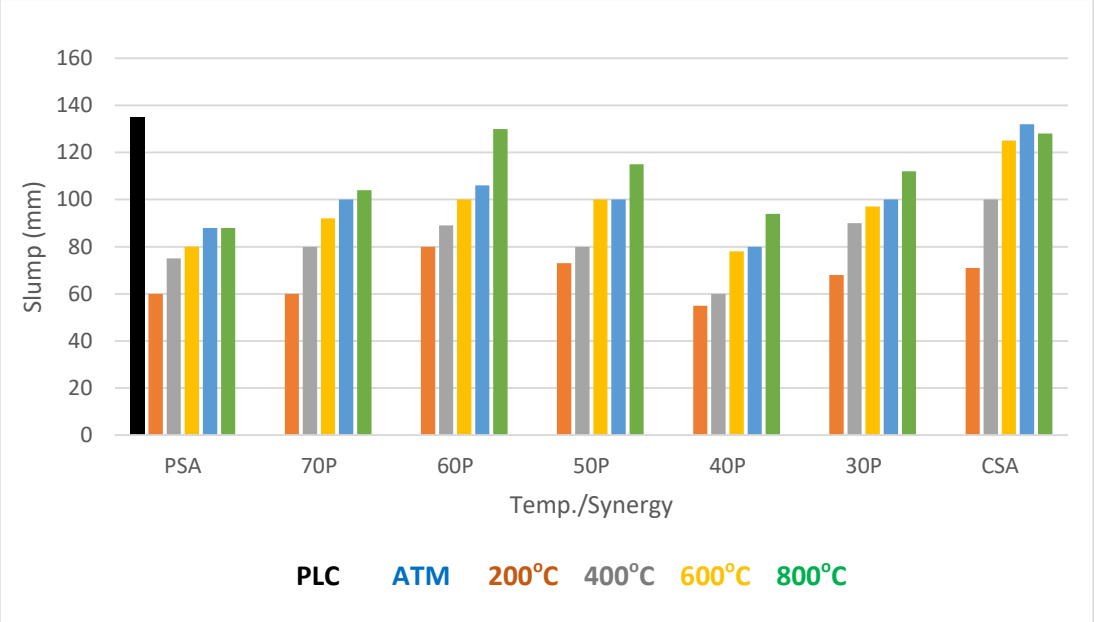

Figure 4.10: **Calcination and synergistic ratio variation of HAP on the workability of HAP cement blended concrete at 40% CRL**

4.2. Mechanical Properties of Agro-based Pozzolan Cement Blended Concrete

The mechanical properties covered are compressive strength and flexural strength. The next six sub sections will cover results and discussions on the mechanical properties of the three main types of pozzolans covered.

4.2.1. Calcination and mixture configuration variations on the compressive strength of periwinkle shell ash cement blended concrete

Figure 4.11 express the relationship between the varying calcination and synergistic ratio levels of PSA to the strength of PSA cement blended concrete. A steady reduction in strength was observed with increasing cement replacement level.

Optimum replacement level for PSA produced at 800^{o}C was at 20% level having a compressive strength of 22.95 N/mm^{2}. This was observed to be 82.7% of the control strength of 27.74 MPa. Important observation from the results show that a total of three specimens met the requirement for cement blended concrete in terms of strength activity index. These are at 600 ^{o}C (20%), 800 ^{o}C (20%) and 800 ^{o}C (30%) having compressive strengths of 21.55 MPa, 22.95 MPa, and 22.55 MPa, with strength activity indexes of 77.7%, 82.7% and 81.3% respectively. These three could hence be incorporated into concrete structures for plain concrete works.

Design factors and observed responses as input and output data for the mechanical and durability properties of PSA cement blended concrete are as shown in Table 4.1. This is raw material used by Design Expert in PSA data analysis, model development and optimisation.

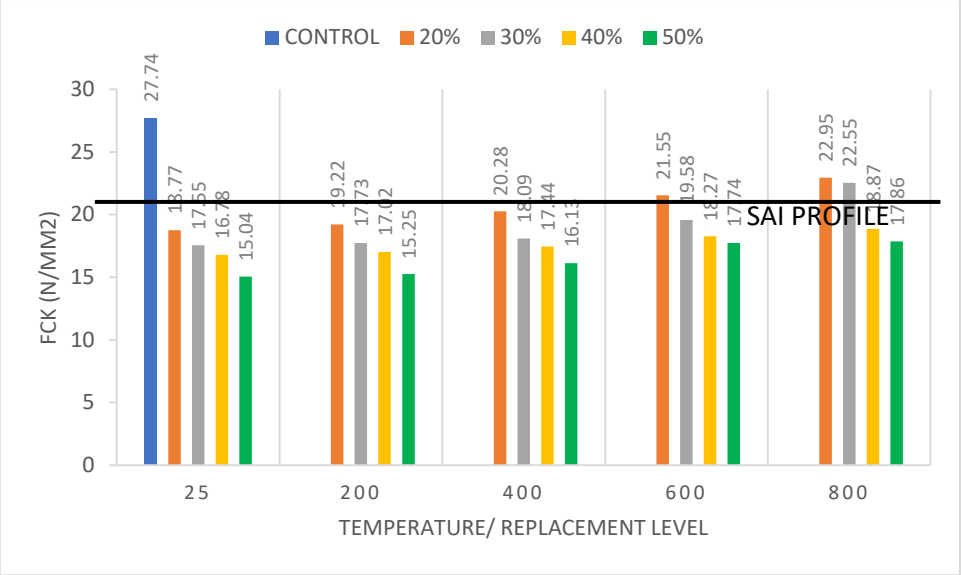

Figure 4.11: Effect of varying temperature at calcination on the compressive strength of PSA cement blended concrete at 28 days

Table 4.1: Design factors and responses as data inputs for PSA data analysis, model development and optimisation

Run	Components PC %	PSA %	Factor TEMP. (^oC)	Response 1 COMP.STR. (N/mm^2)	Response 2 WAI (%)	Response 3 CISLI (%)	Response 4 SISLI (%)	Response 5 SIMLI (%)
1	100	0	800	27.74	1.98	24.56	16.47	9.29
2	80	20	600	21.55	1.74	9.14	-14.69	9.01
3	70	30	25	17.55	3.43	15.78	0.25	8.98
4	70	30	400	18.09	3.18	-8.06	-23.2	8.93
5	50	50	400	16.13	3.58	23.62	20.51	8.63
6	80	20	400	20.28	2.89	1.34	-37.58	8.39
7	60	40	200	17.02	3.52	3.4	-8.99	8.6
8	70	30	600	19.58	1.87	19.63	-0.98	9.02
9	60	40	25	16.78	3.58	11.8	-21.97	9.02
10	70	30	800	22.55	2.05	34.17	22.89	8.98
11	100	0	25	27.74	1.98	24.56	16.47	9.28
12	80	20	200	19.22	3.04	9.19	-14.75	7.82
13	50	50	800	17.86	3.03	21.6	-7.96	8.55
14	50	50	25	15.04	3.83	28.46	-30.99	8.63
15	50	50	400	16.13	3.58	23.62	20.51	8.63
16	80	20	800	22.95	1.86	32.03	-0.89	8.02
17	60	40	600	18.27	2.84	19.34	-10.97	9.13
18	60	40	800	18.87	2.94	22.55	-15.04	8.45
19	80	20	25	18.77	3.17	19.14	-13.2	8.79

The probable model equations for the Compressive Strength (CS) of PSA cement blended concrete is as shown in Equation 4.1 below;

$$\text{CSpsa} = (0.277 * \text{PC}) - (0.588 * \text{PSA}) + (0.012 * PC * PSA) + (8.191 * 10^{-4} * PSA * T) - (1.502 * 10^{-5} * PC * PSA * T) - \left(1.183 * 10^{-4} * PC * PSA * (PC - PSA)\right) + \left(1.422 * 10^{-7} * PC * PSA * T * (PC - PSA)\right) \quad (4.1)$$

Where;

CSpsa = Compressive strength of PSA cement blended concrete (MPa)

PC = Mass concentration of Portland cement in total binder (%)

PSA =Mass concentration of Periwinkle shell ash in total binder (%)

T = Calcination temperature for the production of PSA (^{o}C).

The response summary table (Appendix B-2) indicates that the trend of results for the compressive strength of PSA cement blended concrete is government by a cubic mixture and linear process factors.

Appendix B-3, is The analysed variance and regression coefficients of the model Table for the compressive strength of PSA cement blended concrete. The models generated are of cubic and linear mixtures involving the interaction between two mixture components (PC and PSA) and one-factor component (Calcination temperature). All but one (ABC (A-B)) of the model components had significant interaction negating the hypothesis for nullification ($P < 0.05$). The integrated model has a ratio between the mean square to the residual mean square (F value) of 103.6, and $P < 0.0001$. The P-value obtained implies there is only 0.01% chance of an F-value as large as 103.6 to occur due to noise, hence the model is significant and as such, we do not accept the hypothesis for nullification

Unexplained variations in the response was mainly attributed to the lack of fit component of residuals having a value of 4.33, as such, no pure error was observed in the analysis, however, 4.33 predictions by the model fell out of the 228.83 total observations.

An index of the variation between the total observations and the residuals produced a regression coefficient of (R-squared) of 0.9811, which implies a 98.11% prediction capacity. Upon model modification and removal of non-significant model terms, the R-squared was adjusted to 0.9716.

For optimisation and prediction preferences, the Adjusted R-square was further reduced to a Predicted R-Square of 0.9585 to allow for the model's ability to predict variations outside the inputted observations. The difference between Adjusted R-square and Predicted R-Square was observed to be greater than 0.2 hence both R-squares can be said to be in reasonable agreement with each other indicating the absence of a large block effect, outliers or model errors.

Adequate Precision indicated that the signal to noise ratio is 34.681. This is 774.5% greater than the minimal requirement of4 and contributes to the acceptability of the model.

Other notable observations are the Standard error, mean, coefficient of variance, predicted residual error sum of squares, -2Log likelihood, BIC and AICc having respective values of 0.6, 19.59, 3.07, 9.53, 25.84, 43.5 and 44.84.

The Standard error of 0.6 over a mean of 19.59 is statistically reasonable, and the percentage error of the model, derived from the ratio of the Standard error and the mean (Coefficient of Variance) was observed to be 3.07% and categorised as statistically 'very good' seeing that it falls below 10%. Appendix B-4, represents the coefficients for the individual components of the model, their degrees of freedom, standard error, 95% low and high confidence intervals, and variation inflated factors.

The coefficient generated for the model terms are analysed using the variation inflated factors (VIF). The VIF's obtained are within the acceptable range of 1 – 10, which implies the absence of multicollinearity, as such no significant interaction between the independent variables was observed. This therefore means that the model can allow

for fixing all but one independent variable and monitoring the effect of the unfixed on the dependent variable.

Accordingly, the analysed model with a prediction capacity of 95.85%, having gone various checks, has proven to be statistically satisfactory to be used by the industry in predicting variables at levels of interest in a bid to optimise concrete parameters relative to the compressive strength of Periwinkle shell ash blended cement.

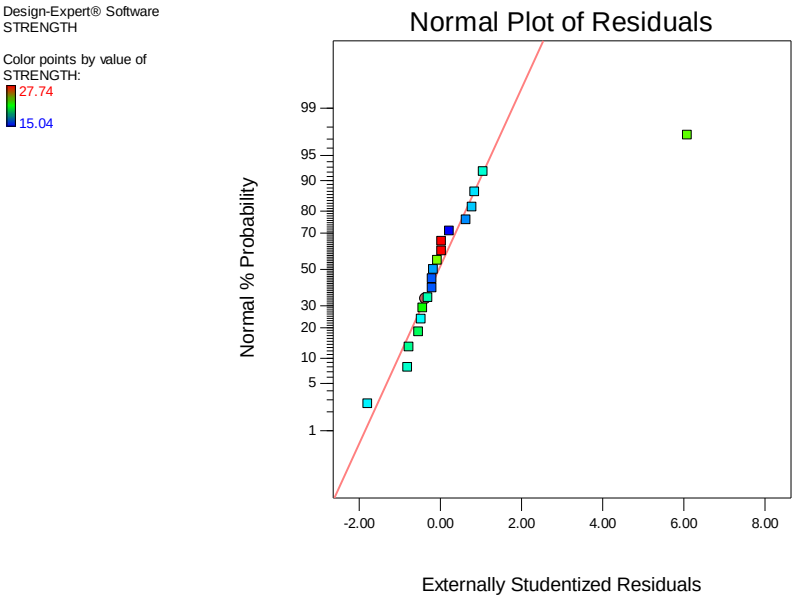

Figure 4.12: Residuals Distribution for the Compressive Strength PSA pozzolan Concrete

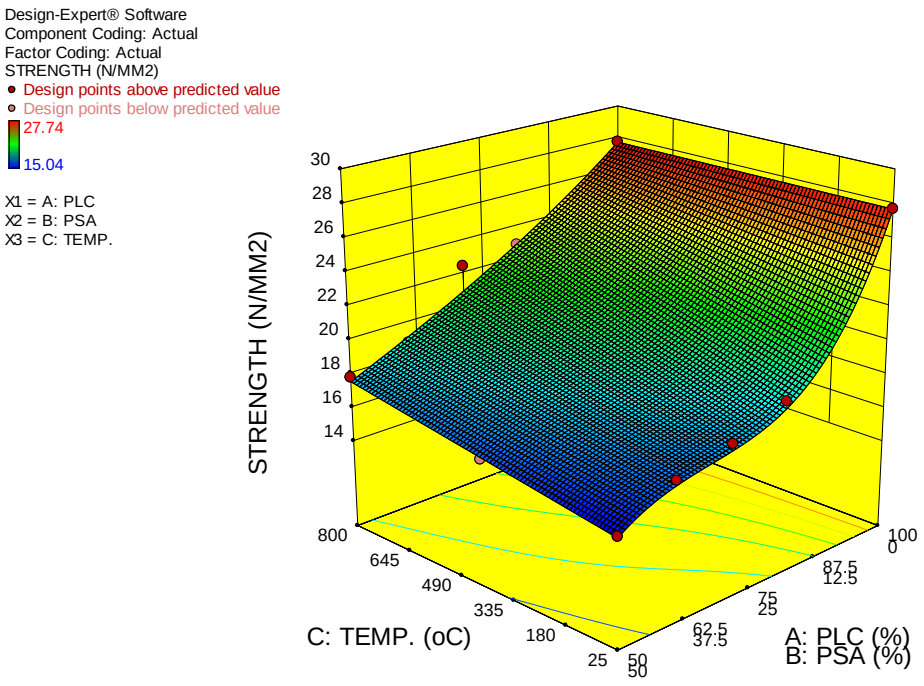

Figure 4.13: Three-dimensional model plot for the compressive strength of PSA cement blended concrete

The externally studentised residuals are distributed well in Figure 4.12, and as a result, the model can be stated to be logically sound and doesn't need to be transformed. Appendix B5, is a representation of the total research factorials, the goals/constraints, lower and upper limits as well as assigned level of importance. The primary objective is enhancing cement replaceability to meet global sustainability demands, as such, Portland cement content was constrained to minimal between a weight replacement range of 50% - 100%. The Periwinkle shell content which is the pozzolanic material was set to maximum on grounds of aiding the sustainability indicators. The process factor (Calcination temperature), was set to minimum as higher temperatures logically imply higher energy demands, CO_2 emissions and cost. The response variables were set to maximum for compressive strength, and minimum for all durability indicators for conventional reasons. Compressive strength was set within a range of 20.8 MPa and 27.74 MPa, as lower and upper limits. This is to ensure that the lowest result obtained does not fall below the 75% SAI criteria.

Optimised model gave 7 best solutions as shown in Table 4.2. Suggested solution had a desirability of 0.567, having a requirement of 80.35%, 19.70%, 425 ^{o}C for PC content, PSA content and Calcination temperature respectively, at optimum responses of 20.8 MPa, 2.46, 2.103, -33.161, and 8.489 for compressive strength, WAI%, CISLI%, SISLI% and SIMLI% respectively.

The effect of temperature of periwinkle shell ash on its inducement to the compressive strength of PSA cement blended concrete can be said to be constant through the boundaries of this experimental framework, having a direct proportionality as seen in Figure4.63. Consequently, increasing calcination temperature yields increasing compressive strength. This was observed to be of similar trend with the findings of Ubong and Effiong (2017), however they observed additionally that a drop in compressive strength at calcination temperatures beyond 800^{o}C is inherent.

Table 4.2: Model Optimisation for PSA Pozzolan Concrete

Solutions N0.	PC	PSA	TEMP.	STR.	WAI	CISLI	SISLI	SIMLI	Desir.	
1	80.352	19.648	424.737	20.800	2.463	2.103	-33.16	8.489	0.567	Selected
2	80.437	19.563	421.871	20.800	2.466	2.069	-33.37	8.491	0.567	
3	80.270	19.730	427.500	20.800	2.460	2.140	-32.96	8.488	0.567	
4	80.525	19.475	418.866	20.800	2.469	2.036	-33.58	8.493	0.567	
5	80.108	19.892	432.946	20.800	2.455	2.219	-32.54	8.485	0.566	
6	81.239	18.761	394.72	20.800	2.492	1.891	-35.12	8.510	0.565	
7	86.158	13.842	182.013	20.800	2.662	8.115	-26.565	8.771	0.482	

An established property of cement-based concrete is its ability to increase strength with time. However, Portland cement concrete is known to reach 99% its total compressive strength within 28 days of curing in fresh water, (CIVL 1101, 2021). Additionally, it has been established that at the completion of the hydration cycle of Portland cement, pozzolanic reaction sets in and secondary hydration begins using the silicic acid component from the pozzolan and the portlandite by-product component from the cement hydration process to form secondary binder gel (Walker and Pavia, 2011). Hence further gain in compressive strength of cement blended concrete is inherent at ages beyond 28 days. Yet, whereas this is not a disputable fact, the engineering society is still keen on feasible applicable results at ages 28 days. As such, model developed for 28 days was opined on the 28 day strength activity index criteria for cement blended concrete being positively optimal that later ages will only yield better strengths.

Afif and Haifaa, (2018) modelled the effect of 'Tal Shihan' content, a natural pozzolan, on the compressive strength of concrete. To avoid multiple interactions and multicollinearity between dependent variables, they developed separate models for the compressive strength per curing age tested. Hence time/ concrete age was not made a factor in the design build-up.

The mixture component of the analysis as seen in Figure 4.13 shows a trend in which increasing cement content increases strength and increasing PSA content reduces strength. The findings agree with existing studies (Afif and Haifaa, 2018, and Walker and Pavia 2011,).

Attah *et al*. (2018), Afif and Haifaa (2018), Ubongand Godwin (2017), Walker and Pavia (2011) and many more, having researched at different levels on the use of pozzolans in concrete production process have recommended minimum levels of pozzolans (0 – 15%) considering the observed limitations and loss in strength associated with higher cement replacement levels. Interestingly, the trend observed from this research as shown in Figure 4.63 validates existing results; however, it is noteworthy that the replacement level when optimised by the process factor of calcination temperature was improved to 19.65%. This is novel but perhaps not a

sufficient enough level of increase in the compressive strength of concrete when compared to already existing results.

4.2.2. Calcination and mixture configuration variations on the compressive strength of clam shell ash cement blended concrete

Figure 4.14 is a preliminary indication of the trend of compressive strength developed as a result of mixture configuration and calcination. Optimum replacement level for CSA produced at 800 ^{o}C was observed at 20% having a compressive strength of 23.22 MPa. This was observed to be 83.7% of the control strength of 27.74 MPa. Important observation from the results show that a total of two specimens met the requirement for a cement blended concrete in terms of strength activity index. These are at 600 ^{o}C (20%) and 800 ^{o}C (20%) having compressive strengths of 22.28 MPa, and 23.22 MPa with strength activity indexes of 80.3% and 83.7% respectively. These two could hence be incorporated into concrete structures for plain concrete works.

Making reference to the physical observations (colouration), there appears to be a need to increase the calcination temperature of CSA beyond 800 ^{o}C in a vein to improve on its cement replaceability as a pozzolanic material.

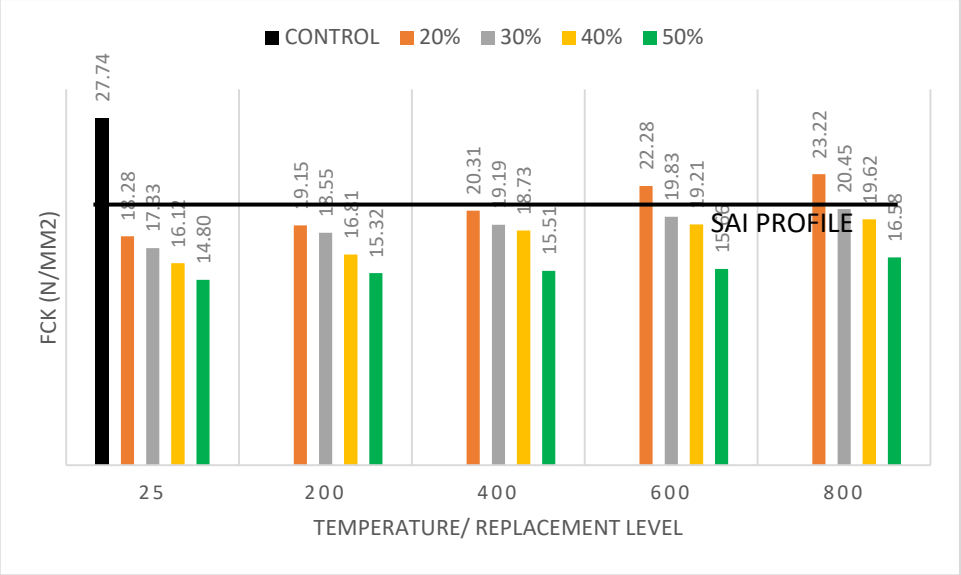

Figure 4.14: Calcination Effect on the Compressive strength of CSA cement blended concrete at 28 days

The design summary page (Appendix C1) indicates that the trend of results for the compressive strength of CSA cement blended concrete is government by a cubic mixture and linear process factors.

Coefficient of regression(Appendix C3) and Analysis of Variance (Appendix C2) for the compressive strength of CSA cement blended concrete, informs that developed model is a cubic mixture component and linear factor model, which has six model classes (linear mixture, AB, BC, ABC, AB(A-B), and ABC(A-B)). Except for ABC(A-B), all model components were significant, refuting the hypothesis for nullification. The Regression coefficient was 0.9919 when the model to cumulative summed up squares ratio was calculated. As a result, adjusted and projected regression coefficients were obtained as 0.9879 and 0.9817, respectively, suggesting a statistically sound model's ability to predict. Standard error was 0.41, with a mean of 19.46 and a 2.1% error margin (C.V). The model's precision was determined to be 53.001, which means that one inaccuracy can be anticipated for every 53 predictions. Given that this is 1225% higher than the permissible related error threshold of 4, the model suggests a sufficient signal and can be utilized to explore the design space.

With the absence of a variance inflated factor higher than 30, the coefficients of the model (Appendix C4) indicates that multicollinearity impact doesn't exist for all the model components, and as such, independent variables can vary independently statistically, which is a useful prerequisite for determining how different isolated causes affect the response variable.

Figure 4.15's illustration of model diagnostics depicts the relative distribution for the model's externally studentised deviations. Thus, the model can be accepted as statistically valid.

Table 4.3: Design factors and responses as data inputs for CSA data analysis, model development and optimisation

Components		Factor	Response 1	Response 2	Response 3	Response 4	Response 5
PC	CSA	TEMP.	COMP.STR.	WAI	CISLI	SISLI	SIMLI
%	%	(oC)	(N/mm2)	(%)	(%)	(%)	(%)
100	0	800	27.74	1.98	24.56	16.41	9.28
80	20	600	22.28	2.08	10.29	-26.17	9.11
70	30	25	17.33	3.17	31.44	10.7	8.47
70	30	400	19.19	3.24	0.5	-36.27	8.86
50	50	400	15.51	4.06	8.66	-10.2	9.04
80	20	400	20.31	2.92	2.94	-33.57	8.93
60	40	200	16.81	3.26	2.28	3.68	9.07
70	30	600	19.83	2.96	6.81	-22.53	8.7
60	40	25	16.12	3.69	25.31	-13.95	9.13
70	30	800	20.45	2.64	18.14	-6.18	8.57
100	0	25	27.74	1.98	24.56	16.41	9.28
80	20	200	19.15	2.96	1.07	-31.6	9.02
50	50	800	16.58	3.69	11.7	14.81	8.96
50	50	25	14.8	4.45	24.19	-1.83	7.98
50	50	400	15.51	4.06	8.66	-10.2	9.04
80	20	800	23.33	2.17	17.21	-5.34	8.85
60	40	600	19.21	3.25	0.44	-16.88	9.04
60	40	800	19.62	3.16	16.85	4.18	8.13
80	20	25	18.28	1.22	28.62	-2.79	8.17

Developed model for the compressive strength of CSA cement blended concrete is as shown in Equation (4.2) below;

$$\mathrm{CScsa} = (0.277 * \mathrm{PC}) - (0.592 * \mathrm{CSA}) + (0.012 * PC * CSA) + (4.550 * 10^{-4} * CSA * T) - (8.047 * 10^{-6} * PC * CSA * T) - \left(1.213 * 10^{-4} * PC * CSA * (PC - CSA)\right) + \left(1.033 * 10^{-7} * PC * CSA * T * (PC - CSA)\right) \quad (4.2)$$

Where;

CScsa = Compressive strength of CSA cement blended concrete

PC = Mass concentration of Portland cement in total binder (%)

CSA =Mass concentration of Clam shell ash in total binder (%)

T = Calcination temperature for the production of CSA (^{o}C).

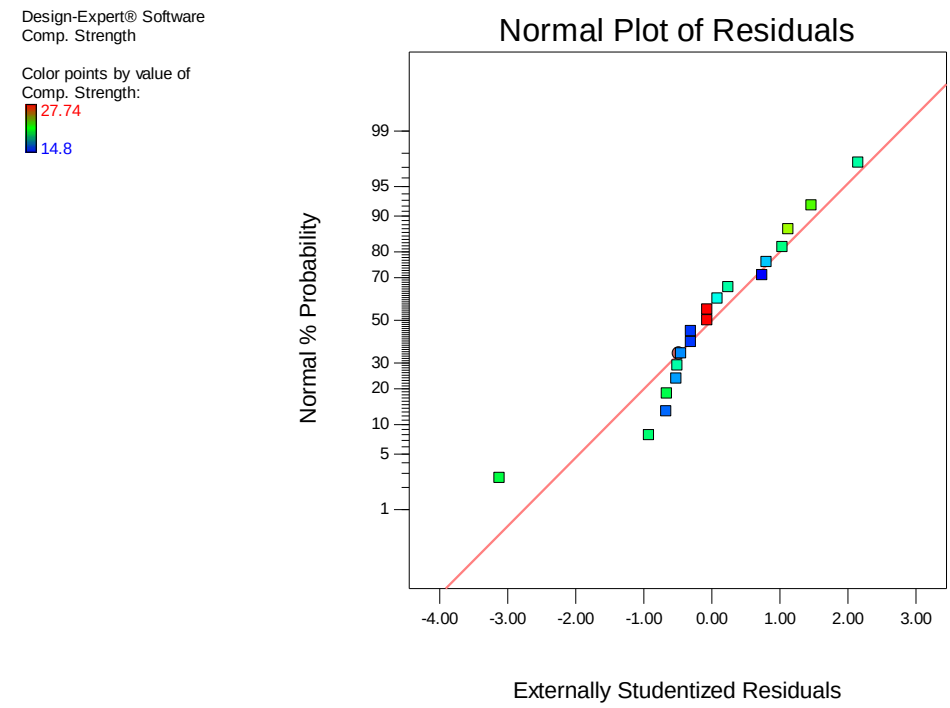

Figure 4.15: Error distribution of the model for the compressive strength of CSA cement blended concrete

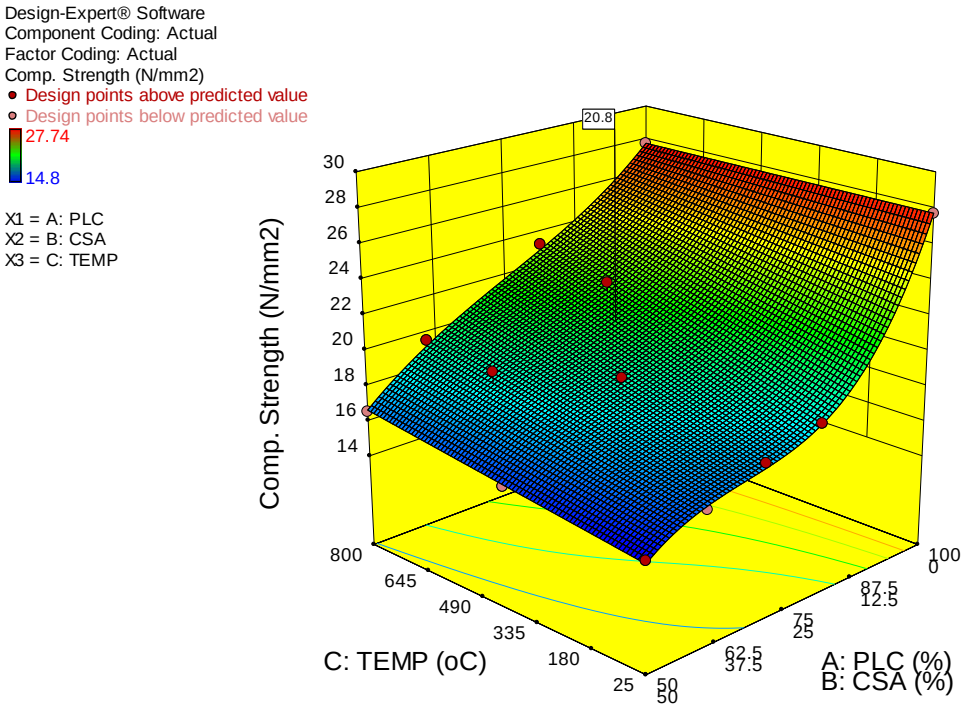

Figure 4.16: Model plot of compressive strength for CSA cement blended concrete

Figure 4.16 represents a cubic mixture interaction and a linear process interaction for the compressive strength of CSA cement blended concrete. The model's process factor component interaction indicates that higher calcination temperature yields higher compressive strength and vice versa. Concurrently, the cubic mixture component indicates the formation of the first crest at about 37.5% CSA concentration and trough at about 25% CSA concentration followed by a continuous rise in compressive strength at increasing PC concentration content.

Olutoge *et al*., (2016), observed a linear interaction for the mixture component at 0%,5%,10%,15%, and 20% of clam content. The linearity observed was decreasing compressive strength at increasing clam content. Strengths measured ranged from 22.56 MPa at 0% CSA concentration to 8.58 MPa at 20% CSA concentration. As such an optimal concentration of 5% CSA was suggested. Bamigboye *et al*., (2020), reviewed on the use of sea shells and forwarded that the mixture of sea shells and cement in concrete has a linear effect on the compressive strength of the concrete however on the decreasing side of the compressive strength, however, between 5% to 15%, concrete water absorption and porosity properties are enhanced when compared to control. Ong, and Kassim (2019), replaced cement to with calm shell ash to concentration levels of 4% - 8% at 2% intervals, they forwarded that within that range, the mixture developed a hugging quadratic curve having its low points at 4% and 8% and its crest at 6% CSA concentration level, they however recommended on the need to investigate on effect of calcination of clam shell ash on the replaceability of cement in concrete. Very similar to Ong and Kassim (2019), Olivia *et al*., (2015) had earlier reported findings using same range of clam shell ash concentration and observing same quadratic mixture effect on the compressive strength of the concrete. They however forwarded 4% replacement level as optimum. Mohammad *et al*., (2017), reviewed sea shells including cockle, clam, oyster, mollusc, periwinkle, snail, and green mussel shell as partial replacements for cement in concrete. 9 papers reviewed between 2007 and 2015, led to their recommendation of 4% - 5% CSA as optimum concentration in concrete, the trend of reviewed results was observed to be approximately linear on the mechanical properties of concrete. Olivia and Oktaviani (2017), experimentally contributed that due to the high concentration of calcium oxide

in clam shell ash, it performed favourably better that 100% cement concrete in areas of setting time, density and strength when used at 4% concentration in concrete.

In respect to the process factor, very little information is available in literature on the effect of calcination on the mechanical properties of clam shell in concrete. Hence, whilst the mixture component and its effect have had a great deal of attention, the combined effect of mixture and temperature factor appears to be novel, however, the linearity for the mixture component effect on compressive strength, as observed in most of the reviewed literature is in tandem with the observations of this research work.

With the introduction of a process factor (calcination temperature), the optimised response of compressive strength of 20.8 N/mm^2 as seen in Table 4.4, was obtained at a mixture configuration of 23.13% CSA:76.87% PC produced at 527 ^oC.

At 20.8 N/mm^2, 75% of the control concrete (100% PC) has been achieved which satisfies the strength activity index criteria for cement blended concrete. Additionally, concrete produced at this specification can be used for various construction works including but not limited to flooring, rigid pavements, structural elements, walk ways, etc.

The cement and SCM industries are therefore encouraged to integrate clam shell in the production of cement and cementitious materials by optimising the production parameters using the model as developed above, all in a bid encourage the global strides of sustainability.

Table 4.4: Optimized solutions of factors and responses for CSA cement blended concrete

Solutions N0.	PC	CSA	TEMP	Comp. Strength	WAI	CISLI	SISLI	SIMLI	Desir.	
1	76.871	23.129	526.812	20.800	2.516	3.055	-31.467	8.654	0.571	Selected
2	76.753	23.247	529.928	20.800	2.521	3.119	-31.323	8.650	0.571	
3	77.171	22.829	518.810	20.800	2.503	2.901	-31.817	8.664	0.571	
4	76.349	23.651	540.616	20.800	2.539	3.359	-30.800	8.638	0.571	
5	76.137	23.863	546.197	20.800	2.548	3.496	-30.508	8.632	0.571	
6	76.026	23.974	549.090	20.800	2.553	3.570	-30.350	8.630	0.570	
7	77.750	22.250	503.186	20.800	2.477	2.648	-32.431	8.686	0.570	
8	81.418	18.582	394.286	20.800	2.329	2.634	-34.678	8.874	0.542	
9	85.906	14.094	208.602	20.800	2.173	9.666	-31.564	9.114	0.452	

4.2.3. Calcination and mixture configuration variations on the Compressive Strength of Hybrid Agro-Based Pozzolan Cement blended concrete

Figures 4.17 – 4.20 are preliminary indicators of the suggested trend of the compressive strength of HAP-cement blended concrete, relative to variations in mixture configuration and calcination temperature.

From Figure 4.17, HAP performed better in strength when compared to the AP, this could be seen at between 70% PSA: 30% CSA and 30% PSA: 70%CSA. All samples produced at calcination temperatures beyond 200 ^{o}C met the Strength Activity Index criteria of 75%. Optimum synergy was at 60% PSA: 40% CSA produced at 800 ^{o}C with a compressive strength of 27.04 MPa, and a SAI of 97.5%.

From Figure 4.18, a general drop in compressive strength was observed between 20% and 30% cement replacement levels for all synergistic ratios. At 30% cement replacement level, the synergy of 60% PSA: 40% CSA was observed to be the likely optimum synergy and at a temperature of 800 ^{o}C, having a compressive strength of 25.42 MPa with a SAI of 91.63%. At all synergies, compressive strength increases steadily with increase in calcination temperature. The general trend appeared like that of an arc, having its crest at 60% PSA: 40% CSA. In regards to Strength Activity Index, 50% PSA: 50% CSA and 60% PSA: 40% CSA specimens have the best performance at all temperatures, and met the SAI criteria.

From Figure 4.19, a general drop in compressive strength was observed between 30% and 40% cement replacement levels for all synergistic ratios. 60% PSA: 40% CSA was observed to be the tentative optimum synergy and at a temperature of 800 ^{o}C. At all synergies, compressive strength increases steadily with increase in calcination temperature. The general trend appeared like that of a cosine wave having its crest at 60% PSA: 40% CSA. In regards to Strength Activity Index, 60P specimens have the best performance at temperatures between 400 ^{o}C and 800 ^{o}C, the SAI criteria was met. However, other specimens such as 70% PSA: 30% CSA at 800 ^{o}C, and 30% PSA: 70% CSA at 800 ^{o}C at lower strengths when compared to that of 60% PSA: 40% CSA, also met the SAI requirements at 40% cement replacement level. Likely

optimum result of 23.71 MPa with a SAI of 85.47% was obtained for 60% PSA: 40% CSA at 800 ^{o}C.

From Figure 4.20, the trend with respect to calcination temperature remains the same; increasing calcination temperature accompanied by increasing compressive strength of specimens. Compressive strength reduces steadily with increasing cement replacement level. At 50% cement replacement level, trend in terms of synergy had the shape of an arc with its crest at around 60P. likely optimum result obtained was at 60P produced at 800 ^{o}C having a compressive strength of 19.73 MPa and a SAI of 71.12% which is lower than the SAI criteria for a pozzolanic concrete. At this replacement level (50%), no specimen met the SAI criteria, as such, this research has been successful in replacing cement up to 40% but further work on the properties of the pozzolans must be done to improve cement replaceability beyond 40%.

It is however noteworthy that while the primary pozzolans could barely replace 20% of cement in previous works, results at this level of study informs the possibility of successfully replacing 40% of cement in cement blended concrete meeting the SAI criteria.

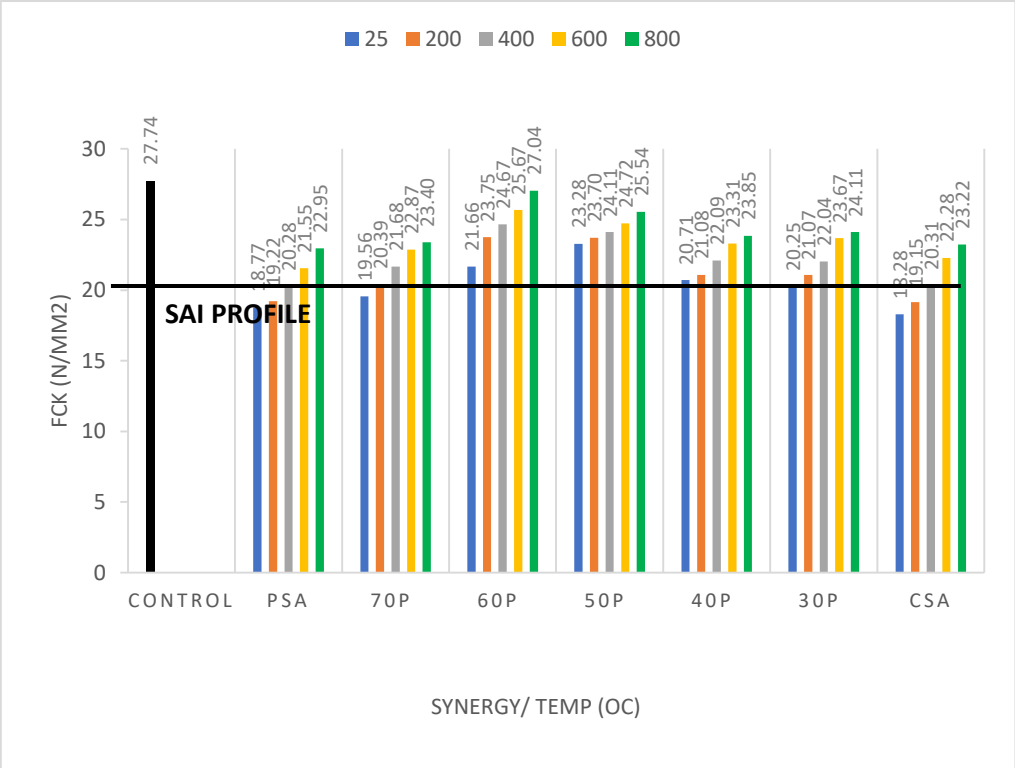

Figure 4.17: Calcination temperature and hybrid ratio variations on the 28 days compressive strength of HAP Concrete at 20% cement replacement level

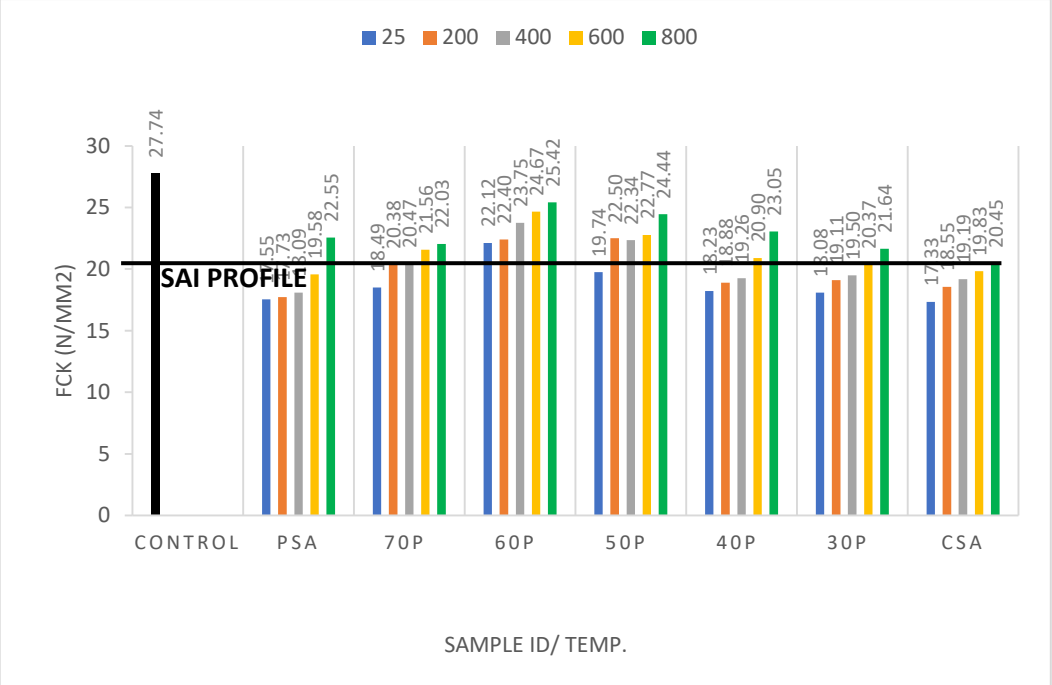

Figure 4.18: Calcination temperature and hybrid ratio variations on the 28 day compressive strength of HAP Concrete at 30% cement replacement level

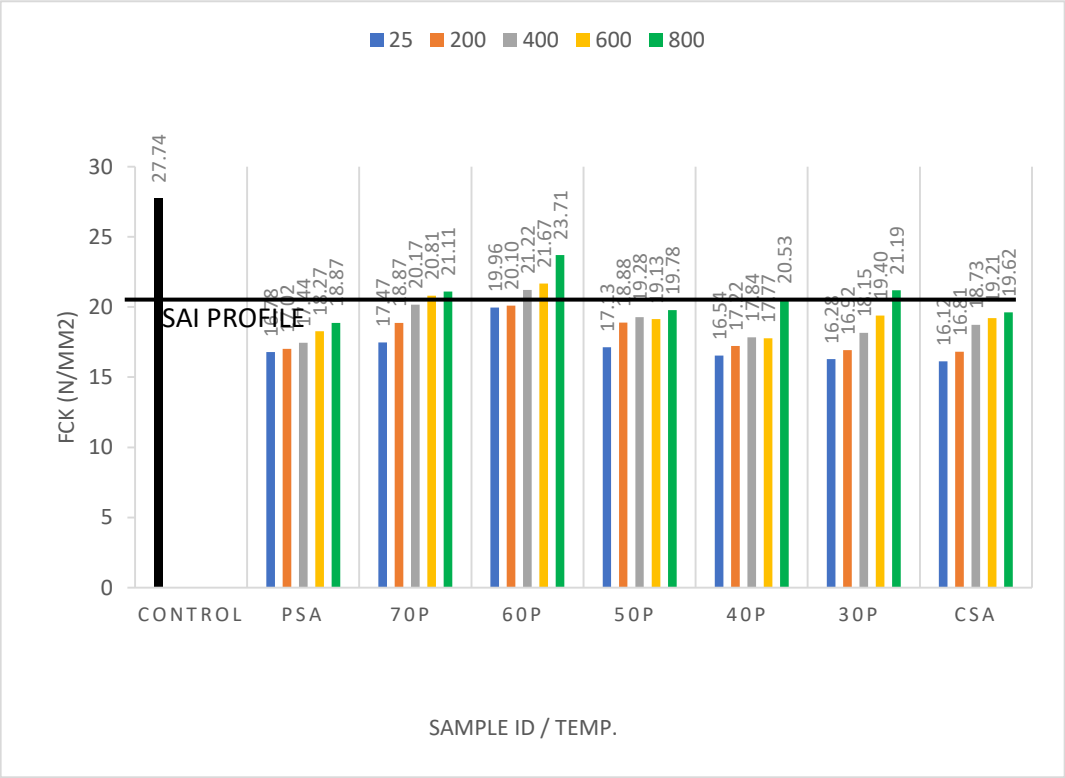

Figure 4.19: **Calcination temperature and hybrid ratio variations on the 28 days compressive strength of HAP Concrete at 40% cement replacement level**

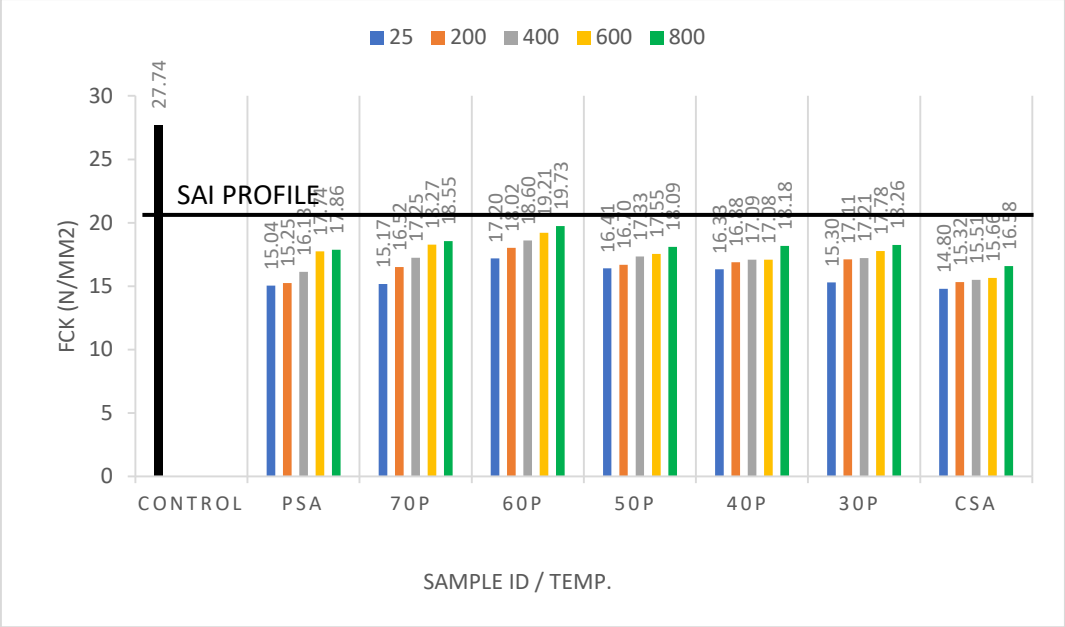

Figure 4.20: Calcination temperature and hybrid ratio variations on the 28 days compressive strength of HAP Concrete at 50% cement replacement level

Experimental inputs for modelling and optimisation of the independent and dependent variables of PSA and CSA hybrid Pozzolan cement blended concrete is as shown in Table 4.5

Table 4.5: Experimental inputs for data analysis, modelling and optimisation of HAP blended cement concrete

Run	A:PC	B:PSA	C:CSA	D:Calc. Temp	Comp. Strength	WAI	CISLI	SISLI	SIMLI
	%	%	%	^oC	N/mm^2	%	%	%	%
1	50	25	25	400	17.33	3.87	16.07	9.8	9.11
2	70	0	30	25	19.26	3.16	31.44	-0.14	8
3	50	0	50	25	14.8	4.45	24.19	-1.83	7.98
4	50	0	50	800	16.58	3.69	11.7	14.81	8.96
5	60	24	16	200	20.1	3.45	11.59	0.5	9.14
6	70	0	30	400	19.26	3.16	0.5	-0.14	8
7	80	0	20	400	19.26	3.16	2.94	-0.14	8
8	50	25	25	800	18.09	2.96	19.13	15.65	9
9	70	30	0	400	19.26	3.16	-8.06	-0.14	8
10	50	0	50	400	15.51	4.06	8.66	-10.2	9.04
11	100	0	0	800	27.74	1.98	24.56	16.47	9.28
12	60	24	16	600	21.67	2.74	16.1	-17.12	9.16
13	80	20	0	400	19.29	19.29	1.34	19.29	8.39
14	80	20	0	25	19.29	19.29	19.14	19.29	8.79
15	80	0	20	25	23.22	1.22	28.62	-2.79	8.71
16	50	25	25	600	17.55	3.62	4.78	-5.19	9.09
17	100	0	0	25	27.74	1.98	24.56	16.47	9.28
18	60	40	0	800	18.87	2.94	22.55	-15.04	8.45
19	70	30	0	600	19.58	1.87	13.63	-0.98	9.02
20	50	50	0	400	16.13	3.58	23.62	20.51	8.63
21	60	24	16	400	21.22	3.18	14.12	2.26	9.08
22	50	50	0	25	15.04	3.83	28.46	-30.99	7.89
23	50	50	0	800	17.86	3.03	21.6	-7.96	8.55
24	60	0	40	800	19.82	3.16	16.85	4.16	8.13
25	50	25	25	25	16.41	4.49	18	-0.41	10.24
26	60	16	24	600	17.77	2.49	12.61	-8.64	8.78
27	60	16	24	200	20.1	3.86	9.7	9.97	9.06
28	80	10	10	400	19.29	19.29	14.44	19.29	8.95

Analysis of variance (Appendices D2) and regression coefficient (Appendices D3) for the compressive strength of HAP concrete, indicates that the equation (model) as developed, is inclusive of cubic mixture and linear process factor components. The developed equation has sixteen components for which all but BCD was significant, hence the integrated model was significant with a confidence interval much greater than 95% ($P<<0.05$) which validates the model. The regression coefficient was 0.9963 when the model to cumulative summed up squares ratio was calculated. As a result, adjusted and projected regression coefficients were obtained as 0.9901, and 0.9162, respectively, suggesting a statistically valid model to make predictions

Standard error was 0.31 over a mean of 19.22, which produced a minimum coefficient of variation of 1.61%. The adequacy of the model's precision was 52.42, which implies that an error could exist in every 52.42 predictions. In essence, the least expected error of 4, is significantly above the model's maximum probable error, accordingly, the model's signal is adequate enough within its design scope for statistical simulation purposes. Statistical check on model's performance as seen in Figure 4.21 indicates a relatively linear error distribution that was studentised. Consequently, the model can be regarded as statistically accurate..

The coefficients of the model (Appendix D4) indicates that multicollinearity impact is absent for all model components, as no factor exceeded 10 by reason of inflation as a result of the model's variance. This suggests that independent variables can be varied statistically, which is a useful prerequisite for examining the impact of changing independent factors on responses.

At a regression coefficient of 0.9162, the model has the capacity to predict the 28 day compressive strength of PSA/CSA cement blended concrete at a statistically acceptable level of 91.62% when the calcination temperature, synergy as well as cement replacement level fall outside the boundaries of the data used in this study. As such, the model (Equation 4.3) is recommended for use in the cement and SCM industry.

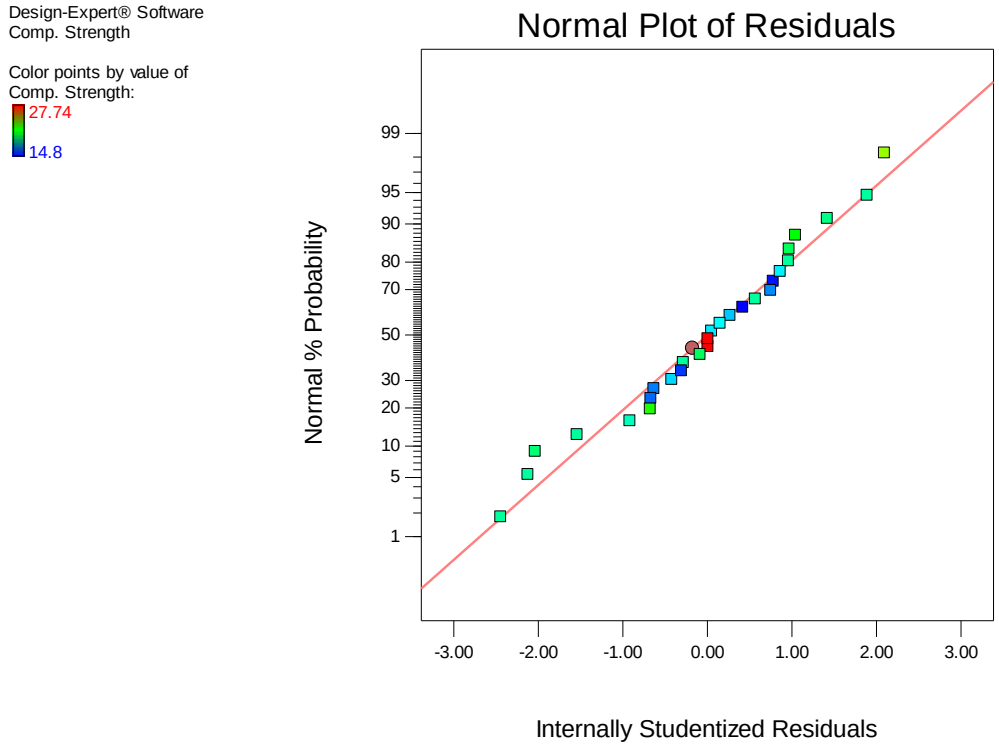

Figure 4.21: Error distribution of the model for the compressive strength of HAP concrete

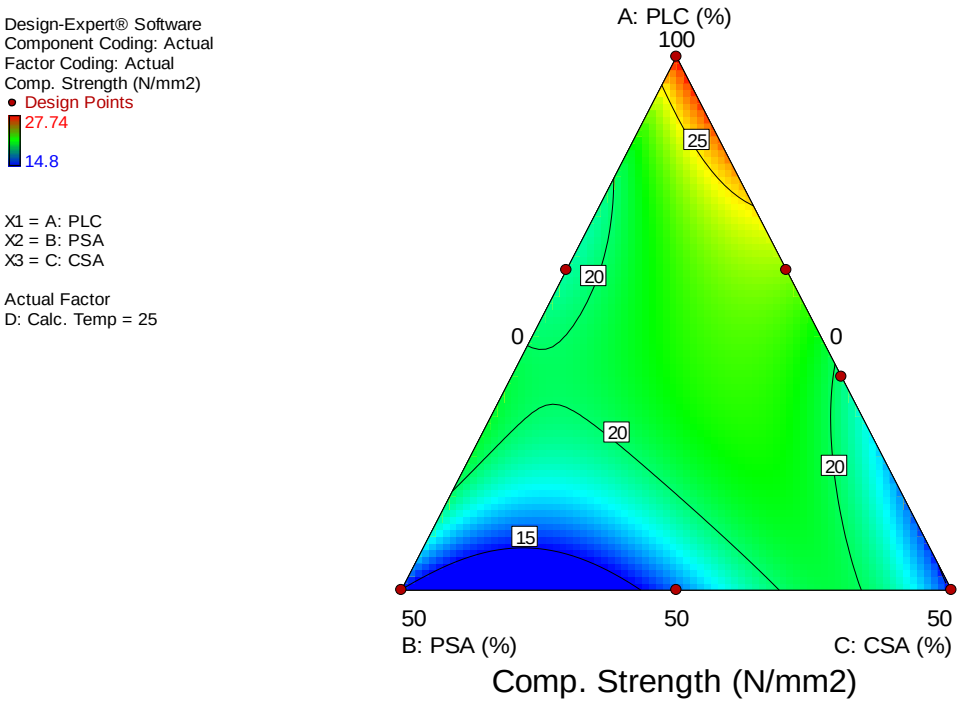

Figure 4.22: Three-dimensional model at 25^{o}C for the compressive strength of HAP concrete

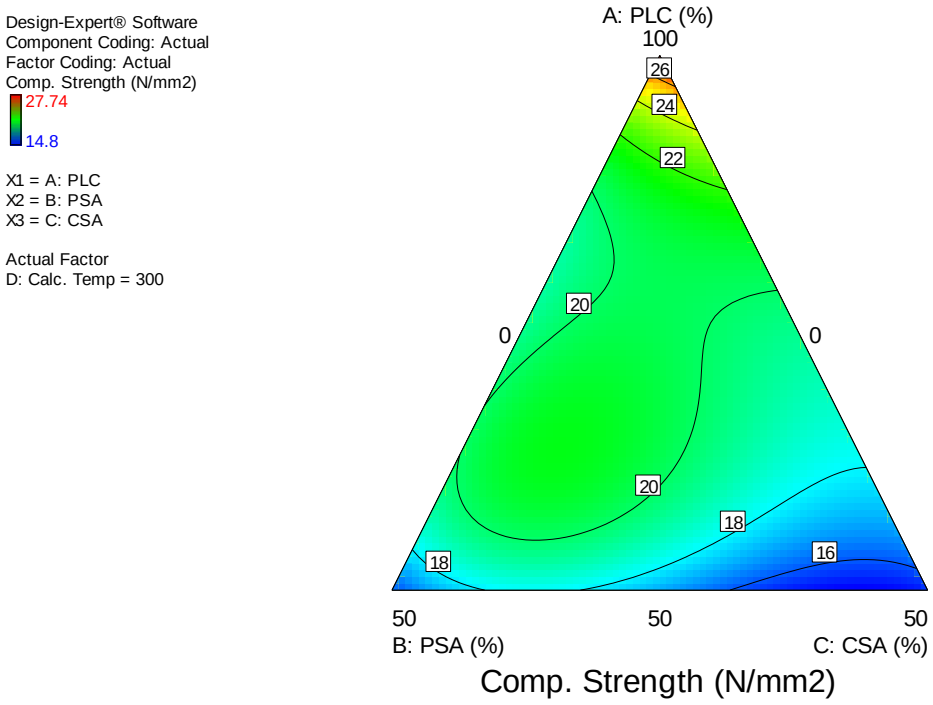

Figure 4.23: **Three-dimensional model at 300^{o}C for the compressive strength of HAP concrete**

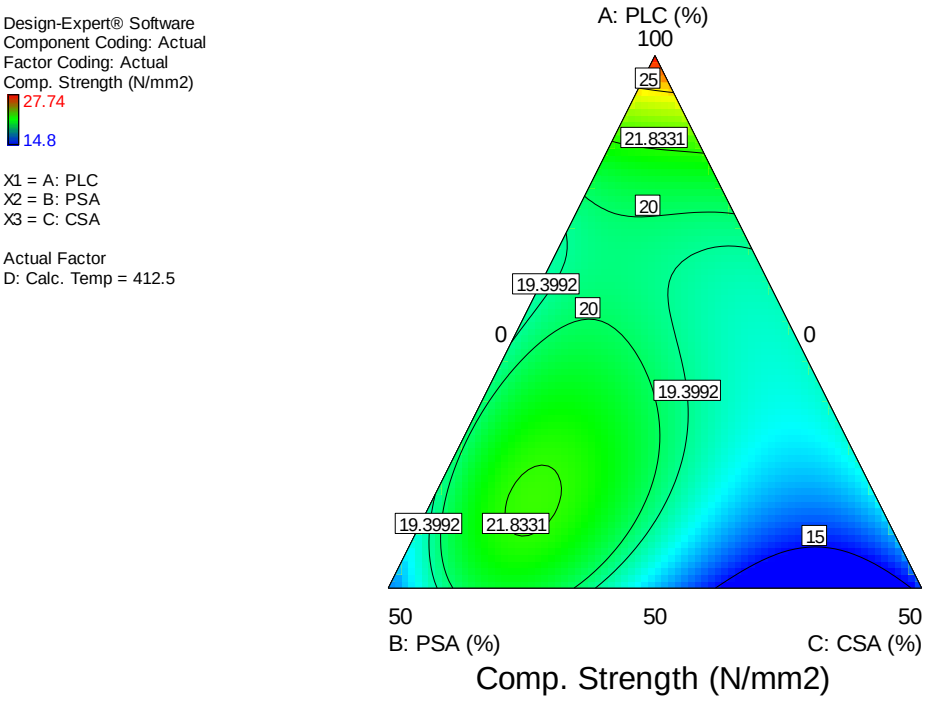

Figure 4.24: **Three-dimensional model at 412.5^{o}C for the compressive strength of HAP concrete**

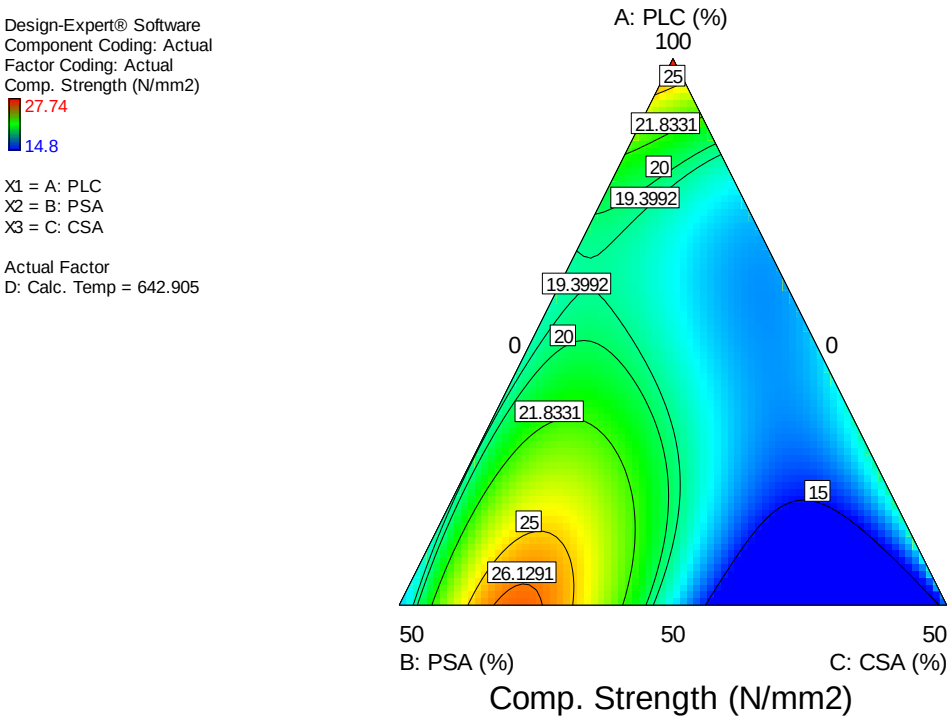

Figure 4.25: Three-dimensional model at 643 ^{o}C for the compressive strength of HAP concrete

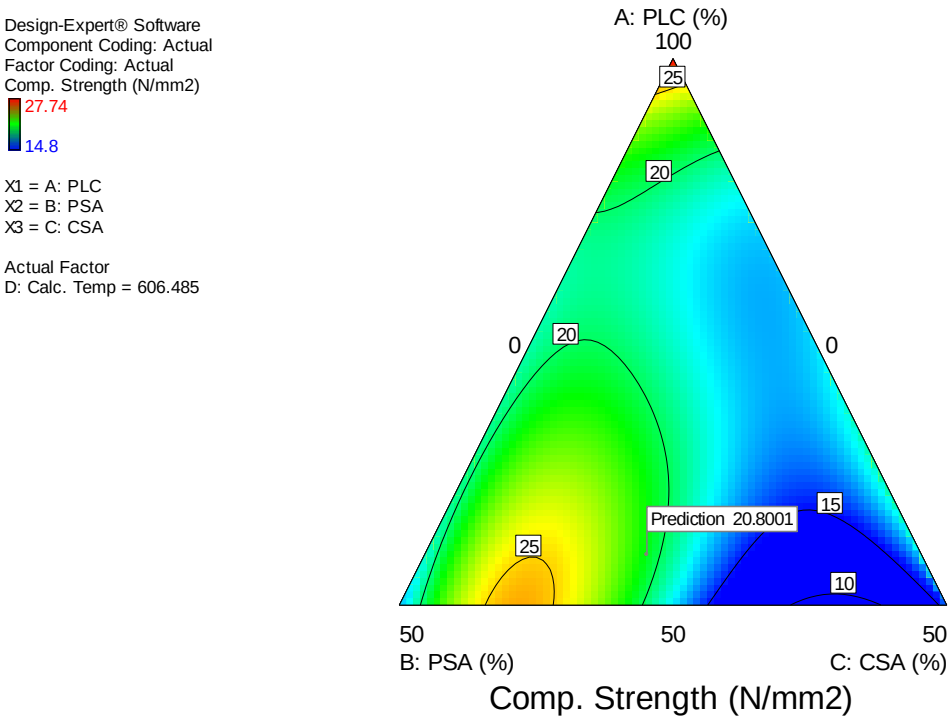

Figure 4.26: Three-dimensional and optimised model variables for compressive strength of HAP concrete

Figures 4.22 to 4.26 represents the model's simulations at varying mixture components as well as processes for HAP cement blended concrete model. The variation of temperature at calcination on the compressive strength of the HAP concrete is mostly linear as increasing calcination temperature leads to increase in compressive strength however in favour of increasing PSA content. However, this relationship barely favours increasing CSA content in the mix, as Figure 4.22 – 4.26 represents reduction in compressive strength at increasing temperature and CSA content. The mixture component in isolation of the factor represents a cubic relationship creating at peaking PSA concentration range of 30-40% and sagging at a PSA range of 5-15%. This generally indicates a need to increase calcination temperature beyond 300 ^{o}C and increasing PSA content above 15% concentration within the total mixture.

At optimisation, 38 suggested solutions where developed as shown in Table 4.6, based on the customised constraint shown in Appendix D5. Selected solution having a desirability of 0.64 requires constraint of 54.62% PC:25.07% PSA:20.31% CSA and a process factor of 606.3 ^{o}C, yielding a compressive strength of 20.8 N/mm^2 which is 75% of the control. However, for an environment that is free from severe environmentally related attacks, solution 10 might be more appropriate having mixture constraints of 56.50% PC:29.4% PSA:14.1% CSA produced at a calcination temperature of 349 ^{o}C and yielding a compressive strength of 20.84 N/mm^2

Table 4.6: Solutions for the optimisation of factors and responses for HAP concrete

N0	PC	PSA	CSA	Calc. Temp	Comp. Strength	WAI	CISLI	SISLI	SIMLI	Desirability	
1	54.611	25.073	20.317	606.758	20.800	2.507	12.724	-0.078	8.966	0.640	Selected
2	54.588	25.113	20.299	603.685	20.800	2.502	12.684	-0.002	8.970	0.640	
3	54.528	25.115	20.357	609.410	20.802	2.507	12.828	-0.002	8.966	0.640	
4	55.065	24.825	20.110	596.927	20.800	2.521	12.247	-0.518	8.959	0.640	
5	54.862	24.845	20.293	613.556	20.800	2.527	12.696	-0.505	8.947	0.640	
6	55.340	24.642	19.718	558.930	20.800	2.492	11.454	-0.233	8.995	0.640	
7	56.103	24.669	18.928	500.964	20.800	2.483	10.302	-0.001	9.033	0.637	
8	58.786	23.203	18.012	485.531	20.800	3.151	8.178	-1.668	8.950	0.631	
9	57.665	24.806	17.529	424.373	20.800	2.612	9.013	0.252	9.057	0.628	
10	56.514	29.358	14.98	349.004	20.840	1.466	11.395	-0.000	9.110	0.619	
11	67.403	17.922	14.675	170.501	20.800	7.761	12.469	16.411	9.002	0.418	
12	67.362	17.811	14.827	171.658	20.800	7.745	12.411	16.456	9.002	0.417	
13	67.346	18.208	14.446	164.918	20.800	7.701	12.824	16.411	9.009	0.417	
14	73.186	3.866	22.948	155.727	20.800	6.358	15.487	9.921	8.497	0.415	
15	72.952	3.865	23.183	151.351	20.800	6.307	15.822	9.942	8.498	0.415	
16	73.175	4.221	22.604	160.777	20.800	6.618	15.007	10.723	8.515	0.414	
17	67.265	17.186	15.550	176.453	20.800	7.732	12.172	16.809	8.998	0.414	
18	74.055	3.868	22.077	171.030	20.800	6.551	14.381	9.987	8.491	0.413	
19	67.601	17.032	15.367	180.288	20.800	7.937	11.879	16.779	8.985	0.413	
20	73.031	4.678	22.291	164.525	20.800	6.909	14.606	11.699	8.539	0.413	
21	74.304	2.743	22.952	159.763	20.800	5.655	15.537	7.198	8.429	0.411	
22	72.899	2.926	24.175	131.738	20.800	5.587	17.704	7.586	8.450	0.410	
23	68.278	18.286	13.435	167.117	20.800	8.272	12.499	16.525	8.981	0.408	
24	67.578	18.821	13.602	146.767	20.800	7.777	13.976	16.800	9.017	0.404	
25	68.292	18.650	13.058	155.145	20.800	8.247	13.275	16.805	8.990	0.401	
26	70.885	6.390	22.725	155.098	20.800	7.298	14.891	15.267	8.642	0.400	
27	67.798	15.762	16.439	184.485	20.800	8.080	11.694	17.626	8.965	0.398	
28	67.736	19.018	13.246	135.998	20.800	7.852	14.709	17.222	9.020	0.393	
29	72.642	2.092	25.266	100.557	20.800	4.894	20.814	5.133	8.409	0.393	
30	68.978	15.555	15.467	191.092	20.800	8.777	11.128	17.777	8.932	0.388	
31	69.371	12.385	18.244	186.703	20.800	8.657	11.730	18.968	8.869	0.355	
32	67.904	19.335	12.761	105.827	20.800	7.919	16.990	18.590	9.037	0.354	
33	92.042	4.591	3.367	751.513	20.800	13.602	21.557	5.286	8.831	0.230	
34	92.101	4.531	3.368	757.024	20.800	13.497	21.837	4.836	8.830	0.230	
35	92.405	4.232	3.363	785.655	20.800	12.956	23.302	2.423	8.826	0.229	
36	91.097	6.044	2.859	718.388	20.800	16.152	19.387	5.283	8.868	0.224	
37	92.153	3.670	4.176	685.134	20.800	11.572	19.204	15.041	8.787	0.215	
38	94.108	5.862	0.000	724.077	23.436	17.575	20.210	8.519	9.109	0.001	

Developed model for the compressive strength of HAP concrete is as shown in Equation 4.3 below;

$$\text{CShap} = (0.277 * \text{PC}) - (2.209 * \text{PSA}) + (0.659 * CSA) + (0.045 * PC * PSA) - (0.013 * PC * CSA) - (8.180 * 10^{-3} * PSA * CSA) + (1.908 * 10^{-3} * PSA * T) - (4.05 * 10^{-3} * CSA * T) + (4.426 * 10^{-4} * PC * PSA * CSA) - (3.672 * 10^{-5} * PC * PSA * T) + (8.190 * 10^{-5} * PC * CSA * T) + (1.913 * 10^{-5} * PSA * CSA * T) - (3.136 * 10^{-4} * PC * PSA * (PC - PSA) + (8.864 * 10^{-5} * PC * CSA * (PC - CSA)) - \left(4.191 * 10^{-4} * PSA * CSA * (PSA - CSA)\right) + (2.133 * 10^{-7} * PC * PSA * T * (PC - PSA) - (6.259 * 10^{-7} * PC * CSA * T * (PC - CSA)) + (1.784 * 10^{-6} * PSA * CSA * T * (PSA - CSA) \quad (4.3)$$

Where;

CShap = Compressive strength of hybrid agro-pozzolan cement blended concrete (MPa)

PC = Mass concentration of Portland cement in total binder (%)

PSA =Mass concentration of Periwinkle shell ash in total binder (%)

CSA =Mass concentration of Clam shell ash in total binder (%)

T = Calcination temperature for the production of CSA (^{o}C).

4.2.4. Calcination and mixture configuration variations on the Flexural Strength of Periwinkle Shell Ash Cement blended concrete

Figures 4.27. and 4.28 are preliminary indicators of the trend of the flexural strength and deflection of PSA cement blended concrete. From Figure 4.27, flexural strength is observed to reduce with increase in cement replacement level using Periwinkle shell ash as the pozzolanic material. A similar trend can be seen in Figure 4.28 for which the relationship between deflection and calcination temperature is shown.

For both Figure 4.27 and Figure 4.28, it can be seen that both flexural strength as well as deflection are tentatively optimum at 800 ^{o}C. it is however noteworthy to establish that optimum flexural strength and deflection obtained at 800 ^{o}C were 2.83 MPa and 125 mm respectively at 40% cement replacement level which were observed to be 53.5% and 59.52% respectively of the control. At 50% cement replacement level, the results obtained at tentative optimum are 2.27 MPa and 88 mm for flexure and deflection respectively. These are again 42.9% and 41.9% respectively of the control's flexural strength (5.29 MPa) and deflection (210 mm).

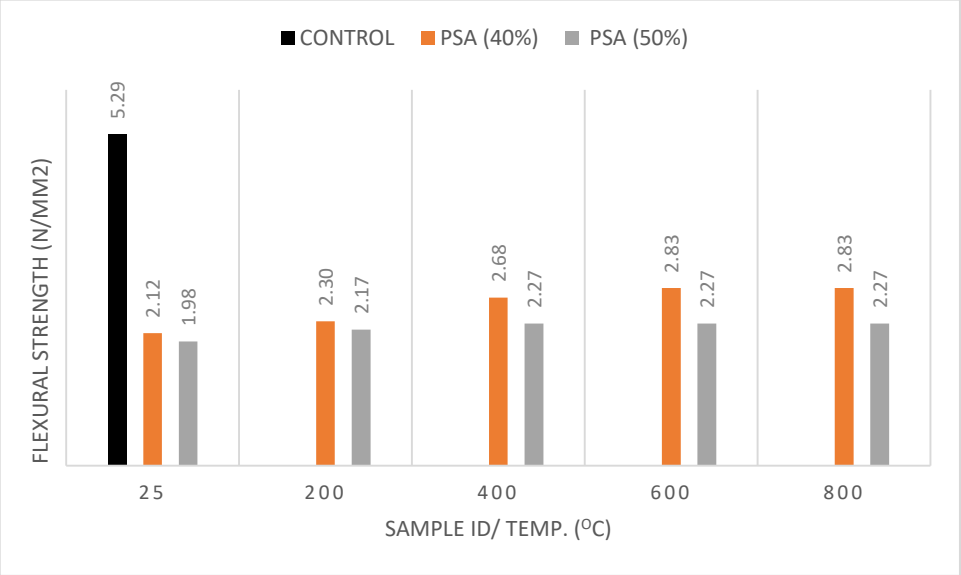

Figure 4.27: Flexural Strength of PSA integrated Cement blended concrete produced at 40% and 50% Cement Replacement Level

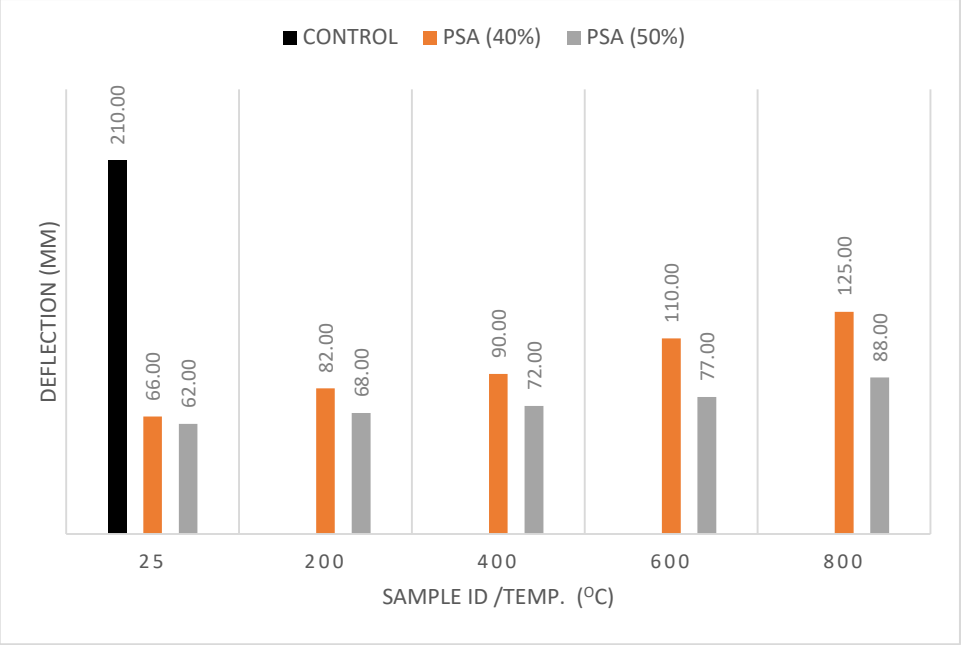

Figure 4.28: Deflection of PSA integrated Cement blended concrete produced at 40% and 50% Cement Replacement Level

Experimental inputs for modelling and optimisation of the independent and dependent variables of periwinkle shell ash cement blended concrete is as shown in Table 4.7

Table 4.7: **Experimental inputs for data analysis, modelling and optimisation of the flexural strength of PSA Pozzolan cement concrete**

Run	Component 1 A:PC %	Component 2 B:PSA %	Factor 3 C:TEMP ^{o}C	Response 1 Flexural strength N/mm^2
1	60	40	600	2.83
2	100	0	400	5.29
3	50	50	400	2.27
4	100	0	400	5.29
5	60	40	25	2.08
6	50	50	400	2.27
7	60	40	800	2.65
8	50	50	25	2.08
9	100	0	25	5.29
10	60	40	400	2.83
11	60	40	800	2.65
12	60	40	25	2.08
13	50	50	800	2.27
14	100	0	800	5.29
15	60	40	200	2.3
16	50	50	200	2.27
17	100	0	200	5.29
18	50	50	800	2.27
19	50	50	600	2.27

The design summary page (Appendix E1) indicates that the trend of results for the flexural strength of PSA cement blended concrete is government by a quadratic mixture and quadratic process factors, indicating that somewhere around the median of both variables lies the optimum.

The analysed variance and regression coefficients of the model (Appendices E2 and E3) for the compressive strength of PSA cement blended concrete, informs that The equation (model) as developed, has eight model classes of linear mixture, AB, AC, BC, ABC, AC^2, BC^2, and ABC^2. Of these, AC, AC^2 and BC^2 were in tandem with the hypothesis for nullification requiring a much lower confidence level than ideal. However, the other five models were significant, enabling the overall model to have a confidence level greater than 95%.

The model's ratio to the square of its total sum produced a regression coefficient of 0.9987. as a result, regression coefficients derived (adjusted and predicted) were 0.9976, and 0.9956, which implies that the model is sound enough for predictions and simulations. Standard error was 0.065 over a mean of 3.14, which produced a minimum coefficient of variation of 2.09%. The adequacy of the model's precision was 72.00, which implies that an error could exist in every 72 predictions. The error being sufficiently below the least permissible error of 4, accordingly, the model's signal is adequate enough within its design scope for statistical simulation purposes.

The coefficients of the model (Appendix E4) indicates that multicollinearity impact is absent for all model components, as no factor exceeded 10 by reason of inflation as a result of the model's variance. This suggests that independent variables can be varied statistically, which is a useful prerequisite for examining the impact of changing independent factors on responses.

Statistical check on model's performance as seen in Figure 4.29 shows a near linear spread of the statistically moderated errors. As such, the developed equation can be satisfactorily utilised for predictions and simulations.

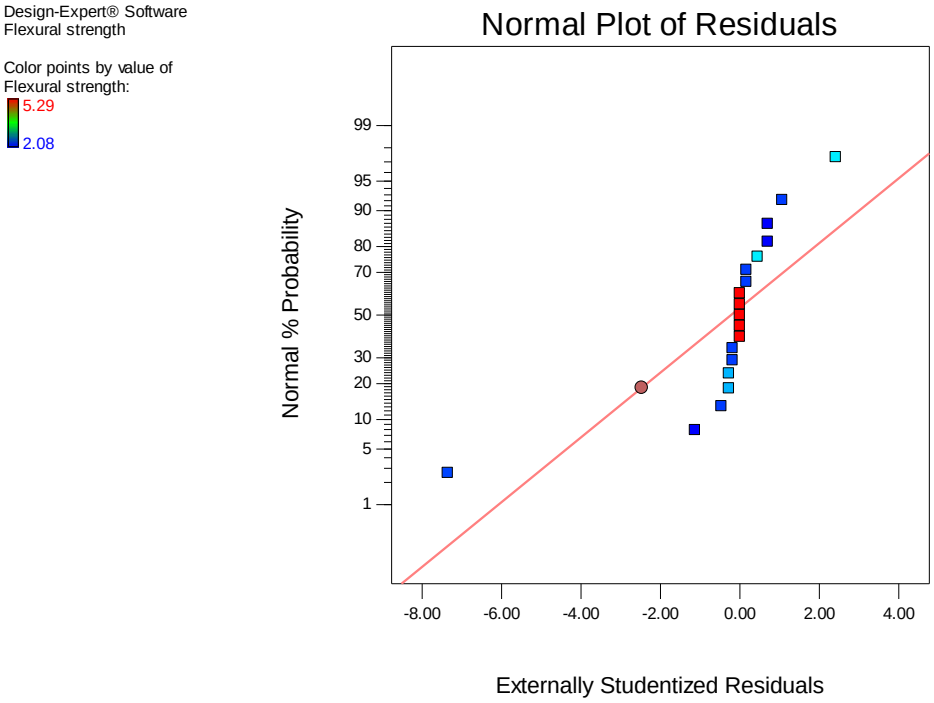

Figure 4.29: Studentised error spread for the flexural strength of PSA cement blended concrete

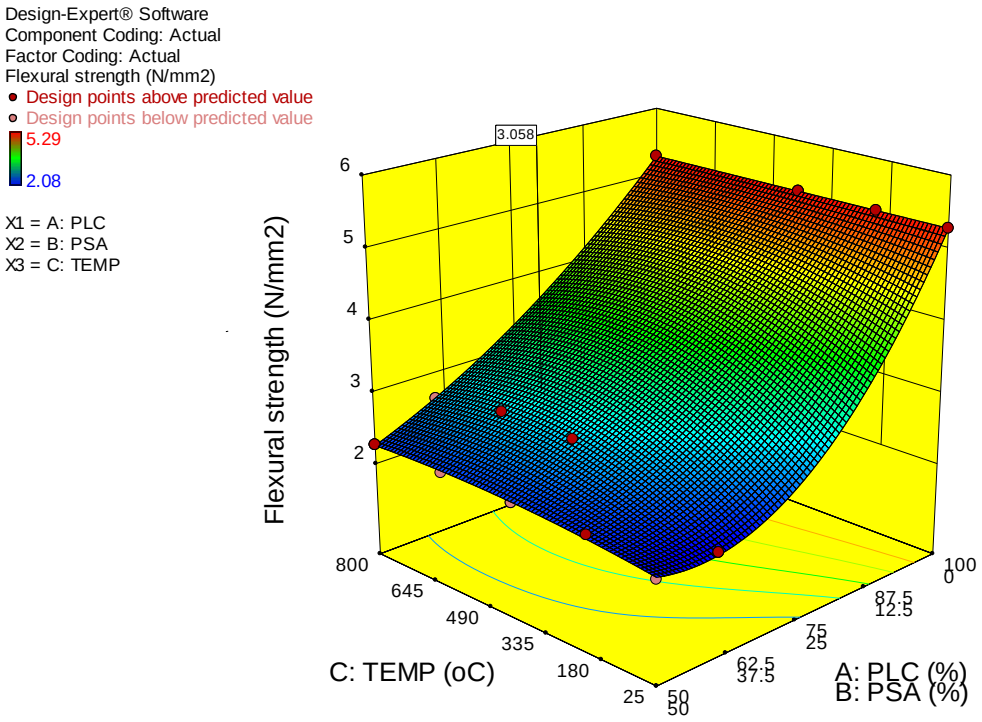

Figure 4.30: Three-dimensional and optimised model variables for flexural strength of PSA concrete

The flexural behaviour of PSA cement blended concrete has been analysed, modelled and optimised. The analysis provides logical reasons for the adoption of the model. As shown in Figure4.30, the mixture factor is quadratic but informs the need for higher PC content in favour of flexural strength. Similarly, calcination temperature is observed to be moderately quadratic, and troughing between 335 ^{o}C and 645 ^{o}C, also in favour of the flexural strength of PSA cement blended concrete.

The flexural behaviour of concrete is often conventionally perceived as a secondary indicator in concrete structures, this is due to its relatively low contribution when compared to compressive strength. However, it's essential that at every introduction of a new/potential binder to the construction industry, certain basic properties require attention.

Olusola and Umoh (2012), informed that the compressive and flexural behaviour of PSA cement blended concrete is best enhanced at a concentration of 10% cement replacement level. This is probably ideal as optimum results presented in Table 4.2, suggested a replacement level of 19.65% as a constraint to meet SAI criteria not to exceed or match up with the control. At 40% replacement level, the flexural behaviour of PSA cement blended concrete, indicated a loss of 28% strength when compared to its control (Olusola and Umoh, 2012). Using the equation (model) as developed, of this research, at 40% cement replacement level, and at the optimized temperature of 565 ^{o}C, a flexural strength of 2.8 N/mm^2 was obtained, and observed to be 47% lower than the control of 5.29 N/mm^2. This is in disparity with the results obtained by Olusola and Umoh (2012), however, they measure flexural behaviour by means of tensile test and not direct flexural test.

At optimisation, optimum variables as shown in Table 4.8, were observed at 65%PC, 35% PSA and at a calcination temperature of 565 ^{o}C. At this configuration, optimum obtainable flexural strength is 3.06 N/mm^2, which is 42.16% below the control.

A practical use of this concrete if for non-reinforced structural works, where limited need for flexural resistance exists. In essence, the model is adoptable and so is the integration of PSA in plain concrete works.

Equation 4.4 below represents the model for the flexural strength of PSA cement blended concrete;

$$\text{FSpsa} = 0.0529\text{PC} + 0.0835\text{PSA} - (1.89 * 10^{-3} * PC * PSA) - (1.272 * 10^{-19} * PC * T) - (2.813 * 10^{-4} * PSA * T) + (5.92 * 10^{-6} * PC * PSA * T) + (8.933 * 10^{-23} * PC * T^2) + (2.490 * 10^{-7} * PSA * T^2) - (5.240 * 10^{-9} * PC * PSA * T^2) \quad (4.4)$$

Where;

FSpsa = Flexural strength of PSA cement blended concrete (MPa)

PC = Mass proportion of Portland cement in total binder (%)

PSA = Mass proportion of PSA in total binder (%)

T = Calcination Temperature (^{o}C)

Table 4.8: Solutions for the optimisation of factors and responses for the flexural strength of PSA cement blended concrete

Solutions						
Number	**PC**	**PSA**	**TEMP**	**Flexural strength**	**Desirability**	
1	64.601	35.399	565.175	3.058	0.535	Selected
2	50.000	50.000	564.849	2.298	0.408	

4.2.5. Calcination and mixture configuration variations on the Flexural Strength of Clam Shell Ash Cement blended concrete

Figures 4.31. and 4.32 are preliminary indicators of the trend of the flexural strength and deflection of CSA cement blended concrete. From Figure 4.31, a quadratic trend of the flexural strength effected by variations in calcination temperature was observed at 40% cement replacement level. This is an early indication that at 40% cement replacement level, optimum calcination temperature is between 400 ^{o}C and 600 ^{o}C. The effect of variations in calcination on the flexural strength of CSA cement blended concrete at 50% cement replacement level was observed to be minimal (constant) between 200 ^{o}C and 800 ^{o}C. Deflection was observed to be directly proportional to calcination temperature. Also, deflection was higher for specimens produced at 50% cement replacement level when compared to those of 40%, regardless of calcination temperature. Noting that increasing deflection reduces structural serviceability, it is of structural importance that structures exhibit limited deflection while resisting maximum structural loads.

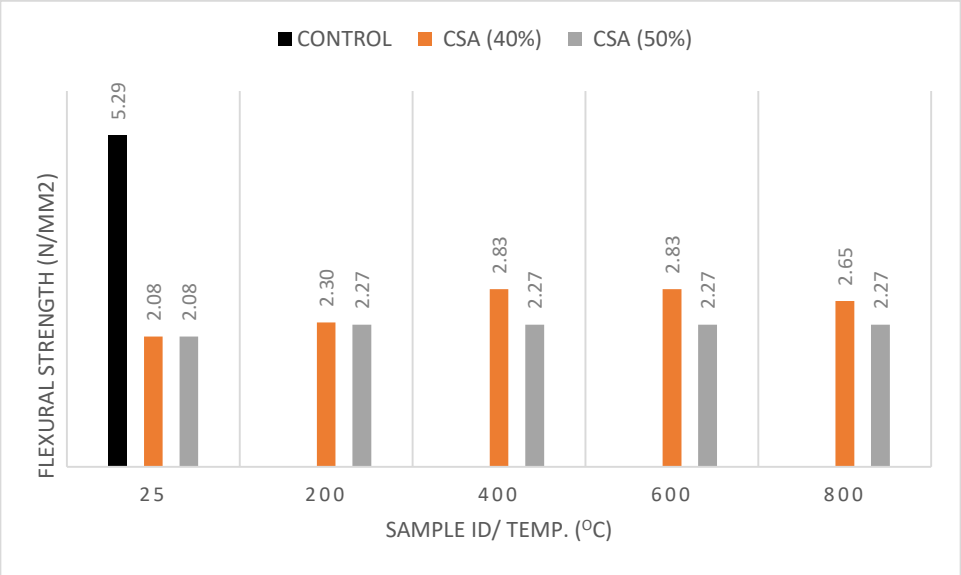

Figure 4.31: Flexural Strength of CSA integrated Cement blended concrete produced at 40% and 50% CRL

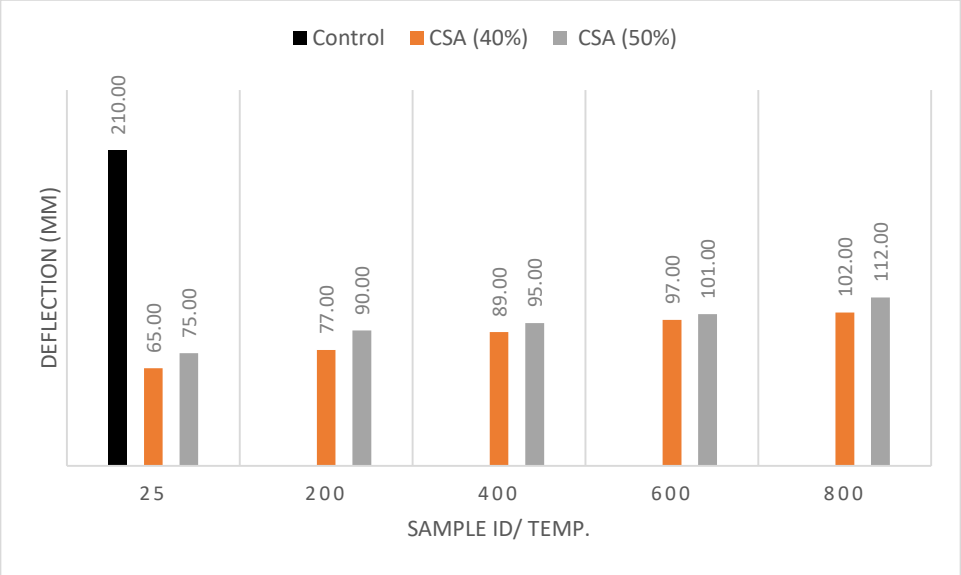

Figure 4.32: Deflection of CSA integrated Cement blended concrete produced at 40% and 50% CRL

Experimental inputs for analysis, modelling and optimisation of the flexural strength of clam shell ash cement blended concrete is as shown in Table 4.9

Table 4.9: Experimental inputs for analysis, modelling and optimisation of the flexural strength of clam shell ash cement blended concrete

Run	Component 1 A:PC %	Component 2 B:CSA %	Factor 3 C:TEMP ^{o}C	Response 1 Flexural strength N/mm^2
1	60	40	400	2.83
2	60	40	200	2.3
3	100	0	25	5.29
4	50	50	800	2.31
5	50	50	400	2.27
6	50	50	400	2.25
7	50	50	25	2.08
8	50	50	25	2.05
9	60	40	600	2.91
10	60	40	800	2.65
11	60	40	25	2.08
12	50	50	800	2.27
13	100	0	25	5.35
14	50	50	25	2.11
15	60	40	600	2.85
16	100	0	25	5.28
17	100	0	25	5.08
18	60	40	600	2.83
19	60	40	400	2.83

The design summary page (Appendix F1) indicates that the trend of results for the flexural strength of CSA cement blended concrete is government by a linear mixture and mean process factors, indicating that increasing the cement content, directly increases the flexural strength of CSA cement blended concrete. Variations in calcination temperature had no significant effect on the flexural strength of CSA cement blended concrete.

The analysed variance and regression coefficients of the model (Appendices F2 and F3) for the flexural of CSA cement blended concrete, informs that the equation (model) as developed, is significant having a confidence interval greater than 95%.

The model's ratio to the square of its total sum produced a regression coefficient of 0.9678. as a result, regression coefficients derived (adjusted and predicted) were 0.9659, and 0.9626, which implies that the model is sound enough for predictions and simulations. Standard error was 0.22 over a mean of 3.03, with a deviation coefficient of 7.38%. The adequacy of the model's precision was 42.665, which implies that an error could exist in every 42 predictions. The error being sufficiently below the least permissible error of 4, accordingly, the model's signal is adequate enough within its design scope for statistical simulation purposes.

The coefficients of the model (Appendix F4) coefficients were 1.03 for PC and CSA, indicating a close to perfect orthogonality, and desired flexibility of a statistically model.

Statistical check on model's performance as seen in Figure 4.33 shows a near linear spread of the statistically moderated errors. As such, the developed equation can be satisfactorily utilised for predictions and simulations.

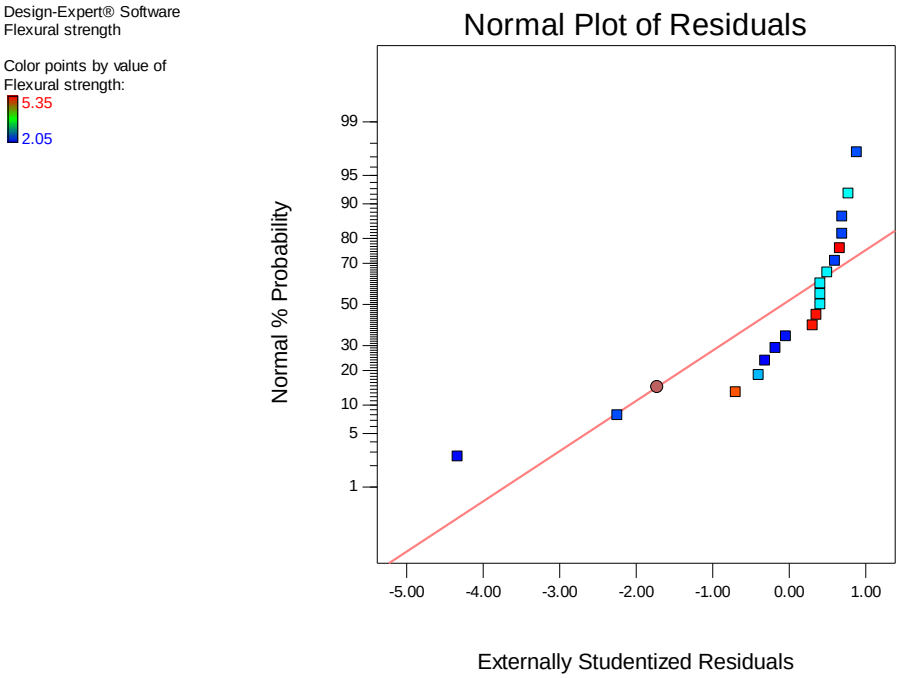

Figure 4.33: Studentised error spread for the flexural strength of CSA cement blended concrete

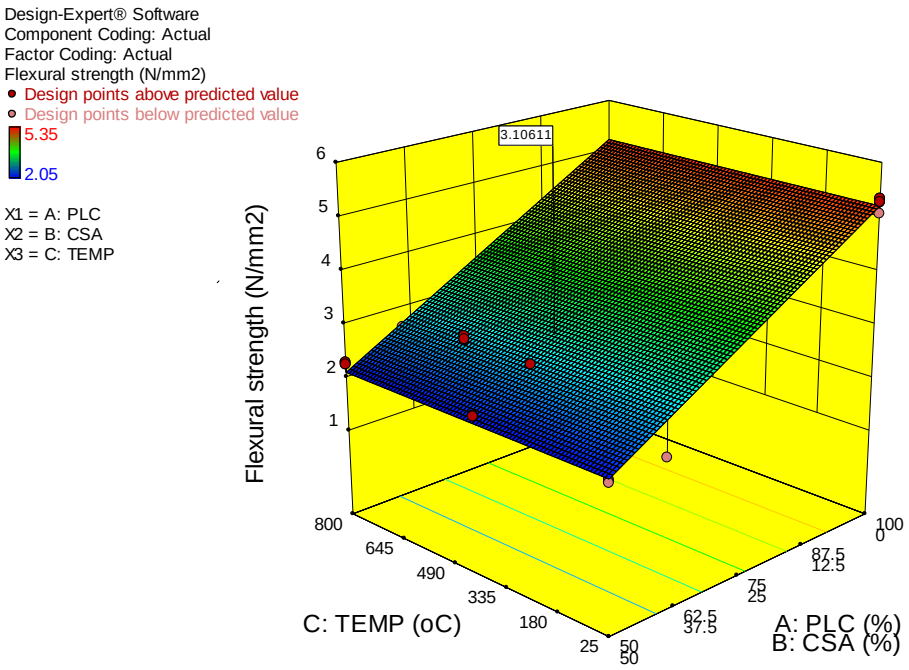

Figure 4.34: Three-dimensional and optimised model variables for flexural strength of CSA cement blended concrete

The flexural behaviour of CSA cement blended concrete has been analysed, modelled and optimised. The analysis provides logical reasons for the adoption of the model. As shown in Figure 4.34, the mixture factor is directly linear to the flexural strength of CSA cement blended concrete. Flexural strength was therefore observed to be minimally affected by variations in CSA production temperature.

Olutoge *et al*. (2016) reported on the flexural behaviour of clam shell ash cement blended concrete, Having produced the ash by uncontrolled burning process they observed a 49.3% reduction in tensile strength at 28 days of curing, due to the integration of 20% concentration of CSA as a partial replacement for cement, and hence recommended an optimum replacement level of 5%. Similarly, Ong and Kassim (2019), observed a drop in split tensile strength of about 33.33% at 8% cement replacement level, at a controlled production temperature of 800 ^{o}C for 2 hours. In same vein, relative to flexural performance of CSA blended concrete, Othman *et al*., (2013) and Olivia *et al*. (2015) recommended optimum cement replacement levels of 5% and 4% respectively.

From the observations of analysed data in this study, developed model for the flexural strength of CSA cement blended concrete, indicates that the flexural behaviour of CSA cement blended concrete is not a function of calcination temperature, but solely a function of cement replacement level. Testing this hypothesis, at 5% cement replacement level, a loss in flexural strength of 7.2% was observed; at 8% replacement, a loss of 11.77% was observed, at 20% replacement, a loss of 24.76% was observed and at the model recommended level of 34% (Table 4.10), a loss of 41.28% was recorded. The ultimate implication of this is that the application of CSA in concrete as a cement replacement material at levels beyond 5%, is only suitable for non-flexural load bearing structures, such as blinding of foundation beds, flooring formations, non-load bearing concrete wall partitions, lining for dykes, etc.

The limitation of CSA in cement blended concrete is not with the CSA itself, but with the oxide composition of Portland cement. CSA is primarily calcareous in nature, and about 70% of Portland cement is made up of materials with calcareous origins, hence there appears to be no more room for more calcareous additions. This is also why CSA

does not scientifically fall into the class of pozzolanic materials according to relevant standards but can be classified as an SCM.

Equation 4.5 is a model for simulating the most probable responses at different levels of the variables within the boundaries of the model of CSA cement blended concrete

$$\text{FScsa} = 0.052\text{PC} - 9.80 * 10^{-3}CSA \quad (4.5)$$

Where;

FScsa = Flexural strength of CSA cement blended concrete (MPa)

PC = Mass proportion of Portland cement in total binder of CSA Pozzolan concrete (%)

CSA = Mass proportion of CSA in total binder of CSA Pozzolan concrete (%)

Table 4.10: Solutions for the optimisation of factors and responses for the flexural strength of CSA cement blended concrete

Solutions Number	PC	CSA	TEMP*	Flexural strength	Desirability	
1	65.922	34.078	427.333	3.106	0.530	Selected
2	65.918	34.082	533.829	3.106	0.530	
3	65.927	34.073	555.156	3.106	0.530	
4	65.918	34.082	201.806	3.106	0.530	
5	65.928	34.072	485.381	3.106	0.530	
6	65.928	34.072	468.972	3.106	0.530	
7	65.929	34.071	264.420	3.107	0.530	
8	65.916	34.084	541.228	3.106	0.530	
9	65.916	34.084	511.080	3.106	0.530	
10	65.915	34.085	700.136	3.106	0.530	
11	65.915	34.085	447.253	3.106	0.530	
12	65.914	34.086	297.515	3.106	0.530	
13	65.931	34.069	255.021	3.107	0.530	
14	65.932	34.068	127.640	3.107	0.530	
15	65.933	34.067	146.424	3.107	0.530	
16	65.934	34.066	558.843	3.107	0.530	
17	65.911	34.089	655.930	3.105	0.530	
18	65.935	34.065	287.109	3.107	0.530	
19	65.911	34.089	342.177	3.105	0.530	
20	65.935	34.065	261.506	3.107	0.530	

4.2.6. Calcination and mixture configuration variations on the Flexural Strength of Hybrid Agro-Based Pozzolan Cement blended concrete

Having identified that PSA is limited by insufficient calcium while CSA is limited by insufficient silicon, this section will explain the results of the hybrid produced, relative to the flexural behaviour of concrete at varying cement replacement levels.

Figures 4.35 and 4.36 are plotted data on the flexural and deflection performance of PSA and CSA hybrid mixture at varying synergies and calcination temperatures, replacing cement at 40% and 50% in concrete.

From both figures, the tentative illustration is that calcination temperature is directly proportional to flexural strength with optimum result obtained at about 800 ^{o}C. Cement Replacement level was seen to be inversely proportional to flexural strength. At 40% cement replacement level, a synergy of 60P produced at 800 ^{o}C appeared to be more desirable relative to other synergies. At this configuration, a flexural strength of 3.5 MPa was obtained, which is approximately 66.2% of the control and higher than PSA and CSA counterparts of 2.83 MPa and 2.83 MPa by 19.14% respectively. A similar trend was observed for results obtained at 50% cement replacement level.

Deflection curve for primary as well as synergised pozzolans are similar in form, having a near arc formation at 40% replacement level and somewhat of a slanted ‘Z’ formation at 50% replacement level. Deflection was seen to increase steadily with temperature for all synergies. At 40% replacement level, optimum deflection was obtained at 60% PSA: 40% CSA with Pozzolan specimen produced 800 ^{o}C having a deflection at failure of 167 mm which is approximately 79.5% of the control deflection and superior in deflection to that of PSA and CSA cement blended concrete (125 mm and 102 mm respectively) by 25% and 39% respectively.

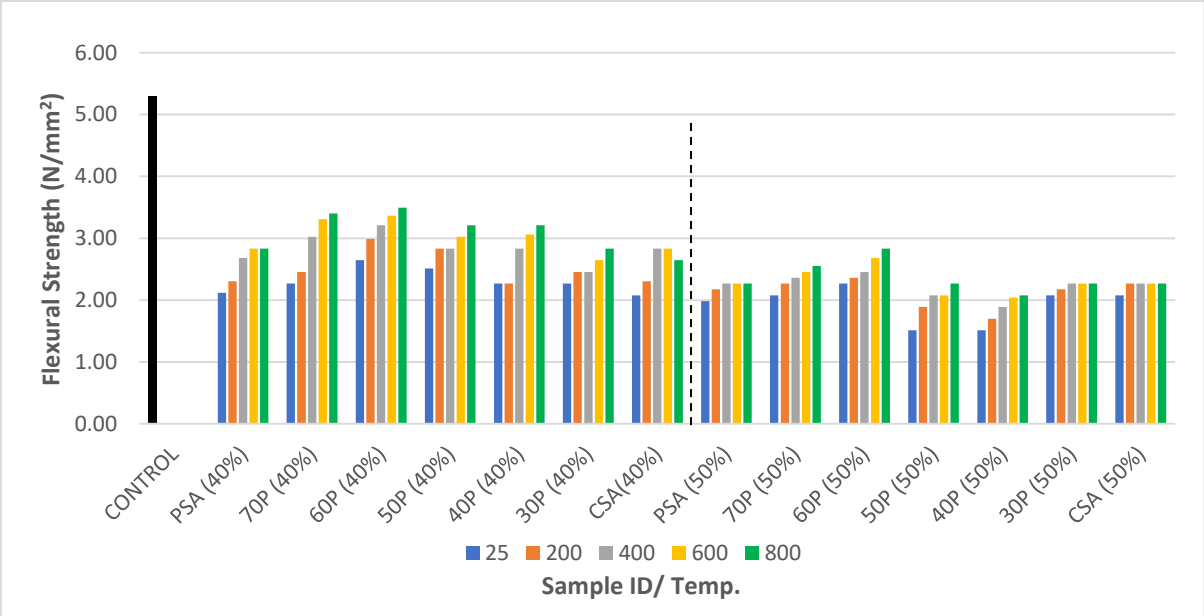

Figure 4.35: Flexural strength of HAP concrete produced at 40% and 50% cement replacement Levels

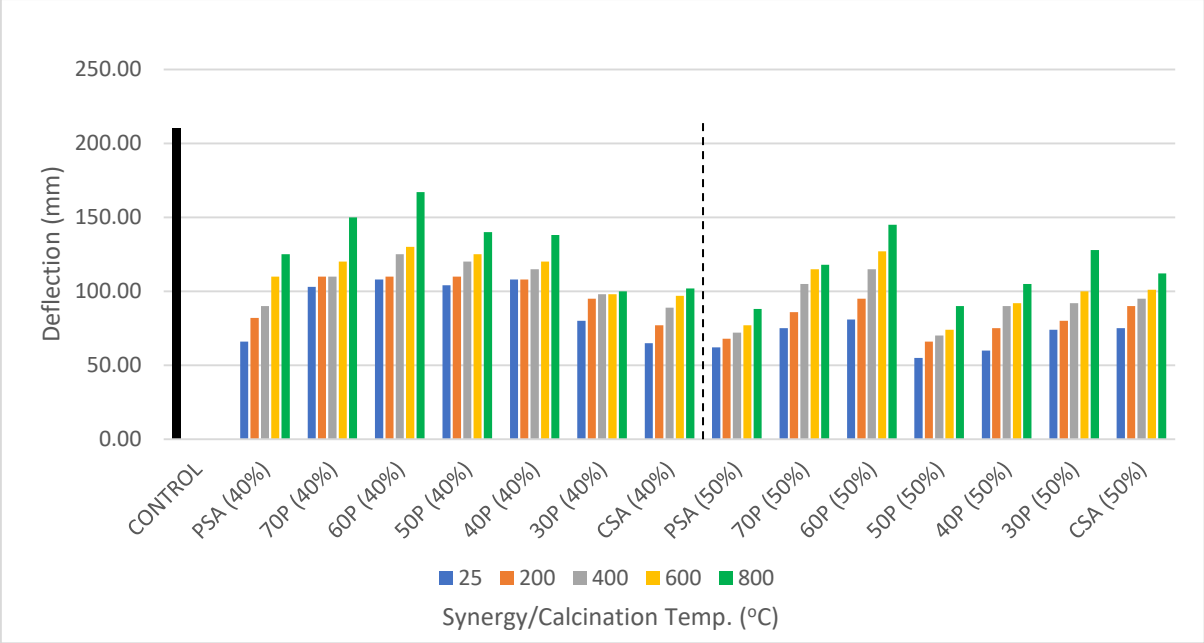

Figure 4.36: Deflection of HAP concrete produced at 40% and 50% cement replacement levels

In analysing the obtained data for the flexural strength of PSA and CSA hybrid mixture, the experimental data were utilised as inputs based on the custom template o the statistical tool used (Design Expert). Table 4.11 represents the data using for the analysis, modelling and optimisation of PSA/CSA hybrid Pozzolan cement blended concrete.

Table 4.11: **Experimental inputs for analysis, modelling and optimisation of the flexural strength of HAP cement blended concrete**

Run	Component 1 A:PC %	Component 2 B:PSA %	Component 3 C:CSA %	Factor 4 D:Calc. Temp. ^{o}C	Response 1 Flexural Strength N/mm2
1	60	0	40	600	2.83
2	60	16	24	400	2.83
3	60	24	16	200	2.99
4	50	50	0	800	2.27
5	50	50	0	25	1.98
6	60	24	16	25	2.65
7	100	0	0	25	5.29
8	60	24	16	800	3.5
9	50	0	50	400	2.27
10	60	24	16	600	3.36
11	100	0	0	400	5.29
12	50	15	35	400	2.36
13	60	40	0	600	2.83
14	100	0	0	800	5.29
15	60	0	40	400	2.83
16	60	20	20	600	3.02
17	60	20	20	800	3.21
18	60	40	0	400	2.68
19	50	25	25	600	2.08
20	50	15	35	25	2.08
21	60	20	20	200	2.83
22	50	0	50	800	2.27
23	50	25	25	400	2.08
24	50	30	20	400	2.46
25	50	25	25	25	1.52
26	100	0	0	25	5.29
27	50	35	15	400	2.36
28	50	25	25	800	2.27

The trend of data for the flexural strength of HAP cement blended concrete is governed by a linear mixture component and a linear process factor, as shown in the design summary page (Appendix G1), suggesting that raising the cement content as well as the calcination temperature, directly enhances the flexural strength of HAP cement blended concrete.

Variable inflated factors (Appendix G4)for the flexural strength model of HAP cement blended concrete were all within the range of 1-2, indicating a very sharp closeness to orthogonally between variations of the independent variables. This is a good measure of the statistical predictability of the model.

The spread of studentised errors was relatively linear and is represented by model diagnostics, as shown in Figure 4.37. As a result, the model can be accepted as statistically acceptable.

The created model is significant, with a confidence interval more than 95%, according to the variance as analysed ($P < 0.05$), and regression coefficient (Appendices G2 and G3) for the flexural strength of HAP Pozzolan cement blended concrete. The Regression coefficient was 0.9653 when the model was compared to the cumulative summed up squares. As a result, the adjusted and projected regression coefficients were 0.9574 and 0.9406, respectively, suggesting a solid model prediction and simulation capacity. The Standard error was 0.22, with an error coefficient (C.V.) of 7.45%, based on a mean of 2.95. The model's sufficient precision was determined to be 34.04, implying that one inaccuracy might be expected for every 34 predictions. The equation developed is precise enough within its boundary conditions, seeing the error associated with its strength of prediction is significantly lower than the maximum permissible error of 4.

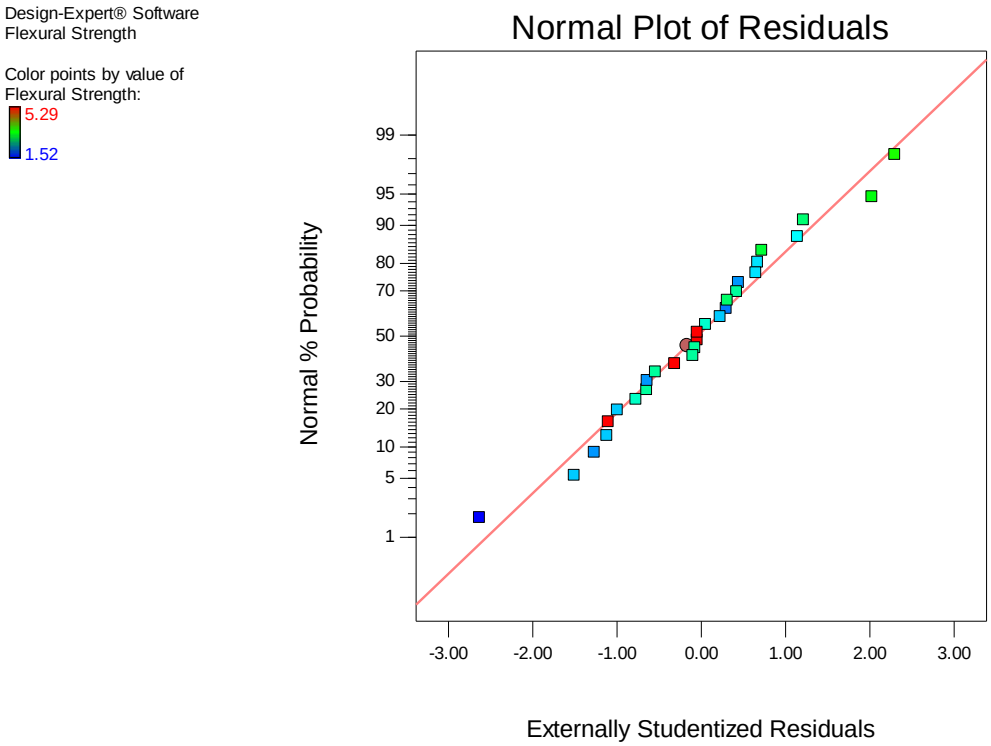

Figure 4.37: **Studentised error spread for the flexural strength of HAP cement blended cement blended concrete**

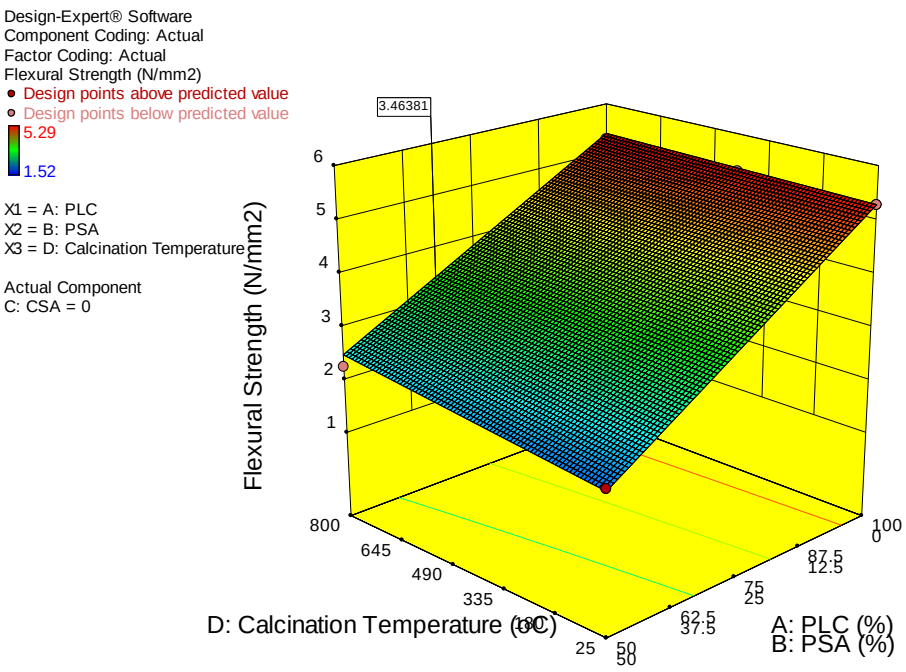

Figure 4.38: Three-dimensional and optimised model variables for flexural strength of HAP cement blended cement blended concrete

Hybrid agro-based pozzolan cement blended concrete's flexural behaviour has been studied, modelled, and optimized, as shown in Figure 4.38. Figure 4.38 is therefore a representation of the flexural behaviour of HAP cement blended concrete, under the influence of calcination variations as well as mixture configuration. As earlier stated by the design summary (Appendix G1), it can be seen from the figure that increasing PC content directly increases flexural strength, and at a more notable rate, relative to the direct proportionality observed between calcination and flexural strength.

About a handful of literature pay attention to the flexural behaviour of Pozzolan cement blended concretes. This is partly due to the conventional assumption the concrete is primarily built for compressive load resistance. Dembo *et al*. (2017) realised that silica fume is very reactive in improving the flexural strength of cement blended concrete, and could be used by up to 30% as cement replacement, without compromising the flexural strength of concrete. A combination of silica fume with calcined clay was observed to lead to a drastic reduction in flexural strength. This is a logical outcome as flexural performance is not only enhanced by sufficient SiO2 content, but also, by the fineness of the pozzolanic material. Silica fume if amongst the finest of pozzolans and very rich in SiO_2, therefore exhibited its high support to the flexural strength of concrete as reported by Dembo *et al*. (2017). On fineness, observed data from this study showed CSA as a finer pozzolan than PSA, however, literature informs that PSA is very much richer in SiO2 content that CSA. As such, increasing PSA content provides a more chemical balance, CSA content tends to proffer a better fineness contribution to the hybrid pozzolanic mix. No marvel as singular materials, both optimal replacement levels was observed to be around 35% yielding a flexural strength of about 3.1 N/mm^2. A synergy of both however, informs the need for the total dependence on PSA for its chemical contribution, or the total dependence on CSA for its fineness contribution, or the need for smaller concentration of CSA in the hybrid mix (Table 4.12). However, in any case, the flexural strength of concrete was yet reduced about 33.8% at replacement levels of 33.5%, produced at 800^oC. Conclusively, regardless of the mix configuration or calcination temperature, at cement replacement levels greater than 30%, cement blended concrete will decline in flexural strength by roughly 30% and as such should not be used in the production of concrete intended for flexural load resistance.

Table 4.12 Solutions for the optimisation of factors and responses for the flexural strength of HAP cement blended concrete

Solutions Number	PC	PSA	CSA	Calcination Temperature	Flexural Strength	Desirability	
1	66.525	33.475	0.000	800.000	3.464	0.588	Selected
2	67.253	30.755	1.993	799.999	3.503	0.587	
3	66.924	25.714	7.362	800.000	3.477	0.586	
4	66.782	22.846	10.372	799.999	3.465	0.585	
5	66.653	21.645	11.702	799.998	3.456	0.585	
6	67.070	19.880	13.050	799.993	3.478	0.585	
7	66.672	18.501	14.827	799.999	3.453	0.585	
8	68.049	2.033	29.918	799.976	3.513	0.581	
9	67.230	0.000	32.770	800.000	3.462	0.581	
10	75.000	25.000	0.000	799.998	3.956	0.568	

Equations 4.6 is developed for navigating the design space of the flexural strength of HAP cement blended concrete, relative to mixture configuration and calcination temperature.

$$\text{FShap} = 0.053\text{PC} - 0.015\text{PSA} - 0.013\text{CSA} + (1.427 * 10^{-6} * PC * T) + (1.311 * 10^{-5} * PSA * T) + (9.251 * 10^{-6} * CSA * T) \quad (4.6)$$

Where;

FS_{hap} = Flexural strength of hybrid Agro-based Pozzolan concrete (MPa)

PC = Mass proportion of Portland cement in total binder of HAP concrete (%)

PSA = Mass proportion of PSA in total binder of HAP concrete (%)

CSA = Mass proportion of CSA in total binder of HAP concrete (%)

T = Calcination temperature for producing HAP in HAP Pozzolan concrete (^{o}C)

4.3. Durability Properties of Agro-based Pozzolan concrete

This section will focus on the data, analysis, models and discussions on the durability indices of concrete containing blends of PSA, CSA and the hybrids as partial replacements for Portland cement.

4.3.1. Calcination and mixture configuration variations on the Water Absorption Index of Periwinkle Shell ash Cement blended concrete

Figure 4.39 is a preliminary illustration of the data generated for the water absorption index of PSA cement blended concrete. Data informs that Water absorption Index (WAI) increases with increase in cement replacement level and reduce with increase in calcination temperature. This indicates that PSA demands high calcination temperature in order to increase its potentials as a cement replacement material relative to WAI resistance. Data suggests that the bests results for WAI are obtained at a calcination temperature of 600 ^{o}C, replacing cement at 20%. At 20% PSA concentration and at 800 ^{o}C, WAI of 1.74% was obtained and observed to be 12% lower than the control value of 1.98%. Referencing 40% findings as a good draw down based on SAI criteria (compressive strength results), at 40% cement level, PSA at 600 ^{o}C had a WAI of 2.84% and was 43.43% higher than the control.

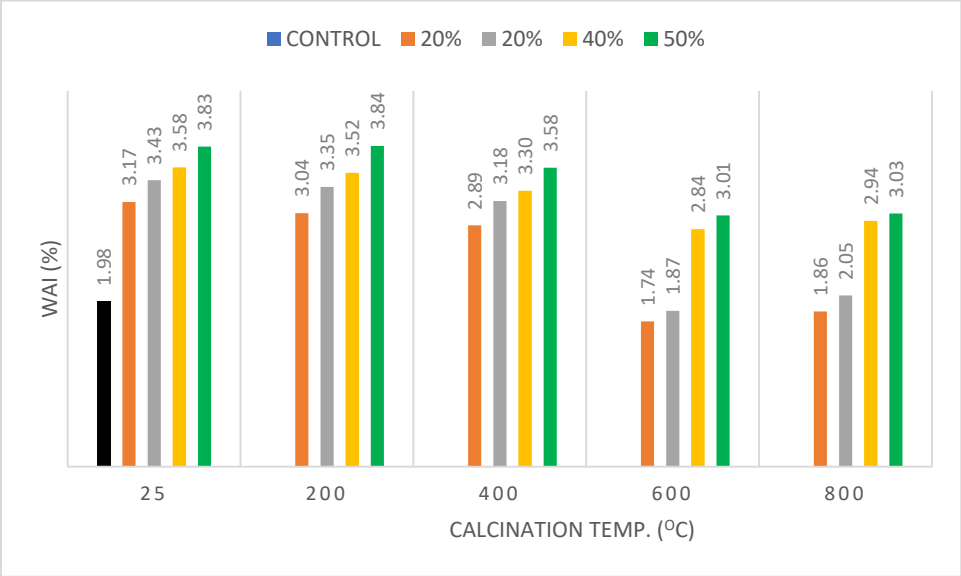

Figure 4.39: **Water Absorption Index for PSA cement blended concrete**

ANOVA Table for water absorption index (Appendix H1) shows a quadratic and linear mixture of the model components. The linear mixture had interactions with $P < 0.0001$, the interactions of PC and PSA (AB) and PSA and Calcination temperature (BC), conformed with the hypothesis for nullification by having P-values of 0.4929 and 0.1431 respectively. The quadratic model of calcination temperature, PC and CSA was observed to have a significant P-value of 0.0021. Consequently, the all integrated model was significant having $P < 0.05$. Hence, the model negates the hypothesis for nullification. Regression analysis shown in Table 4.8 shows the Standard error for the observed data is 0.27 over a mean of 2.85.A percentage ratio of the Standard error to the mean represent the error percentage of the data (C.V%) was observed to be 9.66% which is satisfactory based on the allowable range of 0 – 30%.

The Regression coefficient (Appendix H2) obtained for the model prediction of the water absorption index of PSA cement blended concrete are 0.8819, 0.8481, and 0.8057 for the R^2, Adjusted R^2 and Predicted R^2 respectively. A difference of 0.0424 between the adjusted and predicted R^2 values is an indication of model clarity in prediction analysis. Adequate Precision indicated that the signal to noise ratio is 14.108. This is 253.45% greater than the minimal requirement of 4.0 and contributes to the acceptability of the model. Minimal observations of 1.74 and -0.94 for predicted residual sum of squares (PRESS) and -2log likelihood respectively, are good indicators for minimal errors associated with the predictive capacity of the model. The equation (model) as developed, for the Water Absorption Index of PSA cement blended concrete is as shown in Equation (4.7).

Appendix H3 is associated with all model components, their respective coefficients, degrees of freedom, standard error, low and high range of confidence level as well as the Variance Inflated Factors. The VIF's obtained are within the acceptable range of 1 – 10, which implies the absence of multicollinearity, as such no significant interaction between the independent variables was observed. Consequently, the model is flexible enough to fix one independent variable and monitor the effect of the unfixed variable on the dependent variable.

Figure 4.40 represents a normal distribution of the externally studentized residuals as it obeys the 'fat pencil test' rule of thumb, as such the model can be said to be statistically sound

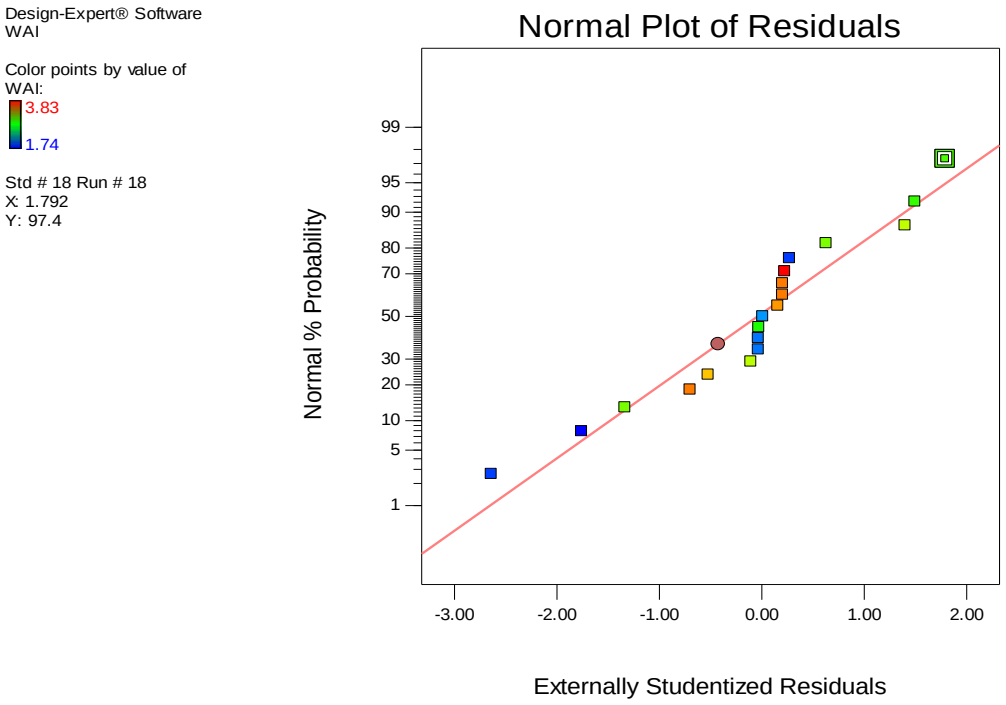

Figure 4.40: Residuals Distribution for Water Absorption Index of PSA pozzolan Concrete

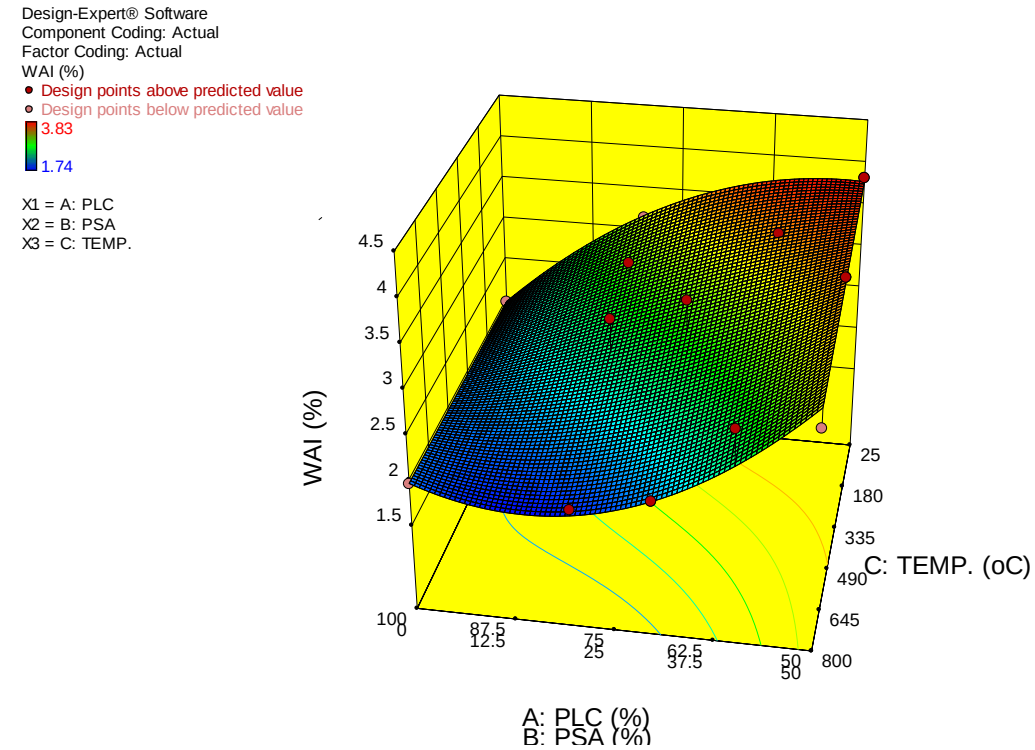

Figure 4.41 Three-dimensional Plot of model simulation for the Water Absorption Index of PSA Cement blended concrete

Figure 4.41 is a representation of the combined effect of mixing Portland cement (PC) and Periwinkle Shell Ash (PSA) and variations in calcination on the water absorption index of PSA cement blended concrete. Calcination temperature is observed to affect the concretes ability to resist the absorption of water positively as increasing calcination temperatures reduces WAI. This can mostly be attributed to the activation of the reactive silica required for the development of secondary C-S-H gel, however, it is noteworthy that this reaction is theoretically dependent on the presence of the hydrated by product of Portland cement (CaOH); a process that requires up to 28 days to complete 99% of its cycle. Consequently, the concrete cubes being allowed to complete its 28 days hydration cycle before a secondary curing of additional 28 days for water absorption testing, it can be said that the WAI collected measures only the effect of the pozzolanic activity within 28 days of post hydration period. This period (28 days), can be argued to be inadequate as a much longer period logically appears more ideal for tests pertaining to the durability of concrete, however, the very concept of pozzolanicity suggests a continuous built-up of mechanical and durability properties of concrete associated with the development of secondary C-S-H gel. As such, any variable (process or mixture) that develops the reactive component of pozzolans (SiO_2), would invariably improve the pozzolanicity of the material by increasing the rate of pozzolanic reaction. Hence, results obtained within the first 28 days of post hydration are expected to be the minimum obtainable results. Accordingly, literature validates findings of this research such that increasing temperature increases pozzolanic activity and reduces water absorption index of cement blended concretes (Siddique and Khan, 2011; Alexandre *et al*., 2014; Ubong and Effiong, 2017).

Figure 4.41 also shows the mixture effect of PSA and PC on the water absorption index of PSA cement blended concrete. Findings show that PSA content between 0 and 30% had minimal effect on the water absorption index of the concrete, however, at PSA concentrations beyond 30%, a steady increase in WAI was observed. This trend suggests that the development of Calcium silicate hydrate gel is primarily depended on the concentration of the basic compounds of cement (C3S, C2S, C3A, and C4AF), which would logically reduce at the partial replacement of cement. As such, a limitation in the concentration of portlandite (CaOH) upon hydration of cement is

inherent. This partly explains the limitations of acceptable concentration of pozzolans in the construction industries to levels below 20% as seen in literature.

Figure 4.41 is a graphical presentation of the optimized findings for limiting the water absorption index of PSA cement blended concrete. An optimized water absorption index of 2.463%was suggested as the best solution with a desirability of 0.564, at factor constraints of 80.35%PC, 19.65% PSA and 425 ^{o}C calcination temperature. At a WAI of 1.98%, the control specimen is observed to be 24.24% lower than the suggested optimised solution.

All other conditions being ideal, results obtained at optimal level for the Water absorption Index of PSA cement blended concrete are satisfactory at local and global levels for the adoption into the production of plain concrete for the construction industry.

The model for navigating the design space of the water absorption index of PSA cement blended concrete, relative to calcination temperature and mixture configuration is as shown in equation 4.7.

$$\text{WAIpsa} = 0.020\text{PC} + 0.012\text{PSA} + (8.758 * 10^{-4} * PC * PSA) + (1.134 * 10^{-4} * PSA * T) - (2.547 * 10^{-6} * PC * PSA * T) \quad (4.7)$$

Where;

WAIpsa = Water absorption index of PSA cement blended concrete

PC = Mass proportion of Portland cement in total binder of PSA cement blended concrete (%)

4.3.2. Calcination and mixture configuration variations on the Water Absorption Index of Clam Shell Ash Cement blended concrete

Laboratory developed data on the water absorption index (WAI) of CSA cement blended concrete are as illustrated on the plot in Figure 4.42. From the data, WAI is observed to increase with increase in cement replacement level and reduce with increase in calcination temperature. At 600 ^{o}C, WAI was minimal and particularly for 20% cement replacement specimens, having a WAI of 2.08% and 5% higher than the control WAI of 1.98%. At a value of 2.17%, 20% CSA at 800 ^{o}C, was 9.6% higher than the control. Referencing 40% findings as a good draw down based on SAI criteria from compressive strength results, at 40% cement level, CSA at 600 ^{o}C had a WAI of 3.25% and was about 64% higher than the control.

Whilst it is eminent that cement be replaced for reasons of sustainability and durability, the material property should enhance the replaceability of cement relative to the desired durability and mechanical indices. In this case, calcination temperature has been seen as a parameter that reduces the adverse WAI indices associated with increasing CSA content. The industry is therefore encouraged to optimise calcination temperature in the production of CSA so as to enhance cement replaceability to optimal levels.

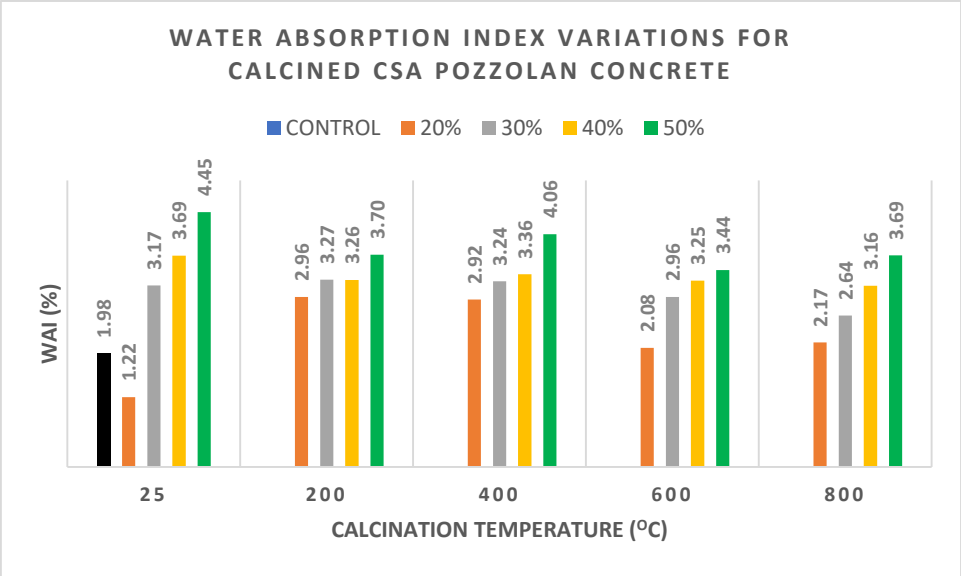

Figure 4.42: Water Absorption Index Variations for Calcined CSA Cement blended concrete

Appendix I1 and I2 represents the analysed variance and regression coefficients of the model for water absorption index of CSA cement blended concrete. The equation (model) as developed, is a combination of a mixture of quadratic terms and mean process terms, having two model terms of 'linear mixture' and 'AB'. All model components were significant having a confidence interval exceeding 95% ($P<0.05$).

The model's ratio to the square of its total sum produced a regression coefficient of 0.8038. Consequently, the 'adjusted' and 'predicted' regression coefficients were 0.7793 and 0.7438, which implies that the model is sound enough for predictions and simulations.

Standard error was 1.18 over a mean of 6.0, with a deviation coefficient of 19.62%. The adequacy of the model's precision was 13.89, which implies that an error could exist in every 13.89 simulations. In essence, the least expected error of 4, is significantly above the model's maximum probable error, accordingly, the model's signal is adequate enough within its boundary conditions for statistical simulation purposes.

The coefficients of the model shown in Appendix I3, expresses that no factor (mixture or process) was inflated above 30 as a result of the model's variance, and as such, prevents multicollinearity amongst the variables. This suggests that independent variables can be varied statistically, which is a useful prerequisite for examining the impact of changing independent factors on responses.

Statistical check on model's performance as seen in Figure 4.43 shows a near linear spread of the statistically moderated errors. As such, the developed equation can be satisfactorily utilised for predictions and simulations.

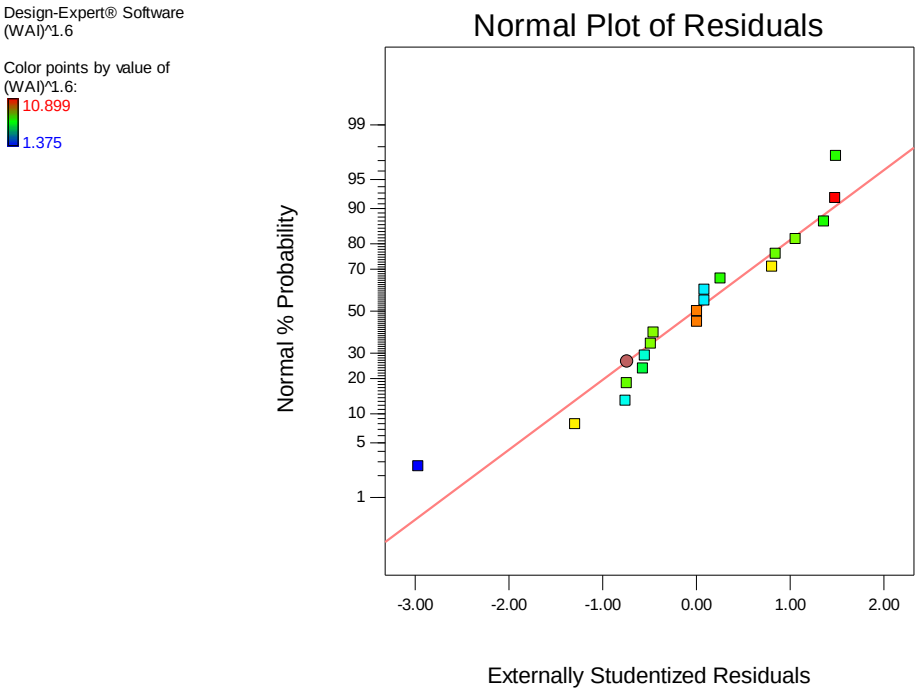

Figure 4.43 Studentised error spread for the water absorption index of CSA cement blended concrete

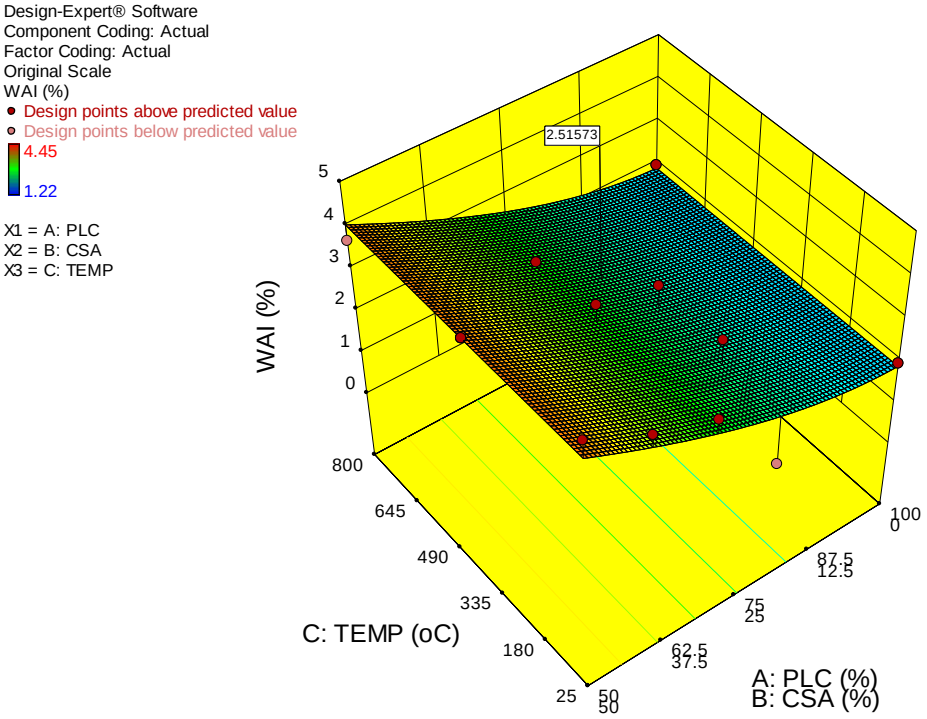

Figure 4.44 Plot of model simulation for the water absorption index of CSA cement blended concrete

Figure 4.44 represents a quadratic mixture interaction and a mean process interaction on the water absorption index of CSA cement blended concrete. The model's process factor component interaction indicates relatively mean/constant result of calcination on the water absorption index of CSA cement blended concrete. The quadratic mixture component of the model, developed a sagging quadratic curve troughing between 0% CSA and 12.5% CSA concentration. The model generally suggests a need to reduce CSA concentration if the sole objective is minimising water absorption index of CSA cement blended concrete.

Bamigboye et al. (2020), reviewed over 50 publications and in their conclusion described the effect of sea shell mixture with cement in concrete as having a sagging quadratic effect on the water absorption index of the cement blended concrete, troughing at a concentration range of 10 – 20%. This validates the research findings of this investigation. Additionally, research works are limited in the area of combined mixture effect and calcination temperature process effect on the water absorption index response of CSA cement blended concrete, however, this research observed the calcination temperature process factor had a mean effect (constant effect) on the water absorption index of CSA cement blended concrete. At optimisation, WAI of 2.516% was obtained at a mixture of 76.87% PC:23.13 CSA produced at a calcination temperature of 527 ^{o}C. The optimized WAI of 2.516% was observed to be 27% higher than control of 1.98%.

Application of the optimized solution in the construction industry is recommended as it reduces the energy demand required for calcination and enhances the replaceability of cement which is a drive in the direction of sustainability.

Developed model for the Water Absorption Index of CSA cement blended concrete is as shown in Equation 4.8.

$$\text{WAIcsa} = \left(0.029\text{PC} + 0.278\text{CSA} - (2.377 * 10^{-3} * PC * CSA)\right)^{\frac{1}{1.6}} \quad (4.8)$$

Where;

WAIcsa = Water absorption index of CSA cement blended concrete

PC = Mass proportion of Portland cement in total binder of CSA cement blended concrete (%)

4.3.3. Calcination and mixture configuration variations on the Water Absorption Index of Hybrid Agro-Based Pozzolan Cement blended concrete

Laboratory data obtained for the WAI of HAP cement blended concrete are as plotted in Figures 4.45 to 4.48. From plotted data, WAI can be said to generally reduce with increasing temperature for most of the synergies at all the cement replacement levels. WAI generally increases with an increase in cement replacement level for all sample types. A trend mostly seen between 20% and 40% suggests an inverted movement of WAI at 800 ^{o}C. Whilst, a downward movement was been observed between ATM and 600 ^{o}C in most cases, at 800 ^{o}C a forced increase in WAI was observed, implying a need to calcinate at temperatures below 800 ^{o}C. At 40% cement replacement level, synergistic ratio of 60% PSA: 40% CSA at 600 ^{o}C had a WAI of 2.75% found to be about 39% higher that the control. This is yet the best result when compared to that of PSA and CSA (2.84% and 3.25% respectively) which were 43.34% and 64% higher than control

Absorbed moisture in concrete has been shown in literature to reduce with increase in cement replacement level (Otunyo and Okechukwu, 2017), however, this is dependent on the specific gravity as well as oxide composition of the material. The synergy of PSA/CSA as studied, shows that WAI increases with increasing cement replacement level, however, this slope of WAI increase was reduced at increasing calcination temperature. Evidently, the calcination treatment enhances specific gravity and activates the pozzolanic chemistry of the samples by cutting off impurities.

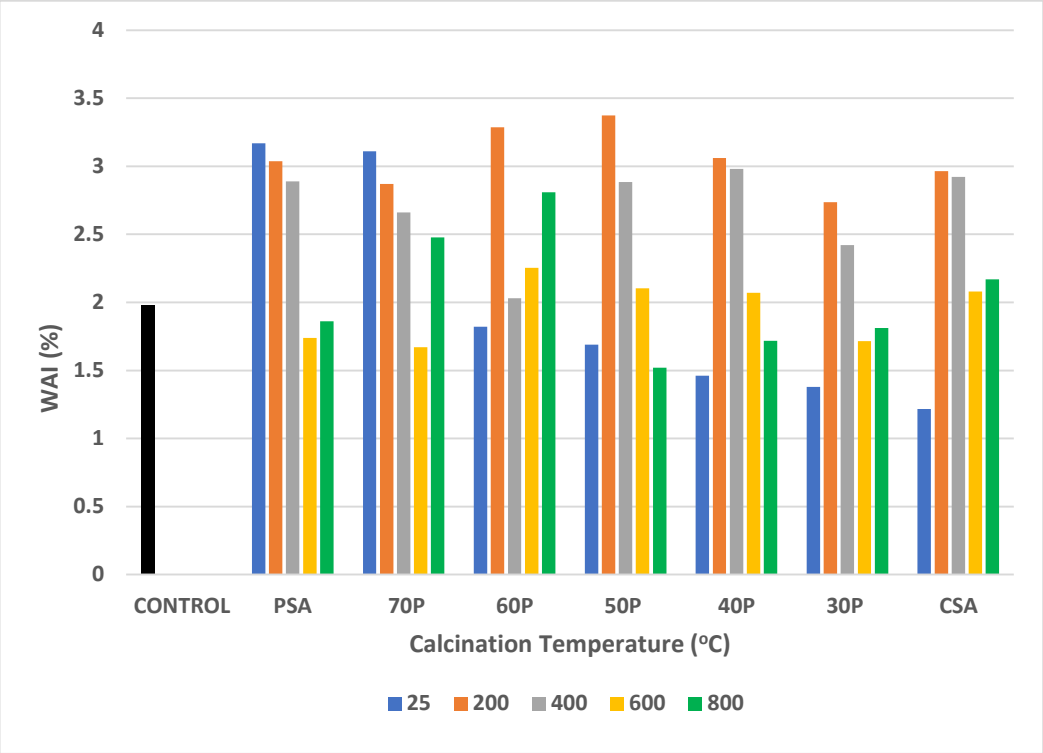

Figure 4.45: Effect of Temperature on the Water Absorption Index of HAP concrete specimens at 20% Replacement Level

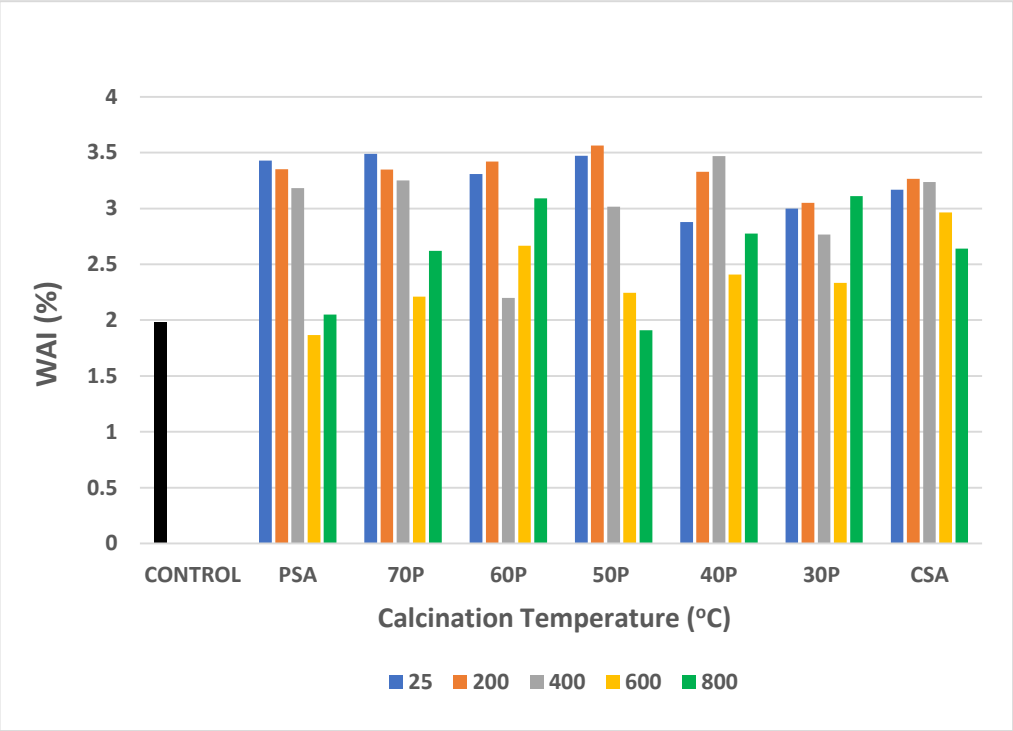

Figure 4.46: **Effect of Temperature on the Water Absorption Index of HAP concrete specimens at 30% Replacement Level**

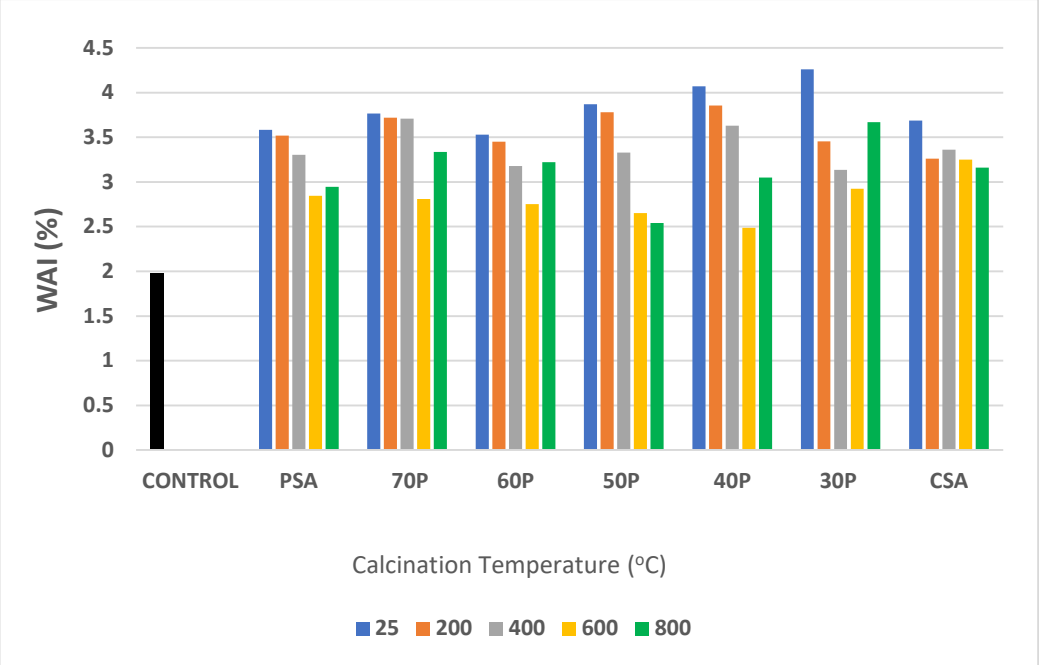

Figure 4.47: Effect of Temperature on the Water Absorption Index of HAP concrete specimens at 40% Replacement Level

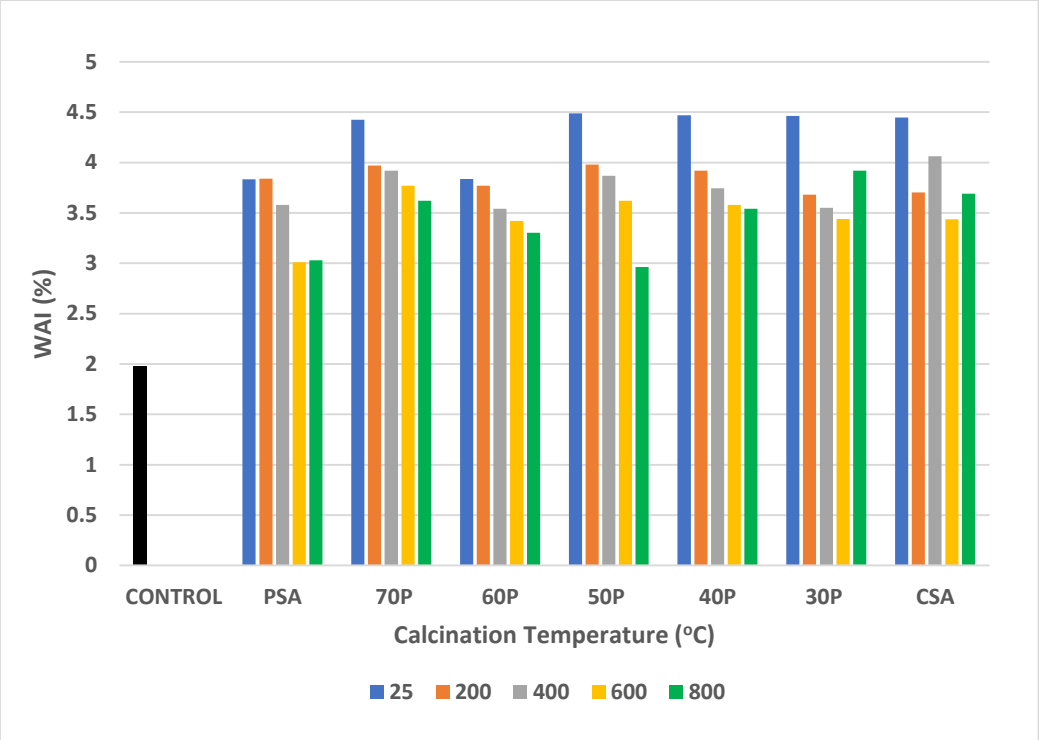

Figure 4.48: Effect of Temperature on the Water Absorption Index of HAP concrete specimens at 50% Replacement Level

The analysed variance and regression coefficients of the model for the water absorption index of HAP concrete are shown in Appendix J1 and J2. The created model is a combination of 'cubic mixture' and 'mean process' terms with four (4) linear mixture terms, AB, BC, and AB(A-B), all of which are combined into the developed equation (model), with a confidence interval exceeding 95% ($P<<0.05$).

The model's ratio to the square of its total sum produced a regression coefficient of 0.8538. Adjusted and Predicted regression coefficients were 0.8205, and 0.6616, which implies that the model is sound enough for predictions and simulations.

Standard error was 2.18 over a mean of 4.18, with a deviation coefficient of 44.47%. The adequacy of the model's precision was 22.39, which implies that an error could exist in every 22.39 predictions. In essence, the least expected error of 4, is significantly above the model's maximum probable error, accordingly, the model's signal is adequate enough within its design scope for statistical simulation purposes.

No factor was observed to be inflated beyond 10 as a result of variance, the model's coefficients as shown in Appendix J3 indicates that all the components of the model are free from bounds of multicollinearity. This implies a high level of statistical flexibility between independent variables, as well as a strong signal strength for examining the cause and effect of each variable and response whilst fixing other model variables.

Statistical check on model's performance as seen in Figure 4.49 shows a near linear spread of the statistically moderated errors. As such, the developed equation can be satisfactorily utilised for predictions and simulations.

Figures 4.49 to 4.53 represents the model's simulations at varying mixture terms as well as varying process inputs.

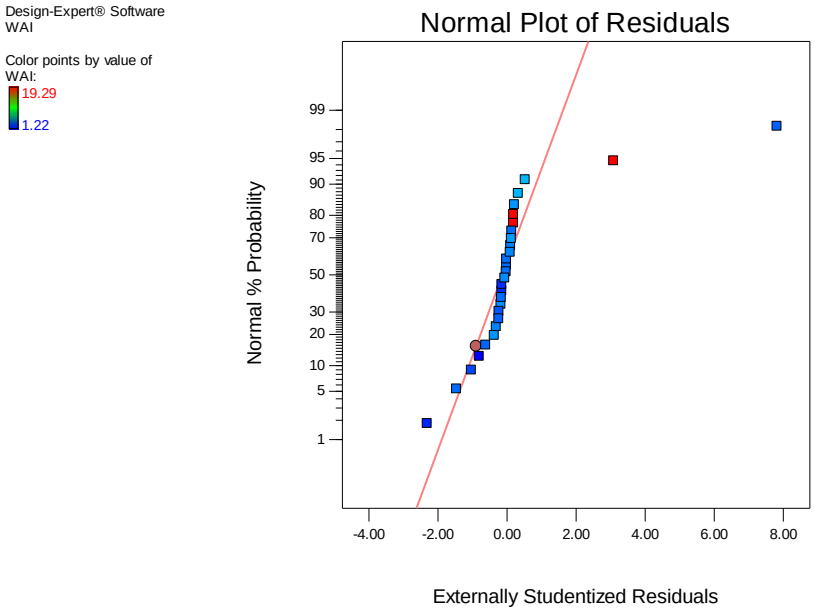

Figure 4.49: **Studentised error spread for the water absorption index of HAP cement blended concrete**

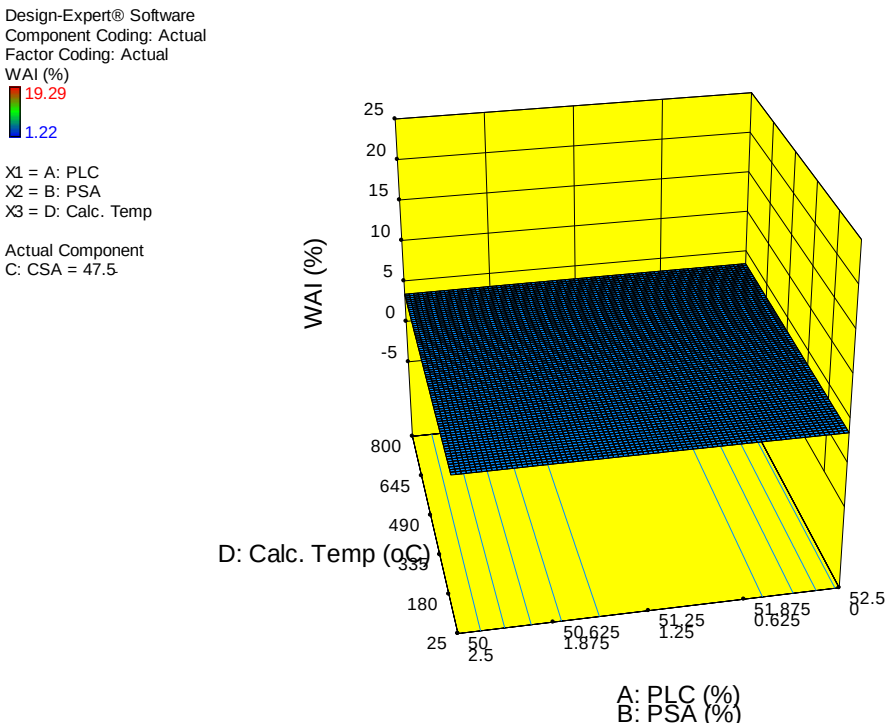

Figure 4.50: Three-dimensional model at 47.5% CSA concentration on the water absorption index of HAP cement blended concrete

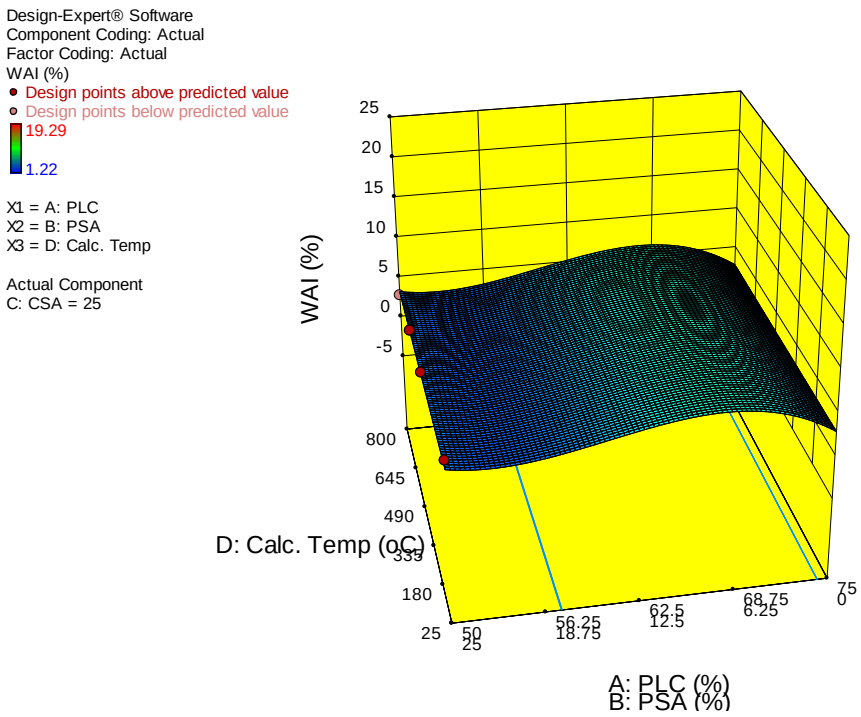

Figure 4.51: Three-dimensional model at 25% CSA concentration on the water absorption index of HAP cement blended concrete

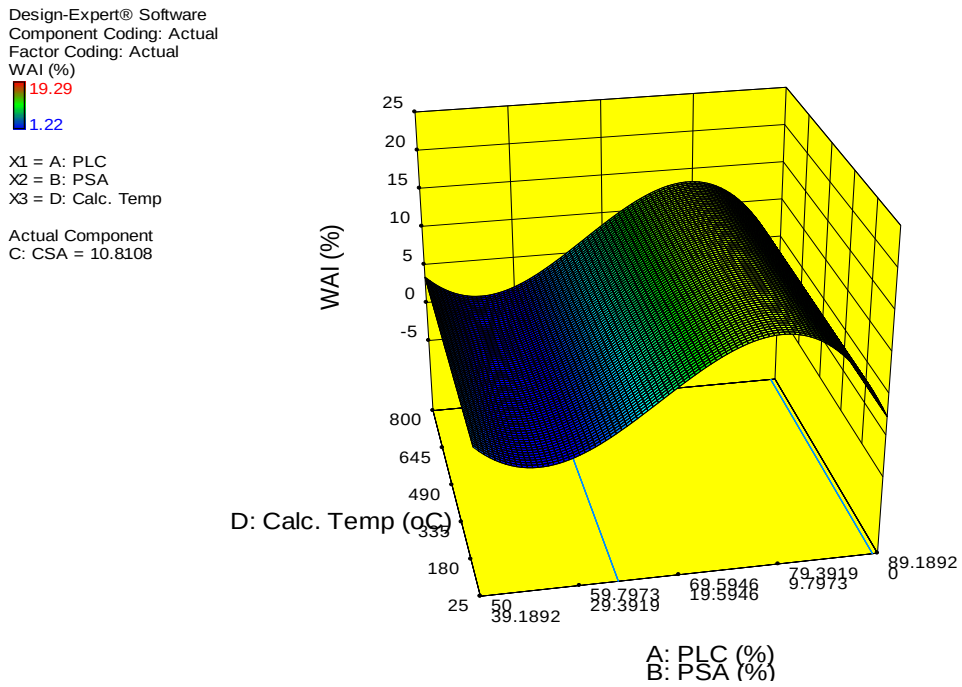

Figure 4.52: Three-dimensional model at 10.81% CSA concentration for the water absorption index of HAP cement blended concrete

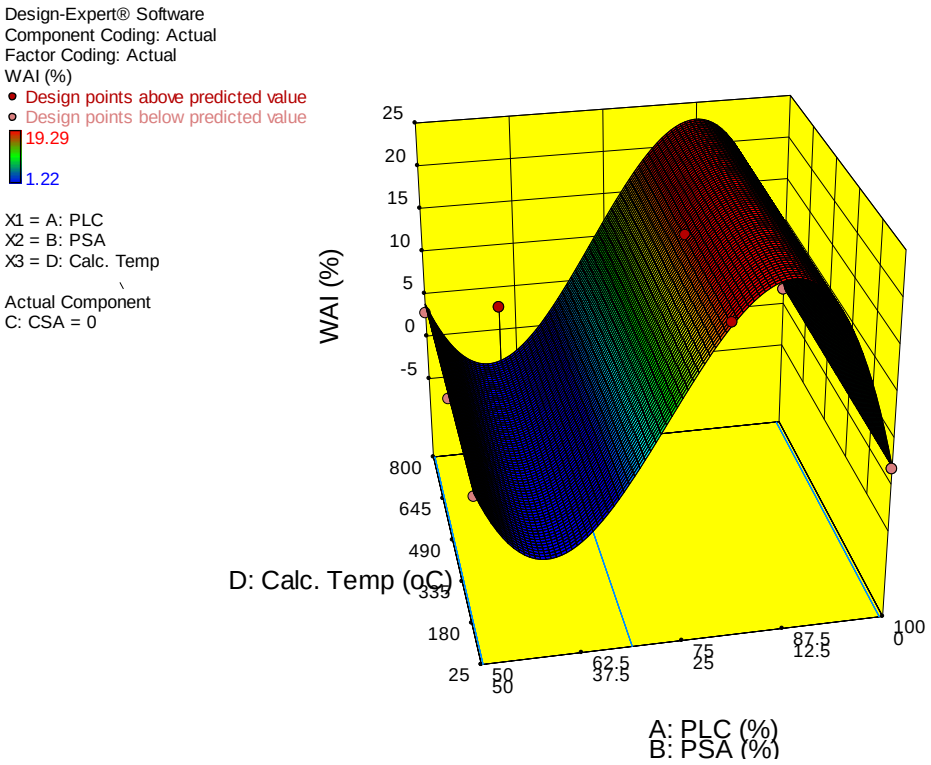

Figure 4.53: Three-dimensional model at 0% CSA concentration for the water absorption index of HAP cement blended concrete

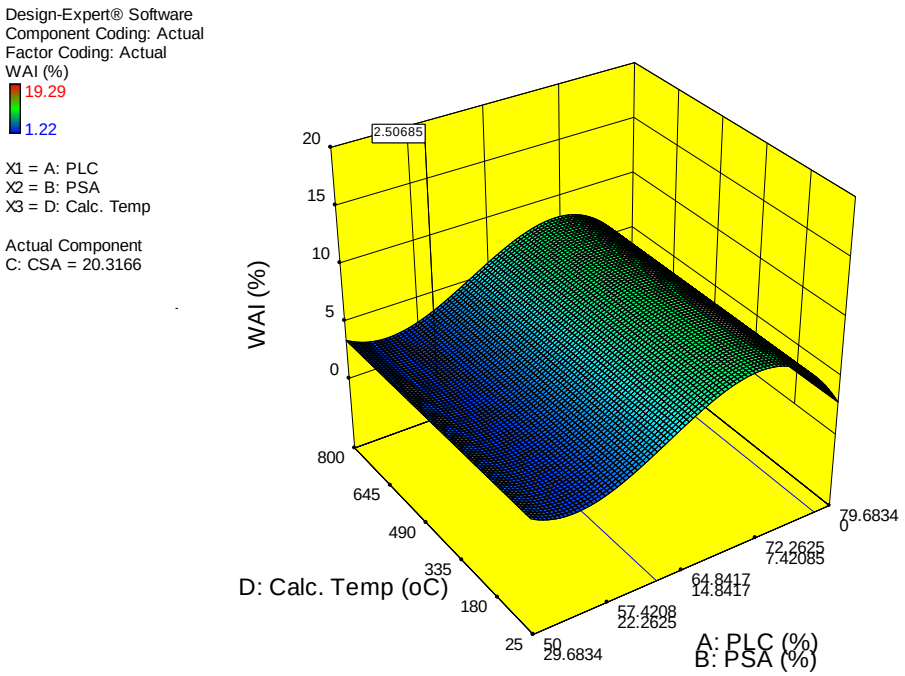

Figure 4.54: Plot of Optimised WAI at 20.316% CSA Concentration.

Figures 4.50 to 4.54 represents the model's simulations at varying mixture terms as well as varying process inputs. Results on the outcome of variations of the process variable (calcination temperature), on water absorption index of HAP concrete, was observed to have a mean effect for mixture composition. In other words, for a particularly mixture composition, calcination temperature variations have minimal effect on the water absorption index of the cement blended concrete. However, the mixture component of the model expressed changes in interaction mostly dependent on the concentration of clam shell ash as seen in Figures 4.88 to 4.61. At 50% CSA content, WAI was observed to be at its minimal irrespective of calcination temperature (Figure 4.88). Reducing the CSA concentration to 25%, a small amplitude wave was formed for WAI, troughing between 12.5 and 25% PSA concentration and cresting between 12.5 and 0% PSA concentration, suggesting a need for higher concentrations of PSA content. A further reduction in CSA content to 10.81% and finally 0% as shown in Figure 4.60 and 4.61 respectively shows a cubic mixture interaction with depth of amplitude proportional to the concentration of CSA content. Increasing CSA concentration reduces the amplitude of the wave and vice versa. Additionally, minimal WAI was observed at PSA concentration ranging between 30 and 45% PSA content.

At optimisation, synergising the custom constraint of all five responses, similar factors constraint as was in the case of compressive strength, yielded same mixture configuration with a WAI of 2.5% observed to be 126.3% of the control of 1.9%. This is theoretically inversely proportional to age and is expected to reduce with time, hence poses no significant threat to the durability concrete structures. Therefore, it is possible to apply these findings in the building industry, mostly for non or lightly reinforced constructions like mass/plain concrete structures.

The equation (model) as developed, (Equation 4.9) can be applied in simulating the most probable responses at different levels of the variables within the boundaries of the model to meet specific sustainably and friendly design requirements.

$$\text{WAIhap} = 0.022\text{PC} + 7.728\text{PSA} + 0.0538\text{CSA} - (0.153\text{PC} * \text{PSA}) - (0.057\text{PSA} * \text{CSA}) + \left(1.125 * 10^{-3} * PC * PSA * (PC * PSA)\right) \quad (4.9)$$

Where;

WAIhap = Water absorption index of HAP cement blended concrete (%)

PC = Mass proportion of Portland cement in total binder of HAP cement blended concrete (%)

PSA = Mass proportion of PSA in total binder of HAP Concrete (%)

CSA = Mass proportion of CSA in total binder of HAP Concrete (%)

T = Calcination temperature for producing HAP in HAP concrete (^{o}C)

4.3.4. Calcination and mixture configuration variations on the CISLI of Periwinkle Shell Ash Cement Blended Concrete

Figure 4.55 represents the plot of laboratory data gotten for the compressive strength of PSA concrete when cured in a chlorine solution. Similarly, Figure 4.56 represents the losses in compressive strength due to the attack of chloride ions.

From Figures 4.55 and 4.56, control specimen was observed to have a loss in strength of about 24.56% between specimens cured in fresh water and specimens cured in 10% sodium chloride solution. At ATM, 200 ^{o}C, 400 ^{o}C, and 600 ^{o}C, 50% cement replacement levels had the greatest loss in compressive strength. For ATM, 200 ^{o}C, and 800 ^{o}C, cement replacement level had an inverse relationship with strength loss, such that the higher the replacement level, the lower the strength loss Index. However, specimens at 50% replacement level did not follow this trend to the end. Minimal losses were obtained at 30% cement replacement level for specimen produced at 400 ^{o}C having a strength gain of about 8%. All specimens at 600 ^{o}C were observed to have a loss in strength lower than that of the control specimen. At 40% replacement level, a loss of about 19.3% was observed.

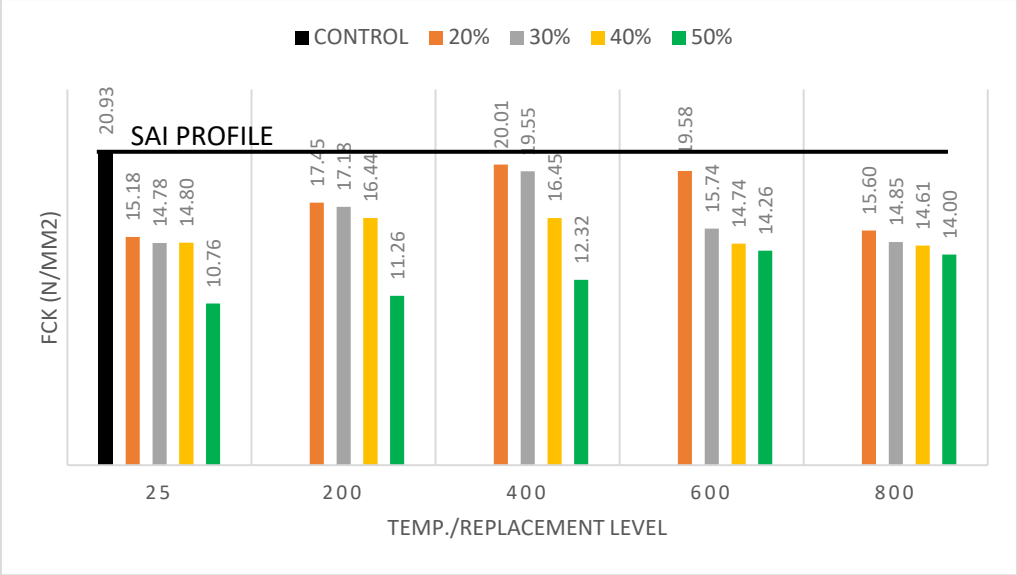

Figure 4.55: Effect of calcination of PSA on the compressive strength performance of PSA cement blended concrete under chloride attack

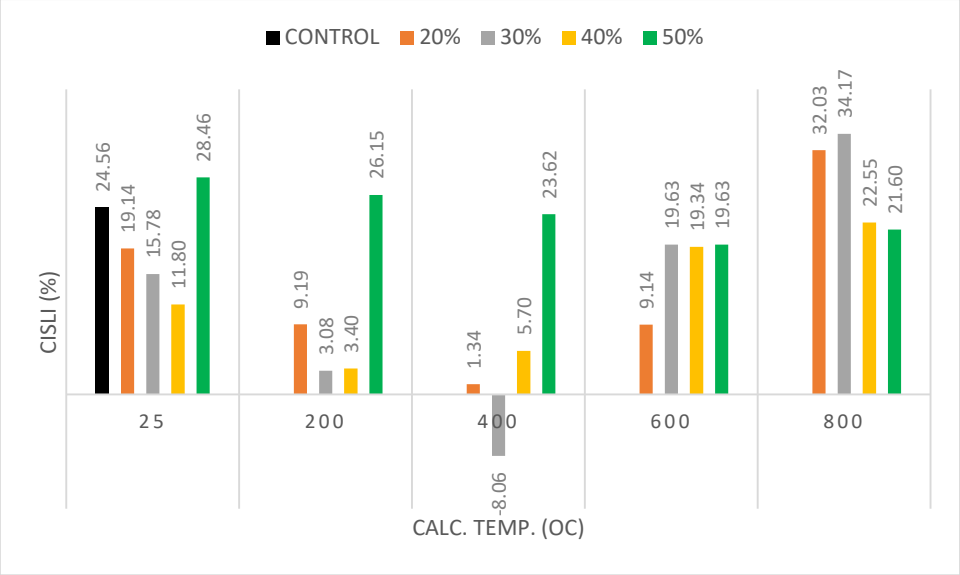

Figure 4.56: Result of calcination and replacement level of PSA on chloride induced strength loss index of PSA cement blended concrete

Appendix K1 is a summary of the analytical findings for the variance as analysed, and variation coefficients for CISLI of PSA cement blended concrete. The components of the equation are linear mixture, AB, ABC, and ABC2. All model components but the linear mixture where observed to be significant having p-value<0.05.

The Linear mixture having a p-value of 0.6519 (>0.05) conforms with the hypothesis for nullification. The integrated model is a quadratic by quadratic model having a significant p-value < 0.05.

Coefficients of regression for the model (Appendix K2) are 0.8194, 0.7678 and 0.7092 for the R^2, adjusted R^2 and predicted R^2 respectively. This is relative to the index of the cumulative summed up squares and the residual sum of squares. The Standard error spreads out of the mean value of 17.68 by 5.23, and the percentage ratio of 29.61% was obtained as the coefficient of variation. The coefficient of variation is below 30% hence the model is statistically satisfactory.

Appendix K3 represents the coefficients of the individual model components, degrees of freedom, standard error associated with each coefficient, range of confidence interval and variance inflated factors. As a check for orthogonality of the process and mixture component factors, ABC interaction had the highest obtainable orthogonality of one and can be said to be perfectly satisfactory and free of the collinearity effect. Other components of the model such PC, PSA, PC/PCA interaction and the squared interaction of all three components all had value inflated factors less than 10 and as such can be said to have satisfactory coefficients.

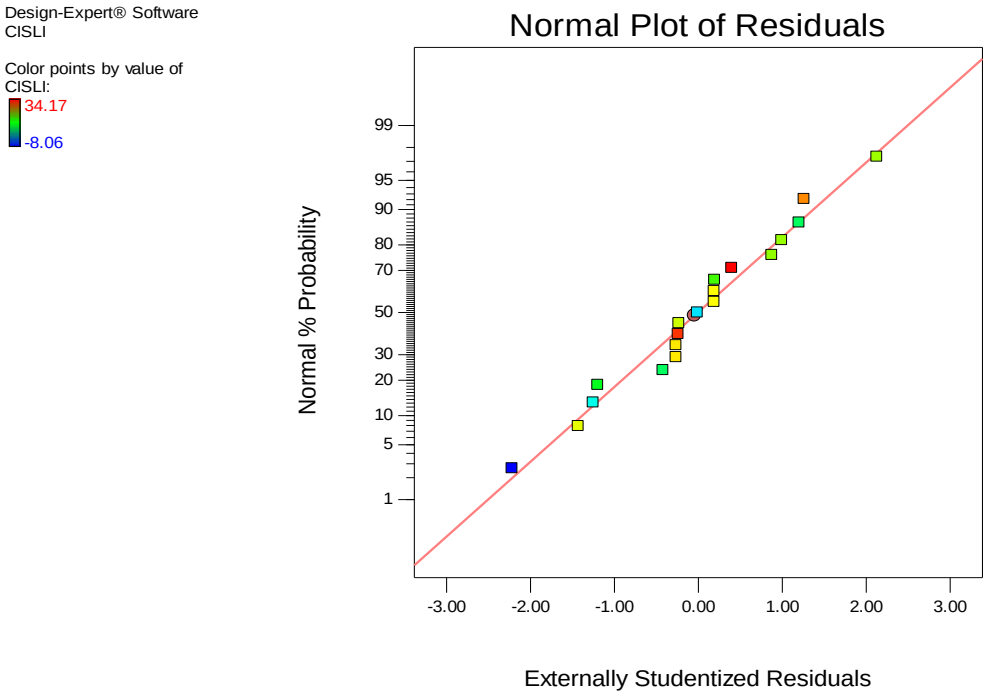

Figure 4.57: Normal plot of residual spread for the CISLI of PSA Cement blended concrete

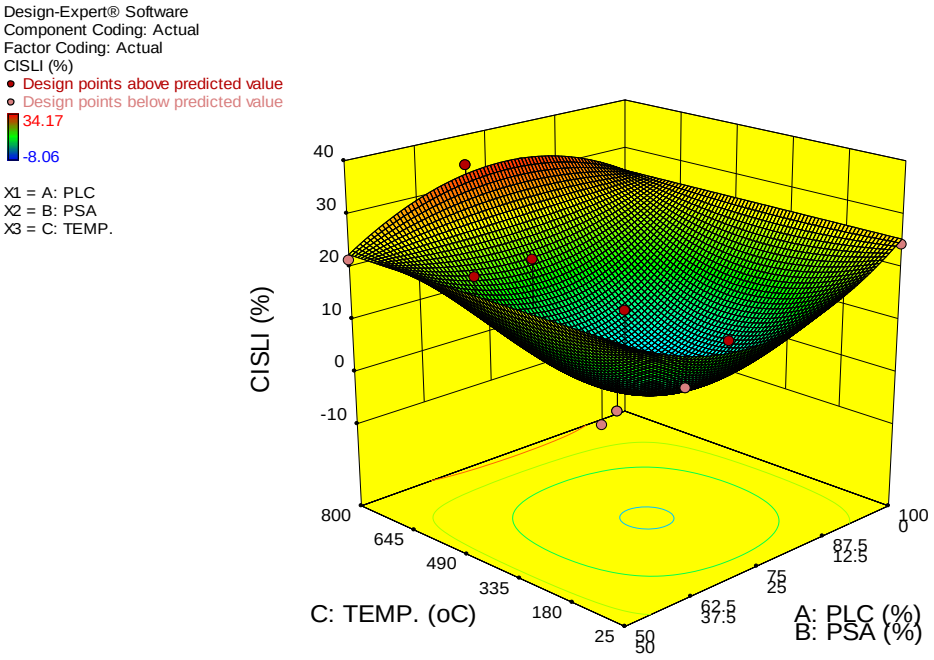

Figure 4.58: Graphical illustration of the effect of PSA content and temperature at calcination on the CISLI of PSA cement blended concrete

Figure 4.57 represents the normal distribution of the externally studentised residual against the probability of occurrence. The externally studentised errors are normally distributed as such model prediction is satisfactory.

Figure 4.58 represents the effect of PSA content and temperature at calcination on the CISLI of PSA cement blended concrete. A quadratic trend is seen for both PSA content as well as calcination temperature, having their peak points about the edges of their boundaries and troughs about the centroids of their axis having a 'bow-like' shape formation. This implies that the linear effect of both calcination temperature and PSA content is directly proportional to CISLI only within the range of the originating points to the centroids of the established boundaries.

The optimized and selected solution for CISLI of PSA cement blended concrete has a desirability of 0.564 and showed a CISLI of 2.10%, observed to be 91.44% lower than the control's observed CISLI of 24.56%. The selected solution was at a constraint level of 80.35PC, 19.65PSA and at a calcination temperature of 425^{o}C.

The predominance of chloride salts is mainly in the marine regions and remains a basic challenge threatening stability of structures. In a bid to ensure the durability of steel in concrete, specific concrete cover is recommended based on the exposed condition of the concrete structure to keep the steel in a state of passivity. Chloride driven strength loss indexes for non-reinforced concrete structures is opined on the destruction of the concrete cover layer which is a primary indication of the concrete's ability to protect and keep any embedded reinforcement in its state of passivity. Guo *et al*. (2018) reported findings in compliance with the observations of this research suggesting a loss in compressive strength of concrete cured in sea water for a period of 28 days. CCAA (2009), after a 34-yearlong study on the compressive strength features of concrete concluded that the aluminate component of the major phases of cement is responsible for the formation of chloro-aluminates (Friedel's salt) which when demobilised reduces the alkalinity of the cement structure and subsequently de-passivates the embedded steel structure. However, findings from their study revealed that no substantial effect was observed on the compressive strength of the tested concrete over the duration of the study. On a conclusive note, literature (Walker and Pavia, 2011;

CCAA 2009), as well as the findings of this validates the need for a pozzolanic reactivity to reduce the non-evaporable pore water as well as voids present in concrete so as to prevent the mobilisation of the Friedel's salt and corrosion activities on and within the concrete. As such, optimized solution suggested by these findings can be adequately adopted as a practice in the engineering society.

Developed model for the CISLI of PSA cement blended concrete is as shown in Equation 4.10 below;

$$\text{CISLIpsa} = 0.256\text{PC} + 0.738\text{PSA} - (0.011\text{CSA} * \text{PC} * \text{PSA}) + (8.478 * 10^{-3} * \text{PSA} * \text{T}) - (1.696 * 10^{-4} * \text{PC} * \text{PSA} * \text{T}) - (1.126 * 10^{-5} * PSA * T^2) + (2.512 * 10^{-7} * PC * PSA * T^2) \quad (4.10)$$

Where;

CISLIpsa = Chloride induced strength loss index of PSA cement blended concrete (%)

PC = Mass proportion of Portland cement in total binder of PSA cement blended concrete (%)

PSA = Mass proportion of PSA in total binder of Cement blended concrete (%)

T = Calcination temperature for producing PSA in PSA Pozzolan concrete (^{o}C)

4.3.5. Calcination and mixture configuration variations on the CISLI of Clam Shell Ash Cement blended concrete

Laboratory obtained data for the compressive strength of CSA cement blended concrete, cured in chloride solution for a period of 28 days post 28 days hydration period, is as shown in Figure 4.59. The resultant losses relative to the chloride attack is illustrated on the plot captured in Figure 4.60. From Figure 4.59 and 4.60, results obtained at ATM and 800 ^{o}C showed greater losses in the compressive strength of CSA cement blended concrete. Results obtained between 200 ^{o}C and 600 ^{o}C showed minimal losses in the compressive strength of CSA cement blended concrete. The least losses in compressive strength was obtained at 200 ^{o}C at a replacement level of 30%, having a strength gain of about 0.5%. At 600 ^{o}C, least strength loss was obtained at 40% cement replacement level, having a CISLI of 0.44%, which is about 98% lower than the control.

Calcination temperatures well as cement replacement variations were both observed to have a quadratic effect on the CISLI of CSA cement blended concrete. The centroid of cement replacement effect was 40% for 25 ^{o}C specimens; 30% for 200 ^{o}C specimens; 30% for 400 ^{o}C specimens, 40% for 600 ^{o}C specimens and 30% for 800 ^{o}C specimens. The centroid of calcination temperature was at 600 ^{o}C. This is an early indication that the optimum variables for optimal concrete resistance to chloride attack are at a configuration around 600 ^{o}C and at 30% cement replacement level.

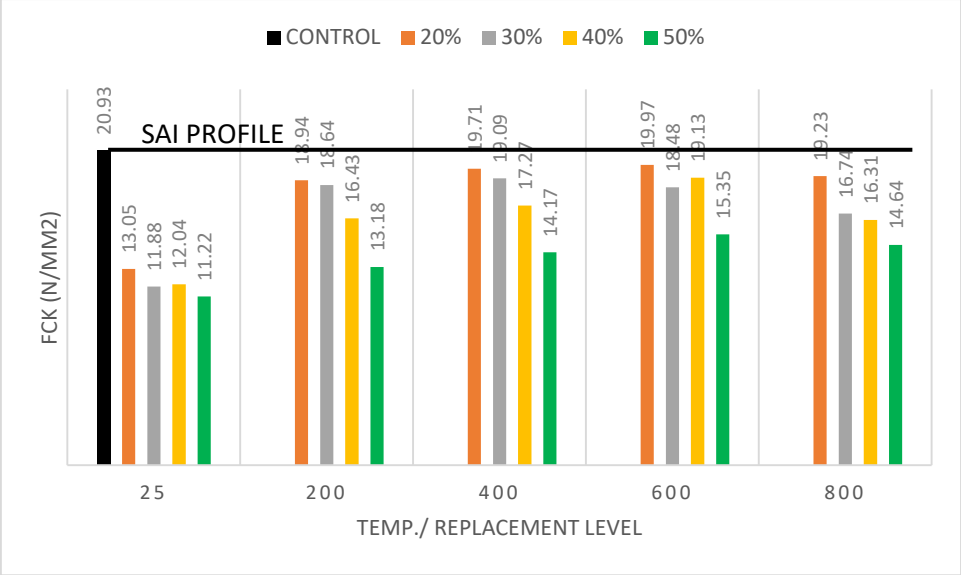

Figure 4.59: Effect of calcination of CSA on the compressive strength performance of CSA cement blended concrete under chloride attack

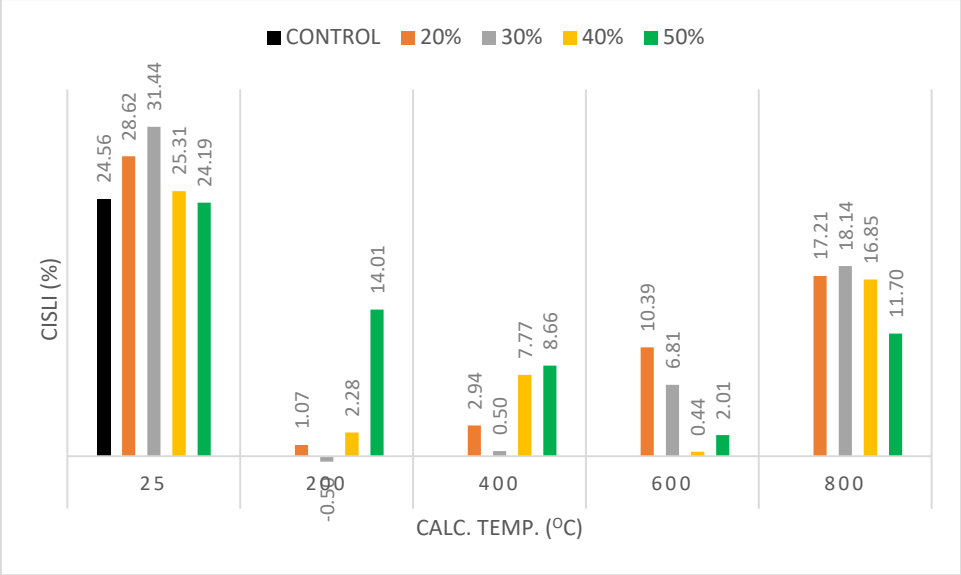

Figure 4.60: Result of calcination and Replacement Level of CSA on the Chloride induced strength loss index of CSA cement blended concrete

Appendix L1and L2 represents the analysed variance and regression coefficients of the model for CISLI of CSA cement blended concrete, respectively. The equation is made up of model terms for "quadratic processes" and "mean mixtures," integrating two (2) model terms for "calcination temperature" and "calcination temperature squared". All model components were significant at a confidence interval exceeding 95% (P <<0.05).

The model's ratio to the square of its cumulative summed up squares produced a regression coefficient of 0.7867. Consequently, the 'adjusted' and 'predicted' regression coefficients were 0.7601 and 0.7095 and having a difference less than 0.2, which implies that the model is sound enough for predictions and simulations.

Standard error was 5.07 over a mean of 13.91, with a deviation coefficient of 36.46%. The adequacy of the model's precision was 11.32, which implies that an error could exist in every 11.32 predictions. In essence, the least expected err or of 4, is significantly above the model's maximum probable error, accordingly, the model's signal is adequate enough within its design scope for statistical simulation purposes.

The coefficients of the model shown in Appendix L3 represents that no factor (mixture or process) was inflated above 30 as a result of the model's variance, and as such, prevents multicollinearity amongst the variables. A perfect orthogonality of 1.0 was obtained for coefficients of the two model terms, which informs the statistical ease with which cause and effect within the model can be simulated with no overlapping variable.

Figure 4.61's statistical analysis of the model's performance shows an externally studentised error distribution that is relatively linear. As a result, the model is considered to be statistically trustworthy.

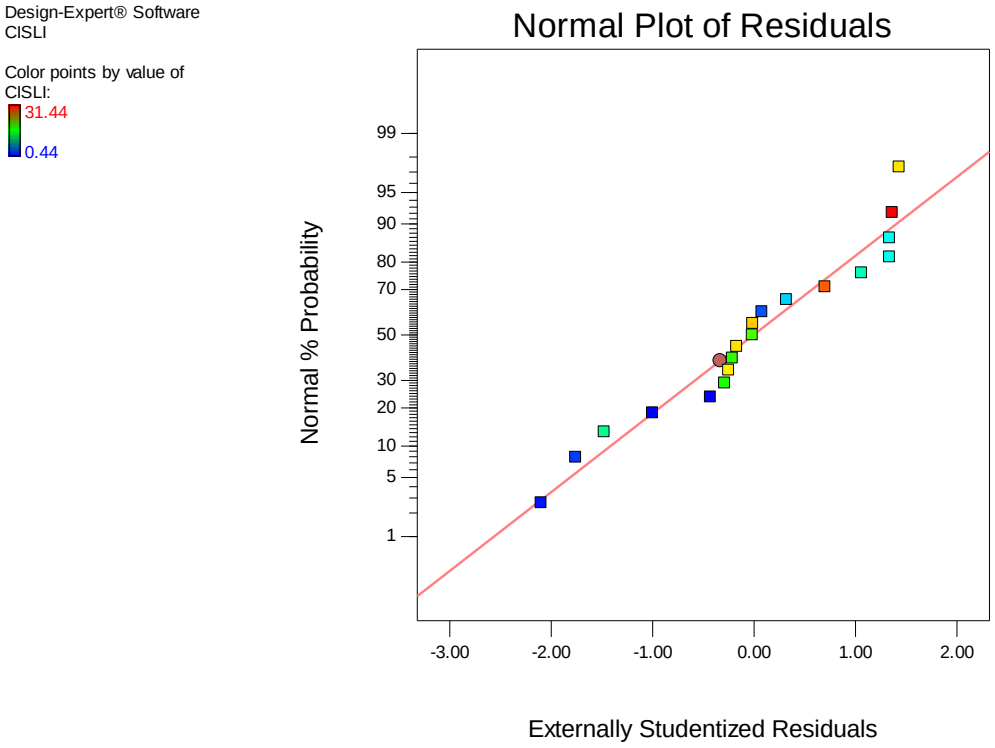

Figure 4.61: Studentised error spread for the CISLI of CSA Pozzolan concrete

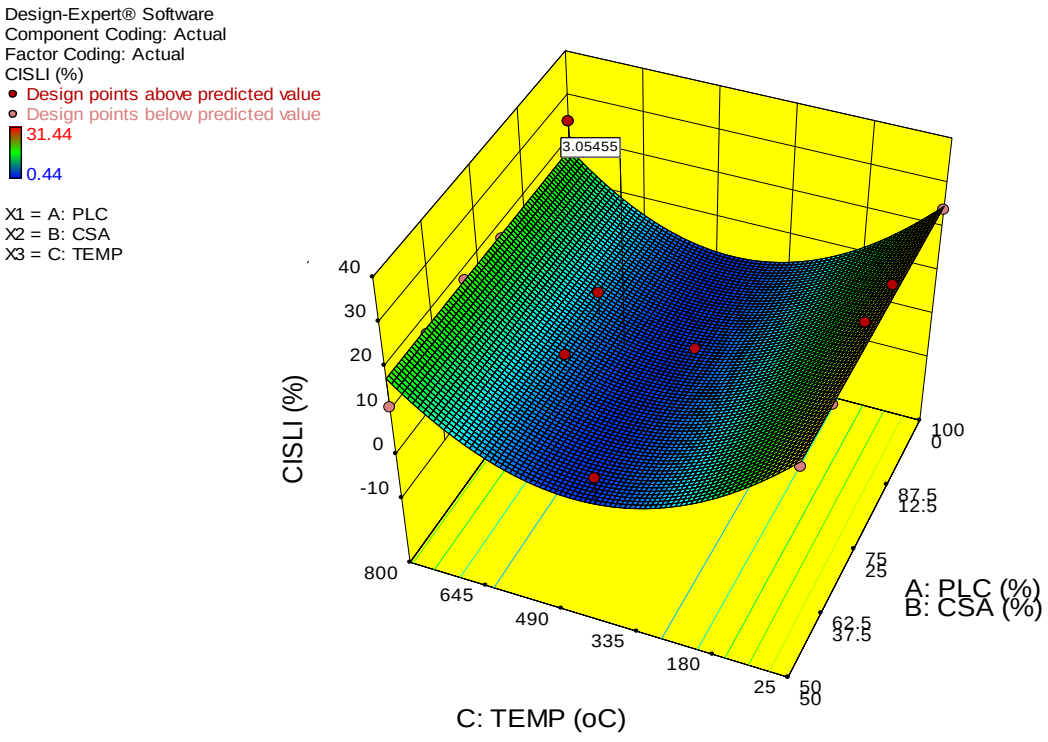

Figure 4.62: Model simulation for the CISLI of CSA cement blended concrete

Figure 4.62 represents a mean mixture interaction and a quadratic process factor interaction on the CISLI of CSA cement blended concrete . The equation's mean mixture component interaction indicates a relatively mean/constant effect of variations in CSA content on the CISLI of CSA cement blended concrete . The 'process' term of the model, developed a sagging quadratic curve troughing between 300 ^{o}C and 600 ^{o}C calcination temperature, peaking at 450 ^{o}C. The model generally suggests a need to constrain the calcination temperature to below 600 ^{o}C to reduce the potentials of strength losses due to chloride attack.

When mussel shell samples were thermogravimetrically analyzed at room temperature up to 200 ^{o}C, the weight loss was approximately 0.4% as a result of the release of absorbed water, at temperatures between 200 ^{o}C and 356 ^{o}C, the weight loss increased to 1.7% due to oxidation and removal of volatile matter, and at temperature levels of 356 ^{o}C to 600 ^{o}C, the weight loss further increased significantly to 2.3%. Felipe-Sese *et al*., (2011). Martinez-Garcia et al. (2017), corroborates earlier findings in which the weight loss of mussel shells was reported to be greater than 40% at temperatures ranging from 670 ^{o}C to 800 ^{o}C Celsius. Similarly, Chiou *et al*. (2014), discovered that oyster shells were virtually fully destroyed at temperatures surpassing 760 ^{o}C, while Mohamed *et al*. (2012), found that increasing the temperature from 700 ^{o}C to 900 ^{o}C resulted in a considerable drop in the weight of cockle shells owing to carbonate breakdown. For seashells and typical limestone, Safi *et al*. (2015) showed a similar pattern in weight loss related to an increase in temperature such that thermogravimetric endothermic peak at 842.5 ^{o}C was linked to the decarbonation of the seashell samples, and a similar peak was discovered for limestone. These led to the conclusion by Mo *et al*., (2018), that calcination of sea shells should exceed 600 ^{o}C in order to fully activate the pozzolanicity of the materials by achieving complete decarbonation and oxidation of the calcium mineral. However, the sustainability implication of this is that, close to half of the material would have been rendered inert and would result in the formation of pores and voids in the hydrated cement blended concrete which will be the transportation route for attacks such as chloride attack. It is however justified that losses in weight or strength be the greater justifier on the effect of calcination on the reactivity of Pozzolans on their mechanical and durability contributions to cement blended concrete.

At optimisation, the optimal chloride induced strength loss index was obtained at 3.06% at constraints of 76.87%PC:23.13% CSA mix produced at a calcination temperature of 527 ^{o}C. This was observed to be 87.5% lower than the losses observed with the 28 day control loss of 24.56%. Consequently, in preference to mechanical, durability, environmental and economic gains, the optimised solution can be adopted and mostly for non-structural engineering works.

Developed model for the CISLI of CSA cement blended concrete is as shown in Equation (4.11)

$$\text{CISLIcsa} = 28.174 - 0.116\text{T} + (1.290 * 10^{-4} * T^{2}) \quad (4.11)$$

Where;

CISLIcsa = Chloride induced strength loss index of HAP cement blended concrete (%)

T = Calcination temperature for producing HAP in HAP concrete (^{o}C)

4.3.6. Calcination and mixture configuration variations on the CISLI of HAP Cement Blended Concrete

Having studied the contributions of PSA and CSA to potentials of concrete resistivity to chloride attack, this section will discuss on the data and analysis of data on the hybrid's contribution relative to synergistic ratio, replacement level and calcination temperature. Laboratory data are illustrated on plots as shown in Figures 4.63 to 4.70.

Figures 4.63 and 4.64, represents the compressive strength and losses in compressive strength of HAP cement blended concrete at 20% cement replacement level, cured for 28 days post hydration period in 10% chloride solution.

From Figures 4.63 and 4.64, a visible trend is the shape of an arc formed by the losses in strength over the various synergistic ratios for all the calcination temperatures. Minimum loss in strength was observed at 400 ^{o}C for most of the synergies. Maximum loss in strength was observed at ATM for all of the synergies. At a synergistic ratio of 60% PSA: 40% CSA, specimens produced at 600 ^{o}C have a loss in strength of about 22.8% which is observed to be 7.3% lower than the control loss of 24.56%

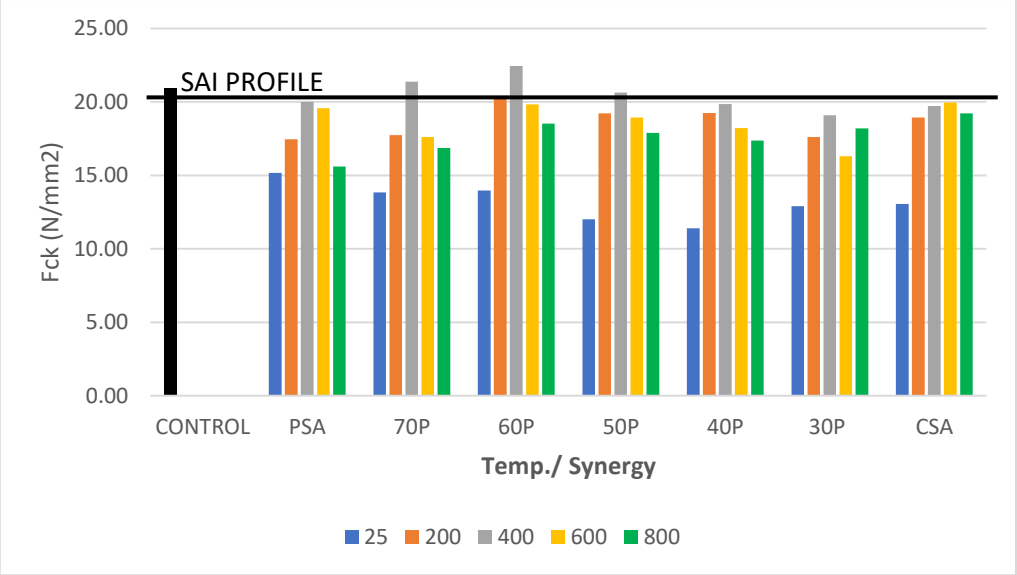

Figure 4.63: Effect of Chloride Attack on the Compressive Strength of HAP Concrete At 20% Cement Replacement Level

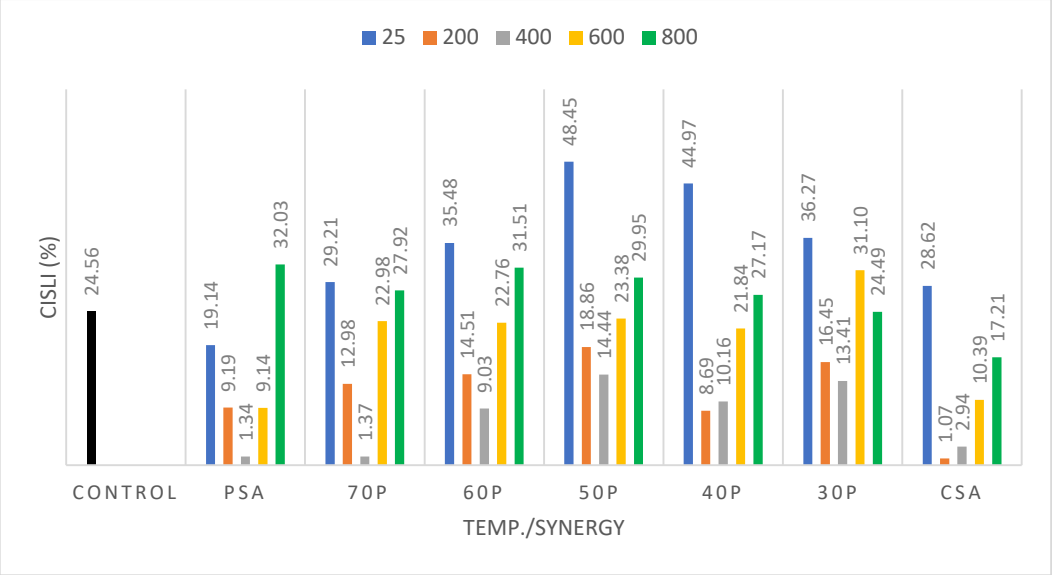

Figure 4.64: Chloride Induced Strength Loss Index of HAP Cement blended concrete at 20% Cement Replacement Level.

Figures 4.65 and 4.66 show the compressive strength and losses in compressive strength of HAP cement blended concrete at30% cement replacement level, cured for 28 days in a 10% chloride solution.

From Figure 4.65 and 4.66, A visible trend is the shape of an arc formed by the losses in strength over the various synergistic ratios for all the calcination temperatures. Minimum loss in strength was observed at 400 ^{o}C for most of the synergies. Maximum loss in strength was observed at ATM and 800 ^{o}C for all of the synergies. Within each synergy, the result of calcination formed a shape like that of letter 'U' having both peak points at ATM and 800 ^{o}C, and its trough at 400 ^{o}C. At a synergistic ratio of 60P, specimens produced at 600 ^{o}C have a loss in strength of about 22.71% which is observed to be 7.5% lower than the control loss of 24.56%

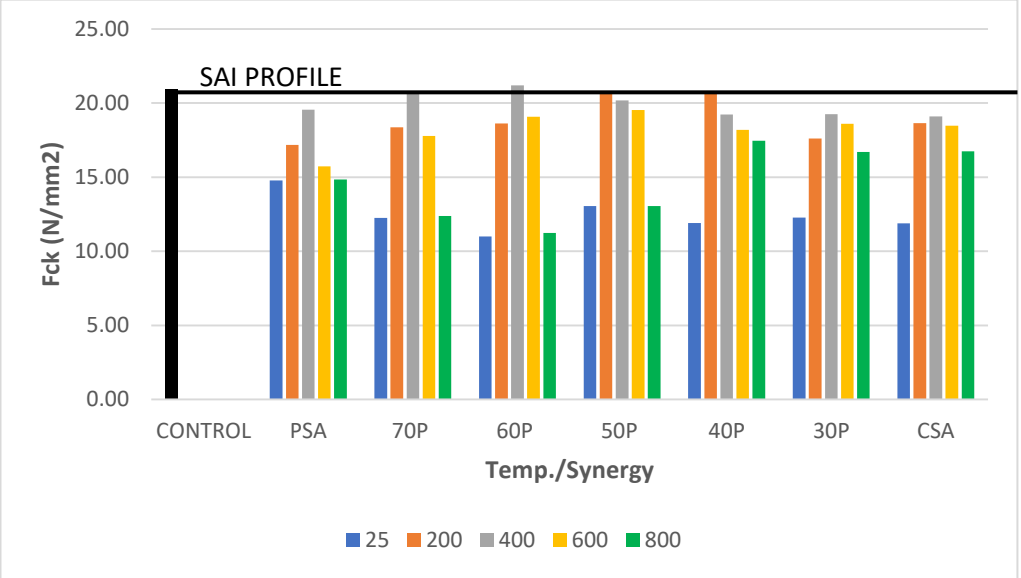

Figure 4.65: Effect of Chloride Attack on the Compressive Strength of HAP Concrete At 30% Cement Replacement Level

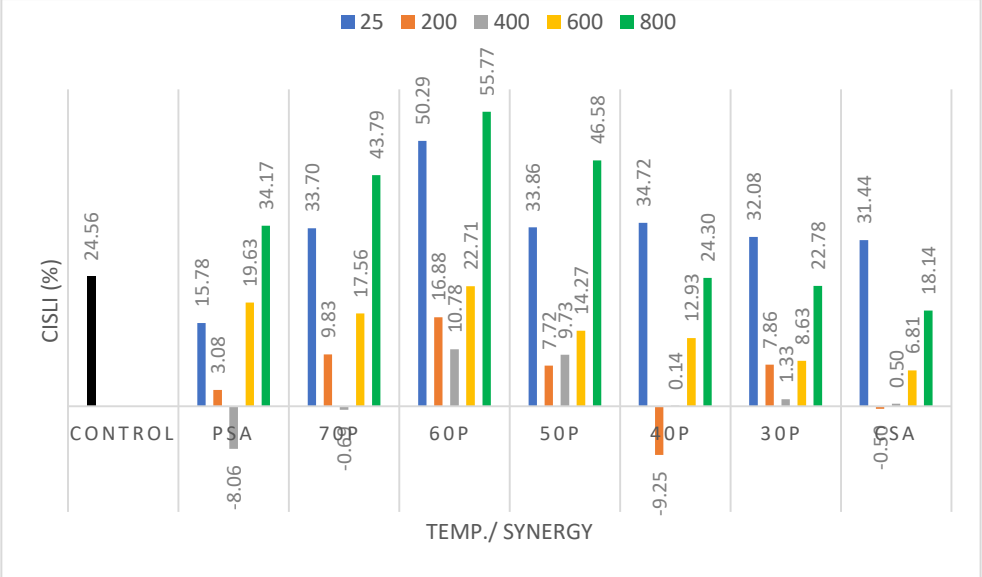

Figure 4.66: Chloride Induced Strength Loss Index of HAP Ternary Blended Cement Concrete at 30% Cement Replacement Level

Figures 4.67 and 4.68 show the compressive strength and losses in compressive strength of HAP cement blended concrete at40% cement replacement level, cured for 28 days in a 10% chloride solution.

From Figure 4.67 and 4.68, A visible trend is the shape of an arc formed by the losses in strength over the various synergistic ratios for calcination temperatures of 200 ^{o}C, 400 ^{o}C and 800 ^{o}C. ATM synergies had somewhat of a distorted arc shape and 600 ^{o}C samples had a U shape, peaking at PSA and CSA and troughing at 40P. Minimum loss in strength was observed at 600 ^{o}C for both 40P and 50P where a gain of about 12.6% and 4.6% was observed. Maximum loss in strength was observed mostly at 800 ^{o}C for all of the synergies. Within each synergy, the result of calcination formed no constant shape on the strength losses of the specimens at varying temperatures. At a synergistic ratio of 60P, specimens produced at 600 ^{o}C have a loss in strength of about 6.1 % which is observed to be 75% lower than the control loss of 24.56%

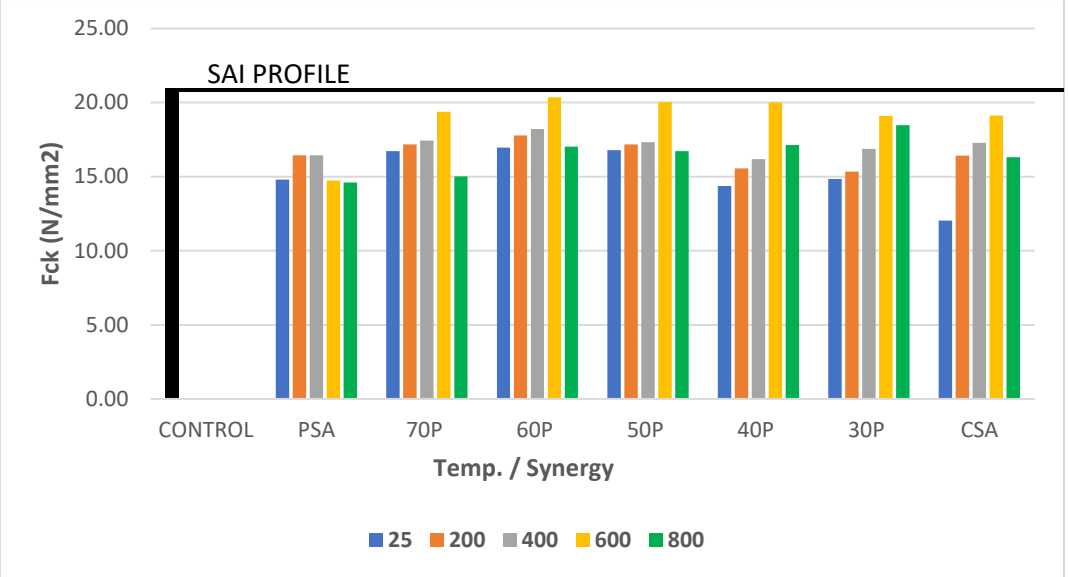

Figure 4.67: Effect of Chloride Attack on the Compressive Strength of HAP Concrete At 40% Cement Replacement Level.

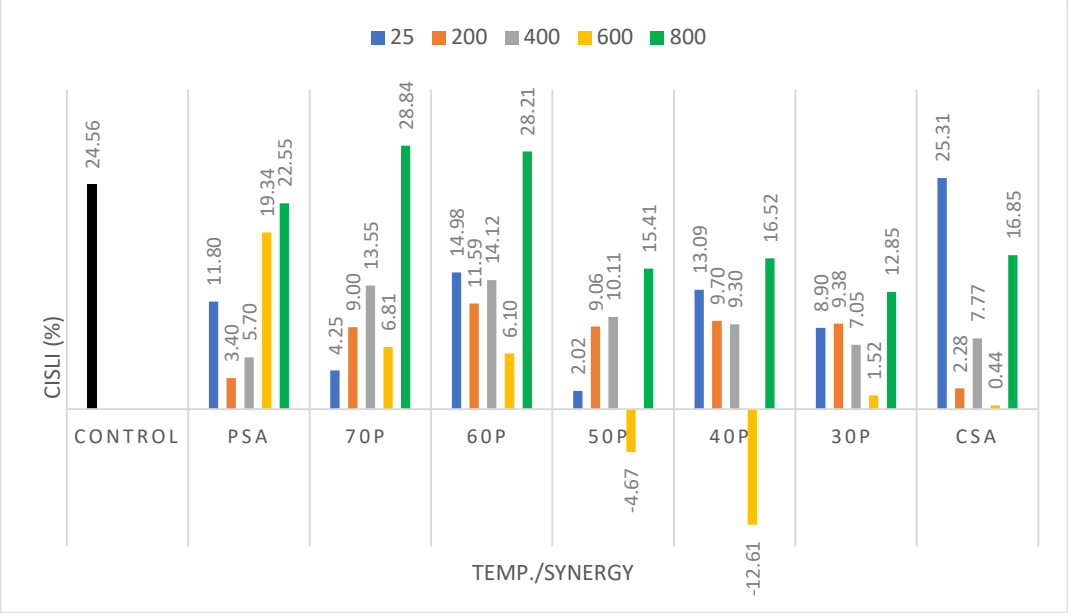

Figure 4.68: Chloride Induced Strength Loss Index of HAP Ternary Blended Cement Concrete at 40% Cement Replacement Level

Figure 4.69 and 4.70, represents the compressive strength and losses in compressive strength of HAP cement blended concrete at 20% cement replacement level, cured for 28 days post hydration period in 10% chloride solution.

From Figure 4.69 and 4.70, a visible trend is the shape of letter 'U' formed by the losses in strength originating from PSA and terminating at 40P beyond which a sharp drop was observed between 40P and CSA. This trend was consistent for all calcination. The effect of temperature within each synergy was observed to be inversely proportional to CISLI such that at higher calcination temperatures, a reduction in strength loss was observed. This was observed to be true up to 600 ^{o}C beyond which a negative turn if behaviour was observed at 800 ^{o}C for most of the synergistic ratios. Minimum loss in strength was observed at 600 ^{o}C for 40P synergistic ratio at 0.32% found to be lower than control loss by about 98.7%. Maximum loss in strength was observed to vary with synergistic ratio, however, ATM and 800 ^{o}C were prominent in most cases. At a synergistic ratio of 60P, specimens produced at 600 ^{o}C have a loss in strength of about 10.65 % which is observed to be 56.6% lower than the control loss of 24.5.

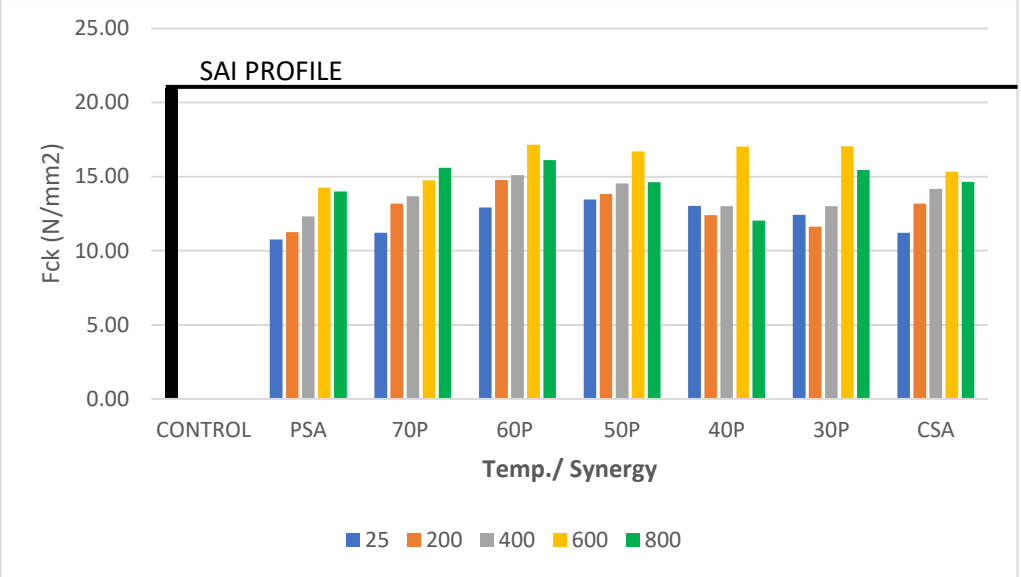

Figure 4.69: Effect of Chloride Attack on the Compressive Strength of HAP Concrete At 50% Cement Replacement Level.

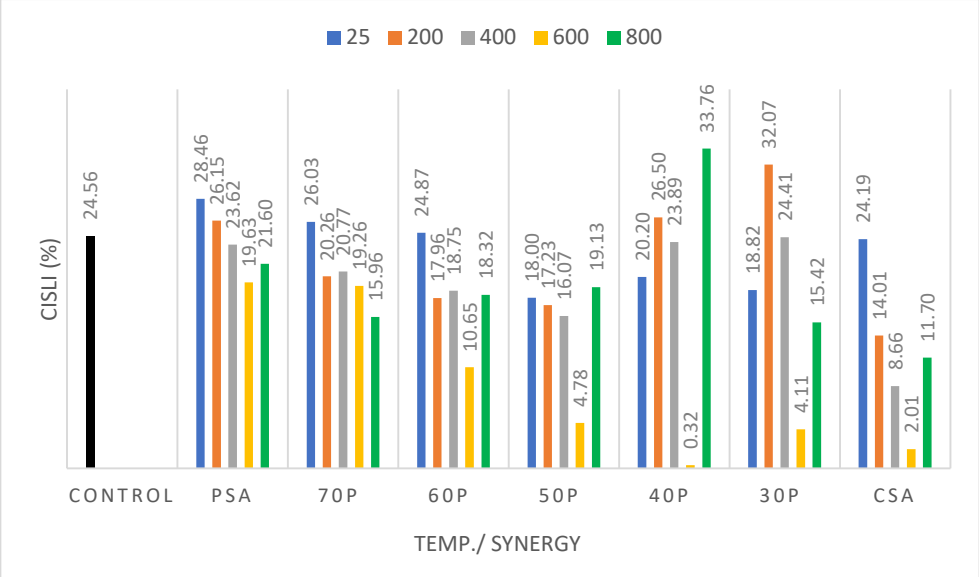

Figure 4.70: Chloride Induced Strength Loss Index of HAP Ternary Blended Cement Concrete at 50% Cement Replacement Level

The analysed variance and regression coefficients of the developed equation for CISLI of HAP concrete is as shown in Appendix M1. The equation (model) as developed, is an equation with combined model terms of 'quadratic mixture and process' origin, involving seven (7) model terms; 'linear mixture', 'AB', 'AC', 'CD', 'CD^2', 'ABD^2' and 'ACD^2', with a confidence interval exceeding 95% ($P<<0.05$) which adequately negates the hypothesis for nullification.

The regression coefficient was calculated as the model's ratio to the square of its entire sum and came to be 0.7631. As a result, the adjusted and anticipated coefficients of regression were found to be 0.6634 and 0.5397, respectively, indicating that the model is reliable enough for simulations and predictions.

Standard error was 5.47 over a mean of 15.56, with a deviation coefficient of 35.38%. The adequacy of the model's precision was 8.56, which implies that an error could exist in every 8.56 predictions. In essence, the least expected error of 4, is significantly above the model's maximum probable error, accordingly, the model's signal is adequate enough within its design scope for statistical simulation purposes.

The coefficients of the model shown in Appendix M3, indicates that multicollinearity impact is absent for all model components, as no factor exceeded 10 by reason of inflation as a result of the model's variance. This suggests that independent variables can be varied statistically, which is a useful prerequisite for examining the impact of changing independent factors on responses.

Statistical check on model's performance as seen in Figure 4.71 indicates a relatively linear error distribution that were externally moderated/trained. Thus, the developed equation can be accepted.

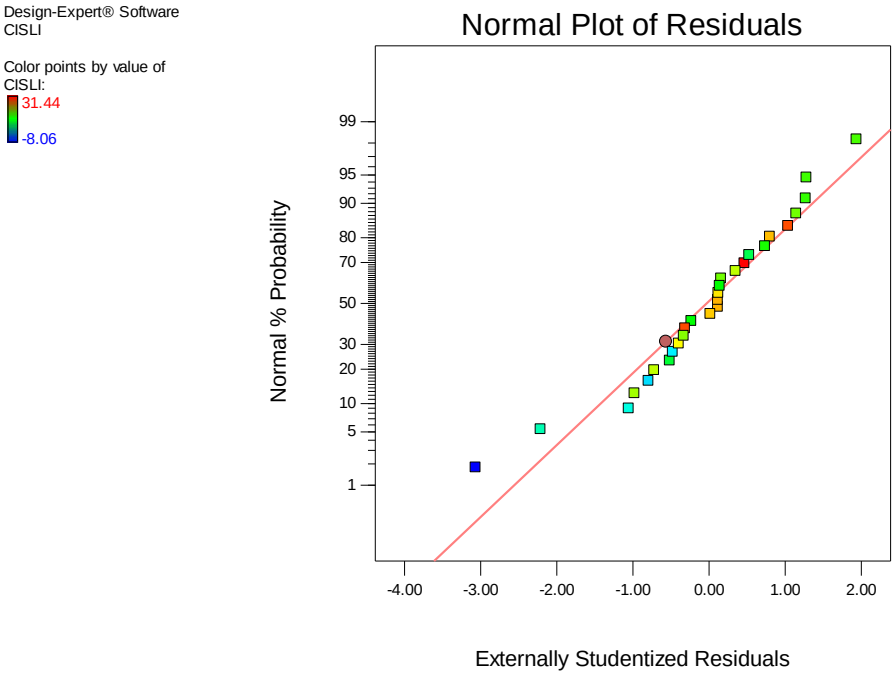

Figure 4.71: Studentised error spread for the CISLI of HAP concrete

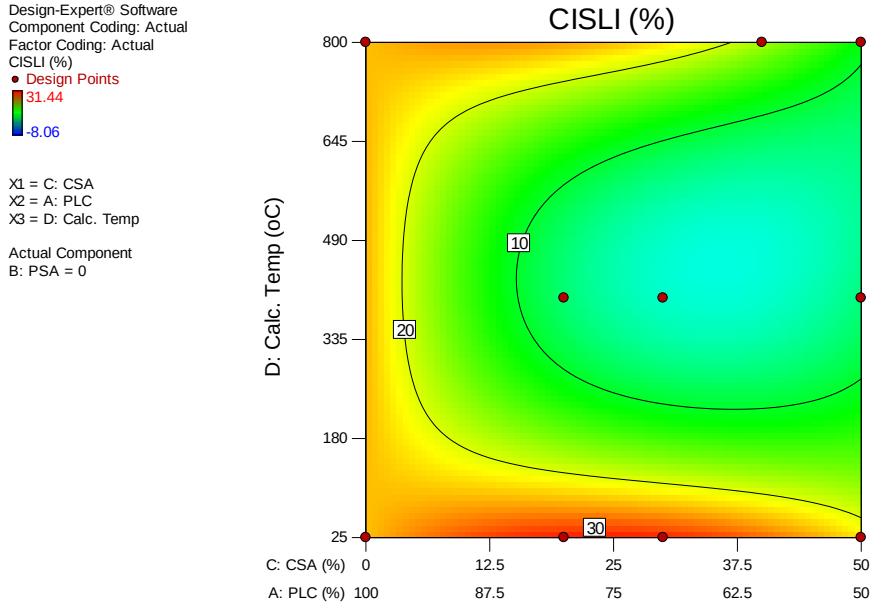

Figure 4.72: Three-dimensional model at 0% PSA level on the CISLI of HAP concrete

Figure 4.72 to 4.75 represents the model's simulations at varying mixture terms as well as varying process inputs. Results on the variations the temperature at calcination on the CISLI of HAP concrete was noted as quadratic, sagging with a trough range of 335 to 490 ^{o}C at all levels of mixture variations. Figure 4.63 – 4.66, is a representation of the CISLI response for HAP cement blended concrete at varying PSA contents. The quadratic curve developed for PC: CSA mix, showed a CISLI troughing between 25 to 50% CSA content. When PSA concentration is increased to 10%, the quadratic trough of CISLI was seen to range between 10% CSA- 30% CSA. Similar to this, a reduction in the CISLI between 0 - 16.25% was seen at a PSA concentration of 17.5%. This is a clear indicator that the CSA concentration must be decreased for every increase in PSA content in order to maintain minimum compressive strength losses in HAP cement blended concrete due to chloride-induced attack.

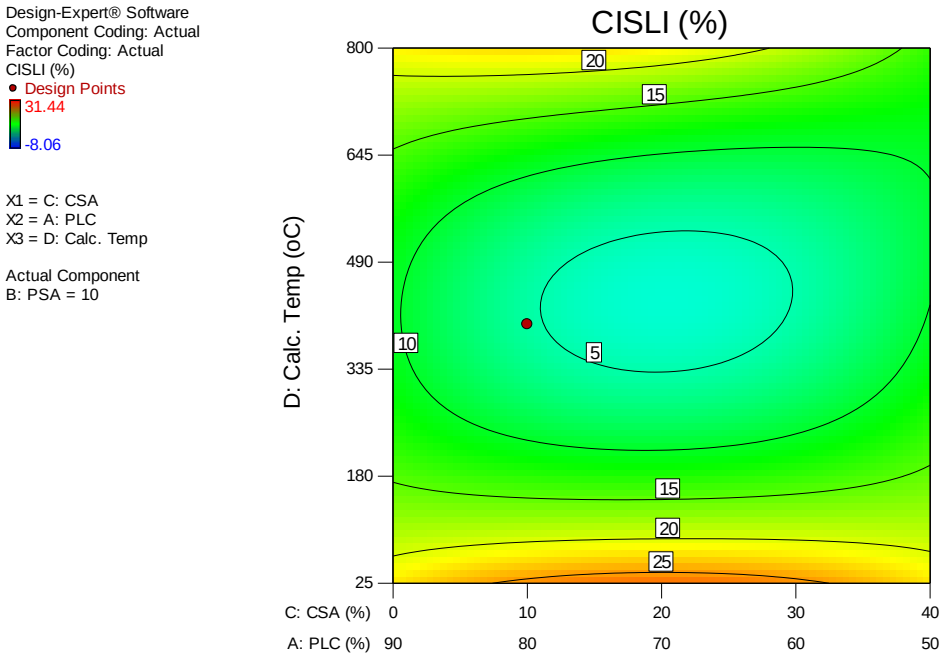

Figure 4.73: Three-dimensional model at 10% PSA level on the CISLI of HAP concrete

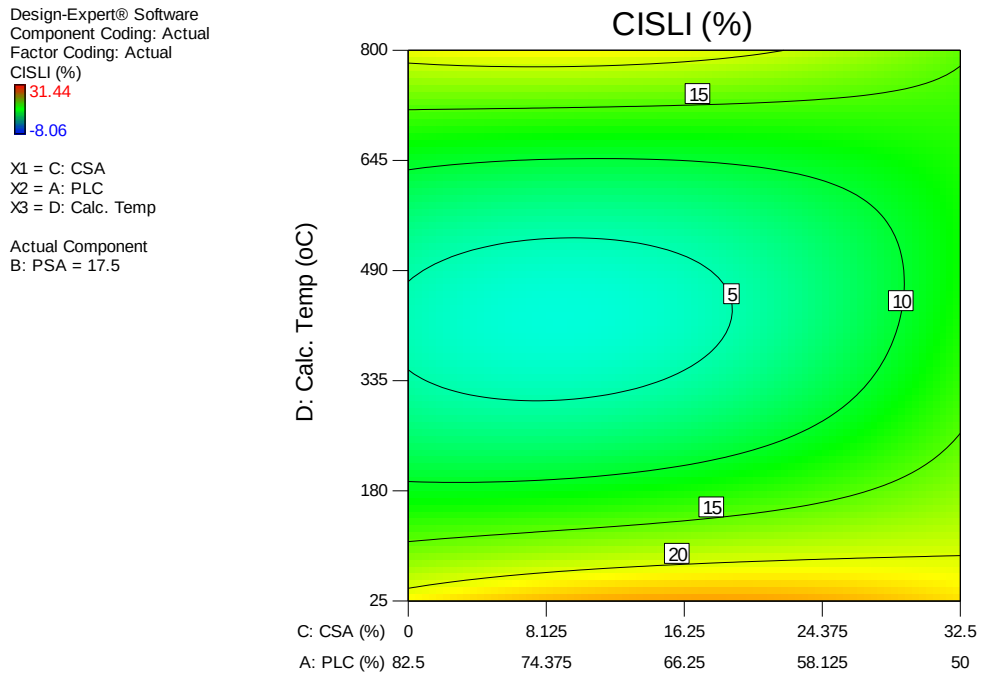

Figure 4.74: Three-dimensional simulation of 17.5% PSA level on the CISLI of HAP concrete

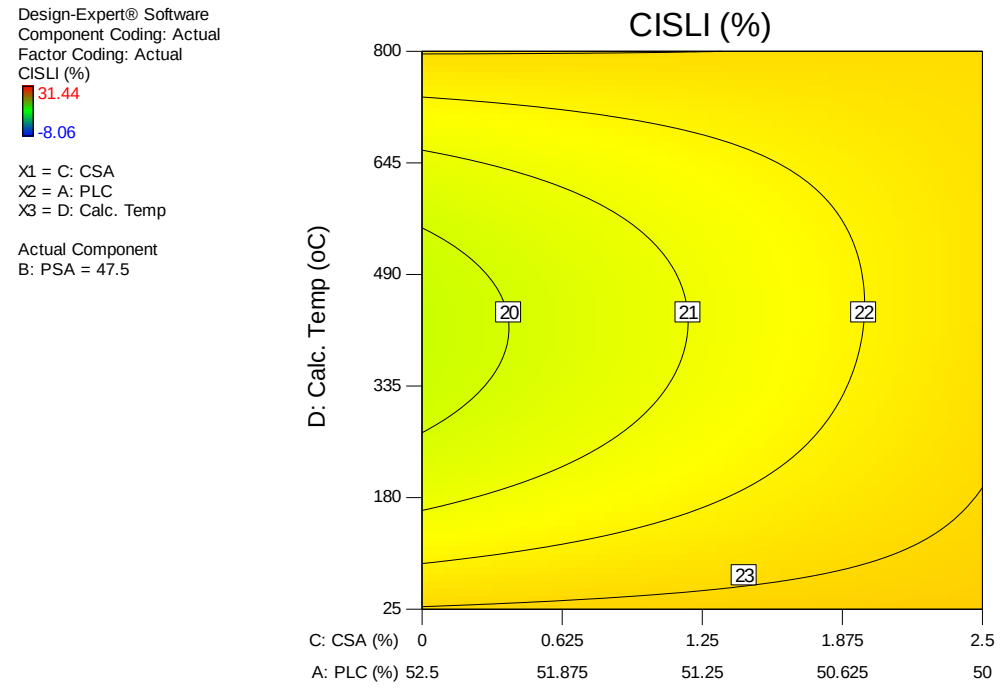

Figure 4.75: Model simulation at 47.5% PSA level for the CISLI of HAP concrete

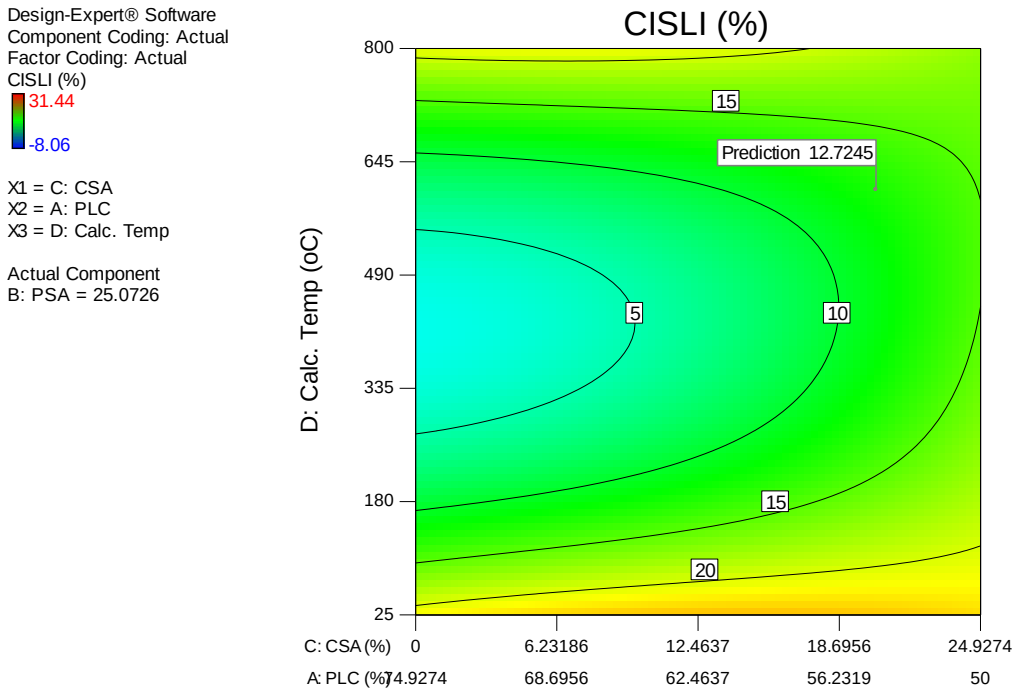

Figure 4.76: Three-dimensional and optimised model variables for the CISLI of HAP concrete

Combining the custom constraint of all five responses with the water absorption index and similar factors constraint as was the case with compressive strength during optimization (Figure 4.76), same mixture configuration with CISLI of 12.72% which was 51.8% of PLC control was obtained. Therefore, it is possible to apply these findings in the building industry, mostly for non or lightly reinforced constructions like mass/plain concrete structures.

The equation (model) as developed, (Equation 4.12) can be applied in simulating the most probable responses at different levels of the variables within the boundaries of the model to meet specific sustainably and friendly design requirements

$$\text{CISLIhap} = 0.241\text{PC} + 0.238\text{PSA} - 0.515\text{CSA} - (1.705 * 10^{-4} * \text{PC} * \text{PSA}) + (0.015 * PC * CSA) + (8.195 * 10^{-3} * PSA * T) + (6.301 * 10^{-3} * CSA * T) - (1.639 * 10^{-4} * PC * PSA * T) - (1.529 * 10^{-4} * PC * CSA * T) - (9.933 * 10^{-6} * PSA * T^2) - (7.974 * 10^{-6} * CSA * T^2) + (1.987 * 10^{-7} * PC * PSA * T^2) + (1.854 * 10^{-7} * PC * CSA * T^2) \quad (4.12)$$

Where;

CISLIhap = Chloride induced strength loss index of HAP cement blended concrete (%)

PC = Mass proportion of Portland cement in total binder of HAP cement blended concrete (%)

PSA = Mass proportion of PSA in total binder of HAP Concrete (%)

CSA = Mass proportion of PSA in total binder of HAP Concrete (%)

T = Calcination temperature for producing HAP in HAP concrete (^{o}C)

4.3.7. Calcination and mixture configuration variations on the SISLI of Periwinkle Shell Ash Cement Blended Concrete

Laboratory data on the compressive strength of PSA cement blended concrete cured in a 2.5% sulphate solution for 28 days post hydration period, and the relative losses are as plotted in Figures 4.77 and 4.78.

From Figure 4.77, control strength was observed to reduce from 27.74 MPa when cured in freshwater to 23.17 MPa when cured in 2.5% sulphate solution, amounting to a loss in strength of about 16.5% after 28 days immersion in sulphate solution. A noticeable increase in strength for PSA cement blended concrete cured in sodium sulphate solution was observed mostly at 20 and 30% replacement levels when compared to their counterparts cured in fresh water. In essence rather than recording a loss in strength, it was rather a gain in strength for most of the PSA cement blended concretes. At 600 ^{o}C, and a replacement of 40%, specimens cured in fresh water had a strength of 18.27 MPa and lower than specimens cured in sulphate solution of 20.28 MPa, amounting to a gain of about 11% after 28 days immersion in 2.5% sulphate solution. Similar observations can be made for other replacement levels and calcination temperatures.

Figure 4.78 is an explicit explanation of the gains and losses in percentage between PSA cement blended concrete specimens cured in freshwater and those cured in 2.5% sulphate solution for 28 days curing period. From Figure 4.78, it's clear that rather than loosing strength, majority of the samples gained strength under sulphate attack. This gain in strength was at its peak for samples produced at 400 ^{o}C.

It is noteworthy that sulphate ions require the presence of calcium hydroxide in the formation of expansive ettringite which weakens, cracks and scales the concrete both internally and externally. The presence of pozzolans eats up the portlandite (by product of the hydration process of cement) and develops secondary binder gel to continue a secondary hydration phase hence the gain being observed under sulphate attack.

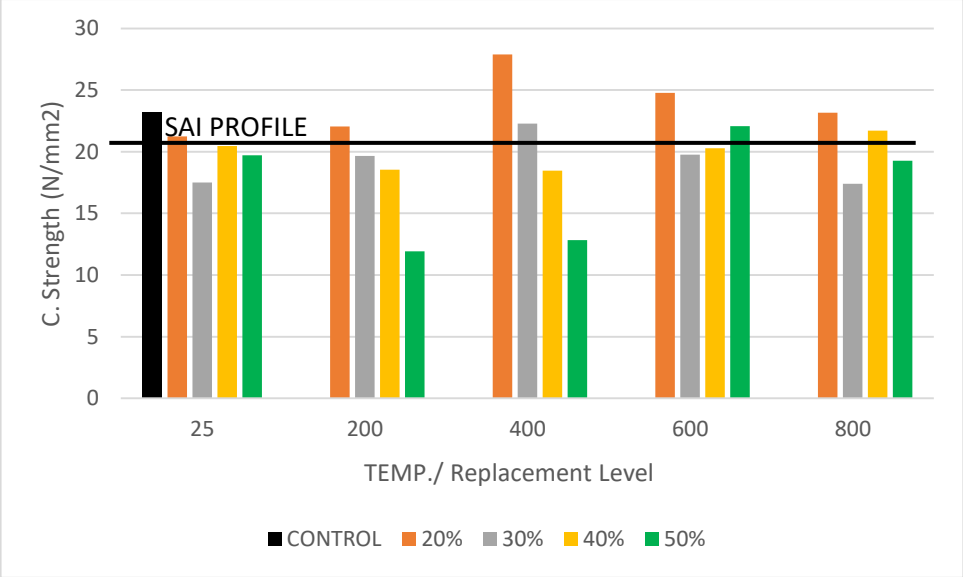

Figure 4.77: Result of calcination and replacement level of PSA on the resistance of PSA cement blended concrete to sulphate attack

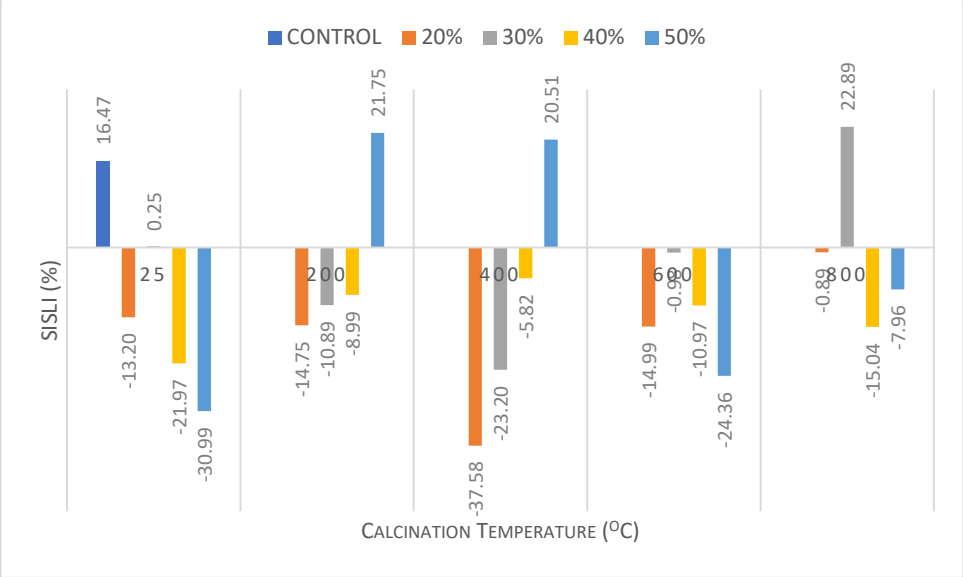

Figure 4.78: Result of calcination and replacement Level of Periwinkle Shell Ash on the SISLI of PSA cement blended concrete

A summary of the findings for the variance as analysed, and variation coefficients for the SISLI of PSA cement blended concrete is as shown in Appendices N1 and N2.

Model components are linear mixture, BC, AC^2, and BC^2. Linear mixture model component and BC Were not significant as seen in Table 4.1, however, components AC^2 and BC^2 were significant with $P < 0.05$. The all integrated and developed equation is a combination of a linear and a quadratic model having a significant P value of 0.0004 and negating the hypothesis for nullification.

Coefficients of regression for the model as seen in Appendix N2 are 0.7498, 0.6783 and 0.6171 for the R^2, adjusted R^2 and predicted R^2 respectively. This is relative to the index of the cumulative summed up squares and the residual sum of squares. The Standard error spreads out of the mean value of 0.84 by 0.18, and the percentage ratio of 21.42% was obtained as the coefficient of variation. The coefficient of variation is below 30% hence the model is statistically satisfactory.

Appendix N3, represents the coefficients of the individual model components, degrees of freedom, standard error associated with each coefficient, range of confidence interval and variance inflated factors for the SISLI of PSA cement blended concrete

Checking for multicollinearity, A, B and ABC had the highest variance inflated factors of 6.13, 3.49 and 5.84 respectively. ABC^2 have a VIF of 3.08 while AB had a perfect orthogonality of 1.0. In essence, all the coefficients of the model components are free from multicollinearity and as such are statistically satisfactory.

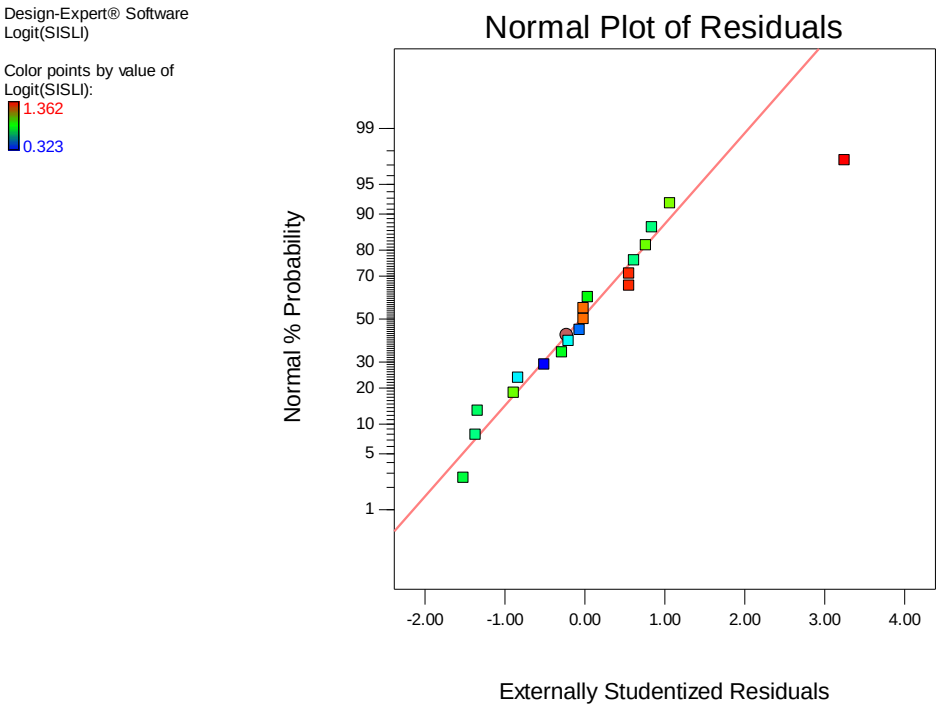

Figure 4.79: Studentised error spread for the SISLI of PSA Pozzolan concrete

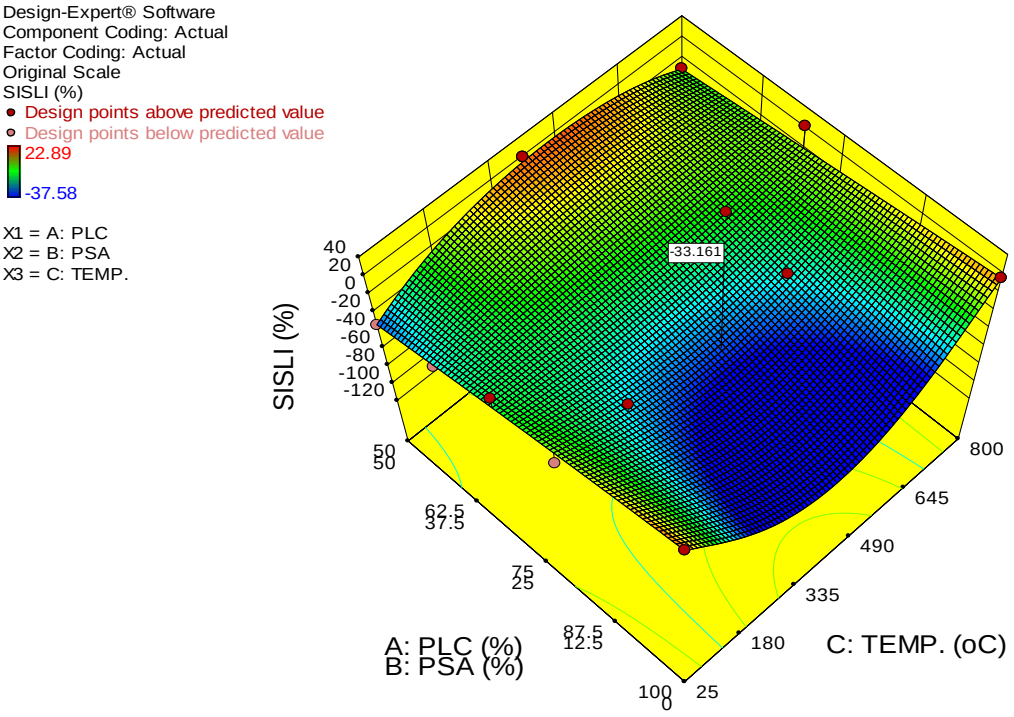

Figure 4.80: Graphical illustration of the effect of PSA content and temperature at calcination on the SISLI of PSA cement blended concrete

Figure 4.79 represents the normal distribution of the externally studentised residual against the probability of occurrence. The externally studentised errors are normally distributed as such model prediction is satisfactory.

Figure 4.80 is an express representation of the effect of the partial replacement of cement with periwinkle shell ash at varying levels of temperature at calcination on the SISLI of PSA cement blended concrete.

Findings on Figure 4.80 show two distinct quadratic curves between PSA concentration ranges of 0 – 25% and 25 to 50% effected by the variations of calcination temperature. Between 0 – 25% PSA concentration range, a sagging quadratic relationship was observed between calcination temperature and SISLI, with a minimum trough SISLI of -60% at a calcination temperature of 412.5 ^{o}C. The second distinct curve is a hugging quadratic curve formed between 25 and 800 ^{o}C, cresting at a peak SISLI of 17% and at a calcination temperature of 412.5 ^{o}C.

Optimisation constrained to maximize compressive strength, minimize cement concentration, maximise periwinkle shell ash content and minimize all durability indicators, produced 7 best solutions, and the selected solution having a desirability of 0.567 suggest mixture constraints of 80.35PC : 19.65PSA and a process factor constraint of 425^{o}C to yield a SISLI of -33.161%.

Having reviewed journals on the trend of loss of compressive strength of PSA cement blended concrete due to variations of cement replacement levels and curing ages up to 180 days, validating the results obtained in Fig. 4.69 as it pertains to the linear relationship existing between PSA concentration and SISLI at calcination temperature ranges of 25 – 120 ^{o}C and 700 – 800 ^{o}C, such that increasing PSA concentration, reduces sulphate induced loss in compressive strength of PSA cement blended concrete.

The application of the suggested optimised solution in the construction industry meets the recommended strength activity index criteria as well as conforms to

durability requirements locally and globally associated with the resistance of concrete to sulphate attack an is hence recommended for local and global adoption.

Developed model on the SISLI of PSA cement blended concrete is as shown in equation 4.13.

$$\frac{\ln(\text{SISLIpsa}+200)}{80-\text{SISLIpsa}} = 0.014\text{PC} - 7.46 * 10^{-3}\text{PSA} - (7.63 * 10^{-5}\text{PC} * \text{T}) + (1.55 * 10^{-4}\text{PSA} * \text{T}) + (9.25 * 10^{-8}\text{PC} * T^2) - (1.77 * 10^{-7}\text{PSA} * T^2) \ldots (4.13)$$

Where;

PC = Mass proportion of Portland cement in total binder of PSA cement blended concrete (%)

PSA = Mass proportion of PSA in total binder of PSA cement blended concrete (%)

T = Calcination temperature for production of PSA in PSA cement blended concrete (^{o}C)

4.3.8. Calcination and mixture configuration variations on the SISLI of Clam Shell Ash Cement Blended Concrete

Figures 4.81 and 4.82 provide laboratory data on the compressive strength of CSA cement blended concrete cured in a 2.5% sulphate solution for 28 days after hydration and the relative losses, respectively.

From Figure 4.81, A noticeable increase in strength for CSA cement blended concrete cured in sodium sulphate solution was observed mostly at 20% and 30% replacement levels when compared to their counterparts cured in fresh water. In essence rather than recording a loss in strength, it was rather a gain in strength for most of the CSA cement blended concretes. At 600 ^{o}C, and a replacement of 40%, specimens cured in fresh water had a strength of 18.27 MPa and lower than specimens cured in sulphate solution of 22.45 MPa, amounting to a gain of about 23% after 28 days immersion in 2.5% sulphate solution. Similar observations can be made for other replacement levels and calcination temperatures. From Fig 4.44, A gain in strength was observed for most of the CSA calcined cement blended concrete. 20 and 30% cement replacement levels had the best gains in strength. At ATM, the best gains were observed at 40% cement content for calcined CSA cement blended concrete specimen. At 200 ^{o}C, 20 and 30% cement replacement level had a superior behaviour to sulphate attack as could be observed at 400, 600 and 800 ^{o}C.

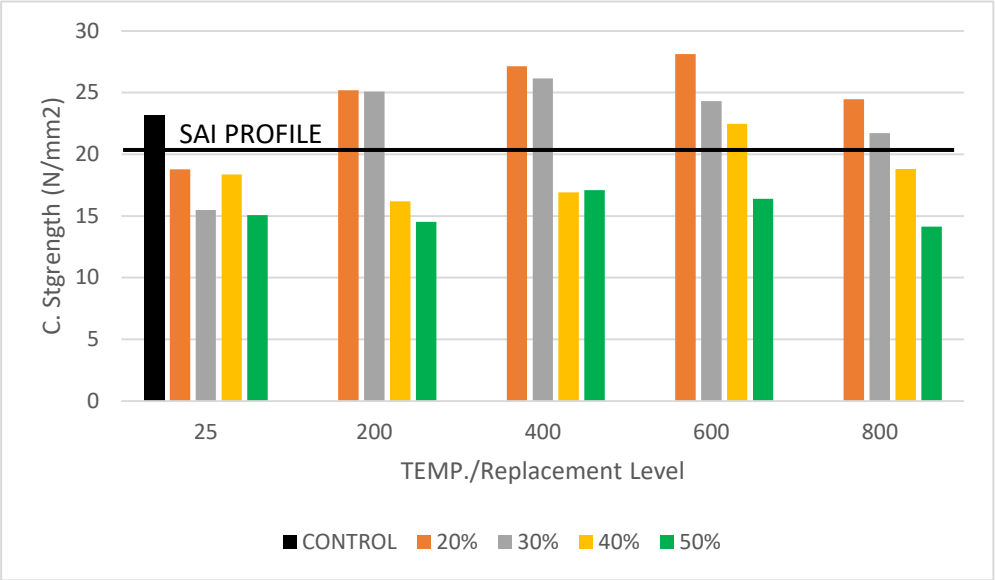

Figure 4.81: Result of calcination and Replacement Level of Clam Shell Ash on the Sulphate Attack Resistivity of CSA Cement blended concrete

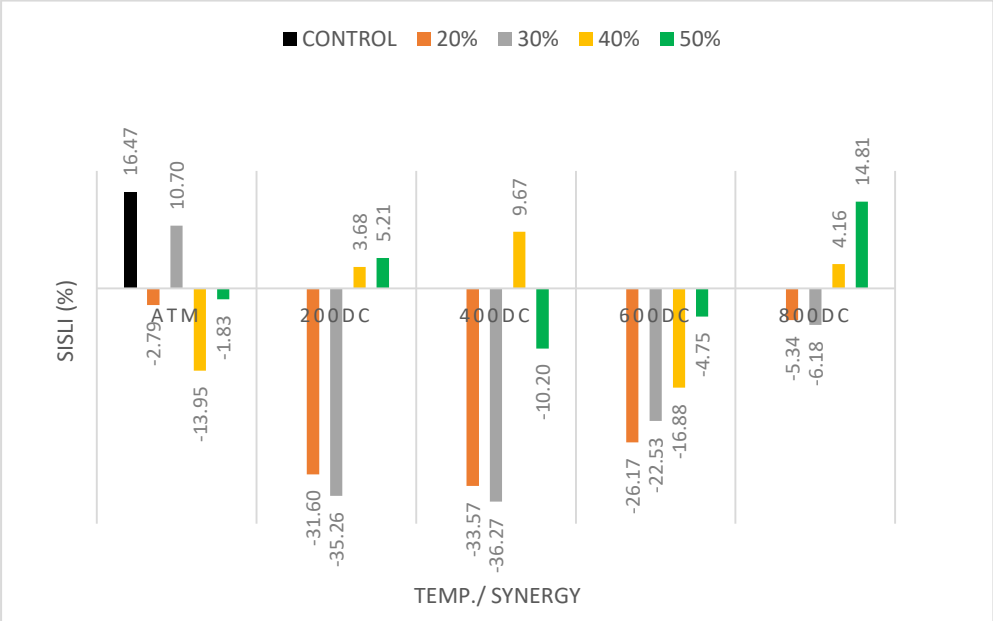

Figure 4.82: Result of calcination and replacement level of CSA on the CISLI of CSA cement blended concrete

Appendix O1 and O2 expresses the analysed variance and regression coefficients of the model for SISLI of CSA cement blended concrete. The equation (model) as developed, is composed of linear terms as mixture variables and quadratic terms as process factors. The model terms are; linear mixture, AC, BC, AC^2 and BC^2. The integrated model was significant with a P value sufficiently less than 0.05 and negating the hypothesis for nullification.

The model's ratio to the square of its total sum produced a regression coefficient of 0.8018. Consequently, the 'adjusted' and 'predicted' regression coefficients were 0.7256 and 0.6260 and having a difference less than 0.2, which implies that the model is sound enough for predictions and simulations.

Standard error was 0.42 over a mean of -2.27, with a deviation coefficient of 18.65%, and considered to be statistically satisfactory. The adequacy of the model's precision was 9.86, which implies that an error could exist in every 9.86 predictions. In essence, the least expected error of 4, is significantly above the model's maximum probable error, accordingly, the model's signal is adequate enough within its design scope for statistical simulation purposes.

The coefficients of the model shown in Appendix O3, represents that no factor (mixture or process) was inflated above 30 as a result of the model's variance, and as such, prevents multicollinearity amongst the variables.

Statistical check on model's performance as seen in Figure 4.83 indicates a relatively linear error distribution that were moderately trained. Thus, the developed equation can be accepted for sound statistical predictions.

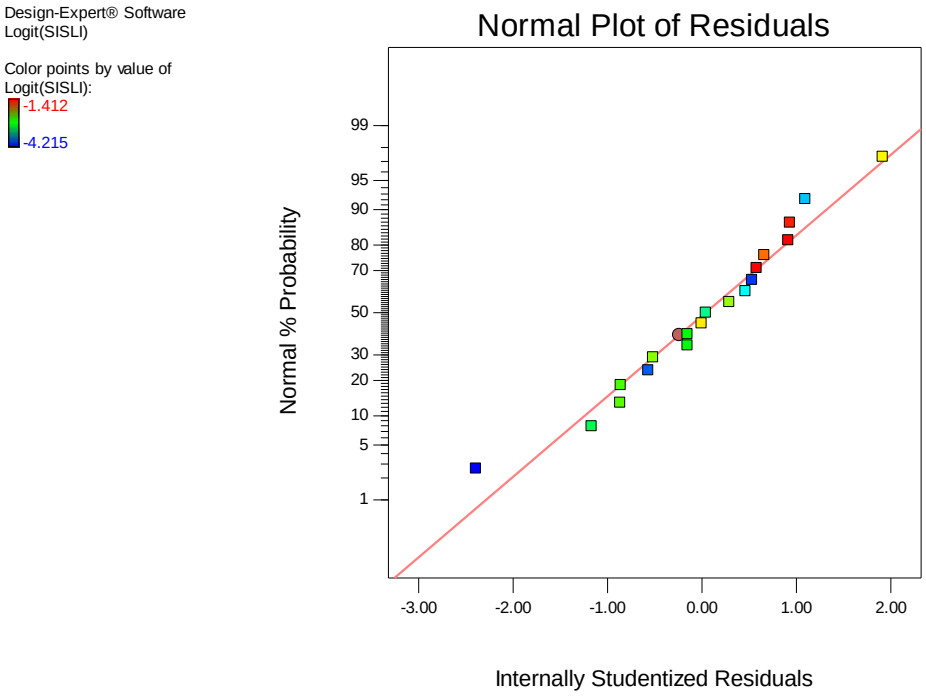

Figure 4.83: Studentised error spread for the SISLI of CSA Pozzolan concrete

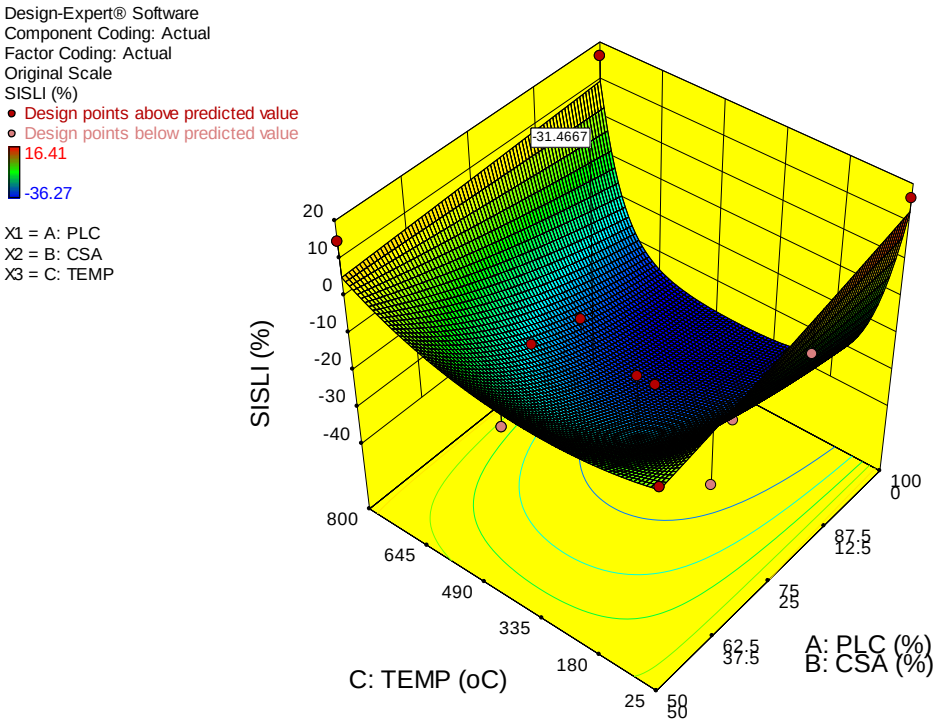

Figure 4.84: Model simulation for the SISLI of CSA cement blended concrete

Figure 4.84 represents a linear mixture interaction and a quadratic process factor interaction on SISLI of CSA cement blended concrete. The model's linear mixture component interaction indicates a direct proportionality between CSA concentration and the sulphate induced strength loss, i.e. increase in CSA content leads to increase in compressive strength losses due to sulphate attack for calcination temperatures between 200 and 700 ^{o}C. The process component of the model, developed a sagging quadratic curve troughing between 180 and 645 ^{o}C calcination temperature, peaking at 450 ^{o}C. The model generally suggests a need to constrain the calcination temperature to below 645^{o}C to reduce the potentials of strength losses due to sulphate attack.

When oyster shells were utilized as a sand substitute, Kuo *et al*., (2013) discovered that the weight loss of concrete owing to sulphate attack increased with increasing sea shell content. Adewumi *et al*., (2015) also contributed findings on the study of three mollusc shells including snail, oyster and periwinkle produced at 800^{o}C. They asserted that increasing mollusc shell concentration reduces the mechanical performance of cement blended concrete and beyond 20% replacement level, only snail shell ash concrete performed acceptably beyond the stipulated bench mark of 15 MPa at 28 days of curing. Similarly, Tayeh *et al*., (2019) monitored the compressive strength of concrete built with 5 - 20% seashell as partial replacement for cement and asserted that specimens produced between 5 - 15% replacement level met the required strength of 25 MPa at 28 days, with 5% being the optimal. The further added that concrete produced with 5% seashell as a cement replacement has about the same resistance to sulphate attacks as regular concrete. As a result, for structures subjected to these types of attacks, a concrete containing 5% seashells may be as durable as regular concrete. They however concluded on the need for calcination if an increased resistance to sulphate attack is needed at higher concentrations of sea shells in concrete. Attah *et al*., (2018), in their study on the effect of sulfuric acid on the mixture interaction of oyster shell on compressive strength, concluded that strength and mass losses due to increasing oyster shell content are directly proportional with increasing oyster shell content. This is in tandem with the objective of this research exercise which seeks to improve the replaceability of cement in concrete without posing challenges on the strength and

durability credentials of concrete and hence incorporating the process factor of calcination temperature.

At optimisation, SISLI was obtained as -31.467% relative to its strength when cured in fresh water at a curing period of 28 days, the optimised constraints are 76.87%PC:23.13% CSA mixture and 527 ^{o}C calcination temperature process factor. Application of equation (model) as developed, is flexible and relatively useful depending on the requirements of strength, durability and sustainability.

Developed model for the SISLI of CSA cement blended concrete is as shown in Equation 4.14 below;

$$\frac{\ln(\text{SISLIcsa}+40.5)}{250-\text{SISLIcsa}} = -0.01\text{PC} - 0.028\text{CSA} - (1.936 * 10^{-4}\text{PC} * \text{T}) + (1.718 * 10^{-4} * \text{CSA} * \text{T}) + (2.335 * 10^{-7}\text{PC} * T^2) - (1.997 * 10^{-7}\text{CSA} * T^2) \quad (4.14)$$

Where;

PC = Mass proportion of Portland cement in total binder of CSA cement blended concrete (%)

CSA = Mass proportion of CSA in total binder of CSA cement blended concrete (%)

T = Calcination temperature for production of CSA in CSA cement blended concrete (^{o}C)

4.3.9. Calcination and mixture configuration variations on the SISLI of HAP Cement blended concrete

Experimental data developed on the compressive strength of HAP cement blended concrete cured in 2.5% sulphuric oxide solution for a period of 28 days post hydration, and the resulting losses, are as plotted in Figures 4.85 to 4.92.

From Figures 4.85 and 4.86, calcination temperature as well as mix configuration for HAP cement blended concrete at 20% cement replacement level, appeared to be quadratically related to the sulphate induced strength losses. However, in some instances of mix configuration such as at 70% PSA: 30% CSA, 40% PSA: 60% CSA and 30% PSA: 70% CSA, a cubic trend was observed. Minimal losses due to calcination were at 400 ^{o}C for PSA, 200 ^{o}C for 70% PSA: 30% CSA, 800 ^{o}C for 60% PSA: 40% CSA, 400 ^{o}C for 50% PSA: 50% CSA, 200 ^{o}C for 40% PSA: 60% CSA, 600 ^{o}C for 30% PSA: 70% CSA and 600 ^{o}C for 100% CSA. Minimal losses due to mix configuration were at 100% CSA and 100% PSA with maximum losses observed between 60% PSA: 40% CSA and 50% PSA: 50% CSA.

The growth in compressive strength generated by the presence of sulphate ions led to most of the specimen classes meeting up and exceeding the SAI criteria (bench mark shown on Figure 4.85), excluding for ATM specimens. However, relative to resistance to sulphate attack, PSA and CSA are superior alone, than in a hybrid form as shown above. In essence, the industry is advised to study the target location and exposure condition of the concrete to be well informed on the ideal cement/cementitious material is to be used.

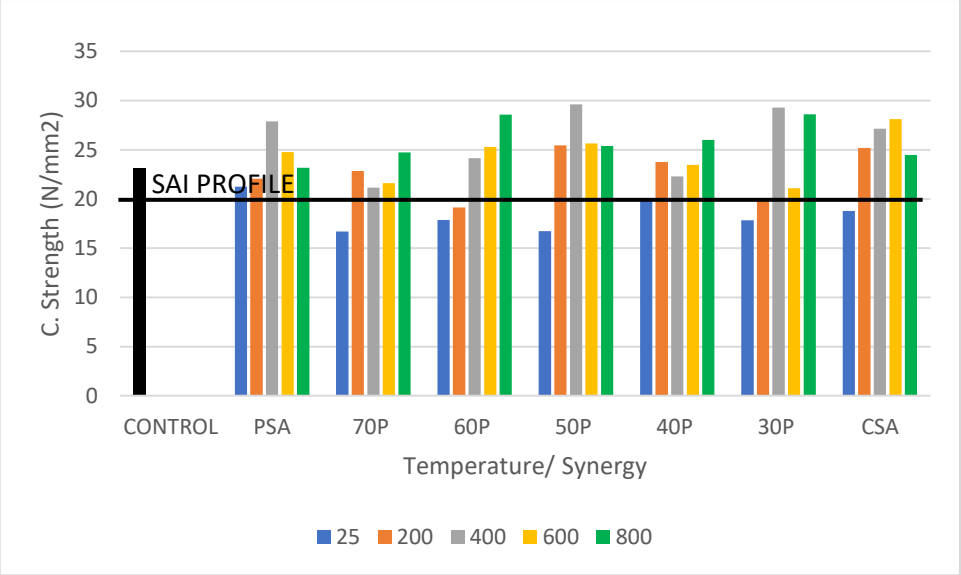

Figure 4.85: Measuring the Sulphate Attack Resistivity of Calcined HAP Concrete At 20% CRL

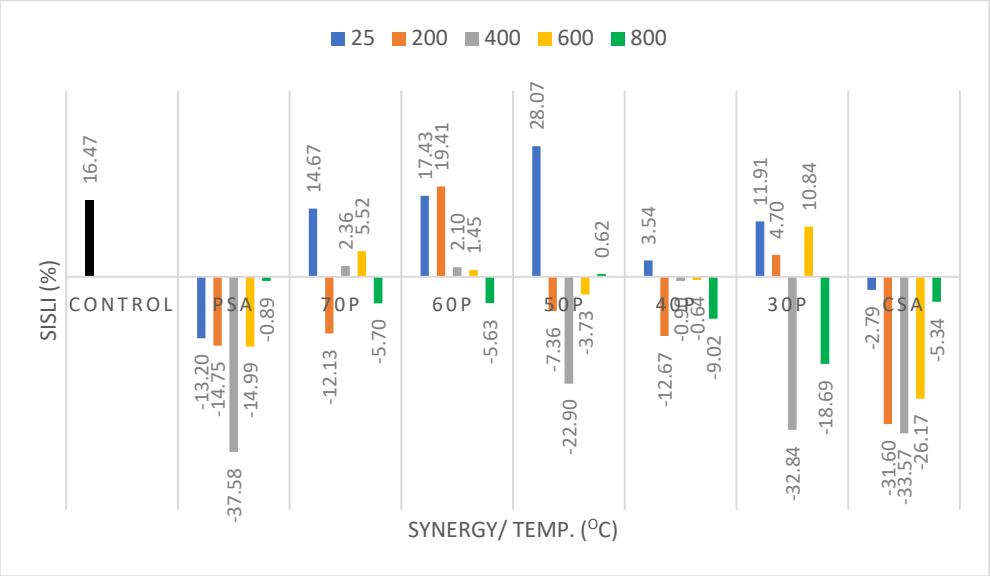

Figure 4.86: Calcination and synergistic ratio variation on SISLI of HAP Concrete at 20% CRL

From Figures 4.87 and 4.88, Mixture configuration of HAP was observed to generate a cubic trend for the losses in strength of HAP cement blended concrete cured in a 2.5% sulphuric oxide solution for 28 days post hydration period. Minimal losses can hence be seen at 100% PSA, 70% PSA: 30% CSA, 30% PSA: 70% CSA and 100% CSA, with greater losses recorded at their middle. Calcination temperature according to the data was mainly quadratic, 70% PSA: 30% CSA, 60% PSA: 40% CSA, 3% PSA: 70% CSA that showed minor deviations. As such minimal losses due to calcination temperature were observed at 400 ^{o}C for 10% PSA, 400 ^{o}C for 70% PSA: 30% CSA, 200 ^{o}C for 60% PSA: 40% CSA, 400 ^{o}C for 50% PSA: 50% CSA, 200 ^{o}C for 40% PSA: 60% CSA, 400 ^{o}C for 30% PSA: 70% CSA and 400 ^{o}C for 100% CSA respectively.

Indices obtained at these levels where observed to be evidently more durable than that of PC. And in most cases, strength was gained and not lost as could be seen in Figure 4.88.

Based on this, the SAI criteria was met and exceeded by 60% PSA: 40% CSA specimens; 100% PSA specimens at 400^{o}C; 70% PSA: 30% CSA, 50% PSA: 50% CSA and 100% CSA specimens at 200, 400, 600 and 800 ^{o}C; 40% PSA: 60% CSA at 800 ^{o}C; and 30% PSA: 70% CSA specimens at 200, 400 and 800 ^{o}C.

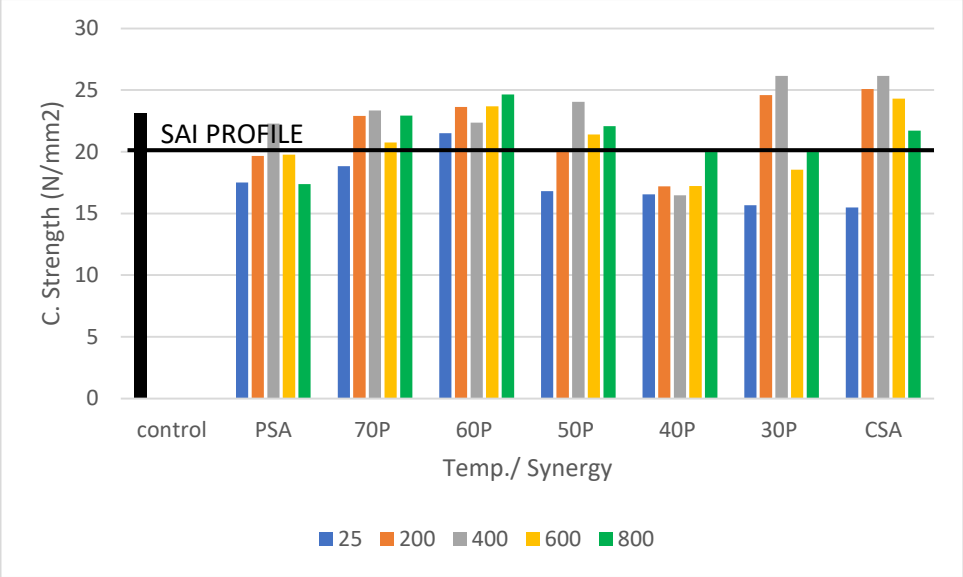

Figure 4.87: Measuring the Sulphate Attack Resistivity of Calcined HAP Concrete At 30% CRL

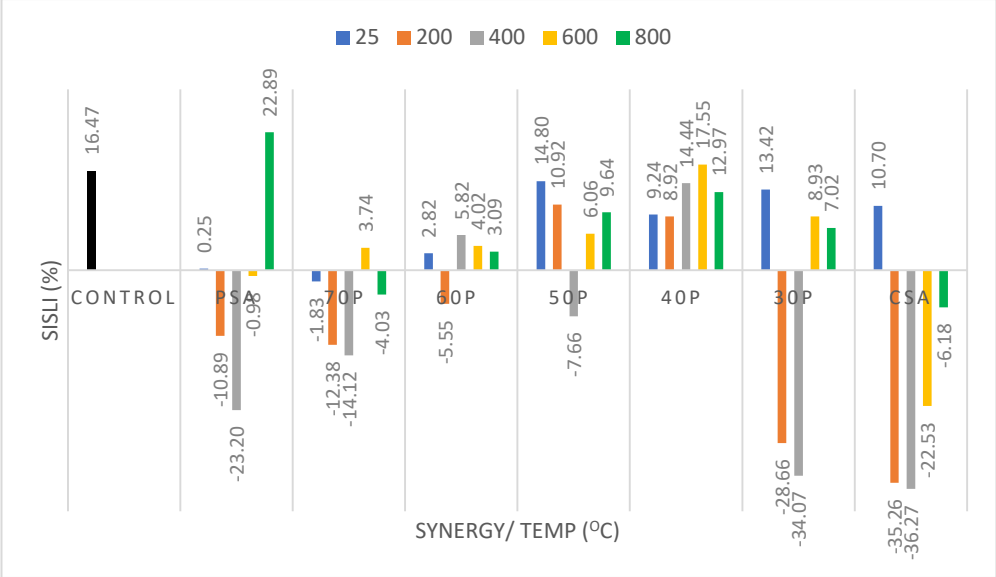

Figure 4.88: Calcination and synergistic ratio variation on SISLI of HAP Concrete at 30% CRL

From Figures 4.89 and 4.90, a representation of HAP cement blended concrete in a sulphated environment is seen, and at a cement replacement level of 40%. Calcination temperature was quadratically related to the SISLI of HAP cement blended concrete at PSA alone, but was cubically related to all other mix configurations as shown by collated data. The mixture configuration was mostly cubic on the SISLI and the synergies with ultimatum performance under sulphated environment were 50% PSA: 50% CSA and 60% PSA: 40% CSA produced at 600 ^{o}C.

Strength activity index bench mark was met and exceeded by PSA (ATM, 600 ^{o}C and 800 ^{o}C) specimens, 60% PSA: 40% CSA (400 ^{o}C and 600 ^{o}C) specimens, and 100% CSA (600 ^{o}C) specimen.

Evidently, a sulphate rich exposure condition has little or no effect on the HAP cement blended concretes when compared to the PLC control. However, the industry should note that optimal parameters associated with the production of PSA/CSA hybrid played quite a significant role in given the concrete additional durability attributes. It is therefore essential that the data generated be analysed and a model developed for easy simulations of the production parameters in a bid to optimise cement replaceability.

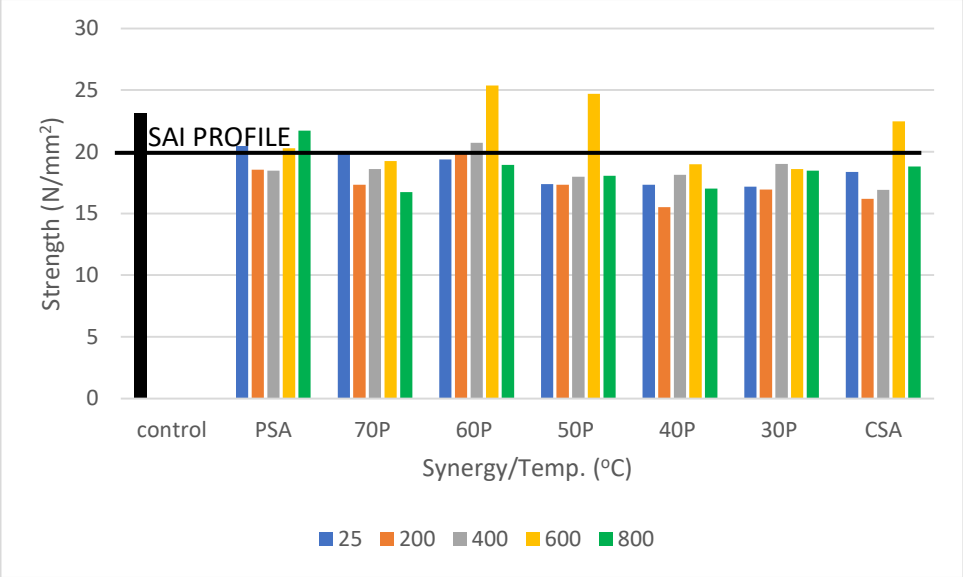

Figure 4.89: Measuring the Sulphate Attack Resistivity of Calcined HAP Concrete At 40% CRL

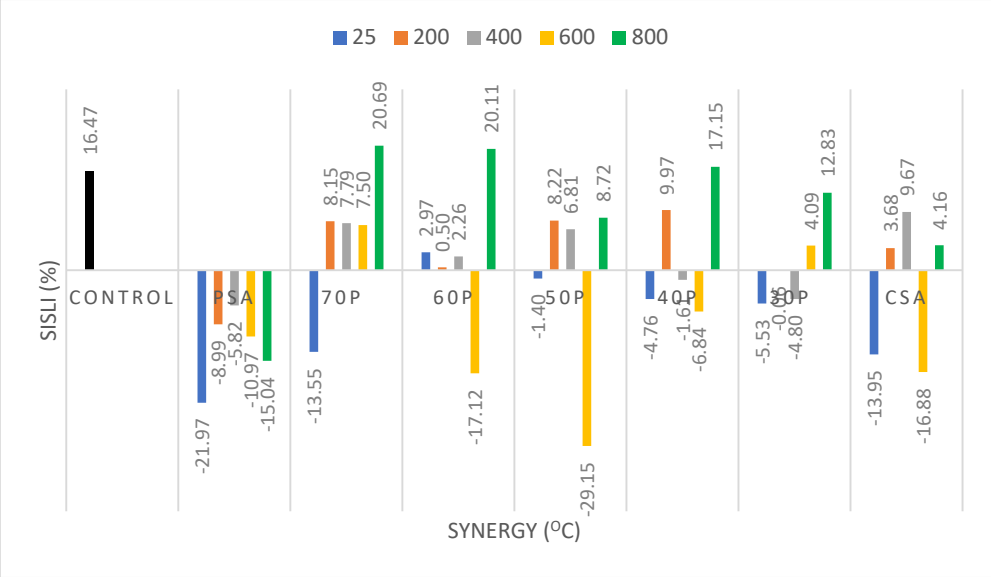

Figure 4.90: Calcination and synergistic ratio variation on SISLI of HAP Concrete at 40% CRL

The laboratory data on SISLI obtained for HAP cement blended concrete at 50% cement concentration is as shown in Figures 4.91 and 4.92. As could be seen from both figures, a significant strength loss in strength due to sulphate attack is observed at this level of cement replacement. Nonetheless, only a handful of specimens had SISLI greater than that of the control. These are 100% PSA (200 and 400 ^{o}C), 70% PSA: 30% CSA (200, and 400 ^{o}C), 60% PSA: 40% CSA (ATM), 40% PSA: 60% CSA (400 ^{o}C), and 30% PSA: 70% CSA (800 ^{o}C).

From Figures 4.85 to 4.92, and laying emphasis on 40% cement replacement level, a general increase in strength was observed for all the concrete specimens due to the presence of sulphate ions. At 40% cement replacement level, under 600 ^{o}C, 60P was observed to grow from 21.67 MPa to 25.38 MPa which is a 17% increase in strength associated with sulphate attack. While this is the optimum growth at that replacement level and temperature, a similar trend can be seen in other replacement levels and calcination temperatures.

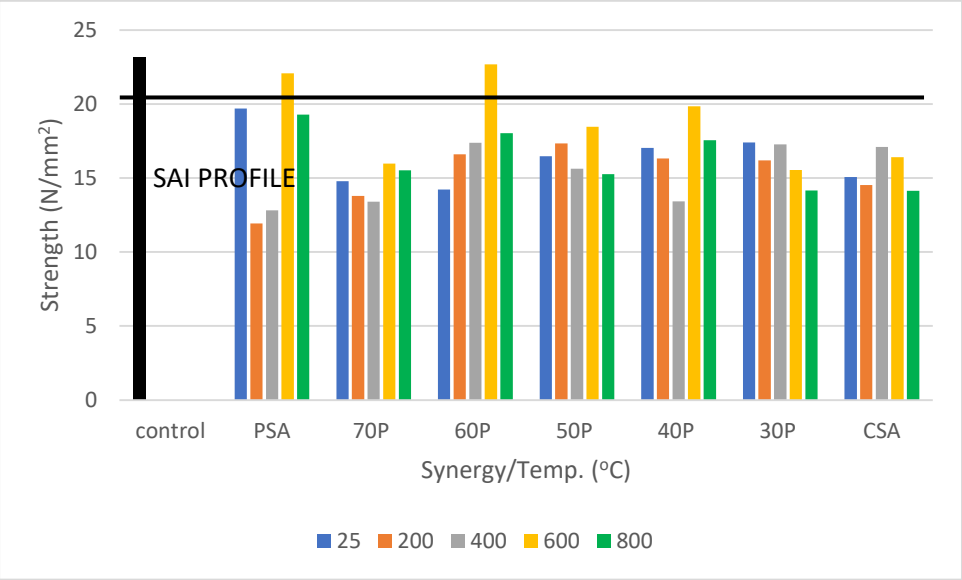

Figure 4.91: Measuring the Sulphate Attack Resistivity of Calcined HAP Concrete At 50% CRL

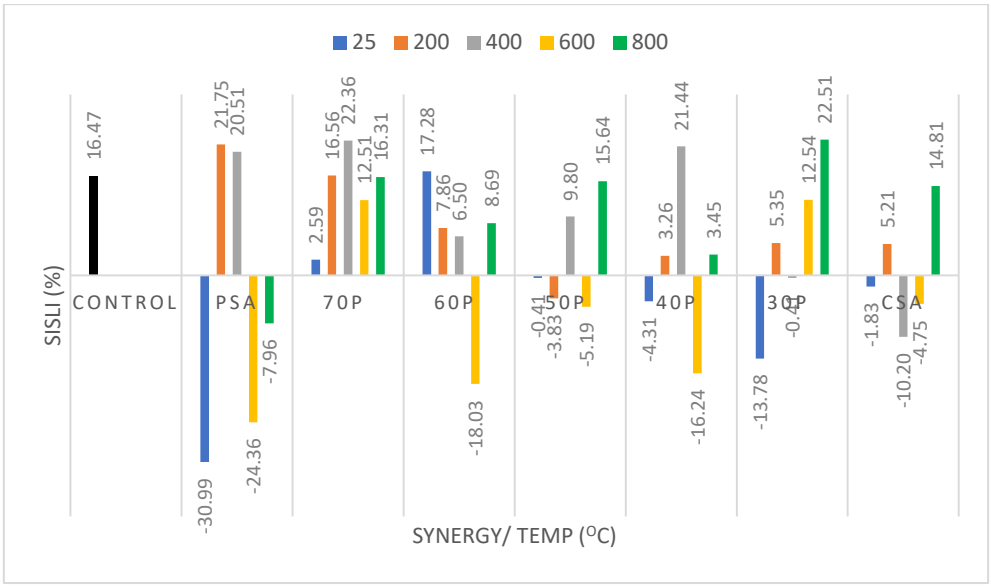

Figure 4.92: Calcination and synergistic ratio variation on SISLI of HAP Concrete at 50% CRL

The analysed variance and regression coefficients of the model for SISLI of HAP concrete are as shown in Appendix P1 and P2. The equation (model) as developed, is an equation with combined model terms of 'quadratic mixture and process' origin, possessing a strong linear mixture component and eleven additional components that integrate into the generated equation (model), refuting the nullification hypothesis and having a 'P' value less than 0.05. With a P > 0.05, amongst the 12 terms of the model, AC, CD, and AD^2 were not significant.

The model's ratio to the square of its total sum produced a regression coefficient of 0.9907. Accordingly, the adjusted regression coefficient was 0.9821, while the predicted regression coefficients was 0.8909. This implies that the model is sound enough for predictions and simulations.

Standard error was 0.27 over a mean of -2.87, with a deviation coefficient of 9.39%. The adequacy of the model's precision was 57.63, which implies that an error could exist in every 57.63 predictions. Given that this is significantly higher lower than the maximum permitted related error of 4, the model's signal is sufficient for statistical simulation purposes within the parameters of its design.

The PC mixed component of the model's coefficients provided in Appendix P3 indicates the presence of multicollinearity, however this is not a cause for alarm because the factors inflated by variance (VIF) is within the range of 0 to 30. The variance inflated factors of all other model components are all lower than 10. As a result, it appears that independent variables can be changed statistically, which is a necessary condition before looking at how changing independent factors affect model responses.

Statistical check on model's performance as seen in Figure 4.93 indicates a relatively linear error distribution that were studentised externally. Thus, the equation as developed can be utilized for statistical predictions.

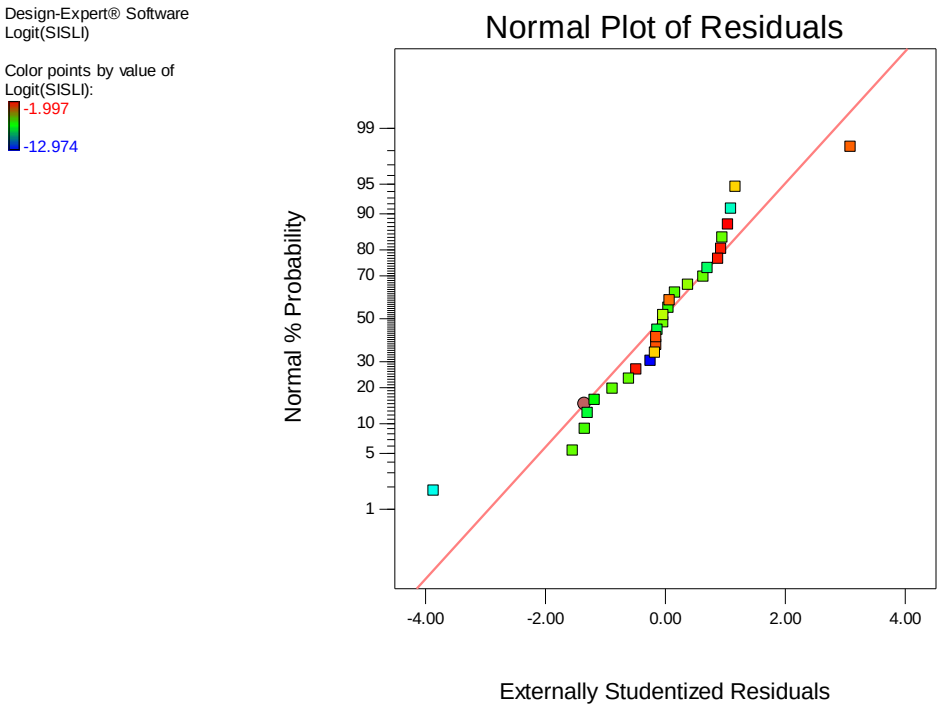

Figure 4.93: **Studentised error distribution for the SISLI of HAP concrete**

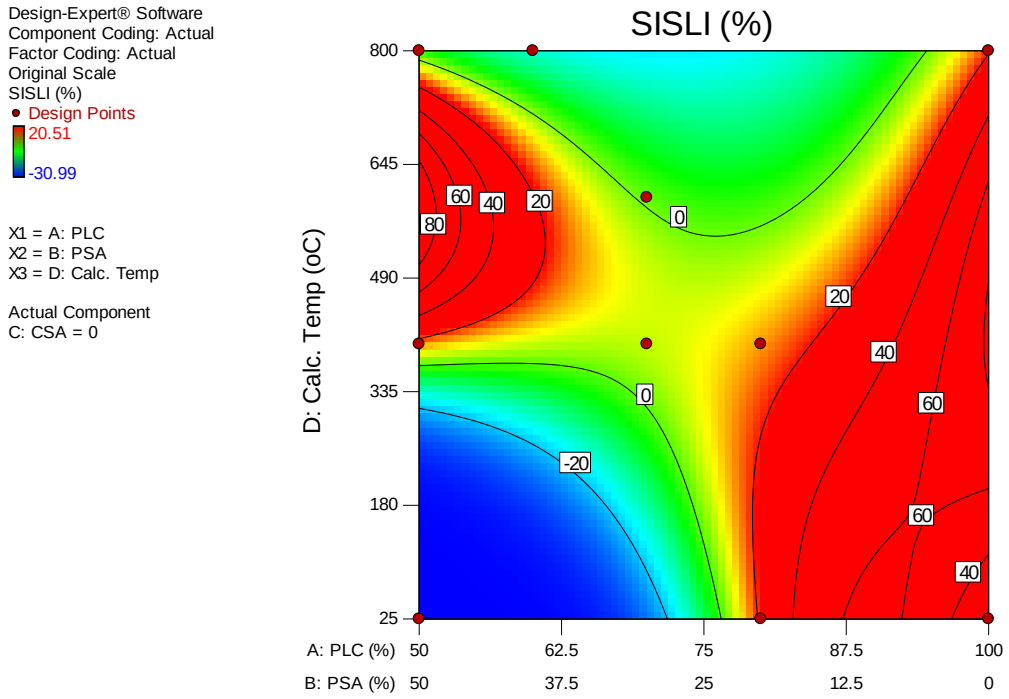

Figure 4.94: Three-dimensional model at 0% CSA level on the SISLI of HAP concrete

The simulations of the SISLI model at various mixture levels and processes are shown in Figures 4.94 to 4.97. Variations in the process variable, which is the temperature at calcination, were seen to have an impact on the SISLI of the HAP concrete in a sloping quadratic relationship with a trough as a function of the changes in the mixture components. The results of altering levels of CSA content on the SISLI of HAP concrete is shown in Figures 4.94 to 4.97. Negligible SISLI was present at 0% to 10% CSA concentration for a PSA level of 25 - 50% PSA and a calcination temperature spanning between 25 – 350 ^{o}C. For a PSA concentration span of 25 - 50% PSA and temperature at calcination span of 25 to 350 ^{o}C, negligible SISLI was present at 0% to 10% CSA. Also, SISLI is seen to be negligible when PSA concentration spans between 20% and 37.5% for all calcination temperatures at a constant CSA content. The calcination temperature needed to reduce SISLI for CSA concentrations between 10 and 20% varies from 25 to 200% for PSA concentrations between 22.5% and 30%. As it comes to reducing SISLI of HAP concrete, a higher distribution of levels of PSA was allowed at temperatures over 335 ^{o}C. The PSA concentration is mostly insignificant at CSA concentrations of 25% (Figure 4.96), as the equation as developed dictates the need for calcination temperatures over 300 ^{o}C in order to minimize SISLI. The SISLI of the concrete at 47.5% CSA content was affected by changes in PSA concentration and calcination temperature on a mean (constant) basis (Figure 4.97). The extract (Figures 4.94 to 4.97) essentially indicates that adding more CSA impedes the attack from sulphate ions whilst reducing the required temperature for dehydroxylation.

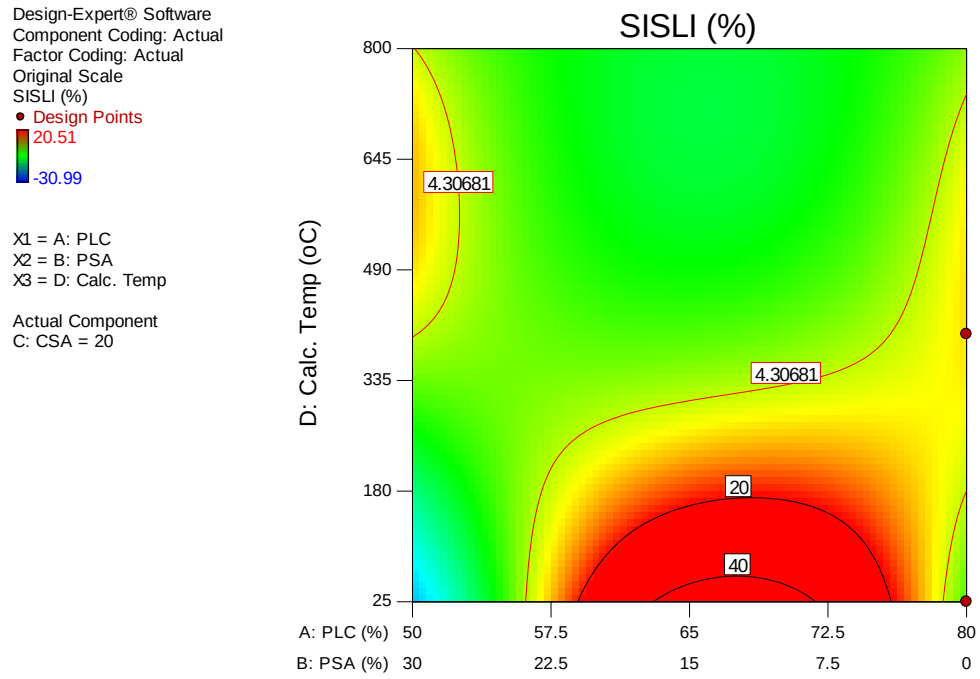

Figure 4.95: Three-dimensional model at 20% CSA level on the SISLI of HAP concrete

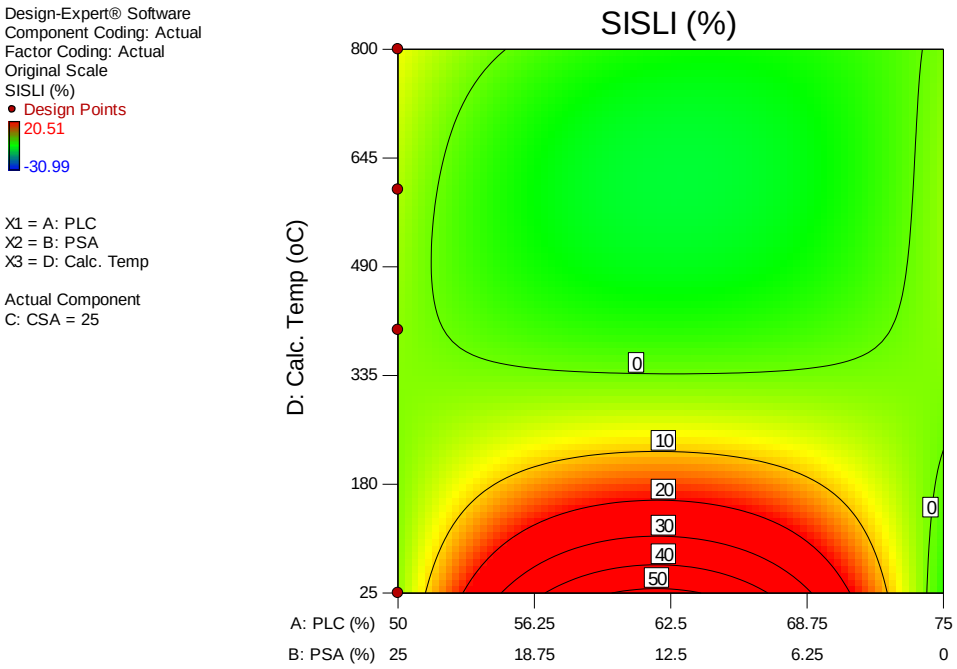

Figure 4.96: Three-dimensional model at 25% CSA level for the SISLI of HAP concrete

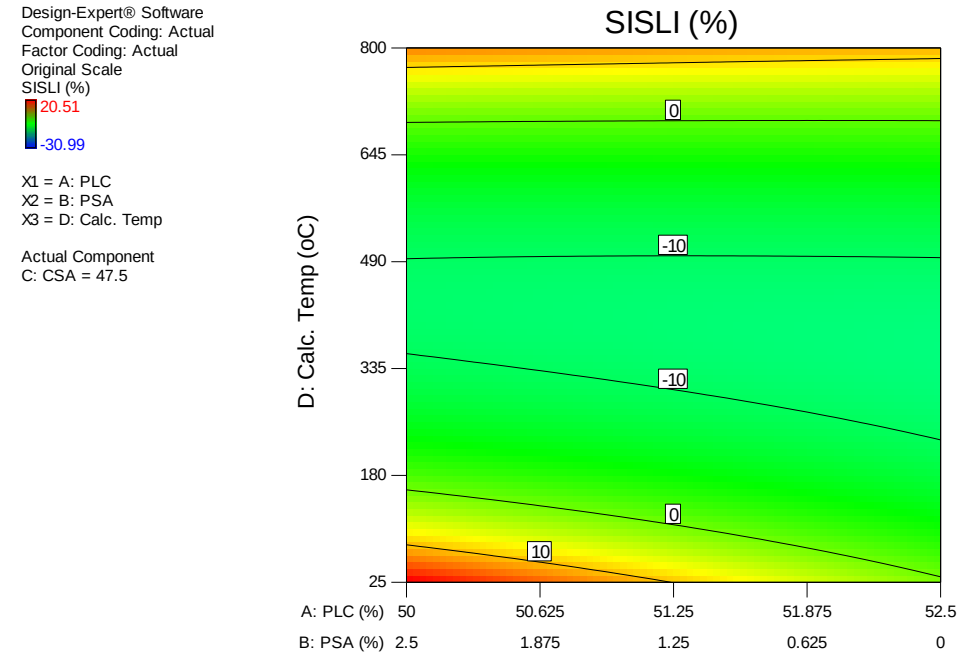

Figure 4.97: Model simulation at 47.5% CSA level for the SISLI of HAP concrete

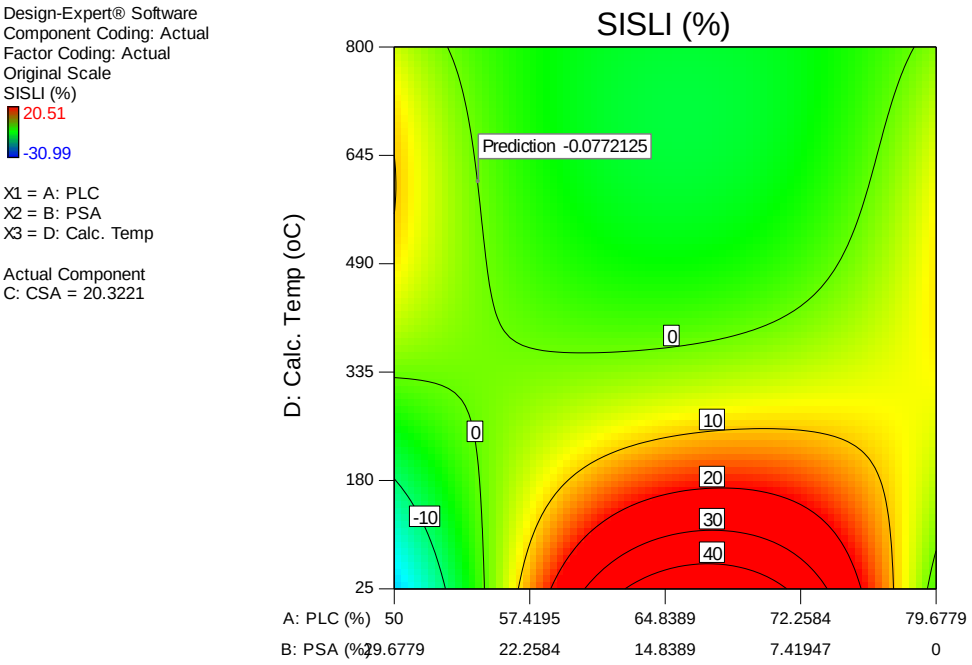

Figure 4.98: Three-dimensional and optimised model variables for the SISLI of HAP concrete

At optimisation (Figure 4.98), calcination temperature played a greater role by separating the active calcination temperature range of 25 – 250 ^{o}C from the stable range of 335 – 800 ^{o}C, relative to the SISLI of HAP concrete. Thus, the optimised production temperature for SISLI obtained was 606.7 ^{o}C and 349 ^{o}C for solutions 1 and 10, respectively, yielding SISLI of -0.078% and 0%, as opposed to a 28 day PLC SISLI of 16.47%.

The analysed model can be adequately utilised in simulations and designs for the production of sulphate resistant pozzolanic concretes.

Developed model for the SISLI of HAP concrete is as shown in Equation 4.15 below;

$$\frac{\ln(\text{SISLIhap}+30.99)}{400-\text{SISLIhap}} = -0.022\text{PC} - 0.671\text{PSA} + 9.958 * 10^{-3}\text{CSA} + (8.227 * 10^{-3} * \text{PC} * \text{PSA}) - (7.242 * 10^{-4}\text{PC} * \text{CSA}) + (5.592 * 10^{-5} * \text{PC} * \text{T}) + (9.228 * 10^{-3} * \text{PSA} * \text{CSA}) + (2.587 * 10^{-3} * PSA * T) - (1.311 * 10^{-4} * CSA * T) - (3.46 * 10^{-4} * PC * PSA * CSA * T) - (3.413 * 10^{-5} * PSA * CSA * T) - (6.778 * 10^{-8} * PC * T^2) - (2.097 * 10^{-6} * PSA * T^2) + (1.701 * 10^{-7} * CSA * T^2) + (2.753 * 10^{-8} * PC * PSA * T^2) + (2.849 * 10^{-8} * PSA * CSA * T^2) \quad (4.15)$$

Where;

SISLIhap = Sulphate induced strength loss index of HAPconcrete (%)

PC = Mass proportion of Portland cement in total binder of HAP concrete (%)

CSA = Mass proportion of CSA in total binder of HAP cement blended concrete (%)

PSA = Mass proportion of PSA in total binder of HAP cement blended concrete (%)

T = Calcination temperature for production of CSA and PSA hybrid in HAP concrete (^{o}C)

4.3.10. Calcination and mixture configuration variations on the SIMLI of Periwinkle Shell Ash Cement Blended Concrete

Under the attack of sulphate ions, concrete mass loss is inherent depending on the concentration of the ions and the quality of the concrete mix. It is essential that mass loss be checked against if long term serviceability and durability is required. At 2.5% sulphate concentration, Figure 4.99 is a plot of the mass loss index of PSA cement blended concrete cured for 28 days post hydration period.

From Figure 4.99, control specimen had a loss in mass of about 9.28% when cured in sulphate solution for a period of 28 days. Mass loss for PSA blended cement blended concrete was observed to increase with increasing cement replacement level at least in most cases. At 600 ^{o}C, 40% cement replacement level, a mass loss of 9.13% was observed which was seen to be lower than that of the control.

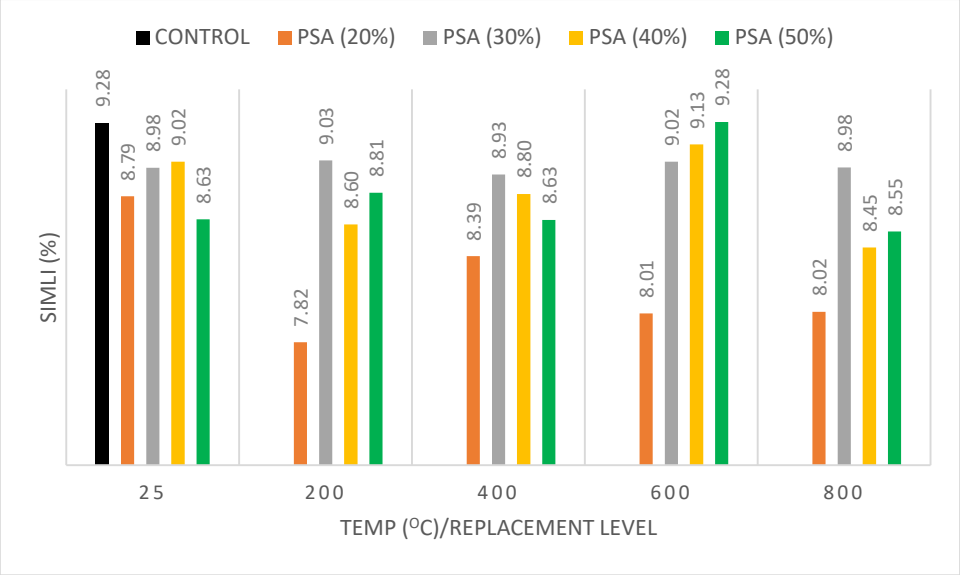

Figure 4.99: Sulphate Induced Mass Loss Index Variations for Calcined PSA Cement blended concrete

Findings from the variance as analysed, and variation coefficients for the SISLI of PSA cement blended concrete are as shown in Appendix Q1 and Q2.

Model components are linear mixture, AB, AB(A-B). All model components are significant having $P < 0.05$. The all integrated equation, combines model terms of a cubic and mean functions with a P value less than 0.0001 and negating the hypothesis for nullification.

Coefficients of regression for the model as seen in Appendix Q2 are 0.8574, 0.8288and 0.6607 for the R2, adjusted R2 and predicted R2 respectively. This is relative to the index of the cumulative summed up squares and the residual sum of squares. The Standard error spreads out of the mean value of 5.27 by 0.72, and the percentage ratio of 13.69% was obtained as the coefficient of variation. The coefficient of variation is below 30% hence the model is statistically satisfactory.

Appendix Q3 represents the coefficients of the individual model components, degrees of freedom, standard error associated with each coefficient, range of confidence interval and variance inflated factors for the SISLI of PSA cement blended concrete checking for multicollinearity, A, B, AB and AB(A-B), had variance inflated factors of 2.29, 2.15, 3.20 and 1.35 respectively. In essence, all the coefficients of the model components are free from multicollinearity and as such are statistically satisfactory.

Figure 4.99 represents the normal distribution of the externally studentised residual against the probability of occurrence. The externally studentised errors pass the fat pencil test and are normally distributed as such model prediction is satisfactory.

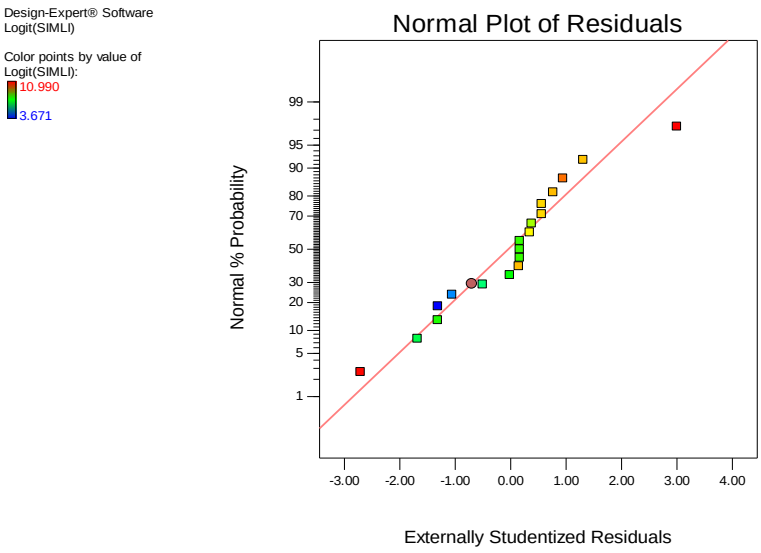

Figure 4.100: Normal plot of residual spread for the SIMLI of PSA Cement blended concrete

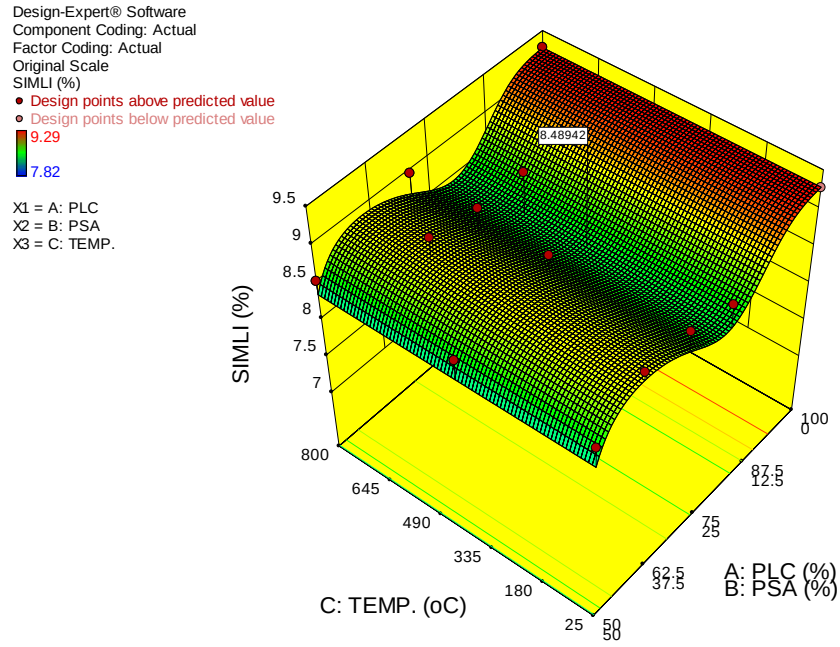

Figure 4.101: Graphical illustration of the effect of PSA content and temperature at calcination on the SIMLI of PSA cement blended concrete

From Figure 4.101, Variation's calcination temperature level was observed to render little or no contribution to PSA concrete's resistance to mass loss generated due to the presence of sulphate ions. The mixture component however, showed a cubic relationship between PSA concentration and SIMLI. The curve, like a sine wave, has two turning points at the crest and trough. First turning point forming the crest was at 40% PSA concentration having a SIMLI of 8.6% and the second turning point forming the trough was at 20% PSA concentration having a SIMLI of 7.82%. Maximum SIMLI was recorded at 100%PC concentration having a SIMLI of 9.3% as shown in Figure 4.99.

Quite information is the nature of the result shown in Figure 4.101, however, a closer look informs that the percentage difference of the SIMLI predicted between the crest and trough points is about 9% and not sufficient enough to contribute effectively in the overall decision-making process. However, the predicted range of calcination temperature for minimum mass loss is between 12.5 and 25% PSA concentration.

Optimized model suggested 7 solutions meeting the set constraints of the five key responses and selected solution has a desirability of 0.567 as shown in Table 4.2. Optimized solution for SIMLI suggested at 8.49% is observed to be a holistic suggestion taking into cognisance the interaction between the mixture and process factors on the other four responses. As such the generalised solution was at mixture components of 80.35PC:19.65PSA at a process factor was at 425 ^{o}C.

The equation (model) as developed, is deemed effective to adequately simulate variables and outcomes within the boundaries of the design to meet localised constraints of the engineering society for the strength and durability requirements of concrete structures without comparatively contributing adversely to the tenets of sustainability.

Developed model on the SIMLI of PSA cement blended concrete is as shown in Equation 4.16

$$\frac{\ln(\text{SIMLIpsa}+50)}{9.29-\text{SIMLIpsa}} = 0.0975\text{PC} - 0.6982\text{PSA} + (0.0138 * \text{PC} * \text{PSA}) - (1.184 * 10^{-4} * PC * PSA\ (PC - PSA)) \ldots \ldots \ldots \ldots \ldots \ldots \ldots \ldots \ldots \ldots \ldots \ldots \ldots \ldots \ldots \ldots . . \ldots . (4.16)$$

Where;

PC = Mass proportion of Portland cement in total binder of PSA concrete (%)

PSA = Mass proportion of CSA in total binder of PSA cement blended concrete (%)

T = Calcination temperature for production of PSA in PSA cement blended concrete (^{o}C)

4.3.11. Calcination and mixture configuration variations on the SIMLI of Clam Shell Ash Cement blended concrete

Experimental data on the resistance of the mass of CSA cement blended concrete to sulphate attack is as shown in Figure 102. The result of calcination on SIMLI was approximately quadratic, however, cement replacement level did not show any clear trend on its contribution to lost masses of CSA cement blended concrete.

From Figure 4.102, Control specimen had a loss in mass of about 9.28% when cured in sulphate solution for a period of 28 days. Mass loss for CSA blended cement blended concrete was observed to reduce with increasing cement replacement calcined CSA cement blended concrete specimens produced at ATM, 400 ^{o}C and 800 ^{o}C. However, at 400 ^{o}C and 800 ^{o}C, 50% replacement level had an upward jump in mass loss greater than their 20% counterparts. At 600 ^{o}C, apart from specimens at 20% cement replacement levels, all other levels were observed to be directly proportional to mass loss, i.e. increase in replacement level increases mass loss. At 600 ^{o}C, 40% cement replacement level, a mass loss of 9.04% was observed which was seen to be lower than that of the control.

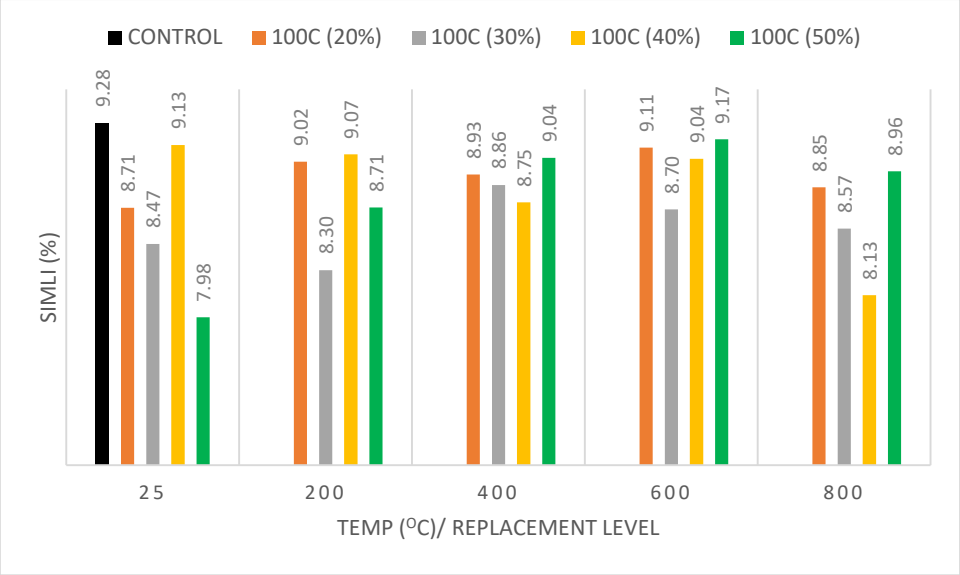

Figure 4.102: Sulphate Induced Mass Loss Index Variations for Calcined CSA Cement blended concrete

Appendices R1 and R2, represents the analysed variance and regression coefficients of the model for the SIMLI of CSA cement blended concrete. The equation as developed, is a combined ‘cubic mixture’ and ‘mean process’ terms, integrated to produce linear mixture, AB, and AB(A-B). The all integrated model as well as individual model component were significant with a ‘P’ values less than 0.05 and suggesting a confidence interval exceeding 95%.

The model’s ratio to the square of its total sum produced a regression coefficient of 0.9468. As such, the coefficients of regressions as adjusted and predicted were obtained as 0.9362 and 0.9180 and having a difference less than 0.2, which implies that the model is sound enough for predictions and simulations.

Standard error was 0.68 over a mean of 5.14, with a deviation coefficient of 13.32%, and considered to be statistically satisfactory seeing that the Standard error is within 30% of the mean. The adequacy of the model’s precision was 27.45, which implies that an error could exist in every 27.45 predictions. In essence, the least expected error of 4, is significantly above the model’s maximum probable error, accordingly, the model’s signal is adequate enough within its design scope for statistical simulation purposes.

The coefficients of the model shown in Appendix R3, indicates that multicollinearity impact is absent for all model components, as no factor exceeded 10 by reason of inflation as a result of the model’s variance.

Statistical check on model’s performance as seen in Figure 4.103 shows a near linear spread of the statistically moderated errors, having passed the ‘Fat pencil test’. As such, the developed equation can be satisfactorily utilised for predictions and simulations.

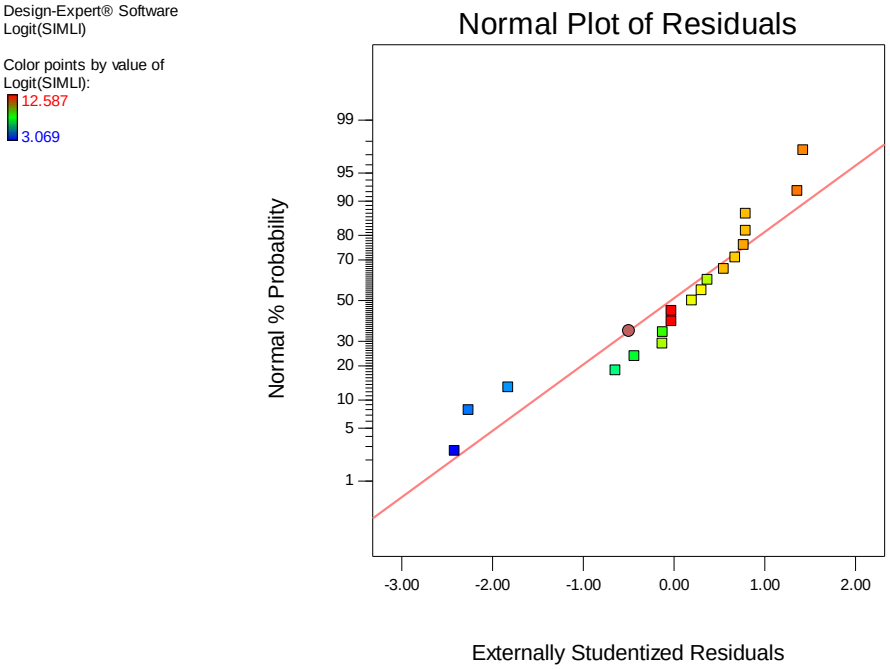

Figure 4.103: Studentised error spread for the SIMLI of CSA cement blended concrete

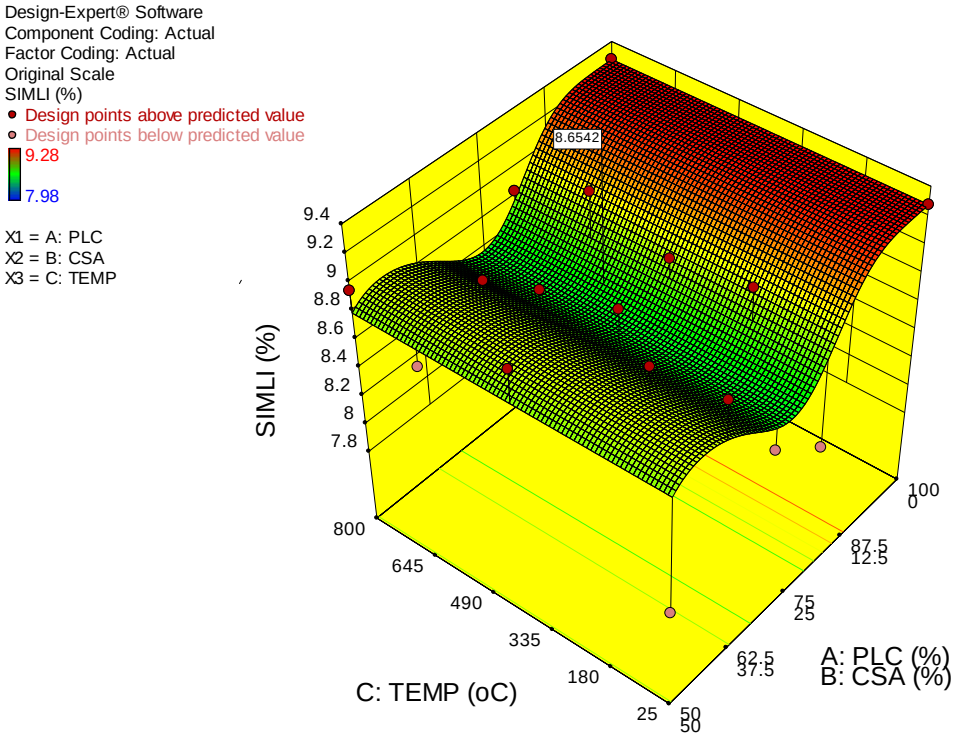

Figure 4.104: Model simulation for the SIMLI of CSA cement blended concrete

Figure 4.104, represents a cubic mixture order of interaction and a mean process factor order of interaction on the SIMLI of CSA cement blended concrete. The model's cubic mixture component interaction indicates a wave-like proportionality between CSA concentration and the sulphate induced mass loss with increasing amplitude. The first wave length formed as shown in Figure 4.81 has its crest at a mixture of 60%PC:40% CSA and troughing at 75%PC:25% CSA. It therefore suggests that CSA concentration should be limited to levels below 25% as a check against losses in mass, associated with the presence of sulphate attack on CSA cement blended concrete. The process component of the model, developed a mean relationship between calcination temperature and the sulphate induced mass loss index for a mixture tested analysed. The model generally suggests that calcination temperature has no significant effect on the mass loss index induced by sulphate attack on CSA cement blended concrete.

When oyster shells were utilized as a sand substitute, Kuo *et al*. (2013) discovered that the weight loss of concrete owing to sulphate attack increased with increasing sea shell content. Compressive strength of concrete built with 5, 10, and 15% seashell as partial replacement for cement met the required strength of 25 MPa at 28 days, with 5% being the optimal. Furthermore, they added that concrete produced with 5% seashell as a cement replacement has about the same resistance to sulphate attacks as regular concrete (Tayeh *et al*., 2019). As a result, for structures subjected to these types of attacks, a concrete containing 5% seashells may be as durable as regular concrete. They however concluded on the need for calcination if an increased resistance to sulphate attack is needed at higher concentrations of sea shells in concrete. Attah *et al*. (2018), in their study on the effect of sulfuric acid on the mixture interaction of oyster shell on compressive strength, concluded that strength and mass losses due to increasing oyster shell content linearize with increasing oyster shell content. This is in tandem with the objective of this research exercise which seeks to improve the replaceability of cement in concrete without posing challenges on the strength and durability credentials of concrete and hence incorporating the process factor of calcination temperature.

At optimisation as shown in Figure 4.49, SIMLI was obtained as 8.654% relative to its mass when cured in fresh water at a curing period of 28 days, the optimised constraints are 77%PC:23% CSA mixture and 527 ^{o}C calcination temperature process factor. Application of The equation (model) as developed, is flexible and relatively useful depending on the requirements of strength, durability and sustainability.

Developed model for the SIMLI of CSA cement blended concrete is as shown in Equation 4.17 below;

$$\frac{\ln(\mathrm{SIMLIcsa}+20)}{9.28-\mathrm{SIMLIcsa}} = 0.126\mathrm{PC} - 0.524\mathrm{CSA} + (9.70 * 10^{-3} * \mathrm{PC} * \mathrm{CSA}) - (1.127 * 10^{-4} * PC * CSA\ (PC - CSA)) \ldots\ldots\ldots\ldots\ldots\ldots\ldots\ldots\ldots\ldots\ldots\ldots\ldots\ldots\ldots \quad (4.17)$$

Where;

PC = Mass proportion of Portland cement in total binder of CSA concrete (%)

CSA = Mass proportion of CSA in total binder of CSA cement blended concrete (%)

T = Calcination temperature for production of CSA in CSA cement blended concrete (^{o}C)

4.3.12. Calcination and mixture configuration variations on the SIMLI of Hybrid Agro-Based Pozzolan Cement Blended Concrete

From Figure 4.100 to 4.103, no significant effect on mass loss was observed due to variations in temperature and synergistic ratio. No significant variation on mass loss was observed due to variations in cement replacement level. Control specimen had a higher slightly SIMLI than majority of the samples. However, no definite trend can be identified from the plots using the laboratory data.

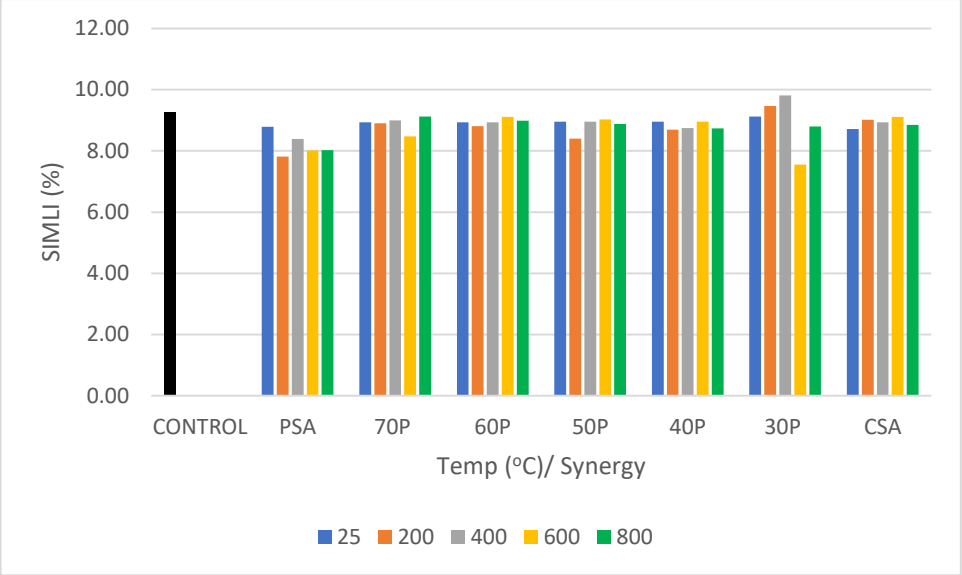

Figure 4.105: Sulphate Induced Mass Loss Index Variations for Calcined HAP Concrete at 20% CRL

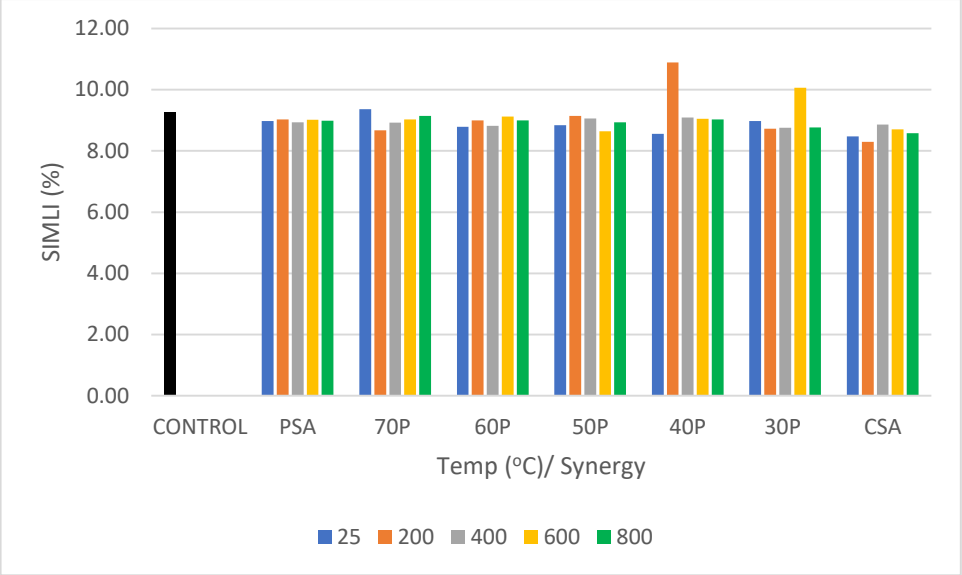

Figure 4.106: Sulphate Induced Mass Loss Index Variations for Calcined HAP Concrete at 30% CRL

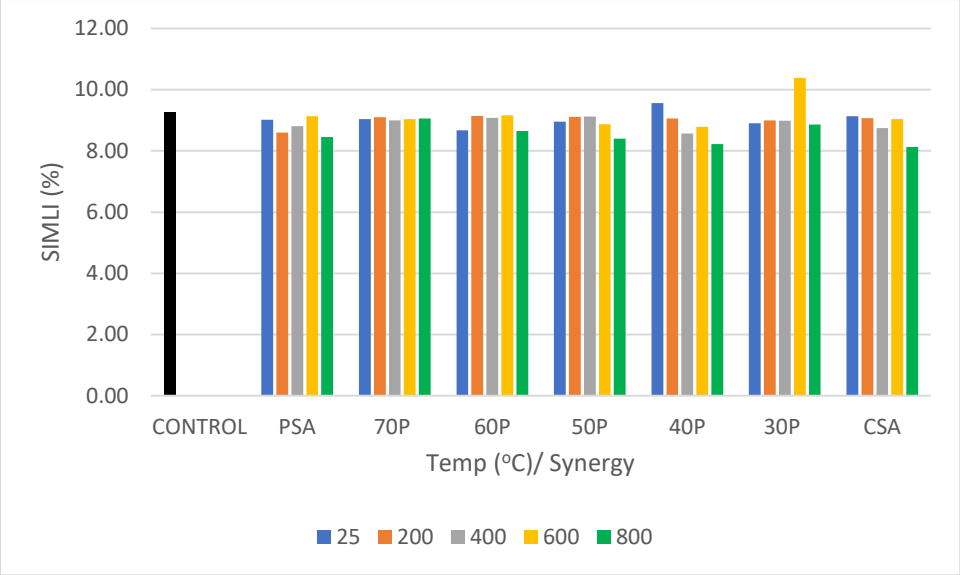

Figure 4.107: Sulphate Induced Mass Loss Index Variations for Calcined HAP Concrete at 40% CRL

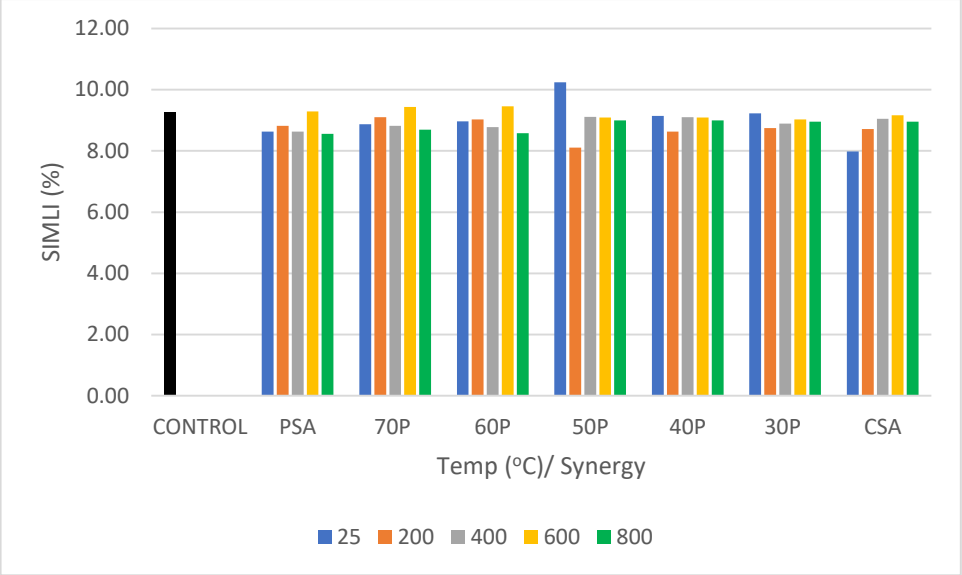

Figure 4.108: Sulphate Induced Mass Loss Index Variations for Calcined HAP Concrete at 50% CRL

Appendix S1, represents the analysed variance and regression coefficients of the model for the sulphate induced mass loss index of HAP concrete. The equation (model) incorporates model terms from "quadratic mixture" and "linear processes" which collectively includes six model terms involving the variables AC (significant), BC (significant), BD (non-significant), CD (significant), and ACD (significant). The all integrated model was observed to be significant a $P<<0.05$ and model's confidence interval exceeding 95%

The model's ratio to the square of its total sum produced a regression coefficient (Appendix S2) of 0.7827. Also, coefficients of regression as adjusted and predicted was obtained as 0.6912, and 0.5147, which implies that the model is sound enough for predictions and simulations.

Standard error was 0.3 over a mean of 8.74, with a deviation coefficient of 3.48%. The adequacy of the model's precision was 12.13, which implies that an error could exist in every 12.13 predictions. In essence, the least expected error of 4, is significantly above the model's maximum probable error, accordingly, the model's signal is adequate enough within its design scope for statistical simulation purposes.

The model's coefficients, which are displayed in Appendix S3, indicate that multicollinearity did not have an impact on any of the six (6) model terms with variance inflated factors smaller than 10. As a result, it appears that independent variables can be changed statistically, which is a necessary condition before looking at how changing independent factors affect replies.

Statistical check on model's performance as seen in Figure 4.109 shows a near linear spread of the statistically moderated errors, having passed the 'Fat pencil test'. As such, the developed equation can be satisfactorily utilised for predictions and simulations.

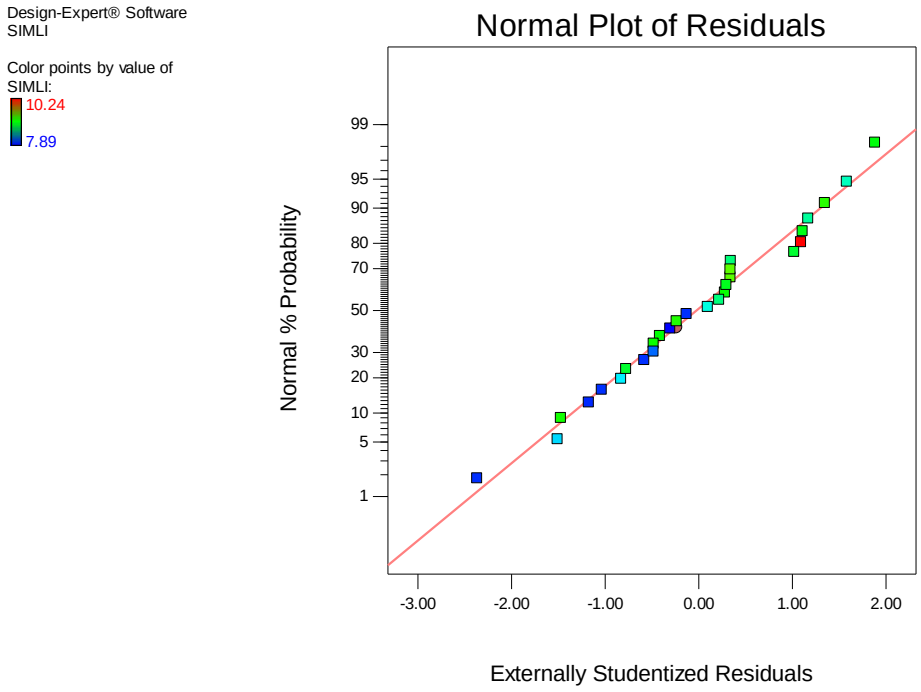

Figure 4.109: Studentised error spread for the SIMLI of HAP concrete

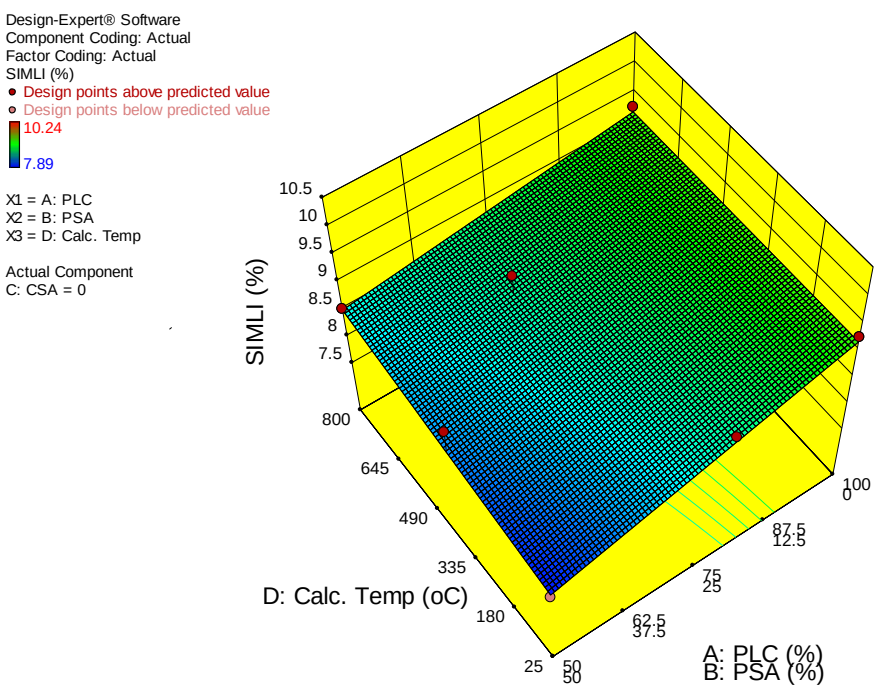

Figure 4.110: Three-dimensional model at 0% CSA level on the SIMLI of HAP concrete

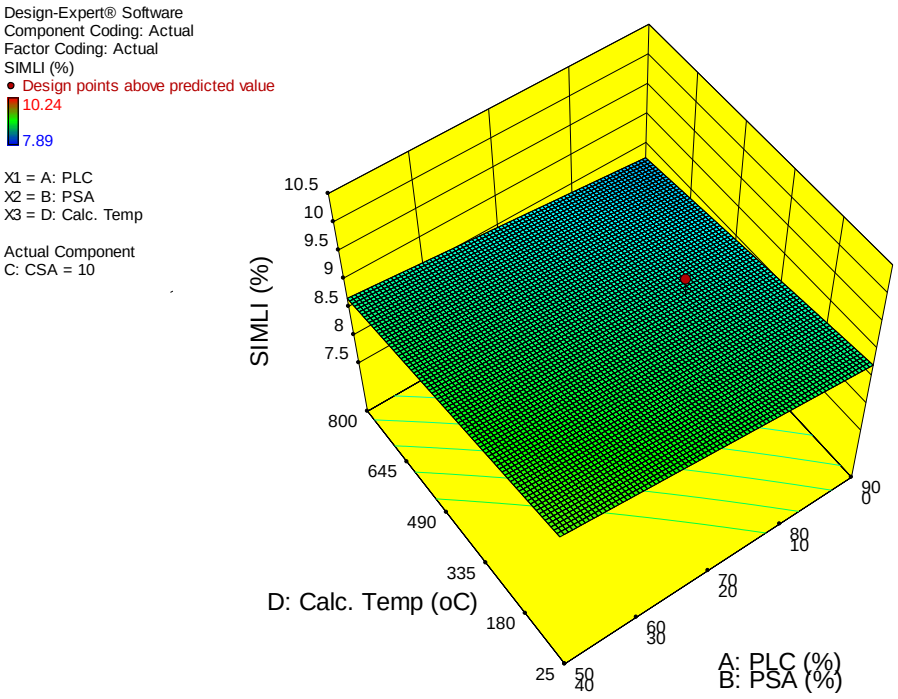

Figure 4.111: Three-dimensional model at 10% PSA level on the SIMLI of HAP concrete

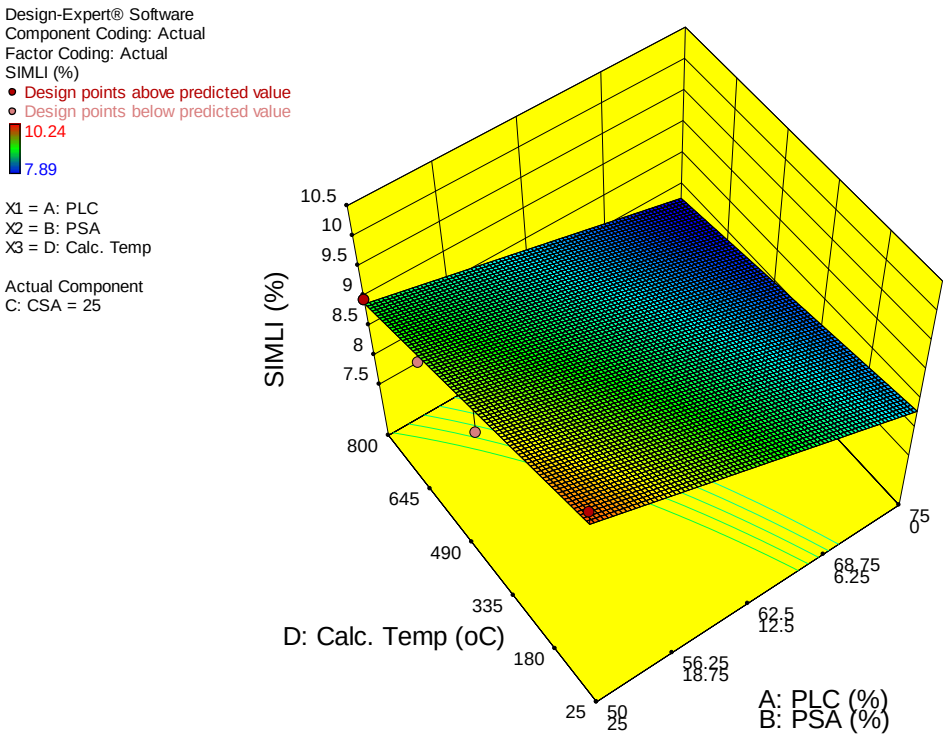

Figure 4.112: Three-dimensional model at 25% CSA level for the SIMLI of HAP concrete

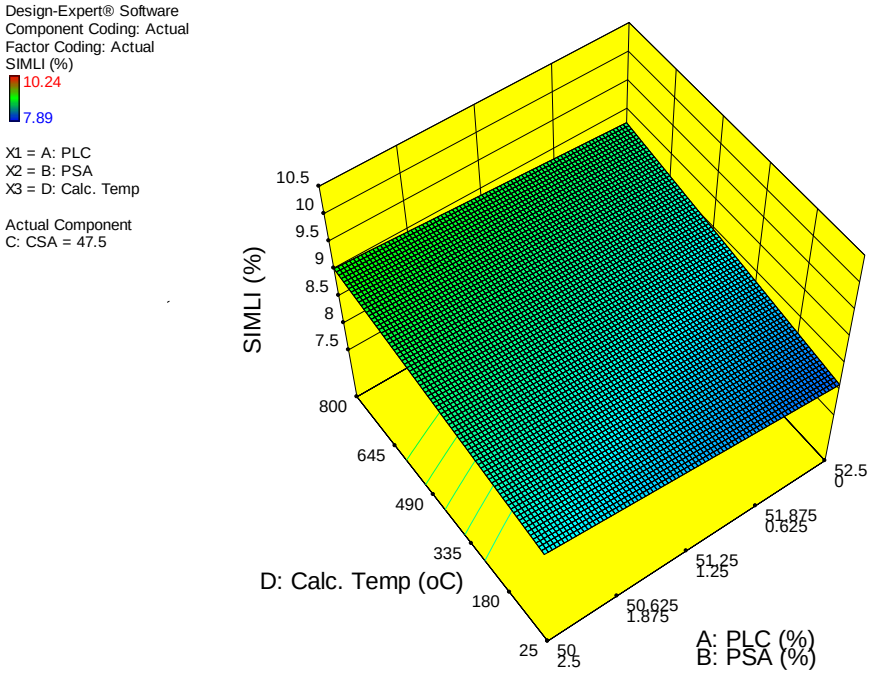

Figure 4.113: Model simulation 47.5% CSA level for the SIMLI of HAP concrete

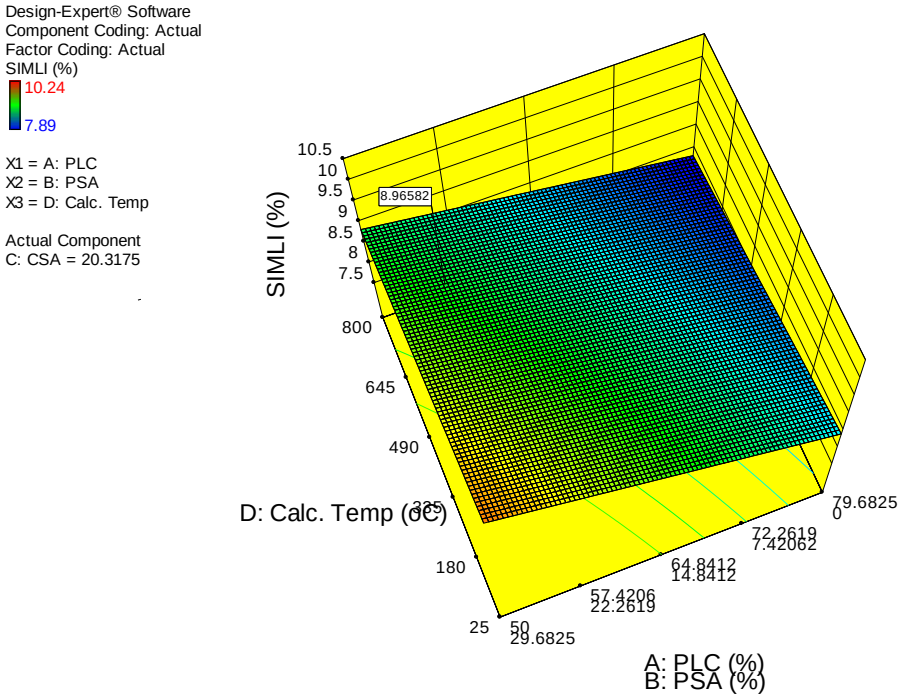

Figure 4.114: Three-dimensional and optimised model variables for SIMLI of HAP concrete

Figure 4.110 to 4.113 represents the model's simulations at varying mixture components as well as processes for SIMLI model. The SIMLI of the HAP concrete was observed to be affected by the mixture factor (calcination temperature) in a hugging quadratic relationship with a depth of crest corresponding to the concentration of PLC in the HAP concrete mix. At minimal cement content (50%PC), the crest was at its peak about an average hybrid synergy of 25% PSA:25% CSA. Increasing cement content reduces the depth of the crest (SIMLI) and flattens at 97.5%PC concentration. At 0% CSA concentration (Figure4.110), minimal SIMLI was observed at 50% PSA content requiring minimum calcination treatment. At 10% CSA concentration, for all PSA concentrations, calcination temperature increase results in the reduction of SIMLI and mostly true for PSA concentration range of 0-20% (Figure 4.111). At 25% CSA concentration, (Fig 4.112), increasing calcination temperature and reducing PSA content enhances the concretes ability in resisting sulphate attack on its mass. At 47.5% CSA concentration (Figure 4.113), reductions in both calcination temperature and PSA concentration are favourable against SIMLI. Hence, with respect to the quadratic mixture factor of the SIMLI model, the introduction of CSA suggests the need for the reduction of PSA concentration in order to increase the concrete's potentials against SIMLI. Additionally, the models (Figure 4.110 and Figure 4.113), suggests that if either of the pozzolanic materials are to be used alone in a mixture with Portland cement, calcination temperature will have a direct proportionality with SIMLI such that increasing calcination temperature increases SIMLI; a scenario suggesting the need to neglect calcination when considering SIMLI in isolation.

At optimisation (Figure 4.114), calcination temperature for SIMLI was relative to the four other equally important responses and hence constrained to 606.7 ^{o}C and 349 ^{o}C for solutions 1 and 10, yielding respective SIMLI of 8.996% and 9.11%, against a 28 day control SIMLI of 9.28%.

The equation as developed is vetted logically ideal to be included into the engineering community, for designs and policy-making processes in relation to the unique characteristics of cost, environment, social, structural, and durability indicators of sustainable engineering practices.

Developed model for the sulphate induced mass loss index of HAP cement blended concrete is as shown in Equation (4.18)

$$SIMLIhap = 0.092\text{PC} - 0.665\text{PSA} + 0.095\text{CSA} - (4.905 * 10^{-4}\text{PC} * \text{CSA}) + (3.287 * 10^{-3} * \text{PSA} * \text{CSA}) + (1.516 * 10^{-5}\text{PSA} * \text{T}) + (1.293 * 10^{-4} * \text{CSA} * \text{T}) - (2.102 * 10^{-6} * \text{PC} * \text{CSA} * \text{T}) - (3.844 * 10^{-6} * PSA * CSA * T) \quad (4.18)$$

Where;

SIMLIhap =	Sulphate induced mass loss index of HAP concrete (%)
PC =	Mass proportion of Portland cement in total binder of HAP concrete (%)
CSA =	Mass proportion of CSA in total binder of HAP cement blended concrete (%)
PSA =	Mass proportion of PSA in total binder of HAP cement blended concrete (%)
T =	Calcination temperature for production of CSA and PSA hybrid in HAP concrete (^{o}C)

Results obtained on the use of HAP in concrete as a partial replacement for cement, based on compressive strength, flexural strength, water absorption index, chloride induced strength loss index, sulphate induced strength loss index and mass loss index, has shown to be a combined function of mix configuration and calcination temperature. Compressive as well as flexural strengths were observed to increase with increasing calcination temperature and PSA concentration content. Water absorption index was observed to reduce with increasing PSA content, with minimal calcination temperature effect. Similarly, chloride induced strength loss index was observed to be affected quadratically on both sides of calcination temperature and mixture configuration, with optimal effects at a temperature and mixture configuration range of 250 ^{o}C – 500 ^{o}C, and 15% PSA - 30% PSA respectively. Sulphate induced strength and loss index was observed to be minimal with increase in clam shell ash concentration at lower calcination temperatures.

Mala *et al*., (2013), using a combination of 10% SF and 10% FA as partial cement replacement materials in concrete, asserted that the combination of ordinary

Portland cement, silica fume and fly-ash in concrete is of ecological and economic relevance as well as possess superior corrosion resistance even in cracked conditions, and concluded that OPC replacement level should be limited to 20% if early strength is required. This is quite logical noting the elemental characteristics of silica fume and fly ash being of similar proportion of low silica to very high lime concentrations. Walker and Pavia, (2011) asserted that the elemental composition of pozzolanic materials is a key ingredient in determining the pozzolanic reactivity of pozzolan concretes structures. While Imoh *et al*., (2019) suggests that a good concentration of CaO is responsible for self-cementing properties in pozzolans, also, pozzolans' very activity relies primarily on the acid-based reaction which requires the presence of SiO_2, according to ASTM C 618, (2008). Bamigboye *et al*., (2021), added that high silica content in mollusc shells suggests that they could be utilised as cementitious materials. Cheng *et al*., (2012) discovered that increasing calcination temperature has a quadratic effect on the SiO_2 content of shale (mudstone) peaking between 650 ^oC and 750 ^oC. Using calcined shale to replace cement in mortar at 20% replacement level, they concluded that although results obtained met the 75% SAI criteria for pozzolans, limitations in CaO content is a shortfall in the use of shale at larger proportions. Memon *et al*. (2020) contributed the variations of CaO content in corn stalk due to variations in calcination temperature, revealing findings that suggest a hugging quadratic relationship peaking around 500 ^oC. Sabir *et al*., (2001) added that pozzolanic reactivity of pozzolans is influenced by the burning or calcining temperature, and the calcining temperature which produces the active state, is normally between 600 ^oC and 800 ^oC. Similarly, Salau and Osemeke, (2015) with findings that validates this research exercise added that compressive strength of the concrete increases as the calcination temperature rises from 450 ^oC to 750 ^oC, until it reaches the optimum temperature of 750 ^oC beyond which a significant deterioration was observed at 900 ^oC.

The above reviews justify the need to limit the calcination of mollusc's shells to temperature below 800 ^oC and affirm on the need for pozzolans with

complementing oxides of CaO and SiO_2 in a bid to increase the replaceability of Portland cement in concrete.

Trend of reviewed literature on the mixture of pozzolans with cement are in tandem with the obtained results in terms of reducing compressing strength resulting from increasing pozzolanic content. However, quite novel is the optimized solutions obtained from this investigation, introducing a new optimised and acceptable replacement level of cement using the synergy of PSA and CSA, produced at a binder mix ratio of 54.6%PC:25.1% PSA:20.3% CSA, subjected to calcination at 607^oC and found to have a desirability of 0.64. Alternatively, the 10th suggested solution with mixture configuration of 56.5%PC:29.4% PSA:14.1% CSA at a calcination temperature of 349 ^oC yielding approximately 21 N/mm2 compressive strength of concrete observed to be 75% of control and a grade M20 concrete acceptable for mass concrete purposes.

The novelty of this research is that in a bid to enhance the replaceability of cement in concrete production, as a route towards a more sustainable binder that is structurally and durably sound, models have been developed analysed incorporating a mix of PSA and CSA as well as well as calcination temperature, which can be used to navigate the design space of Pozzolan properties for use concrete production. Beyond that, knowledge on the potentials of incorporating pozzolans with complementing CaO and SiO2 rich oxides in concrete as more effective cement replacement alternatives explored and shows boundless possibilities surrounding pozzolans and supplementary cementitious materials at large.

4.4. Sustainability Footprint of Hybrid Agro Based Pozzolan

The production of artificial Pozzolans involves energy consumption which translates to economic and environmental costs. This section therefore states the results on the sustainability indicators associated with the pulverisation process as well as the calcination process.

Calcination temperature is directly proportional to rate of pulverisation. As such, higher calcination temperature reduces the time required for pulverisation. Table 4.13, represents that rate of pulverisation in Kilogram/minute as a function of calcination temperature, based on laboratory experience.

Table 4.13: Primary factors for evaluating the result of calcination/pozzolan type relative to pulverisation rate of PSA and CSA pozzolans

CALCINATION TEMPERATURE (^oC)	PSA (Kg/hr)	CSA (Kg/hr)	PSA (Kg/min)	CSA (Kg/min)
25	25	20	0.42	0.33
200	32	25	0.95	0.75
400	35	28	1.00	0.80
600	36	30	1.02	0.83
800	37	31	1.03	0.85

Table 4.14: Result of calcination/pozzolan type relative to pulverisation rate of PSA and CSA pozzolans measured in minutes per kilogram

Calcination Effect on Rate of Pulverization (Mins/Kg)					
SAMPLE ID	25 ^{o}C	200 ^{o}C	400 ^{o}C	600 ^{o}C	800 ^{o}C
PSA	2.40	1.05	1.00	0.98	0.97
70P	2.55	1.12	1.06	1.04	1.02
60P	2.61	1.15	1.09	1.06	1.04
50P	2.67	1.18	1.11	1.08	1.06
40P	2.73	1.20	1.14	1.10	1.08
30P	2.79	1.23	1.16	1.13	1.10
CSA	3.00	1.33	1.25	1.20	1.18

From the engine specifications (Appendix T1) used for pulverisation, fuel consumption rate is at 1.7 L/hr or 0.028 L/min. As such, the fuel consumption per mass of pozzolan produced is as shown in Table 4.15, obtained as the product of Table 4.14 results and 0.028.

ECOSCORE (2021), shows that for every litre of petrol burnt, approximately 2.39 Kg of carbon dioxide is emitted. Consequently, the Table 4.16 below is an approximate indication of the carbon footprint associated with the pulverisation of the pozzolans covered in this study.

Table 4.15: Fuel consumption per pozzolan mass due to pulverization

RATE OF FUEL CONSUMPTION (L/Kg)					
SAMPLE ID	25 ^{o}C	200 ^{o}C	400 ^{o}C	600 ^{o}C	800 ^{o}C
PSA	0.07	0.03	0.03	0.03	0.03
70P	0.07	0.03	0.03	0.03	0.03
60P	0.07	0.03	0.03	0.03	0.03
50P	0.07	0.03	0.03	0.03	0.03
40P	0.08	0.03	0.03	0.03	0.03
30P	0.08	0.03	0.03	0.03	0.03
CSA	0.08	0.04	0.04	0.03	0.03

Table 4.16: CO_2 Emission rate per pozzolan mass production due to pulverisation

Grinding CO_2 emission Rate (gCO_2/kg)					
SAMPLE ID	25 ^oC	200 ^oC	400 ^oC	600 ^oC	800 ^oC
PSA	160.61	70.44	66.92	65.82	64.76
70P	170.86	75.19	71.19	69.59	68.40
60P	174.57	76.92	72.74	70.94	69.71
50P	178.45	78.73	74.36	72.35	71.07
40P	182.51	80.63	76.05	73.81	72.48
30P	186.75	82.62	77.81	75.33	73.94
CSA	200.76	89.23	83.65	80.30	78.73

Having established the CO_2 footprint associated with the pulverisation process, it is needful to analyse for the cost the raw materials as well as the labour cost of processing. Table 4.17 represents the observations made on the cost associated with the purchase and processing of the raw pozzolanic materials.

Table 4.17: Primary Cost evaluation of PSA AND CSA POZZOLANS

Pozzolan	PSA	CSA	Synergy	COST (₦/KG)
KG/BAG	35	55	PSA	29
*WT. LOSS%	10	10	70P	25.1
USED (KG)	31.5	49.5	60P	23.8
COST (N)	800	600	50P	22.5
TRANSPORT	100	100	40P	21.2
Labour	100	150	30P	19.9
total cost	1000	850	CSA	16
Primary Rate (₦/Kg)	28.57143	15.45455		
Aprox. Rate (₦/Kg)	29	16		

*Approximate Loss of pozzolan material due to pulverisation, calcination and handling

Table 4.18: **Grinding Fuel consumption Rate (₦/kg)**

Grinding Cost Due to Fuel consumption (₦/kg)					
SAMPLE ID	25 ^{o}C	200 ^{o}C	400 ^{o}C	600 ^{o}C	800 ^{o}C
PSA	11.09	4.86	4.62	4.54	4.47
70P	11.80	5.19	4.61	4.80	4.72
60P	12.05	5.31	5.02	4.90	4.81
50P	12.32	5.44	5.13	4.69	4.61
40P	12.60	5.57	5.25	5.10	5.00
30P	12.89	5.70	5.37	5.20	5.10
CSA	13.86	6.16	5.78	5.54	5.44

Having noted the mass of Pozzolan material that can be produced per litre of petrol, based on mix configuration and calcination temperature, at petrol cost rate of 165 ₦/L, the cost of petrol will be the product of fuel consumption in L/Kg as shown in Table 4.15, and a constant fuel cost of 165 ₦/Litre. Results obtained are as shown in Table 4.18, representing the cost of fuel associated with the pulverisation process of PSA, CSA and the hybrid.

On calcination, four chambers of the furnace could contain about 20 kg each, its logically assumed that each chamber loses 10% of its mass on calcination and pulverization, as such, a chamber is assumed to yield 18 kg as mass of proceeds from the calcination process. Based on observation, the average rate of increase in temperature within the furnace is at 10 ^{o}C per minute, due to the air inlet valve setting. However, seeing the furnace is not a rotary kiln but a static kiln, grains of samples around the middle of the sample conveyer will not get as much heat treatment as those at the boundaries. For this reason, an additional 30 minutes was allowed to enable a greater percentage of the samples reach their designed calcination temperature. In essence, the calcination time was taking as the sum of ratio of calcination temperature to 10 and 30. This is as shown below;

$$Calcination\ Time = \frac{Calcination\ Tempertaure}{10} + 30 \quad \text{in } ^{o}\text{C} \qquad (4.19)$$

From equation 4.19, the calcination timing for the production of the pozzolanic samples are as shown in Table 4.18. ATM samples were not calcined and as such the column is left blank. Recalling that the above illustration was based on observations for 18 kg of samples being produced. However, per kg of sample will consume a reasonable amount of time which is not a direct proportion to that of 18 kg seeing that the material remains the same. However, the reduced packing factor associated with reduced mass will increase the flow of oxygen within the conveyer and hence increase the rate of heat transfer. For this reduce and due to lack of additional information, a safety factor of 50%-time reduction was applied on calcination rate of 18 kg/min to arrive at the calcination rate of minutes per kilogram pozzolan produced as shown in Table 4.20.

Table 4.19: Approximate Time to Bulk Pozzolan Calcination

Rate of Calcination (min/18 kg)					
SAMPLE ID	25 ^{o}C	200 ^{o}C	400 ^{o}C	600 ^{o}C	800 ^{o}C
PSA	0	50	70	90	110
70P	0	50	70	90	110
60P	0	50	70	90	110
50P	0	50	70	90	110
40P	0	50	70	90	110
30P	0	50	70	90	110
CSA	0	50	70	90	110

Table 4.20: Approximate Time to Specific Pozzolan Calcination

Rate of Calcination (min/ Kg)					
SAMPLE ID	25 ^{o}C	200 ^{o}C	400 ^{o}C	600 ^{o}C	800 ^{o}C
PSA	0	25	35	45	55
70P	0	25	35	45	55
60P	0	25	35	45	55
50P	0	25	35	45	55
40P	0	25	35	45	55
30P	0	25	35	45	55
CSA	0	25	35	45	55

The calcination process involved the use of coal powered by an electric blower on ignition; hence the CO_2 generated is a function of energy consumed by the electric blower per kg of Pozzolan produced and the CO_2 footprint of Coal combustion per kg of Pozzolan produced. Similarly, the cost associated with calcination process is a combination of man hourly labour cost, cost of coal and cost of electricity supply.

A bag of dried charcoal weighs approximately 45 kg which on combustion emits 123,300 grams of CO_2 (Almeida, 2012), as such, a kg of charcoal emits 2,740 g of CO_2 on combustion. Hassan *et al*., (2017) asserted that the average burning rate of wood charcoal is 3.5 g/min, however, laboratory observations revealed that at the air pressure required to raise the temperature levels for calcination, the minimum combustion rate is 7 g/min. Using the time required to reach the desired calcination temperature and the above constants, the mass of charcoal consumed, its cost as well as CO_2 indicator are shown as shown Tables 4.21, 4.22 and 4.23.

Table 4.21: Mass of charcoal consumed due to calcination per kilogram of pozzolan produced

Mass of Charcoal consumed on Pozzolan Production (g/Kg)					
SAMPLE ID	25 ^{o}C	200 ^{o}C	400 ^{o}C	600 ^{o}C	800 ^{o}C
PSA	0	175	245	315	385
70P	0	175	245	315	385
60P	0	175	245	315	385
50P	0	175	245	315	385
40P	0	175	245	315	385
30P	0	175	245	315	385
CSA	0	175	245	315	385

Table 4.22: CO_2 Emission Due to Charcoal Combustion

CO2 EMISSION due to calcination (gCO2/Kg)					
SAMPLE ID	25 ^oC	200 ^oC	400 ^oC	600 ^oC	800 ^oC
PSA	0	479.5	671.3	863.1	1054.9
70P	0	479.5	671.3	863.1	1054.9
60P	0	479.5	671.3	863.1	1054.9
50P	0	479.5	671.3	863.1	1054.9
40P	0	479.5	671.3	863.1	1054.9
30P	0	479.5	671.3	863.1	1054.9
CSA	0	479.5	671.3	863.1	1054.9

Table 4.23: Cost of Charcoal Consumed per Pozzolan Production

Cost of Charcoal Consumed per Pozzolan Production (₦)					
SAMPLE ID	25 ^{o}C	200 ^{o}C	400 ^{o}C	600 ^{o}C	800 ^{o}C
PSA	0	15.56	21.78	28.00	34.22
70P	0	15.56	21.78	28.00	34.22
60P	0	15.56	21.78	28.00	34.22
50P	0	15.56	21.78	28.00	34.22
40P	0	15.56	21.78	28.00	34.22
30P	0	15.56	21.78	28.00	34.22
CSA	0	15.56	21.78	28.00	34.22

The time required for calcination as shown in Table 4.20 is dependent on the mass of pozzolan being calcined. The mass of pozzolan calcined within a chamber of the furnace was 18 kg. As such, Table 4.19 is to be reduced to Table 4.20 which conveys the time required for the calcination of a Kg of pozzolan sample. It is noteworthy that it will be illogical to divide the recorded calcination time by 18 kg as the relationship is not entirely linear, however, it is safe to state that for all calcination temperatures, at half the time, a kg of respective pozzolan would have been completely calcinated.

Charcoal combustion rate is independent of the mass of pozzolan being calcined, but dependent on the rate of calcination. By observation, the useful heat from coal is exhausted at the rate of 20 g/min, bases on the furnace geometry and configuration. Seeing that 10 kg of charcoal has a useful life span of 500 minutes average rate of burning. This resulted in the development of Table 4.21, which is a product of Table 4.20 and 20, representing the rate of charcoal consumption at various calcination temperatures.

Table 4.22 represents the CO_2 footprint associated with charcoal combustion, gotten as a product of Table 4.21 and the standard CO_2 embodiment of charcoal (2.74 kg CO_2 /Kg of Charcoal).

The cost of charcoal is based on the portion of charcoal used as a result of varying burning time. However, at a standard cost of Four thousand Nigerian Naira (₦4,000.00) per 45 kg bag of charcoal, a kg of charcoal can be said to be at Eighty-Nine Nigerian Naira (₦89). Table 4.23 represents the cost of charcoal used by pozzolan production, as the product of Table 4.21 and ₦89.

Table 4.24: Blowing time for the combustion of HAP

Blowing Time (hr/kg)					
SAMPLE ID	25 ^{o}C	200 ^{o}C	400 ^{o}C	600 ^{o}C	800 ^{o}C
PSA	0	0.42	0.58	0.75	0.92
70P	0	0.42	0.58	0.75	0.92
60P	0	0.42	0.58	0.75	0.92
50P	0	0.42	0.58	0.75	0.92
40P	0	0.42	0.58	0.75	0.92
30P	0	0.42	0.58	0.75	0.92
CSA	0	0.42	0.58	0.75	0.92

Table 4.25: **Energy Consumed due to Blower**

Energy Consumed due to Blower (kwh/kg)					
SAMPLE ID	25 ^{o}C	200 ^{o}C	400 ^{o}C	600 ^{o}C	800 ^{o}C
PSA	0	0.25	0.35	0.45	0.55
70P	0	0.25	0.35	0.45	0.55
60P	0	0.25	0.35	0.45	0.55
50P	0	0.25	0.35	0.45	0.55
40P	0	0.25	0.35	0.45	0.55
30P	0	0.25	0.35	0.45	0.55
CSA	0	0.25	0.35	0.45	0.55

Table 4.26: Cost of Energy Consumed due to Blower

Cost of Energy Consumed due to Blower (₦/kwh/kg)					
SAMPLE ID	25 ^{o}C	200 ^{o}C	400 ^{o}C	600 ^{o}C	800 ^{o}C
PSA	0	10	14	18	22
70P	0	10	14	18	22
60P	0	10	14	18	22
50P	0	10	14	18	22
40P	0	10	14	18	22
30P	0	10	14	18	22
CSA	0	10	14	18	22

In a similar vein, the indicators associated with the electric blower used as the source of sending oxygen into the furnace for coal combustion process is dependent on the electricity emission factor, the wattage of the electric blower and the blowing time. Sam-Amobi, (2019) stated the Nigerian electricity emission factor to be 0.439 KgCO2/kwh and the blower used had a wattage of 600 watts. Additionally, Cost of electricity in Nigeria is approximately at 40 ₦/kwh for commercial and industrial purposes and 25 ₦/kwh for domestic use, (Global Petrol Prices, 2021). Table 4.24, the blowing time for Pozzolan production, is simple a representation of Table 4.20, when converted from minutes to hours.

Table 4.25 represents the energy consumed due to the blowing time and power of the lower, obtained as the product of blowing time and blower wattage (0.6 Kw) in kwh/Kg.

Table 4.26 represents the cost of energy associated with the electric blower. It is obtained as the product of the Nigerian electricity cost of 40 N/kwh and the energy demand per kilogram of pozzolan produced of Table 4.25.

By using the Nigerian electricity emission factor of 0.439 $KgCO_2$/kwh, Table 4.27, is developed as the product of the blower consumed energy (Table 4.25) and 0.439 $KgCO_2$/kwh.

Total cost pozzolan production is hence a function of primary costs (Table 4.17), grinding cost (Table 4.18), Cost of charcoal (Table 4.23) and cost of electric blower energy (Table 4.26). As such, Table 4.28 entails the summation of the indices from the aforementioned four tables, to yield a more comprehensive picture of the total cost of pozzolan production.

The calcination process itself releases CO_2 into the environment as the $CaCO_3$ breaks open at high temperatures. Turolla *et al*., (2020) established that a tonne of clam shell embodies about 88kg of carbon which when oxidised amounts to about 323 kg of CO_2 (because 1 kg of carbon produces 3.67 kg of CO_2). This implies that clam shell contains within 32.3% of CO_2. Fayemi *et al*., (2019) informed that for a kg of Portland cement produced, 0.49 KgCO_2 is emitted due to the calcination and clinker production, and 0.89 kgCO_2 is emitted due to coal power source, amounting to a total of 1.38 kgCO_2. This however does not state categorically if the CO_2 emitted due to pulverization is included. It was however clear on the absence of emission factors due to transportation and quarrying. Orgi *et al*., (2017) added that a kilogram of periwinkle shell contains 85% of calcium carbonate ($CaCO_3$) of which by molecular mass results in 44% CO_2 content on calcination. Hence, the maximum CO_2 content obtainable by complete calcination of 1 kg of periwinkle shell is 0.37 kg (0.44*0.85) or 37%. It is logically safe to conclude that a hybrid Pozzolan sample of PSA and CSA on calcination releases 0.35 kg of CO_2 per kg of produced.

Table 4.27: CO_2 Footprint Due to Blower Per Mass of Pozzolan Produced

CO_2 PER Energy Consumed due to Blower (gCO_2/kwh/kg)					
SAMPLE ID	25 ^oC	200 ^oC	400 ^oC	600 ^oC	800 ^oC
PSA	0	109.75	153.65	197.55	241.45
70P	0	109.75	153.65	197.55	241.45
60P	0	109.75	153.65	197.55	241.45
50P	0	109.75	153.65	197.55	241.45
40P	0	109.75	153.65	197.55	241.45
30P	0	109.75	153.65	197.55	241.45
CSA	0	109.75	153.65	197.55	241.45

Table 4.28: Total Production Cost of HAP (Charcoal Present)

SAMPLE ID	Temperature 25 °C	200 °C	400 °C	600 °C	800 °C
PSA	2,005	2,971	3,470	3,977	4,485
70P	1,845	2,793	3,275	3,795	4,302
60P	1,793	2,734	3,230	3,735	4,242
50P	1,741	2,675	3,171	3,660	4,167
40P	1,690	2,617	3,112	3,615	4,121
30P	1,640	2,558	3,053	3,555	4,061
CSA	1,493	2,386	2,878	3,377	3,883

Table 4.29: Total cost of pozzolan production (Charcoal absent)

Total Cost for the Production of 50kg HAP (₦)					
SAMPLE ID	25 ^{o}C	200 ^{o}C	400 ^{o}C	600 ^{o}C	800 ^{o}C
PSA	2,005	2,193	2,381	2,577	2,774
70P	1,845	2,015	2,186	2,395	2,591
60P	1,793	1,956	2,141	2,335	2,531
50P	1,741	1,897	2,082	2,260	2,456
40P	1,690	1,839	2,023	2,215	2,410
30P	1,640	1,780	1,964	2,155	2,350
CSA	1,493	1,608	1,789	1,977	2,172

In comparing the CO_2 footprint of the pozzolans covered in this study with that of Portland cement, only CO_2 emissions due to calcination was considered due to incomprehensive knowledge on the CO_2 footprint associated with the pulverisation of the raw materials, clinker production for Portland cement, as well as electricity supply. Hence, whilst cement emits 0.49 Kg of CO_2 per kilogram of Clinker, PSA and CSA emit 0.35 kg of CO_2 per kilogram of calcined sample due to calcination. This makes PSA and CSA a more environmentally friendly alternative when compared to Portland cement as its inclusion to form a binary or ternary cement blend in concrete or mortar reduces CO_2 emission into the environment by 29%.

Regarding the cost, the total cost for the production of HAP hybrid pozzolan is a combination of the primary material/labour cost, grinding cost, energy cost, and fuel cost. This as shown in Table 4.58, reveals that at a desirable calcination temperature not exceeding 600 ^{o}C, the production cost of 50 kg bag of PSA, CSA or the hybrid is approximately Three Thousand Eight Hundred Naira (₦3,800), when charcoal is used as the energy fuel, and roughly Two Thousand Six Hundred Naira (₦2,600) in the absence of charcoal cost. The second scenario of the absence of charcoal cost is based on the logical assumption that an electrically powered furnace wouldn't require a blower (although at a higher wattage), would drastically reduce pozzolan production cost. As such, an average of both costs will yield a more logical cost of Three Thousand Two Hundred Naira (₦3,200). At a profit and managerial cost of 8%, the market value of calcinated and optimized agro pozzolan becomes approximately Three Thousand Five Hundred Naira (₦3,500). This is about 22% lower than the current market value of Portland cement as at April, 2023, as such, economic savings can be said to have been filled as a gap in this study. Additionally, the environmental and durability components of the research gap of this study have been evidently addressed.

The cement industry is well aware that in 45 years or less, limestone would be no longer be making the list of major solid minerals in Nigeria (AsokoInsights, 2023). Also, the fight to preserve a future for the next generation is also of global interest. It is therefore of timely necessity that the industry gives full attention to findings related to supplementary cementitious materials favour of structural durability and sustainability.

CHAPTER FIVE
SUMMARY, CONCLUSIONS AND RECOMMENDATIONS

5.1. Summary

Portland cement, at production, is environmentally hazardous, economically unfriendly, and in concrete, results in reduced durability. This study, utilizing wastes/by-products from the agricultural sector, adopted an approach of combining ashes rich in siliceous content (periwinkle shell ash) and ashes rich in calcareous content (clam shell ash), and at varying proportions, whilst simultaneously, burning at varying temperatures, to improve on the gap that existed in cement replaceability from 20% to 45%, without adversely affecting the short- term structural integrity of the concrete.

Calcination temperature as well as synergistic ratio variations, have been found by this study, to contribute effectively to the physical, mechanical and durability properties of periwinkle shell ash, clam shell ash and the hybrid, when used in concrete production as a partial cement replacement material. To this effect, this study has developed models for designing concrete mixes incorporating the aforementioned pozzolans and based on the desired mechanical and/or durability properties.

Based on the methodology adopted for calcination, this study informs that no short-term economic benefits can be derived from the application of the optimized pozzolans in the construction industry. However, their durability contribution implies long term economic benefits. Environmentally, this study concludes that increasing the replaceability of Portland cement using the optimized pozzolanic materials, inversely affects the concentration of CO_2 emissions.

5.2. Conclusion

The Study utilized calcination temperature and synergistic ratio as the key production variables in evaluating the enhanced performance of periwinkle and clam shells in concrete as pozzolanic substitutes and partial cement replacements. The following therefore concludes the findings of this research exercise;

1. Calcination temperature significantly affects the physical, mechanical and durability properties of AP and HAP cement blended concretes and as such enhance cement replaceability at optimised levels.
2. The replacement level of cement in concrete, using AP or HAP was observed to be inversely and linearly related with the compressive and flexural strength of AP or HAP cement blended concrete, regardless of synergistic ratio or calcination temperature.
3. The mix configuration (inclusive of cement replacement level and synergistic ratio) was also observed to be a stronger variable on the compressive strength, flexural strength and water absorption indices of the pozzolan cement blended concretes, than the calcination temperature regardless of pozzolan type.
4. Calcination temperature was seen to be a superior dependent variable than mix configuration relative to the resistance of pozzolan cement blended concrete to chemical attack. Hence, close attention must be given to the temperature of pozzolan production mostly, in cases of exposing the concrete to chloride or sulphate rich exposure conditions.
5. At optimal calcination temperature, synergistic ratio and cement replacement levels, HAP cement blended concrete is economically, socially and environmentally friendly.

5.3. Recommendations

The following are the recommendations from the findings of the study for the industry:

1. Produce PSA at 500oC and pulverise to a D50 of 25µm. This would invariably enhance cement replacement to between 20-25% with improved sustainability and durability indices at acceptable mechanical indices
2. Produce CSA at 600oC and pulverise to a D50 of 25µm. This would invariably enhance cement replacement to between 25-30% with improved sustainability and durability indices at acceptable mechanical indices
3. Produce a hybrid of PSA and CSA at a ratio of 1.25:1, calcinate at 650oC and pulverise to a D50 of 25µm. This would invariably enhance cement replacement to between 45-50% with improved sustainability and durability indices at acceptable mechanical indices

The following are the recommendations from the findings of the study for future research:

4. The design and development of a local scale rotary type kiln, powered by an energy source with reduced CO_2 footprint.
5. The design and fabrication of a local scale shell pulveriser, with the capacity of producing a material with fineness less than 75 µm and at a relative economic and environmental cost.
6. A qualitative study of localities and their willingness to participate and adopt locally made supplementary cementitious materials, noting the absence of short-term economic benefits.
7. The design and development of a more inclusive platform that utilises the hydraulic indices of available materials with pozzolanic or hydraulic tendencies, in the establishment of optimal mix configuration as well as calcination temperatures for the production of sustainable cement replacement alternatives.

5.4. Contributions to Knowledge

The following sums up the contributions to knowledge from this study;

- Developed models for the estimation of optimal temperatures, synergistic ratios as well as cement replacement levels in the integration of periwinkle and clam shells in concrete production, relative to compressive strength and durability indices.
- An environmentally feasible approach in the utilisation of periwinkle and clam shells as partial supplementary cementitious materials to mitigate the excessive harvest and processing of limestone for cement production, and hence reduce the relative emissions of carbon dioxide into the atmosphere.
- The design and fabrication of a local scale, charcoal powered furnace

REFERENCES

Abalaka, A.E. 2012. Effects of Methods of Incineration on Rice Husk Ash Blended Concrete. *ATBU journal of Environmental Technology* 5.1: 34-47.

Adam D. N. 2004 'Supplementary Cementitious Materials: Part I: Pozzolanic SCMs - What are SCMs and how can you use them to your advantage? Technical report – National Precast Concrete Association, USA, October 2004

Adewuyi, A. P., Franklin, S. O., and Ibrahim, K. A. 2015. Utilization of mollusc shells for concrete production for sustainable environment. *International Journal of Scientific and Engineering Research* 6.9: 201-208.

Afif, R. and Haifaa, J, 2018. Modelling the Cementitious Effect of the Pozzolan on the Compressive Strength of Concrete. *Cogent Engineering* 5.1:1–13.

Agbede, O. I., and Manasseh, J. 2009. Suitability of periwinkle shell as partial replacement for river gravel in concrete. *Leonardo Electronic Journal of Practices and Technologies* 15.2:59-66.

Ahmad, S., 2002, 'Effect of fineness of cement on properties of fresh and hardened concrete. *Proceedings of the 27th Conference on Our World in Concrete and Structures, Singapore. 29-30th August, 2002*. CI-Premier PTE LTD Eds., Singapore. Singapore Concrete Institute. 1 – 8.

Ahmed, S., Dwivedi, V. K., Chhabra, S.S., and Sahu P. 2016. Partial Replacement of Ordinary Portland Cement with Rice Husk Ash and Coconut Shell Ash in Concrete. *International Journal of Modern Trends in Engineering and Science* 3.5:107-111.

Ajay, G., Hattori K., Hidechiko O., Monika G., Anwar A.M., and Ashraf M., 2007. Synergic Effect of Wheat Straw Ash and Rice Husk Ash on Strength Properties of Mortar. *Journal of Applied Science* 7.21:3256-3261.

Alhamad, A., Yehia, S., Lublóy, É. and Elchalakani, M., 2022. Performance of Different Concrete Types Exposed to Elevated Temperatures: A Review. *Materials* 15.14:1-58.

Alexandre, J.1 , Xavier, G.C. 1Azevedo, A.R.G.1 , Monteiro, S.N.2 , Vieira, C.M.F 2014. Determination of Temperature and Time Calcination of Clays for Production of Metakaolin Based on Pozzolanic Activity. *Characterization of Minerals, Metals, and Materials*. John S. Carpenter, Chenguang Bai, Jiann-Yang Hwang, Shadia Ikhmayies, Bowen Li, Sergio Neves Monteiro, Zhiwei Peng, and Mingming Zhang Eds. Brazil. 25-32.

Almeida A. S., 2012. Charcoal, carbon emissions, and international conventions/protocols. *Proceedings of the Conference on Charcoal and Communities in Africa, Maputo, Mozambique. 16 – 18 June, 2008*. Ralf Kwaschik Eds. 20-34

Amarachi N., Gerald O., Emeka O. and Martin O., 2021. The Future and Prospects of Periwinkle Composites in Reinforced Concretes: A Review. *Journal of Engineering Research and Reports* 21.1:49-67.

Antia M.E., Ajiero I.R. and Anih P.C., 2020. The Effect of Periwinkle shell ash mixed with cement on water absorption and shrinkage of lateritic block. *Baltic Journal of Real Estate Economics and Construction Management* 8.1:22-33.

Anyanwu S.O., Adam J.A., Obi B. and Yelwa M., 2015. Human capital development and economic growth in Nigeria. *Journal of Economics and Sustainable Development* 6.14:16-26.

Arum C., Ikumapayi C. M., and Aralepo G. O., 2013. Ashes of Biogenic Wastes—Pozzolanicity, Prospects for Use, and Effects on Some Engineering Properties of Concrete. *Materials Sciences and Applications* 4.9:521-527.

ASTM C – 618, 2008. Standard Specification for Coal Fly Ash and Raw or Calcined Natural Pozzolan for Use in Concrete. *ASTM international standards*

Attah I. C., Etim R. K., and Ekpo D. U., 2018. Behaviour of Periwinkle Shell Ash Blended Cement Concrete in Sulphuric Acid Environment. *Nigerian Journal of Technology* 37.2:315 – 321.

Bamigboye, G. O., Nworgu, A. T., Odetoyan, A. O., Kareem, M., Enabulele, D. O., and Bassey, D. E. 2020. Sustainable Use of Seashells as Binder in Concrete production: Prospect and challenges. *Journal of Building Engineering* 34.7:1-17.

Ban, C.C. and Norbert, B.H., Mechanical properties of Rice Husk Ash-Ground Granulated Blast Furnace Slag Ternary Blended Cement Mortar. *Journal of Built Environment, Technology and Engineering*1:10-17

Bayuaji, R., and Akhwady, R. 2017. The Influence of Clamshell on Mechanical Properties of Non-Structure Concrete as Artificial Reef. *Asian Journal of Applied Sciences* 5.2:389-395.

Beef2Live, 2017. World Corn Production (Ranking By Country) Online source available at *http://beef2live.com/story-world-corn-production-ranking-country- 0-107183/* last visited on 07/17/2017.

Bharnuke A.J. and Chore H.S, 2014. Experimental Studies on High Performance Concrete Using Blast Furnace Slag as a Cement Replacement Material. *International Journal of Multidisciplinary Approach and Studies* 1.6:1 – 15.

Bheel, N., Mangi, S.A. and Lal, S., 2021. Coconut shell ash as cementitious material in concrete: a review. *Jurnal Kejuruteraan* 33.1:27-38.

BREF, 2010. Best Available Techniques in the Cement, Lime and Magnesium Oxide Manufacturing Industries. *European Commission* JRC-IPTS, IPPC Reference Document, May 2010

British Standard Colour. com, 2023. British Standard Colours - the most used British Standards for colours BS2660, BS381C, BS4800 and BC5252 collected in one fan deck. Online Source at https://www.britishstandardcolour.com/, Last visited 6/28/2023

BS 1881 – 122, 2011. Testing concrete - Method for determination of water absorption. British International Standards.

BS 1881 -124, 1988. Testing concrete - Methods for analysis of hardened concrete' British International Standards.

BS 1881: Part 118:1983. Testing concrete - Method for determination of flexural strength' British International Standards.

BS EN 12350-1, 2009 Testing fresh concrete - Sampling', British International Standards.

BS EN 12350-2, 2009. Testing fresh concrete - Slump-test', British International Standards.

BS EN 12350-4, 2009. Testing fresh concrete - Degree of compatibility', British International Standards.

BS EN 12390 – 13, 2013. Testing hardened concrete - Determination of secant modulus of elasticity in compression', British International Standards.

BS EN 12390 - 3, 2009. Testing hardened concrete - Compressive strength of test specimens. British International Standards.

BS EN 12390 - 5, 2009. Testing hardened concrete - Flexural strength of test specimens. British International Standards.

BS EN 12390 – 7, 2009. Testing hardened concrete - Density of hardened concrete British International Standards.

BS EN 12390 – 8, 2009. Testing hardened concrete - Depth of penetration of water under pressure. British International Standards.

BS EN 14630, 2006. Products and Systems for the protection and repair of concrete structures. Test Methods – Determination of Carbonation depth in hardened concrete by the Phenolphthalein Method. British International Standards.

BS EN 196-3, 1995. Methods of testing cement - Determination of setting time and soundness'. British International Standards.

Busari, A. A., Akinmusuru, J. O., Dahunsi, B. I. O., Ogbiye, A. S., and Okeniyi, J. O. 2017. Self-compacting concrete in pavement construction: Strength grouping of some selected brands of cements. *Proceedings of the International Conference on Technologies and Materials for Renewable Energy, Environment and Sustainability, TMREES17, 21-24 April 2017*. Energy Procedia Eds., Beirut Lebanon: 119:863-869.

Campo, F.P., Tua, C., Biganzoli, L., Pantini, S. and Grosso, M., 2021. Natural and enhanced carbonation of lime in its different applications: a review. *Environmental Technology Reviews* 10.1:224-237

CEFIC, 2013. European Chemistry for growth – Unlocking a competitive, low carbon and energy efficient future. *The European Chemical Industry Council (CEFIC)*, Brussels, Belgium, 2013:1-186

Cemnet 2023. What's driving Nigerian cement demand?. Online source at https://www.cemnet.com/News/story/173376/what-s-driving-nigerian-cement-demand-.html last visited on 6/28/2023

Charles C. 2022. CIVL 1101 – Properties of Concrete. *Department of Civil Engineering, University of Memphis*, Online Source available on http://www.ce.memphis.edu/1101/notes/concrete/section_3_properties.html Last Visited on 5/14/2023.

Cheng, A., Chao, S. J., and Lin, W. T. 2012. Effect of calcination on pozzolanic reaction of calcined shale mortar. *Applied Mechanics and Materials*, Trans Tech Publications Ltd. Eds. 174-177:843-846.

Chiou I.J., C.H. Chen, and Y.H. Li 2014. Using oyster-shell foamed bricks to neutralize the acidity of recycled rainwater. *Construction and Building Materials* 64.3: 480–487.

Chopra, D. and Siddique, R. 2015. Strength, permeability and microstructure of self- compacting concrete containing rice husk ash. *Biosystems Engineering* 130.1:72-80

CIVL 1101, 2021, Properties of Concrete; Department of Civil Engineering at the University of Memphis.

Cook, D. J., Pama, R. and Darner, S. A., 1977. Rice Husk Ash-Lime-Cement Mixes for use in Masonry Units. *Building and Environment* 12.1:281-288

Dan Bloom, 2017. Lime Verses Portland Cement; Which is better? Stone House Masonry Company. Online Source Available on

http://stonehengemasonry.ca/lime-vs-portland-cement-which-is-better/ Last visited on 13/11/2017

Danner, T. and Justnes, H., 2018. The influence of production parameters on pozzolanic reactivity of calcined clays. *Nordic Concrete Research* 59.1:1-12.

Dankwah, J.R. and Nkrumah, E., 2016. Recycling blends of rice husk ash and snail shells as partial replacement for Portland cement in building block production. *Ghana Journal of Technology* 1.1:67-74.

Data Commons, 2023. Nigeria: A country in Africa. Online at *https://datacommons.org/place/country/NGA?utm_medium=explore&mprop=count&popt=Person&hl=en* last visited on 04/16/2023.

Deepa G N., Sivaraman K., and Thomas J. 2013. Mechanical Properties of Rice Husk Ash (RHA) - High strength Concrete. *American Journal of Engineering Research (AJER)* 3.1:14-19

Dembovska, L., Bajare, D., Pundiene, I., and Vitola, L. (2017). Effect of pozzolanic additives on the strength development of high-performance concrete. *Procedia Engineering* 172.1. 202-210.

ECOSCORE, 2021. How to calculate CO2 emissions from fuel Consumption. Online source available on https://ecoscore.be/en/info/ecoscore/co2. Last Viewed on 22/08/2021

EN 197 – 1, 2000. Composition, specifications and conformity criteria for common cements. European Standard.

EPA, 2023. Energy Recovery from the Combustion of Municipal Solid Waste (MSW). United States Environmental Protection Agency (EPA). Available online: https://www.epa.gov/smm/energy-recovery-combustion-municipal-solid-waste-msw/ visited on 4/10/2023.

Ephraim M. E, ThankGod. O, Gbinu. K.S., 2019. Performance of high Strength Concrete Using Oyster Shell Ash as Partial Replacement for Cement. *SSRG International Journal of Civil Engineering (SSRG-IJCE)* 6.6:33 – 38.

Eren Özgür, (2015), Materials of Construction; Lecture Note. *Department of Civil Engineering, Eastern Mediterranean University*. Second Edition: 9 – 16.

Ettu, L.O., Onyeyili, I.O., Anya, U.C., Awodiji, C.T.G. and Amanze, A.P.C., 2013. Strength of binary blended cement composites containing Afikpo rice husk ash. *International Journal of Computational Engineering Research* 3.4:71-76.

Etuk B. R., Etuk I. F., and Asuquo L.O., 2012. Feasibility of Using Sea Shells Ash as Admixtures for Concrete. *Journal of Environmental Science and Engineering* 1: 121-127.

Eziefula, U.G., Obiechefu, G.C. and Charles, M.E., 2020. Use of periwinkle shell by-products in Portland cement-based materials: An overview. *International Journal of Environment and Waste Management* 26.3:362-388.

Fadele O. A, and Ata O., 2016. Compressive Strength of Concrete Containing Palm Kernel Shell Ash. *American Journal of Engineering Research (AJER)* 5.12:32-36.

FAO, 2023. FAO lowers global rice forecast for 2012. *Food and Agricultural Organisation of the United Nations* Online Source available on https://www.fao.org/news/story/en/item/154122/icode/ last visited on 6/28/2023

Fayomi, G. U., Mini, S. E., Fayomi, O. S. I., and Ayoola, A. A. 2019. Perspectives on environmental CO^2 emission and energy factor in Cement Industry. In IOP Conference Series. *Earth and Environmental Science* 331.1: 12-35.

Felipe-Sesé, M., Eliche-Quesada, D. and Corpas-Iglesias, F.A., 2011. The use of solid residues derived from different industrial activities to obtain calcium silicates for use as insulating construction materials. *Ceramics International* 37.8:3019-3028.

Global Petrol Prices, 2021 'Nigeria Electricity Prices'. Online source available on; *https://www.GlobalPetrolPrices.com*, Last Viewed on 22/08/2021

Guo, Q., Chen, L., Zhao, H., Admilson, J. and Zhang, W., 2018. The effect of mixing and curing sea water on concrete strength at different ages. *MATEC Web of Conferences,* EDP Sciences Eds. 142: 02004.

Habert, G., Choupay, N., Escadeillas, G., Guillaume, D. and Montel, J.M., 2009. Clay content of argillites: Influence on cement based mortars. *Applied Clay Science* 43.4:322-330.

Habert, G., 2013. Environmental impact of Portland cement production: *Eco-efficient concrete*. Woodhead Publishing Eds. Chapter 1:3-25.

Hassan, L. G., Sani, N. A., Sokoto, A. M., and Tukur, U. G. 2017. Comparative Studies of Burning Rates and Water Boiling Time of Wood Charcoal and Briquettes Produced from Carbonized Martyniaannua woody Shells. *Nigerian Journal of Basic and Applied Sciences* 25.2:21-27.

Ikuemonisan, E.S., Mafimisebi, T.E., Ajibefun, I. and Adenegan, K., 2020. Cassava production in Nigeria: trends, instability and decomposition analysis (1970–2018). *Heliyon* 6.10:1-9

Intergovernmental Panel for Climate Change, 2022. The evidence is clear: the time for action is now. We can halve emissions by 2030. Online Source on https://www.ipcc.ch/2022/04/04/ipcc-ar6-wgiii-pressrelease/ Visited on 6/27/2023

Inti, S., Sharma, M., and Tandon, V. (2016). Ground granulated blast furnace slag (GGBS) and rice husk ash (RHA) uses in the production of geopolymer concrete. *Geo-Chicago 2016GSP 270: American Society of Civil Engineers* 621-632. Online source available on https://sci-hub.se/http://dx.doi.org/10.1061/9780784480137.059 last visited on 5/14/2023

Isaksson, R. and Steimle, U., 2009. What does GRI-reporting tell us about corporate sustainability?. *The TQM Journal* 21.2:168-181.

IS 4031 part 1., 1996. Method of Physical Tests for Hydraulic Cement: Part 1-Determination of Fineness by Dry Sieving' Indian Standard

Jobberman 2023. Closing the Talent Gap in Nigeria's Agriculture Sector. Online source on https://www.jobberman.com/discover/closing-the-talent-gap-in-nigerias-agriculture-sector#:~:text=While%20the%20sector%20currently%20employs,%2C%20Fishery%2C%20Forestry%20and%20Horticulture. Last visited on 6/27/2023

Kalkanis, K., Alexakis, D.E., Kyriakis, E., Kiskira, K., Lorenzo-Llanes, J., Themelis, N.J. and Psomopoulos, C.S., 2022. Transforming Waste to Wealth, Achieving Circular Economy. Circular Economy and Sustainability, 2, pp.1541–1559

Kamau J., Ash A., Paul H., and Joseph K. 2016. Suitability of Corncob Ash as a Supplementary Cementitious Material. *International Journal of Materials Science and Engineering* 4.4:215-228.

Kannan V., and Ganesan K. 2012. Strength and Water Absorption Properties of Ternary Blended Cement Mortar Using Rice Husk Ash and Metakaolin. *Scholarly Journal of Engineering Research* 1.4:51-59.

Kevern, J.T. and Wang, K., 2010. Investigation of Corn ash as a supplementary cementitious material in concrete. *In Second International Conference on Suitable Construction Material and Technology*, University of Wisconsin Milwakee Centre for by product utilization.

Kim, J. H., Chung, C. W., and Lee, J. Y. 2014. Effects of crushed shells on the physical properties of cement mortar. *Journal of the Korea institute of building construction* 14.1:94-101.

Kulkarni M. S., Mirgal P.G., Bodhale P. P., and Tande S.N. 2014. Effect of Rice Husk Ash on Properties of Concrete. *Journal of Civil Engineering and Environmental Technology* 1.1:26-29.

Kumar A., Tomar A.K,, Gupta S. K., and Kumar A, 2016. Replacement of Cement in Concrete with Rice Husk Ash. *SSRG International Journal of Civil Engineering (SSRG-IJCE)* 3.7:127-129.

Kumar N. and Kumar D. 2014. Utilization of Coconut Shell in Different Forms in Concrete. *International Journal for Scientific Research and Development* 2.7:158-160.

Kurniawan, R.W., Hardiyanto, E. and Faroqi, A.A., 2013. Environmentally friendly material: coconut husk ash and fly ash as supplementary cementitious material. Procedings of the *Asian Academic Society International*. Alessandro P. Fantilli and Daria Jóźwiak-Niedźwiedzka, Eds. 355-358.

Kuo W., Wang H., Shu C., Su D., 2013. Engineering properties of controlled low strength materials containing waste oyster shells. *Construction and Building Materials* 46.1:128–133.

Lertwattanaruk, P., Makul, N. and Siripattarapravat, C., 2012. Utilization of ground waste seashells in cement mortars for masonry and plastering. *Journal of environmental management* 111:133-141.

Li H., Yang L. and Xie Y. 2015. Effect of fineness on the properties of cement past. *Key Engineering Materials* 629-630.1: 366-370.

Mala, K., Mullick, A. K., Jain, K. K., and Singh, P. K. 2013. Effect of relative levels of mineral admixtures on strength of concrete with ternary cement blend. *International Journal of Concrete Structures and Materials* 7.3:239-249.

Malaiskiene J., Skripkiunas G., Vaiciene M., and Karpova E., 2017. The influence of aggregates type on W/C ratio on the strength and other properties of concrete' *IOP Conference Series: Materials Science and Engineering*, 251.12025:1-10

Marcus V. P. (1960), The Ten Books Architecture. *Cambridge Harvard University Press London*. Morris Hicky Morgan Eds. 376

Martinez-Garcia C., Gonzalez-Fonteboa B., Martinez-Abella F., and Carro-Lopez D., 2017. Performance of mussel shell as aggregate in plain concrete. *Construction and Building Materials* 139.1:570–583.

Memon, S. A., Khan, S., Wahid, I., Shestakova, Y., and Ashraf, M. 2020. Evaluating the effect of calcination and grinding of corn stalk ash on pozzolanic potential for sustainable cement-based materials. *Advances in Materials Science and Engineering* 20.1:1-13.

Mindat.org, 2023. Amassoma, Southern Ijaw, Bayelsa State, Nigeria. Mindat.org and the Hudson Institute of Mineralogy Online Source available at https://www.mindat.org/feature-2350172.html, last visited 6/28/2023

Mo, K. H., Alengaram, U. J., Jumaat, M. Z., Lee, S. C., Goh, W. I., and Yuen, C. W. 2018. Recycling of seashell waste in concrete: A review. *Construction and Building Materials* 162:751-764.

Mohamed M., Yusup S., Maitra S., 2012. Decomposition study of calcium, carbonate in cockle shell. *Journal of Engineering Science and Technology* 7.1:1–10.

Mohammad, W. A. S., Othman, N. H., Ibrahim, M. H. W., Rahim, M. A., Shahidan, S., and Abd R. R. 2017. A review on seashells ash as partial cement replacement. *IOP Conference Series: Materials Science and Engineering* 271.1:1-8

Murthi, P., Poongodi, K., and Gobinath, R. (2020, December). Effects of Corn Cob Ash as Mineral Admixture on Mechanical and Durability Properties of Concrete–A Review. *IOP Conference Series: Materials Science and Engineering* 1006.1:1-14

Ndububa, Emmanuel E. and Nurudeen Yakubu .2015. Effect of Guinea Corn Husk Ash as Partial Replacement for Cement in Concrete' *IOSR Journal of Mechanical and Civil Engineering (IOSR-JMCE)* 12.2:40-45.

Nwankwojike B. N., Onwuka O. S. and Ndukwe E. C. 2014. An Appraisal of Different Brands of Portland Cement in Umuahia Industrial Market, Nigeria. *Journal of Research Information in Civil Engineering* 11.2:577-589

Ofuyatan, O.M., Ede, A.N., Olofinnade, O.M., Oyebisi, S.O., Alayande, T. and Ogundipe, J., 2018. Assessment of strength properties of cassava peel ash-

concrete. *International Journal of Civil Engineering and Technology (IJCIET)*, 9.1:965-974.

Ogbonna, C., Mbadike, E. and Alaneme, G.U., 2020. Characterisation and use of cassava peel ash in concrete production. *Computational Engineering and Physical Modeling* 3.2:12-28.

Olivia, M., and Oktaviani, R. 2017. Properties of concrete containing ground waste cockle and clam seashells. *Procedia Engineering* 171.2017: 658-663.

Olivia, M., Mifshella, A. A., and Darmayanti, L. 2015. Mechanical properties of seashell concrete. *Procedia Engineering* 125.2015:760-764.

Olowe, K.O. and Adebayo, V.B., 2015. Investigation on Palm Kernel Ash as partial cement replacement in high strength concrete. *SSRG International Journal of Civil Engineering (SSRG-IJCE)* 2.4:48-55.

Olutoge, F. A., Nwabueze, S. E., Olawale, S. O. A., and Yabefa, B. E. 2016. Performance of Clam (Egeria Radiata) Shell Ash (CSA) as a Substitute for Cement in Concrete. *International Journal of Recent Development in Engineering and Technology* 5.9:33-38.

Ong, B. P., and Kassim, U. 2019. Performance of concrete incorporating of clam shell as partially replacement of ordinary Portland cement (OPC). *Journal of Advanced Research in Applied Mechanics* 55.1:12-21.

Orji, B., G. E. Igbokwe, C. O. Anagonye, and E. U. Modo. Chemical content of the periwinkle shell and its suitability in thin layer chromatography. *International Journal of Chemistry Studies* 1.2:9-11.

Othman, N. H., Bakar, B. H. A., Don, M. M., and Johari, M. A. M. 2013. Cockle shell ash replacement for cement and filler in concrete. *Malaysian Journal of Civil Engineering* 25.2:201-211.

Oti, J.E., Kinuthia, J.M., Robinson, R. and Davies, P., 2015. The use of palm kernel shell and ash for concrete production. *International Journal of Civil and Environmental Engineering* 9.3:263-270.

Otunyo, A.W. and Okechukwu, B.N., 2017. Performance of concrete with partial replacement of fine aggregates with crushed waste glass. *Nigerian Journal of Technology* 36.2:403-410.

Oyedepo, O. J., Olanitori, L. M., and Akande, S. P. (2015). Performance of coconut shell ash and palm kernel shell ash as partial replacement for cement in concrete. *Journal of building materials and structures*, 2.1:18-24.

Premium Times 2023. Nigeria's GDP growth fell to 3.1% in 2022 – NBS. Online source seen on *https://www.premiumtimesng.com/news/headlines/583431-nigerias-gdp-growth-fell-to-3-1-in-2022-nbs.html* visited 4/15.2023

Qureshi, A.S. and Nawab, A., 2013. The role of engineers in sustainable development. *In Proceedings of the Symposium on Role of Engineers in Economic Development and Policy Formulation*, Lahore, Pakistan 107-114.

Raheem, S.B., Arubike, E.D. and Awogboro, O.S., 2020. Effects of cassava peel ash (CPA) as alternative binder in concrete. *International Journal of Constructive Research in Civil Engineering* 1.2:27-32.

Ranganath B. and Kumari S. G. 2018. An Experimental Study on Acid Resistance of Concrete by using Mineral Admixtures. *International Journal for Research in Applied Science and Engineering Technology (IJRASET)* 6.4:2865-2871.

Sabir, B. B., Wild, S., and Bai, J. 2001. Metakaolin and calcined clays as pozzolans for concrete: a review. *Cement and concrete composites* 23.6:441-454.

Safi, B. Saidi, M. Daoui, A. Bellal A. Mechekak A., and Toumi K. 2015. The use of seashells as a fine aggregate (by sand substitution) in self-compacting mortar (SCM), Construction and Building Materials. 78.2015:430–438.

Salau,M. A., Ikponmwosa, E. E., and Olonode, K. A. 2012. Structural Strength Characteristics of Cement-Cassava Peel Ash Blended Concrete. *Civil and Environmental Research* 2.10:68-78.

Salau M. A. and Osemeke, O. J. 2015. Calcination Effect on the pozzolanicity of metakaolin-concrete. *Physical Science International Journal* 6.2015:131-143.

Sam-Amobi, C., Ekechukwu, O. V., and Chukwuali, C. B. 2019. A preliminary assessment of the energy related carbon emissions associated with hotels in Enugu metropolis Nigeria. *AFRREV STECH: An International Journal of Science and Technology* 8.2:19-30.

Sarah, C. 2014. Comparing Concrete Durability Testing Methods' Smart Concrete. Online source available on https://blog.kryton.com/2014/05/comparing-concrete-durability-testing-methods/. Last visited on 13/11/2017

Schorcht, F., Kourti, I., Scalet, B.M., Roudier, S. and Sancho, L.D., 2013. Best available techniques (BAT) reference document for the production of cement, lime and magnesium oxide. *European Commission Joint Research Centre Institute for Prospective Technological Studies, Luxembour*: 1-506.

Science Nigeria, 2023. Rice Husks Sodium Silicate: Tonic For Wealth Creation. Online Source at https://sciencenigeria.com/rice-husks-sodium-silicate-tonic-for-wealth-creation/#:~:text=Nigeria%20produces%205.04%20million%20tons,of%20which%20are%20environmentally%20hazardous. Visited last on 6/28/2023

Shen, J., Liu, X., Zhu, S., Zhang, H. and Tan, J., 2011. Effects of calcination parameters on the silica phase of original and leached rice husk ash. *Materials Letters* 65.8:1179-1183.

Shetty, M.S. 2005. *Concrete Technology-Theory and Practice*, S. Chand and Company Ltd. Publishing. 17th ed. New Delhi.

Siddique, R. and Khan, M.I., 2011. *Supplementary cementing materials-Metakaolin*. Springer Science & Business Media Eds. Engineering Materials (ENG.MAT.). Chapter 4:175-230

Statista 2023. Production of milled rice in Nigeria from 2010 to 2022. Online at https://www.statista.com/statistics/1134510/production-of-milled-rice-in-

nigeria/₦:~:text=In%202022%2C%20the%20quantity%20of,in%20the%20country%20generally%20increased. Visited on 4/16/2023

Stork, M., Meindertsma, W., Overgaag, M. and Neelis, M., 2014. A Competitive and Efficient Lime Industry: Cornerstone for a Sustainable Europe. *European Lime Association: Brussels, Belgium*. Online source available on https://www.eula.eu/wp-content/uploads/2019/02/A-Competitive-and-Efficient-Lime-Industry-Technical-report-by-Ecofys_0.pdf last visited on 5/14/2023:1-72

Sulaiman T. A. and Aliyu I. 2020. Combined Effect of Rice Husk Ash and Cement Kiln Dust as Cement Replacement Materials in Concrete. *FUDMA Journal of science (FJS)* 4.1:446 – 452

Suwanmaneechot, P., Nochaiya, T. and Julphunthong, P., 2015. Improvement, characterization and use of waste corn cob ash in cement-based materials. *IOP Conference Series: Materials Science and Engineering* 103.1:12-23.

Syed, T.Z. and Vaishali, G.G., 2014. Experimental Investigation of Snail Shell Ash (SSA) as Partial Replacement of Ordinary Portland cement in Concrete. *International Journal of Engineering Research & Technology (IJERT)* 3.10: 1049-1053

Tayeh, B.A., Hasaniyah, M.W., Zeyad, A.M. and Yusuf, M.O., 2019. Properties of concrete containing recycled seashells as cement partial replacement: A review. *Journal of Cleaner Production*, 237.1:1-13

TNO, 2012 Techno-economic evaluation for CO_2 capture in lime production plants, *Netherlands Organisation for Applied Scientific Research (TNO)*, Delft, The Netherlands, June 2012.

Tokeshi, M., Ota, N., and Kawai, T. 2000. A comparative study of morphometry in shell- bearing molluscs. *Journal of Zoology* 251.1:31-38.

Turolla, E., Castaldelli, G., Fano, E. A., and Tamburini, E. 2020. Life cycle assessment (LCA) proves that Manila Clam farming (Ruditapesphilippinarum) is a fully sustainable aquaculture practice and a carbon sink. *Sustainability* 12.13:1-13.

Ubong, D. O. and Godwin E. A., 2017. Assessment of Physico- Chemical Properties of Periwinkle Shell Ash as Partial Replacement for Cement in Concrete. *International Journal of Scientific Engineering and Science* 1.7:33-36.

Umoh, A.A., Olaniyi, A., Babafemi, A.J. and Femi, O.O., 2013. Assessing the mechanical performance of ternary blended cement concrete Incorporating periwinkle shell and bamboo leaf ashes. Civil and Environmental Research, 3(1), pp.26-35.

Umoh, A.A. and Olusola, K.O., 2012. Effect of different sulphate types and concentrations on compressive strength of periwinkle shell ash blended cement concrete. *International Journal of Engineering & Technology IJET-IJENS* 12.5:10-17.

Umoh, A. A. and Ujene, A. O., 2015. Improving the Strength Performance of High-Volume Periwinkle Shell Ash Blended Cement Concrete with Sodium Nitrate as Accelerator. *Journal of Civil Engineering, Science and Technology* 6.2:18-22.

Walker, R. and Pavìa S., 2011. Physical properties and reactivity of pozzolans, and their influence on the properties of lime–pozzolan pastes. *Materials and Structures* 44.2011:1139–1150.

Yu, C., Zhang, Y. and Li, Z., 2021. Study on the particle size distribution characteristics and cementitious activity of different fineness components in cement. *In IOP Conference Series: Earth and Environmental Science*, IOP Publishing Eds., 768.1:1-5.

Zaid, O., Ahmad, J., Siddique, M.S. and Aslam, F., 2021. Effect of incorporation of rice husk ash instead of cement on the performance of steel fibers reinforced concrete. Frontiers in materials, 8.2015:1-14.

Zaid, S. T. and Ghorpade, V. G. 2014. Experimental Investigation of Snail Shell Ash (SSA) as Partial Replacement of Ordinary Portland Cement in Concrete. *International Journal of Engineering Research and Technology (IJERT)* 3.10:1049-1053.

Zhang, M.H. and Malhotra, V.M., 1996. High-performance concrete incorporating rice husk ash as a supplementary cementing material. *ACI Materials Journal* 93.6:629-636.

APPENDICES

Appendix A1: Furnace design with cover, without cover and the sectional view

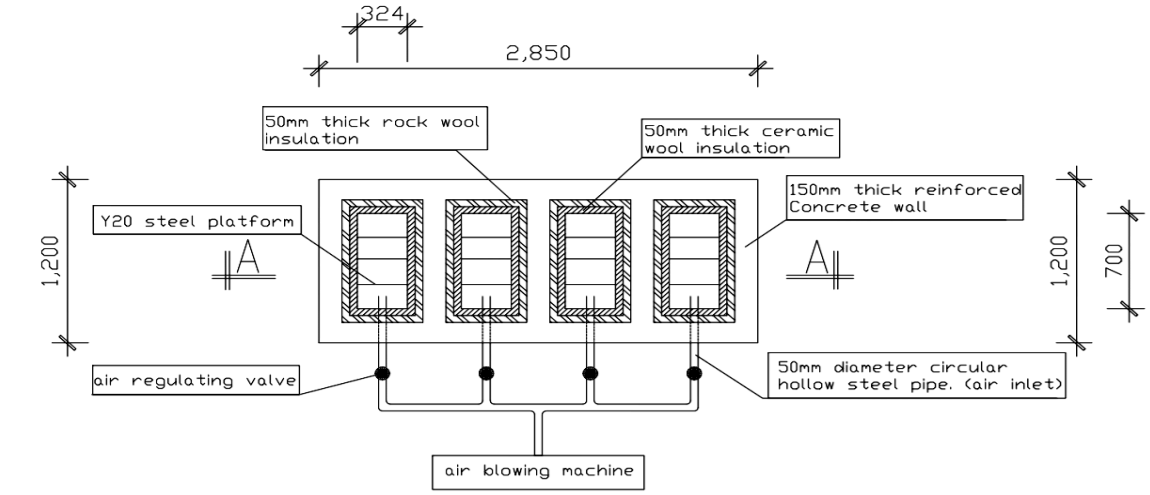

PLAN WITHOUT COVER

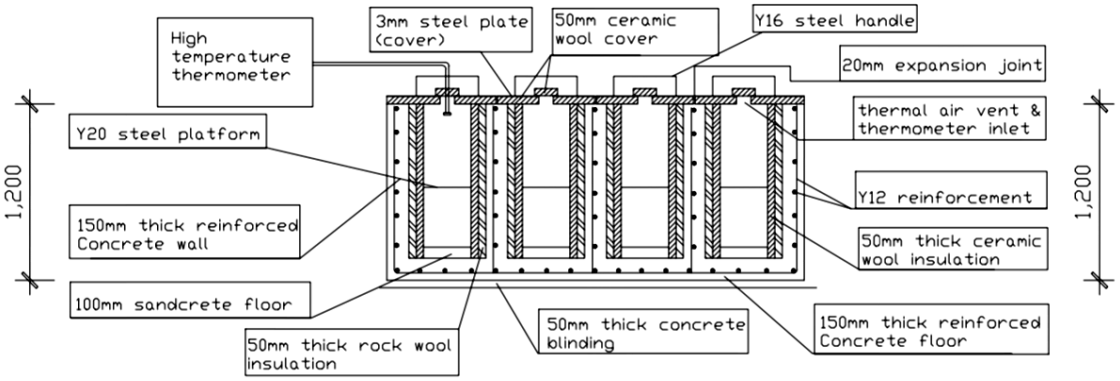

SECTION A–A

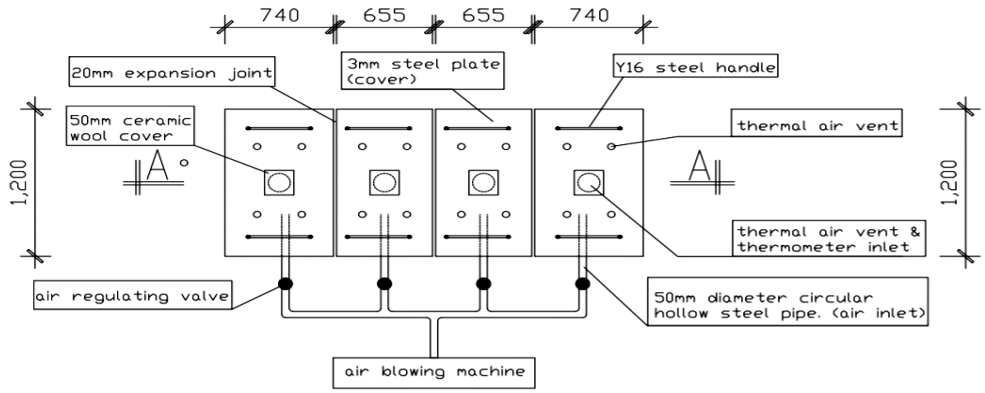

PLAN WITH COVER

Appendix A2: The Grinding Process

Appendix A3: **The Sieving Process**

Appendix A4: **Mould preparation Prior to Concrete Cube production**

Appendix A5: **Concrete Production Ongoing**

Appendix A6: **Concrete slump testing**

Appendix A7: **Concrete casting**

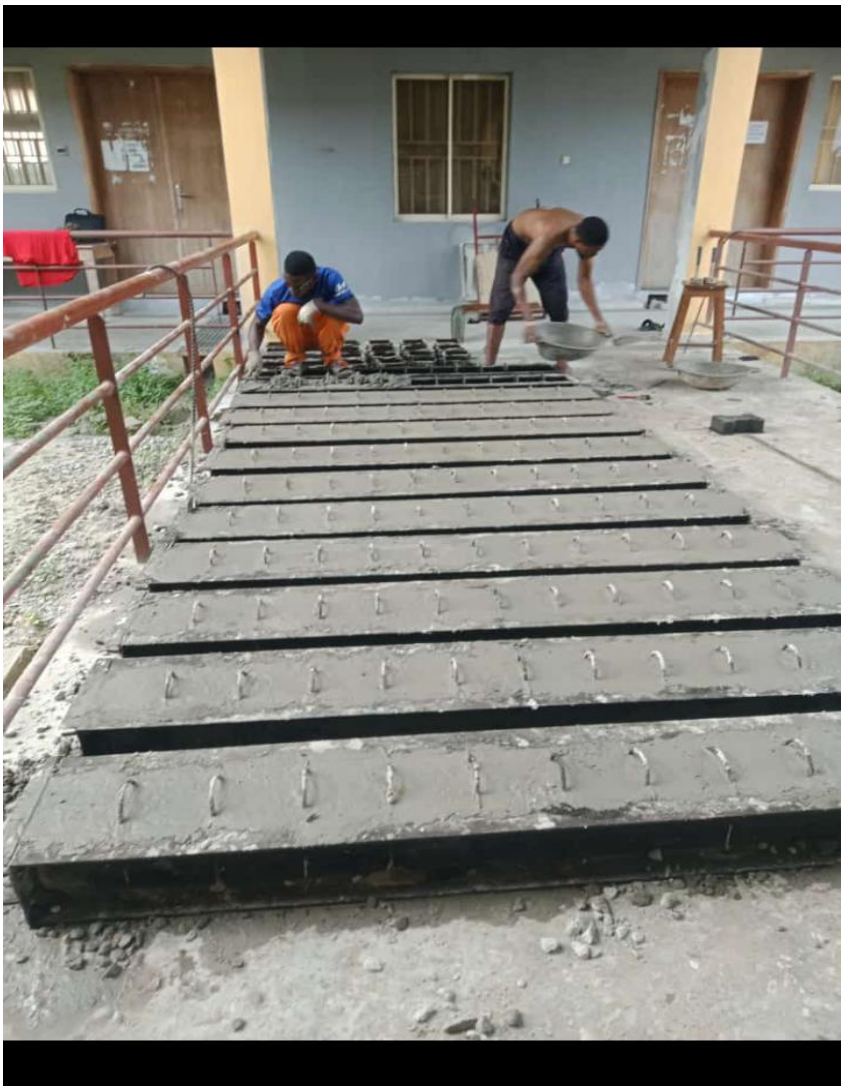

Appendix A8: **Concrete curing**

Appendix A9: Concrete Testing

Appendix B1: **Summary of design method and factors constraints for PSA Pozzolan Concrete data analysis, model development and optimisation**

Design Summary						
File Version	10.0.1.0					
Study Type	Combined		Subtype	Randomized		
Design Type	I-optimal	Point Exchange	Runs	19		
Design Model	Quadratic x Quadratic		Blocks	No Blocks	Build Time (ms)	144.00

Mix Comp.	Units	Type	Min	Max	Mean	Std. Dev.
A: PLC	%	Mixture	50	100	69.4737	15.4466
B: PSA	%	Mixture	0	50	30.5263	15.4466

Factor	Units	Type	Subtype	Min	Max	Mean	Std. Dev.
C: TEMP.	^{o}C	Numeric	Discrete	25	800	417.105	307.098

Appendix B2: **Response Summary for PSA Cement blended concrete Models**

Response	Analysis	Min.	Max.	Mean	Std. Dev.	Ratio	Trans	Model
Comp. Str. (N/mm^2)	Poly.	15.04	27.74	19.58	3.57	1.84	None	Cubic x Linear
WAI (%)	Poly.	1.74	3.83	2.85	0.71	2.20	None	Quadratic x Linear
CISLI (%)	Poly.	-8.06	34.17	17.68	10.86	N/A	None	Quadratic x Quadratic
SISLI (%)	Poly.	-37.58	22.89	-5.49	18.01	N/A	Logit	Linear x Quadratic
SIMLI (%)	Poly.	7.82	9.29	8.74	0.39	1.19	Logit	Cubic x Mean

Appendix B3: **ANOVA Summary for the Compressive Strength of PSA Pozzolan concrete**

Analysis of variance Table [Partial sum of squares - Type III]						
Source	Sum of Squares	Df	Mean Square	F Value	p-value Prob > F	
Model	224.50	6	37.42	103.60	< 0.0001	Significant
[1]Linear Mixture	178.41	1	178.41	494.01	< 0.0001	
AB	15.34	1	15.34	42.46	< 0.0001	
BC	3.56	1	3.56	9.86	0.0085	
ABC	6.55	1	6.55	18.13	0.0011	
AB(A-B)	2.36	1	2.36	6.54	0.0251	
ABC(A-B)	1.19	1	1.19	3.30	0.0943	
Residual	4.33	12	0.36			
Lack of Fit	4.33	11	0.39			
Pure Error	0.000	1	0.000			
Cor Total	228.83	18				
Coefficient of Regression						
Std. Dev.	0.60		R^2	0.9811		
Mean	19.59		Adjusted R^2	0.9716		
C.V. %	3.07		Predicted R^2	0.9584		
PRESS	9.53		Adeq Precision	34.681		
-2 Log Likelihood	25.84		BIC	43.50		
			AICc	44.84		

A = PLC (%), B = PSA (%), C = CALCINATION TEMPERATURE (^oC)

Appendix B4: **The coefficients of the model and Variation Inflated Factors the Compressive strength of PSA cement blended concrete**

Model factors	Coeff.	df	Error	95% CI min	95% CI Max	VIF
A-PLC	27.73	1	0.42	26.80	28.65	2.29
B-PSA	16.28	1	0.30	15.64	16.93	2.15
AB	-8.90	1	1.37	-11.87	-5.92	3.20
BC	1.32	1	0.42	0.40	2.23	2.36
ABC	6.11	1	1.44	2.99	9.24	1.94
AB(A-B)	-7.45	1	2.91	-13.81	-1.10	1.36
ABC(A-B)	6.89	1	3.79	-1.37	15.15	1.37

Appendix B5: **PSA Pozzolan Concrete Optimisation Constraints**

Constraints						
Name	Goal	Lower Limit	Upper Limit	Lower Weight	Upper Weight	Importance
PLC (%)	Minimize	50	100	1	1	3
PSA (%)	maximize	0	50	1	1	3
TEMP. (^{o}C)	Minimize	25	800	1	1	3
COMP. STRENGTH (N/mm^2)	is in range	20.8	27.74	1	1	3
WAI (%)	Minimize	1.74	3.83	1	1	3
CISLI (%)	Minimize	-8.06	34.17	1	1	3
SISLI (%)	Minimize	-37.58	22.89	1	1	3
SIMLI (%)	Minimize	7.82	9.29	1	1	3

Appendix C1: **Summary page of design method and factors constraints for CSA Cement blended concrete data analysis, model development and optimisation**

Design Summary							
File Version	10.0.1.0						
Study Type	Combined		**Subtype**	Randomized			
Design Type	I-optimal	Point Exchange	**Runs**	19			
Design Model	Reduced Quadratic x Quadratic		**Blocks**	No Blocks	**Build Time (ms)**	140.00	

Mixture Components	**A**	**B**
Process Factors		**C**

Comp.	**Name**	**Units**	**Type**	**Min**	**Max**	**Coded**	**Values**	**Mean**	**Std. Dev.**
A	PLC	%	Mixture	50	100	0.000=50	1.000=100	69.4737	15.4466
B	CSA	%	Mixture	0	50	0.000=0	1.000=50	30.5263	15.4466
				Total =	100.00	**L_Pseudo Coding**			

Factor	**Name**	**Units**	**Type**	**Subtype**	**Min**	**Max**	**Coded**	**Values**	**Mean**	**Std. Dev.**
C	TEMP	Oc	Numeric	Discrete	25	800	-1.000=25	1.000=800	417.105	307.098

Response	**Name**	**Units**	**Analy.**	**Min.**	**Max**	**Mean**	**Std. Dev.**	**Ratio**	**Trans**	**Model**
R1	Comp. Strength	MPa	Poly.	14.8	27.74	19.4626	3.70784	1.87432	None	RCubic x Linear
R2	WAI	%	Poly.	1.22	4.45	2.99684	0.832253	3.64754	Power	RQuadratic x Mean
R3	CISLI	%	Poly.	0.44	31.44	13.9068	10.3517	71.4545	None	(Mean x Mean + User Added Terms)
R4	SISLI	%	Poly.	-36.27	16.41	-7.96421	16.8279	N/A	Logit	RLinear x Quadratic
R5	SIMLI	%	Poly.	7.98	9.28	8.82263	0.386492	1.16291	Logit	Cubic x Mean

Appendix C2: **ANOVA Table for the Compressive Strength of CSA Pozzolan Concrete**

ANOVA for Combined Cubic x Linear model						
Mixture	Components	A B				
Process	Factors	C				
Analysis of variance **Table** [Partial sum of squares - Type III]						
Source	Sum of Squares	Df	Mean Square	F Value	p-value Prob > F	
Model	245.47	6	40.91	245.84	< 0.0001	Significant
[1]Linear Mixture	200.06	1	200.06	1202.14	< 0.0001	
AB	11.01	1	11.01	66.18	< 0.0001	
BC	2.14	1	2.14	12.83	0.0038	
ABC	9.14	1	9.14	54.63	< 0.0001	
AB(A-B)	4.12	1	4.12	24.73	0.0003	
ABC(A-B)	0.63	1	0.63	3.78	0.0756	
Residual	2.00	12	0.17			
Lack of Fit	2.00	11	0.18			
Pure Error	0.000	1	0.000			
Cor Total	247.46	18				

Appendix C3: Regression coefficient for the Compressive Strength of CSA Cement blended concrete

Std. Dev.	0.41	R-Squared	0.9919
Mean	19.46	Adj R-Squared	0.9879
C.V. %	2.10	Pred R-Squared	0.9817
PRESS	4.54	Adeq Precision	53.001
-2 Log Likelihood	11.12	BIC	28.78
		AICc	30.12

Appendix C4: **The coefficients of the model and The collinearity effect for the Compressive Strength of CSA cement blended concrete.**

Component	Coefficient Estimate	df	Standard Error	95% CI Low	95% CI High	VIF
A-PLC	27.76	1	0.29	27.13	28.39	2.29
B-CSA	15.66	1	0.20	15.22	16.10	2.15
AB	-7.54	1	0.93	-9.56	-5.52	3.20
BC	1.02	1	0.28	0.40	1.64	2.36
ABC	7.22	1	0.97	5.10	9.35	1.94
AB(A-B)	-9.84	1	1.98	-14.15	-5.53	1.36
ABC(A-B)	5.01	1	2.57	-0.60	10.61	1.37

Appendix C5: **Constraints for the optimisation of factors and responses for CSA cement blended concrete**

Constraints						
Name	Goal	Lower Limit	Upper Limit	Lower Weight	Upper Weight	Importance
A:PLC	minimize	50	100	1	1	3
B:CSA	maximize	0	50	1	1	3
C:TEMP	minimize	25	800	1	1	3
Comp. Strength	is in range	20.8	27.74	1	1	3
WAI	minimize	1.22	4.45	1	1	3
CISLI	minimize	0.44	31.44	1	1	3
SISLI	minimize	0	16.41	1	1	3
SIMLI	minimize	7.98	9.28	1	1	3

Appendix D1: **Summary page of design method and factors constraints for HAP concrete data analysis, model development and optimisation**

Design Summary							
File Version	10.0.1.0						
Study Type	Combined		**Subtype**	Randomized			
Design Type	I-optimal	Point Exchange	**Runs**	28			
Design Model	Quadratic x Quadratic		**Blocks**	No Blocks	**Build Time (ms)**	468.00	

Component	**Name**	**Units**	**Type**	**Min.**	**Max.**	**Mean**	**Std. Dev.**
A	PLC	%	Mixture	50	100	64.2857	15.0132
B	PSA	%	Mixture	0	50	18	16.6311
C	CSA	%	Mixture	0	50	17.7143	16.5929

Factor	**Name**	**Units**	**Type**	**Subtype**	**Min**	**Max**	**Mean**	**Std. Dev.**
D	Calc. Temp	^{o}C	Num.	Discrete	25	800	406.25	284.363

Response	**Units**	**Analysis**	**Min**	**Max**	**Mean**	**Std. Dev.**	**Ratio**	**Trans**	**Model**
Comp. Strength	MPa	Poly.	14.8	27.74	19.22	3.10	1.87	None	Cubic x Linear
WAI	%	Poly.	1.22	19.29	4.89	5.14	15.81	None	Cubic x Mean
CISLI	%	Poly.	-8.06	31.44	15.46	9.43	N/A	None	Quadratic x Quadratic
SISLI	%	Poly.	-30.99	20.51	2.38	12.71	N/A	Logit	Quadratic x Quadratic
SIMLI	%	PolY.	7.89	10.24	8.74	0.55	1.29	None	Quadratic x Linear

Appendix D 2: **ANOVA Table for the Compressive Strength of HAP cement Concrete**

Mix. Process	Factors	A B C D				
Source	Summed Squares	Df	Average Square	F Val.	p-value Prob > F	
Model	259.19	17	15.25	159.56	< 0.0001	significant
[1]Linear Mixture	178.16	2	89.08	932.30	< 0.0001	
AB	12.79	1	12.79	133.90	< 0.0001	
AC	10.67	1	10.67	111.62	< 0.0001	
BC	4.08	1	4.08	42.65	< 0.0001	
BD	4.01	1	4.01	41.97	< 0.0001	
CD	1.53	1	1.53	16.04	0.0025	
ABC	7.40	1	7.40	77.45	< 0.0001	
ABD	0.89	1	0.89	9.34	0.0121	
ACD	7.43	1	7.43	77.73	< 0.0001	
BCD	0.21	1	0.21	2.23	0.1663	
AB(A-B)	6.13	1	6.13	64.19	< 0.0001	
AC(A-C)	6.60	1	6.60	69.07	< 0.0001	
BC(B-C)	4.07	1	4.07	42.62	< 0.0001	
ABD(A-B)	0.63	1	0.63	6.62	0.0277	
ACD(A-C)	7.66	1	7.66	80.17	< 0.0001	
BCD(B-C)	4.65	1	4.65	48.65	< 0.0001	
Residual	0.96	10	0.096			
Cor Total	260.14	27				

Appendix D3: **Regression coefficient for the compressive strength of HAP cement concrete**

Std. Dev.	0.31	R-Squared	0.9963
Mean	19.22	Adj R-Squared	0.9901
C.V. %	1.61	Pred R-Squared	0.9162
PRESS	21.80	Adeq Precision	52.426
-2 Log Likelihood	-15.12	BIC	41.53
		AICc	80.08

Appendix D4: **The coefficients of the model and the collinearity effect for the compressive strength of HAP cement concrete**

Component	Coefficient Estimate	df	Standard Error	95% CI Low	95% CI High	VIF
A-PLC	27.74	1	0.22	27.25	28.23	2.36
B-PSA	16.34	1	0.18	15.95	16.74	2.20
C-CSA	15.61	1	0.18	15.22	16.01	2.15
AB	-11.03	1	0.95	-13.15	-8.91	2.91
AC	-11.22	1	1.06	-13.59	-8.86	3.56
BC	5.21	1	0.80	3.44	6.99	2.47
BD	1.41	1	0.22	0.92	1.89	1.79
CD	0.87	1	0.22	0.39	1.35	1.93
ABC	55.33	1	6.29	41.32	69.34	2.19
ABD	-4.58	1	1.50	-7.91	-1.24	2.44
ACD	-11.61	1	1.32	-14.54	-8.67	2.69
BCD	-1.45	1	0.97	-3.61	0.71	1.63
AB(A-B)	-28.20	1	3.52	-36.05	-20.36	2.99
AC(A-C)	-21.19	1	2.55	-26.87	-15.51	1.52
BC(B-C)	39.61	1	6.07	26.09	53.13	1.16
ABD(A-B)	10.33	1	4.01	1.39	19.28	2.11
ACD(A-C)	-30.32	1	3.39	-37.86	-22.77	1.71
BCD(B-C)	86.42	1	12.39	58.81	114.03	1.04

Appendix D5: **Constraints for the optimisation of factors and responses for the compressive strength of HAP cement concrete**

Constraints						
Name	Goal	Lower Limit	Upper Limit	Lower Weight	Upper Weight	Importance
A:PLC	minimize	50	100	1	1	3
B:PSA	maximize	0	50	1	1	3
C:CSA	maximize	0	50	1	1	3
D:Calc. Temp	is in range	25	800	1	1	3
Comp. Strength	is in range	20.8	27.74	1	1	3
WAI	minimize	1.22	19.29	1	1	3
CISLI	minimize	-8.06	31.44	1	1	3
SISLI	minimize	0	20.51	1	1	3
SIMLI	minimize	7.89	10.24	1	1	3

Appendix E1: **Summary page of design method and factors constraints for data analysis, model development and optimisation for the flexural strength of PSA cement blended concrete**

Design Summary

File Version	10.0.1.0						
Study Type	Combined		**Subtype**	Randomized			
Design Type	I-optimal	Point Exchange	**Runs**	19			
Design Model	Quadratic x Quadratic		**Blocks**	No Blocks	**Build Time (ms)**	61.00	

Mixture Components A B
Process Factors C

Component	Name	Units	Type	Min	Max	Coded	Values	Mean	Std. Dev.
A	PLC	%	Mixture	50	100	0.000=50	1.000=100	66.8421	20.8307
B	PSA	%	Mixture	0	50	0.000=0	1.000=50	33.1579	20.8307
				Total =	100.00	**L_Pseudo Coding**			

Factor	Name	Units	Type	Subtype	Min	Max	Coded	Values	Mean	Std. Dev.
C	TEMP	oC	Numeric	Discrete	25	800	-1.000=25	1.000=800	415.789	294.181

Response	Name	Units	Analysis	Min.	Max.	Mean	Std. Dev.	Ratio	Trans	Model
R1	Flexural strength	N/mm2	Poly.	2.08	5.29	3.13526	1.34169	2.54327	None	Quadratic x Quadratic

Appendix E2: **ANOVA Table for the flexural strength of PSA cement concrete**

ANOVA for Combined Quadratic x Quadratic model

***** Mixture Component Coding is L_Pseudo. *****

Mixture Components A B

Process Factors C

Analysis of variance table [Partial sum of squares - Type III]

Source	**Sum of Squares**	**df**	**Mean Square**	**F Value**	**p-value Prob > F**	
Model	32.36	8	4.04	943.50	< 0.0001	significant
[1]Linear Mixture	*31.17*	*1*	*31.17*	*7270.70*	*< 0.0001*	
AB	*0.026*	*1*	*0.026*	*6.05*	*0.0337*	
AC	*0.000*	*1*	*0.000*	*0.000*	*1.0000*	
BC	*0.019*	*1*	*0.019*	*4.46*	*0.0609*	
ABC	*0.14*	*1*	*0.14*	*32.81*	*0.0002*	
AC^2	*0.000*	*1*	*0.000*	*0.000*	*1.0000*	
BC^2	*0.012*	*1*	*0.012*	*2.87*	*0.1210*	
ABC^2	*0.072*	*1*	*0.072*	*16.90*	*0.0021*	
Residual	0.043	10	4.287E-003			
Lack of Fit	*0.043*	*5*	*8.574E-003*			
Pure Error	*0.000*	*5*	*0.000*			
Cor Total	32.40	18				

Appendix E3: **Regression coefficient for the flexural strength of PSA cement concrete**

Std. Dev.	0.065	R-Squared	0.9987
Mean	3.14	Adj R-Squared	0.9976
C.V. %	2.09	Pred R-Squared	0.9956
PRESS	0.14	Adeq Precision	72.002
-2 Log Likelihood	-61.87	BIC	-38.31
		AICc	-31.47

Appendix E4: **The coefficients of the model and the collinearity effect for the Flexural strength of PSA cement concrete**

Component	Coefficient Estimate	df	Standard Error	95% CI Low	95% CI High	VIF
A-PLC	5.29	1	0.042	5.20	5.38	2.22
B-PSA	2.28	1	0.038	2.20	2.37	3.81
AB	-0.85	1	0.35	-1.63	-0.080	5.04
AC	0.000	1	0.044	-0.098	0.098	1.12
BC	0.077	1	0.036	-4.237E-003	0.16	1.99
ABC	1.55	1	0.27	0.95	2.15	1.98
AC^2	0.000	1	0.065	-0.14	0.14	2.20
BC^2	-0.098	1	0.058	-0.23	0.031	4.52
ABC^2	-1.97	1	0.48	-3.03	-0.90	5.67

Appendix E 5: **Constraints for the optimisation of factors and responses for the flexural strength of PSA cement concrete**

Constraints						
Name	Goal	Lower Limit	Upper Limit	Lower Weight	Upper Weight	Importance
A:PLC	minimize	50	100	1	1	3
B:PSA	maximize	0	50	1	1	3
C:TEMP	is in range	25	800	1	1	3
Flexural strength	maximize	2.08	5.29	1	1	3

Appendix F1: **Summary page of design method and factors constraints for data analysis, model development and optimisation for the flexural strength of CSA cement blended concrete**

Design Summary

File Version	10.0.1.0						
Study Type	Combined		**Subtype**	Randomized			
Design Type	I-optimal	Point Exchange	**Runs**	19			
Design Model	Quadratic x Quadratic		**Blocks**	No Blocks	**Build Time (ms)**	57.00	

Mixture Components A B
Process Factors C

Component	Name	Units	Type	Min	Max	Coded	Values	Mean	Std. Dev.
A	PLC	%	Mixture	50	100	0.000=50	1.000=100	64.7368	19.2551
B	CSA	%	Mixture	0	50	0.000=0	1.000=50	35.2632	19.2551
				Total =	100.00	**L_Pseudo Coding**			

Factor	Name	Units	Type	Subtype	Min	Max	Coded	Values	Mean	Std. Dev.
C	TEMP	oC	Numeric	Discrete	25	800	-1.000=25	1.000=800	326.316	303.85

Name	Units	Analysis	Min	Max	Mean	Std. Dev.	Ratio	Trans	Model
Flexural strength	N/mm2	Polynomial	2.05	5.35	3.03263	1.21319	2.60976	None	Linear x Mean

Appendix F 2: **ANOVA Table for the flexural strength of CSA cement concrete**

Mixture Process	**Factors**	**A B**	**C**			
Source	**Summed Squares**	**df**	**Average Square**	**F Value**	**p-value Prob > F**	
Model	25.64	1	25.64	511.50	< 0.0001	significant
[1]Linear Mixture	*25.64*	*1*	*25.64*	*511.50*	*< 0.0001*	
Residual	0.85	17	0.050			
Lack of Fit	*0.80*	*7*	*0.11*	*24.11*	*< 0.0001*	*significant*
Pure Error	*0.048*	*10*	*4.767E-003*			
Cor Total	26.49	18				

Appendix F 3: **Regression coefficient for the flexural strength of CSA cement concrete**

Std. Dev.	0.22	R-Squared	0.9678
Mean	3.03	Adj R-Squared	0.9659
C.V. %	7.38	Pred R-Squared	0.9626
PRESS	0.99	Adeq Precision	42.665
-2 Log Likelihood	-5.06	BIC	-2.12
		AICc	-2.83

Appendix F4: **The coefficients of the model and the collinearity effect for the Flexural strength of CSA cement concrete**

Component	Coefficient Estimate	Df	Standard Error	95% CI Low	95% CI High	VIF
A-PLC	5.22	1	0.11	4.99	5.45	1.03
B-CSA	2.12	1	0.065	1.98	2.26	1.03

Appendix F5: **Constraints for the optimisation of factors and responses for the flexural strength of CSA cement concrete**

Constraints

Name	Goal	Lower Limit	Upper Limit	Lower Weight	Upper Weight	Importance
A:PLC	minimize	50	100	1	1	3
B:CSA	maximize	0	50	1	1	3
C:TEMP	is target = 412.5	25	800	1	1	3
Flexural strength	maximize	2.05	5.35	1	1	3

Appendix G 1: **Summary page of design method and factors constraints for data analysis, model development and optimisation for the flexural strength of HAP cement blended concrete**

Design Summary							
File Version	10.0.1.0						
Study Type	Combined		**Subtype**	Randomized			
Design Type	I-optimal	Point Exchange	**Runs**	28			
Design Model	Quadratic x Quadratic		**Blocks**	No Blocks	**Build Time (ms)**	350.00	

Mixture Components A B C
Process Factors D

Component	**Name**	**Units**	**Type**	**Min.**	**Max.**	**Coded**	**Values**	**Mean**	**Std. Dev.**
A	PLC	%	Mixture	50	100	0.000=50	1.000=100	61.4286	16.7142
B	PSA	%	Mixture	0	50	0.000=0	1.000=50	19.5357	15.3345
C	CSA	%	Mixture	0	50	0.000=0	1.000=50	19.0357	15.4308
				Total =	100.00	**L_Pseudo Coding**			

Factor	**Name**	**Units**	**Type**	**Subtype**	**Min**	**Max**	**Coded**	**Values**	**Mean**	**Std. Dev.**
D	Temp.	^{o}C	Numeric	Discrete	25	800	-1.000=25	1.000=800	426.786	276.463

Name	**Units**	**Obs**	**Analysis**	**Min**	**Max**	**Mean**	**Std. Dev.**	**Ratio**	**Trans**	**Model**
Flexural Strength	N/mm2	28	Polynomial	1.52	5.29	2.95429	1.06673	3.48026	None	Linear x Linear

Appendix G2: **ANOVA Table for the flexural strength of HAP cement blended concrete**

ANOVA for Combined Linear x Linear model

***** Mixture Component Coding is L_Pseudo. *****

Mixture Factors A B C D

Process

Source	**Summed Squares**	**df**	**Average Square**	**F Value**	**p-value Prob > F**	
Model	29.66	5	5.93	122.41	< 0.0001	significant
[1]Linear Mixture	*29.07*	*2*	*14.53*	*299.94*	*< 0.0001*	
AD	*8.837E-003*	*1*	*8.837E-003*	*0.18*	*0.6735*	
BD	*0.22*	*1*	*0.22*	*4.52*	*0.0450*	
CD	*0.083*	*1*	*0.083*	*1.71*	*0.2041*	
Residual	1.07	22	0.048			
Lack of Fit	*1.07*	*21*	*0.051*			
Pure Error	*0.000*	*1*	*0.000*			
Cor Total	30.72	27				

Appendix G3: **Regression coefficient for the flexural strength of HAP cement blended concrete**

Std. Dev.	0.22	R-Squared	0.9653
Mean	2.95	Adj R-Squared	0.9574
C.V. %	7.45	Pred R-Squared	0.9406
PRESS	1.83	Adeq Precision	34.035
-2 Log Likelihood	-12.05	BIC	4.61
		AICc	0.68

Appendix G4: **The coefficients of the model and the collinearity effect for the Flexural strength of HAP cement blended concrete**

Component	Coefficient Estimate	Df	Standard Error	95% CI Low	95% CI High	VIF
A-PLC	5.35	1	0.11	5.12	5.58	1.13
B-PSA	2.22	1	0.098	2.02	2.43	1.35
C-CSA	2.23	1	0.10	2.02	2.44	1.43
AD	0.055	1	0.13	-0.21	0.32	1.10
BD	0.28	1	0.13	6.898E-003	0.56	1.31
CD	0.21	1	0.16	-0.12	0.53	1.40

Appendix G5: **Constraints for the optimisation of factors and responses for the flexural strength of HAP cement blended concrete**

Constraints

Name	Goal	Lower Limit	Upper Limit	Lower Weight	Upper Weight	Importance
A:PLC	minimize	50	100	1	1	3
B:PSA	is in range	0	50	1	1	3
C:CSA	is in range	0	50	1	1	3
D:Calcination Temperature	is in range	25	800	1	1	3
Flexural Strength	maximize	1.52	5.29	1	1	3

Appendix H1: **ANOVA Table for the water absorption index of PSA cement Blended concrete**

Source	Sum of Squares	Df	Mean Square	F Value	p-value Prob > F	
Model	7.90	4	1.98	26.13	< 0.0001	Significant
[1]Linear Mixture	4.24	1	4.24	56.07	< 0.0001	
AB	0.037	1	0.037	0.50	0.4929	
BC	0.18	1	0.18	2.41	0.1431	
ABC	1.07	1	1.07	14.15	0.0021	
Residual	1.06	14	0.076			
Lack of Fit	1.06	13	0.081			
Pure Error	0.000	1	0.000			
Cor Total	8.96	18				

Appendix H2: **Regression coefficient for the water absorption index of PSA cement blended concrete**

Coefficient of Regression			
Std. Dev.	0.27	R^2	0.8819
Mean	2.85	R^2 Adjusted	0.8481
C.V. %	9.66	R^2 Predicted	0.8057
PRESS	1.74	Adeq. Precision	14.108
-2 Log Likelihood	-0.94	BIC	10.83
		AICc	9.91

Appendix H3: **The coefficients of the model and the collinearity effect for the water absorption index of PSA cement blended concrete**

Factora	Coeff. Esti.	df	Std Error	95% CI lower	95% CI Upper	VIF
A-PLC	1.99	1	0.19	1.58	2.39	2.15
B-PSA	3.52	1	0.13	3.25	3.79	1.84
AB	-0.44	1	0.62	-1.77	0.89	3.16
BC	-0.27	1	0.17	-0.64	0.10	1.93
ABC	-2.47	1	0.66	-3.87	-1.06	1.93

Appendix I1: **ANOVA Table for the water absorption index of CSA cement Blended concrete**

Mixture	Components	A B				
Process	Factors	C				
Analysis of variance Table [Partial sum of squares - Type III]						
Source	Sum of Squares	Df	Mean Square	F Value	p-value Prob > F	
Model	90.79	2	45.39	32.78	< 0.0001	significant
[1]Linear Mixture	83.85	1	83.85	60.55	< 0.0001	
AB	6.94	1	6.94	5.01	0.0397	
Residual	22.16	16	1.38			
Lack of Fit	22.16	15	1.48			
Pure Error	0.000	1	0.000			
Cor Total	112.95	18				

Appendix I2: Regression coefficient for the water absorption index of CSA cement blended concrete

Std. Dev.	1.18	R-Squared	0.8038
Mean	6.00	Adj R-Squared	0.7793
C.V. %	19.62	Pred R-Squared	0.7438
PRESS	28.93	Adeq Precision	13.894

Appendix I3: **The coefficients of the model and the collinearity effect for the water absorption index of CSA cement blended concrete**

Component	Coefficient Estimate	df	Standard Error	95% CI Low	95% CI High	VIF
A-PLC	2.91	1	0.81	1.20	4.61	2.15
B-CSA	9.40	1	0.54	8.26	10.54	1.84
AB	-5.94	1	2.65	-11.57	-0.32	3.16

Appendix J1: **ANOVA Table for the water absorption index of HAP cement blended concrete**

Mix. Process	Factors	A B C D				
Source	Summed Squares	Df	Average Square	F Value	p-value Prob > F	
Model	607.87	5	121.57	25.69	< 0.0001	significant
[1]Linear Mixture	62.60	2	31.30	6.61	0.0056	
AB	218.43	1	218.43	46.16	< 0.0001	
BC	0.97	1	0.97	0.21	0.6545	
AB(A-B)	389.07	1	389.07	82.22	< 0.0001	
Residual	104.11	22	4.73			
Cor Total	711.97	27				

Appendix J2: **Regression coefficient for the water absorption index of HAP cement blended concrete**

Coefficient of Regression

Std. Dev.	2.18	R-Squared	0.8538
Mean	4.89	Adj R-Squared	0.8205
C.V. %	44.47	Pred R-Squared	0.6616
PRESS	240.91	Adeq Precision	22.389
-2 Log Likelihood	116.23	BIC	132.89
		AICc	128.96

Appendix J3: **The coefficients of the model and the collinearity effect for the water absorption index of HAP cement blended concrete**

Component	Coefficient Estimate	Df	Standard Error	95% CI Low	95% CI High	VIF
A-PLC	2.25	1	1.29	-0.42	4.61	1.65
B-PSA	4.15	1	1.24	1.59	6.72	2.14
C-CSA	3.81	1	1.05	1.64	5.99	1.51
AB	38.33	1	5.64	26.63	50.03	2.06
BC	-2.18	1	4.81	-12.17	7.80	1.81
AB(A-B)	140.57	1	15.50	108.42	172.72	1.17

Appendix K1: **ANOVA Table for the chloride induced strength loss index of PSA cement blended concrete**

Mix. Process	Factors	A B C				
Source	Summed Squares	df	Average Square	F Value	p-value Prob > F	
Model	1740.14	4	435.03	15.88	< 0.0001	Significant
[1]Linear Mixture	5.82	1	5.82	0.21	0.6519	
AB	1162.70	1	1162.70	42.44	< 0.0001	
ABC	451.43	1	451.43	16.48	0.0012	
ABC^2	982.65	1	982.65	35.87	< 0.0001	
Residual	383.58	14	27.40			
Lack of Fit	383.58	13	29.51			
Pure Error	0.000	1	0.000			
Cor Total	2123.72	18				

Appendix K2: **Regression coefficient for the CISLI of PSA cement blended concrete**

Coefficient of Regression			
Std. Dev.	5.23	R-Squared	0.8194
Mean	17.68	Adj R-Squared	0.7678
C.V. %	29.61	Pred R-Squared	0.7092
PRESS	617.65	Adeq Precision	12.005
-2 Log Likelihood	111.02	BIC	122.79
		AICc	121.87

Appendix K3: **The coefficients of the model and the collinearity on CISLI of PSA cement blended concrete**

Component	Coeff. Estimate	Df	Std Error	95% CI Lower	95% CI Upper	VIF
A-PLC	25.60	1	3.58	17.92	33.29	2.16
B-PSA	22.71	1	2.39	17.58	27.84	1.84
AB	-94.69	1	14.58	-126.27	-63.72	4.82
ABC	36.52	1	9.00	17.22	55.82	1.00
ABC^2	94.31	1	15.75	60.53	128.08	2.69

Appendix L1: **ANOVA Table for the CISLI of CSA cement blended concrete**

Mix. Process	Factors	A B	C			
Source	Summed Squares	df	Average Square	F Value	p-value Prob > F	
Model	1517.50	2	758.75	29.51	< 0.0001	Significant
C-TEMP	*144.38*	*1*	*144.38*	*5.62*	*0.0307*	
C^2	*1355.31*	*1*	*1355.31*	*52.72*	*< 0.0001*	
Residual	411.35	16	25.71			
Lack of Fit	*411.35*	*15*	*27.42*			
Pure Error	*0.000*	*1*	*0.000*			
Cor Total	1928.85	18				

Appendix L2: **Regression coefficient for the CISLI of CSA cement blended concrete**

Regression Coefficients			
Deviation (STD)	5.07	R-Squared	0.7867
Average	13.91	R-Squared (Adj)	0.7601
Variation Coeff. (%)	36.46	R-Squared (Pred)	0.7095

Appendix L3: **The coefficients of the model and its collinearity on the CISLI of CSA cement blended concrete**

Component	Coefficient Estimate	Df	Standard Error	95% CI Low	95% CI High	VIF
Intercept	2.42	1	1.97	-1.75	6.60	
C-TEMP	-3.57	1	1.51	-6.77	-0.38	1.00
C^2	19.37	1	2.67	13.71	25.02	1.00

Appendix M1: **ANOVA Table for the CISLI of HAP cement blended concrete**

Mix. Process	Factors	A B C	D			
Source	Summed Squares	Df	Average Square	F Value	p-value Prob > F	
Model	1831.64	8	228.96	7.65	0.0001	significant
[1]Linear Mixture	21.37	2	10.69	0.36	0.7043	
AB	814.51	1	814.51	27.22	< 0.0001	
AC	135.38	1	135.38	4.52	0.0467	
CD	107.75	1	107.75	3.60	0.0730	
CD^2	89.11	1	89.11	2.98	0.1006	
ABD^2	291.19	1	291.19	9.73	0.0056	
ACD^2	232.53	1	232.53	7.77	0.0117	
Residual	568.48	19	29.92			
Cor Total	2400.13	27				

Appendix M2: **Regression coefficient for the CISLI of HAP cement blended concrete**

Regression Coefficient

Deviation (STD)	5.47	R-Squared	0.7631
Average	15.46	R-Squared (Adj)	0.6634
Variation Coef. (%)	35.38	R-Squared (Pred)	0.5397
PRESS	1104.76	Precision (Adeq)	8.563

Appendix M3: **The coefficients of the model and its collinearity on the CISLI of HAP cement blended concrete**

Mix. Process	Factors	A B C D				
Source	Summed Squares	Df	Average Square	F Value	p-value Prob > F	
Model	1831.64	8	228.96	7.65	0.0001	Significant
[1]Linear Mixture	21.37	2	10.69	0.36	0.7043	
AB	814.51	1	814.51	27.22	< 0.0001	
AC	135.38	1	135.38	4.52	0.0467	
CD	107.75	1	107.75	3.60	0.0730	
CD^2	89.11	1	89.11	2.98	0.1006	
ABD^2	291.19	1	291.19	9.73	0.0056	
ACD^2	232.53	1	232.53	7.77	0.0117	
Residual	568.48	19	29.92			
Cor Total	2400.13	27				

Appendix N1: **ANOVA Table for SISLI of PSA cement blended concrete**

Mix. Process	**Comp. Fact.**	**A B C**				
Source	**Summed Squares**	**Df**	**Average Square**	**F Value**	**p-value Prob > F**	
Model	1.33	4	0.33	10.49	0.0004	Significant
[1]Linear Mixture	*0.028*	*1*	*0.028*	*0.88*	*0.3654*	
BC	*0.14*	*1*	*0.14*	*4.58*	*0.0505*	
AC^2	*1.05*	*1*	*1.05*	*33.29*	*< 0.0001*	
BC^2	*0.58*	*1*	*0.58*	*18.43*	*0.0007*	
Residual	0.44	14	0.032			
Lack of Fit	*0.44*	*13*	*0.034*			
Pure Error	*0.000*	*1*	*0.000*			
Cor Total	1.77	18				

Appendix N2: **Regression coefficient for SISLI of PSA cement blended concrete**

Regression Coefficients

Std. Dev.	0.18	R-Squared	0.7498
Mean	0.84	R-Squared (Adj)	0.6783
C.V. %	21.17	R-Squared (Pred)	0.6171
PRESS	0.68	Precision (Adeq)	9.144

Appendix N3: **The coefficients of the model and its collinearity on the SISLI of PSA cement blended concrete**

Comp.	Coeff. Estimate	df	Std Error	95% CI Lower	95% CI Higher	VIF
A-PLC	-0.16	1	0.21	-0.61	0.29	6.31
B-PSA	1.24	1	0.11	1.00	1.48	3.49
AB	0.17	1	0.081	-4.356E-004	0.35	1.00
ABC	1.39	1	0.24	0.87	1.91	5.84
ABC^2	-0.64	1	0.15	-0.95	-0.32	3.08

Appendix O1: **ANOVA Table for the SISLI of CSA cement blended concrete**

Mix. Process	Comp. Factors	A B C				
Source	Summed Squares	df	Average Square	F Value	p-value Prob > F	
Model	9.41	5	1.88	10.52	0.0003	Significant
[1]Linear Mixture	*0.043*	*1*	*0.043*	*0.24*	*0.6314*	
AC	*4.042E-003*	*1*	*4.042E-003*	*0.023*	*0.8828*	
BC	*0.057*	*1*	*0.057*	*0.32*	*0.5822*	
AC^2	*6.71*	*1*	*6.71*	*37.51*	*< 0.0001*	
BC^2	*0.093*	*1*	*0.093*	*0.52*	*0.4827*	
Residual	2.33	13	0.18			
Lack of Fit	*2.33*	*12*	*0.19*			
Pure Error	*0.000*	*1*	*0.000*			
Cor Total	11.74	18				

Appendix O2: **Regression coefficient for the SISLI of CSA cement blended concrete**

Regression Coefficients

Std. Dev.	0.42	R-Squared	0.8018
Mean	-2.27	Adj R-Squared	0.7256
C.V. %	18.65	Pred R-Squared	0.6260
PRESS	4.39	Adeq Precision	9.868
-2 Log Likelihood	14.01	BIC	28.73
		AICc	28.63

Appendix O3: **The coefficients of the model and its collinearity on the SISLI of CSA cement blended concrete**

Component	Coefficient Estimate	df	Standard Error	95% CI Low	95% CI High	VIF
A-PLC	-5.09	1	0.50	-6.16	-4.02	6.31
B-CSA	-2.10	1	0.27	-2.67	-1.52	3.49
AC	-0.038	1	0.25	-0.58	0.50	1.17
BC	0.12	1	0.21	-0.33	0.57	1.17
AC^2	3.51	1	0.57	2.27	4.74	5.84
BC^2	0.25	1	0.35	-0.51	1.01	3.08

Appendix P1: **ANOVA Table for the SISLI of HAP cement blended concrete**

Mix. Process Source	Comp. Factors Summed Squares	A B C D Df	Average Square	F Value	p-value Prob > F	
Model	108.65	13	8.36	115.26	< 0.0001	Significant
[1]Linear Mixture	17.97	2	8.99	123.94	< 0.0001	
AB	0.43	1	0.43	5.96	0.0285	
AC	0.33	1	0.33	4.52	0.0518	
BD	52.81	1	52.81	728.32	< 0.0001	
CD	0.098	1	0.098	1.35	0.2648	
ABD	8.29	1	8.29	114.29	< 0.0001	
BCD	11.32	1	11.32	156.06	< 0.0001	
AD^2	0.31	1	0.31	4.27	0.0578	
BD^2	28.45	1	28.45	392.29	< 0.0001	
CD^2	0.59	1	0.59	8.08	0.0130	
ABD^2	2.13	1	2.13	29.42	< 0.0001	
BCD^2	10.30	1	10.30	142.08	< 0.0001	

Appendix P2: Regression coefficient for SISLI of HAP cement blended concrete

Regression Coefficients

Std. Dev.	0.27	R-Squared	0.9907
Mean	-2.87	Adj R-Squared	0.9821
C.V. %	9.39	Pred R-Squared	0.8909
PRESS	11.96	Adeq Precision	57.634
-2 Log Likelihood	-13.42	BIC	29.90
		AICc	38.58

Appendix P3: The coefficients of the model and its collinearity on the SISLI of HAP cement blended concrete

Component	Coeff. Estimate	df	Std Error	95% CI Lower	95% CI Higher	VIF
A-PLC	-1.04	1	0.50	-2.12	0.034	16.38
B-PSA	-1.97	1	0.23	-2.47	-1.47	4.63
C-CSA	-3.09	1	0.22	-3.56	-2.62	4.31
AB	-3.42	1	1.40	-6.43	-0.42	8.29
AC	-1.81	1	0.85	-3.64	0.016	3.01
BD	5.08	1	0.19	4.68	5.49	1.77
CD	0.18	1	0.15	-0.15	0.51	1.29
ABD	-11.53	1	1.08	-13.85	-9.22	1.67
BCD	-10.29	1	0.82	-12.05	-8.52	1.54
AD^2	-1.02	1	0.49	-2.07	0.039	9.97
BD^2	-5.92	1	0.30	-6.56	-5.28	4.16
CD^2	0.77	1	0.27	0.19	1.35	3.75
ABD^2	10.33	1	1.91	6.25	14.42	4.42
BCD^2	10.70	1	0.90	8.77	12.62	1.50

Appendix Q1: **ANOVA Table for the SIMLI of PSA cement blended concrete**

Mix. Process **Source**	**Components Factors** **A B C** **Summed Squares**	**Df**	**Average Square**	**F Value**	**p-value Prob > F**	
Model	46.94	3	15.65	30.05	< 0.0001	Significant
[1]Linear Mixture	21.19	1	21.19	40.71	< 0.0001	
AB	19.13	1	19.13	36.74	< 0.0001	
AB(A-B)	9.30	1	9.30	17.85	0.0007	
Residual	7.81	15	0.52			
Lack of Fit	7.81	14	0.56			
Pure Error	0.000	1	0.000			
Cor Total	54.75	18				

Appendix Q2: **Regression coefficient for the SIMLI of PSA cement blended concrete**

Regression Coefficient

Std. Dev.	0.72	R-Squared	0.8574
Mean	5.27	Adj R-Squared	0.8288
C.V. %	13.69	Pred R-Squared	0.6607
PRESS	18.57	Adeq Precision	16.231
-2 Log Likelihood	37.03	BIC	45.86
		AICc	44.63

Appendix Q3: **The coefficients of the model and its collinearity on the SIMLI of PSA cement blended concrete**

Component	Coefficient Estimate	Df	Standard Error	95% CI Low	95% CI High	VIF
A-PLC	9.75	1	0.51	8.67	10.84	2.29
B-PSA	4.38	1	0.36	3.62	5.14	2.15
AB	-9.93	1	1.64	-13.42	-6.44	3.20
AB(A-B)	-14.78	1	3.50	-22.24	-7.32	1.35

Appendix R1: **ANOVA Table for the SIMLI of CSA cement blended concrete**

Mix. Process Source	Comp. Factors Summed Squares	A B C df	Average Square	F Value	p-value Prob > F	
Model	124.65	3	41.65	88.98	< 0.0001	significant
[1]Linear Mixture	57.87	1	57.87	123.62	< 0.0001	
AB	62.99	1	62.99	134.56	< 0.0001	
AB(A-B)	8.45	1	8.45	18.04	0.0007	
Residual	7.02	15	0.47			
Lack of Fit	7.02	14	0.50			
Pure Error	0.000	1	0.000			
Cor Total	131.97	18				

Appendix R2: **Regression coefficient for the SIMLI of CSA cement blended concrete**

Regression Coefficients

Std. Dev.	0.68	R-Squared	0.9468
Mean	5.14	Adj R-Squared	0.9362
C.V. %	13.32	Pred R-Squared	0.9180
PRESS	10.83	Adeq Precision	27.451
-2 Log Likelihood	35.01	BIC	43.84
		AICc	42.61

Appendix R3: **The coefficients of the model and its collinearity on the SIMLI of CSA cement blended concrete**

Component	Coefficient Estimate	df	Standard Error	95% CI Low	95% CI High	VIF
A-PLC	12.60	1	0.48	11.57	13.63	2.29
B-CSA	4.32	1	0.34	3.60	5.04	2.15
AB	-18.02	1	1.55	-21.33	-14.71	3.20
AB(A-B)	-14.09	1	3.32	-21.16	-7.02	1.35

Appendix S1: **ANOVA Table for the SIMLI of HAP cement blended concrete**

Mix. Process Source	Comp. Factors summed Squares	A B C D df	Average Square	F Value	p-value Prob > F	
Model	6.34	8	0.79	8.55	< 0.0001	Significant
[1]Linear Mixture	0.011	2	5.434E-003	0.059	0.9432	
AC	1.44	1	1.44	15.53	0.0009	
BC	3.65	1	3.65	39.37	< 0.0001	
BD	0.24	1	0.24	2.61	0.1227	
CD	0.47	1	0.47	5.12	0.0356	
ACD	0.33	1	0.33	3.55	0.0751	
BCD	1.48	1	1.48	15.94	0.0008	
Residual	1.76	19	0.093			
Cor Total	8.10	27				

Appendix S2: **Regression coefficient for the SIMLI of HAP cement blended concrete**

Regression Coefficients

Deviation (STD)	0.30	R-Squared	0.7827
Average	8.74	R-Squared (Adj)	0.6912
Variation Coef. (%)	3.48	R-Squared (Pred)	0.5147
PRESS	3.93	Precision (Adeq)	12.126

Appendix S3: **The coefficients of the model and its collinearity on the SIMLI of HAP cement blended concrete**

Component	Coefficient Estimate	df	Standard Error	95% CI Low	95% CI High	VIF
A-PLC	9.19	1	0.18	8.82	9.56	1.60
B-PSA	8.24	1	0.15	7.92	8.55	1.57
C-CSA	8.61	1	0.17	8.25	8.96	2.01
AC	-3.39	1	0.86	-5.20	-1.59	2.41
BC	4.25	1	0.68	2.83	5.67	1.83
BD	0.29	1	0.18	-0.087	0.67	1.29
CD	0.47	1	0.21	0.035	0.90	1.82
ACD	-2.04	1	1.08	-4.30	0.23	1.87
BCD	-3.72	1	0.93	-5.68	-1.77	1.55

Appendix T1: **Specification of Engine used for Pozzolan Pulverisation**

Pulverising Engine Specification	
Part No:	Honda GX200-QX3 Petrol Engine
Gross Hp	6.5
Net Hp (SAE J1349)	5.5
Cont. rated Hp @ 3600 rpm	5.0
fuel tank capacity	3.1 L
fuel consumption @ 3600 rpm	1.7 L/h
oil capacity	0.6 L
Air cooled 4-stroke OHV engine	
Oil alert and recoil start	
3/4" parallel key horizontal shaft	
313L x 376W x 346H (mm), 16 Kg	